Tectonometamorphic evolution of the Likhu Khola study area, east-central Nepal

A Thesis Submitted to the College of

Graduate Studies and Research

In Partial Fulfillment of the Requirements

For the Degree of Masters of Geology

In the Department of Geological Sciences

University of Saskatchewan

Saskatoon

By

Richard E. From

Permission to use:

In presenting this thesis in partial fulfilment of the requirements for a Postgraduate degree from the University of Saskatchewan, I agree that the Libraries of this University may make it freely available for inspection. I further agree that permission for copying of this thesis in any manner, in whole or in part, for scholarly purposes may be granted by the professor or professors who supervised my thesis work or, in their absence, by the Head of the Department or the Dean of the College in which my thesis work was done. It is understood that any copying or publication or use of this thesis or parts thereof for financial gain shall not be allowed without my written permission. It is also understood that due recognition shall be given to me and to the University of Saskatchewan in any scholarly use which may be made of any material in my thesis.

Requests for permission to copy or to make other use of material in this thesis in whole or part should be addressed to:

Head of the Department of Geological Sciences
University of Saskatchewan
114 Science Place
Saskatoon, Saskatchewan
S7N 5E2, Canada

ABSTRACT

Recent models for the evolution of the Himalaya and adjacent regions have changed our understanding of how large mountain belts form. The key data that govern these models has largely been extracted from the exhumed mid-crustal core of the orogen, the Greater Himalayan sequence, and its bounding structures. Targeted mapping in the Likhu Khola region was carried out across the Greater Himalayan sequence as the initial phase of a project aimed to evaluate the viability of those models. The exhumed mid-crustal core in the study area exposes upper greenschist to upper amphibolite grade metamorphic rocks that have been pervasively deformed by ductile shearing. Mantled porphyroclasts and c, c' and s fabrics record top-to-the-south directed shear. As with most transects across the Himalaya, metamorphic grade increases up structural section. Pressure and temperature estimates using THERMOCALC v.3.26 in average-PT mode with the internally consistent data set of Holland & Powell (1998) were conducted on eleven specimens at different structural positions. Temperatures increase slightly up structural section but become constant within error for the upper portion of the study area. Pressure estimates increase up structural section followed by an abrupt pressure decrease once partial-melting increases to form migmatitic rocks. This may indicate a potential tectonometamorphic discontinuity that separates two distinct domains that have different structural, thermal and metamorphic histories (e.g., Larson et al, 2010a; Yakymchuk and Godin, 2012). In situ U-Th-Pb Monazite geochronology was utilized on six of the specimens used for P-T analyses to constrain the P-T data. Multiple domains of ages were obtained ranging from 27.2 Ma to 15.1 Ma and are interpreted to represent several recorded metamorphic events. These metamorphic events are best interpreted in conjunction with the relative concentration of trace elements present at each U-Th-Pb data point that was collected using a split stream LA-MC-ICP-MS. More specifically, certain

rare earth elements provide insight into whether garnet was growing, resorbing into melt or being homogenized at high temperatures during specific U-Th-Pb age dates. The relationships between metamorphism, crustal melting, P-T conditions and monazite/garnet growth and resorption are critical to evaluating if current models proposed for the evolution of the Himalaya are applicable in east-central Nepal.

ACKNOWLEDGMENTS

The creation of this thesis wouldn't have been possible without the support from numerous people. Many thanks goes to Dr. Kyle Larson whose initiation of this project and selection of myself for graduate research made my dreams of a mountainous Masters project come true. The University of Saskatchewan is thanked for the usage of facilities and the Professors for stimulating discussions. Saskatchewan Research Council for usage of analytical facilities and Microprobe time with Dr. Creighton. Dr. Cottle and G. Lederer at the University of Santa Barbara for assistance with laboratory analyses. The support of my family and friends is greatly acknowledged for helping me through this process and making it such an enjoyable experience.

TABLE OF CONTENTS

page

LIST OF TABLES

LIST OF FIGURES

CHAPTER 1

THE HIMALAYAN OROGEN

1.1 Introduction

Mountain belts are some of the most imposing geologic features on Earth with none more so than the Himalaya. The Himalaya are home to the highest topography on the planet and sit at the nexus of dynamic interaction between tectonics, landscape development, global atmospheric circulation, and climate patterns (Molnar and England, 1990; Burbank et al., 1993; Ruddiman, 1997; Owen, 2006).

The Himalayan orogenic belt extends laterally for over 2500 km from Pakistan in the west to Bhutan in the east and forms the southern margin of the Tibetan Plateau (Figure 1.1A). This iconic mountain range serves as the modern-day paradigm of orogenesis, but due to remoteness, oppressive topography and political instability it has only recently become the subject of earnest geologic research. The insights gained from this well-exposed and evolving orogenic system can be applied to our understanding of orogenic events that have occurred in the past across the globe.

1.2 Orogenic evolution

The precursor to actual continental collision between India and Eurasia, which serves as the engine behind the continuing rise of the Himalaya and the Tibetan plateau, was the breakup of the Gondwana supercontinent and the subduction of the Indian plate beneath the southern margin of the Eurasian plate during the closing of the intercontinental Tethys sea (Hodges, 2000). During this period, the Eurasian plate evolved as an accretionary margin formed through

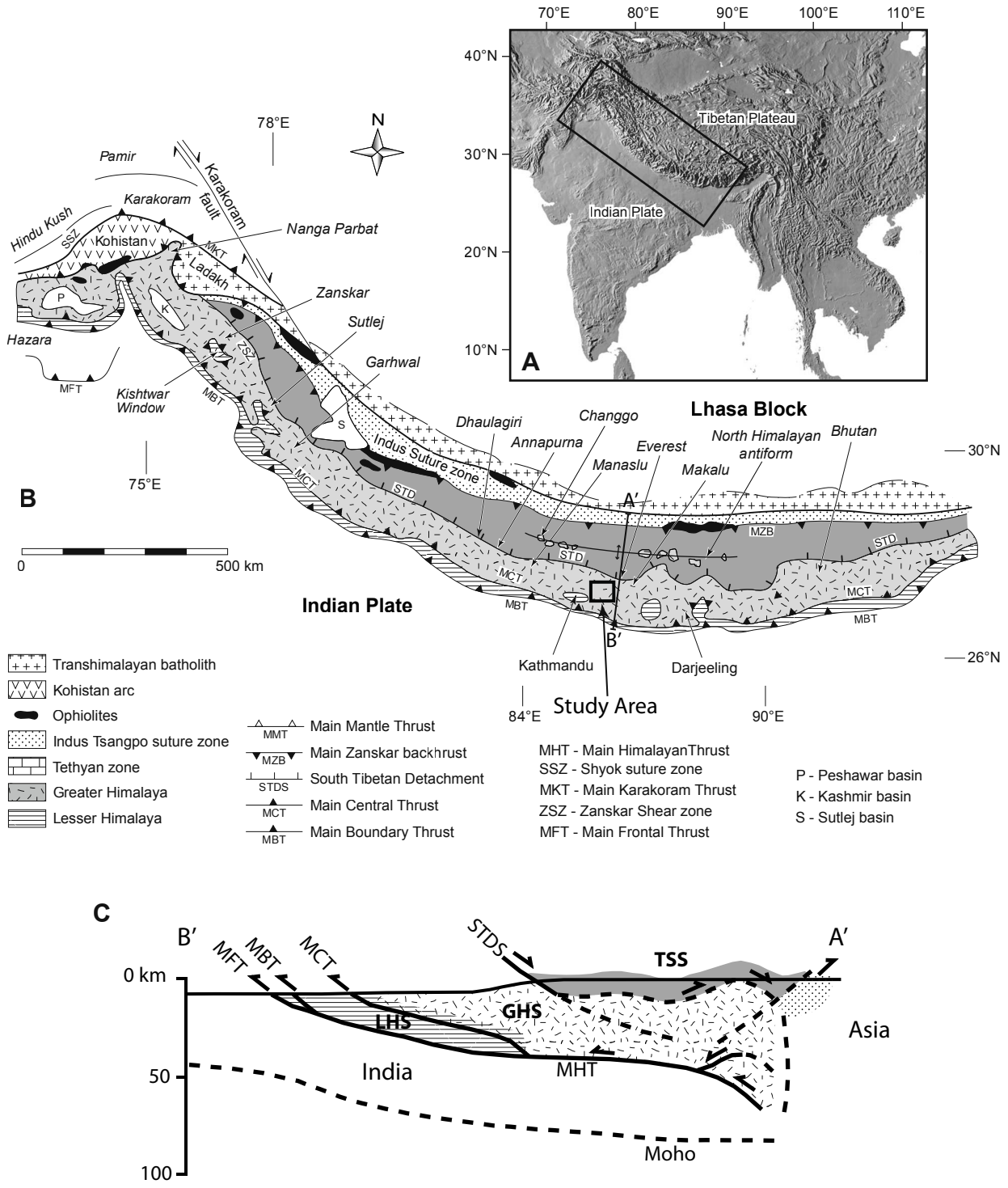

Figure 1.1 - A) Shaded relief map of the Indian and Eurasian plates showing the post-collisional uplifted Himalayan orogenic arc. Black rectangle outlines the region shown in B. B) Simplified geologic map of the Himalayan orogen. Study area investigated as part of this thesis is outlined with a black box. Modified from Searle et al. (2008). C) Simplified vertical geologic section along the line A' to B' as shown above. Modified from Hauck et al. (1998).

the collision and docking of exotic terranes through Early Proterozoic to Cretaceous time, culminating with the Lhasa (east) and Karakorum (west) blocks accreting in the Early Cretaceous (Allégre et al., 1984) and the Kohistan-Ladakh island-arc complex in the Late Cretaceous (Figure 1.2; Petterson and Windley, 1985; Coward et al., 1987).

Based on paleomagnetic data, analysis of magnetic anomalies in the Indian Ocean, cessation of marine sedimentation and the onset of continental molasse-type sedimentation along the Indus (also referred to as the Yarlung-Tsangpo) suture between India and Eurasia (Figure 1.1B; see review in Yin and Harrison, 2000), the initiation of continental collision between the Indian and Eurasian plates is interpreted to be late Eocene ~50 Ma (Besse et al., 1984; Patriat and Achache, 1984; Molnar, 1984; Hodges, 2000, Najman et al., 2010). The exact timing of initiation of continent-continent collision, however, is not yet resolved and debate continues around the best method of determination (e.g., Yin and Harrison, 2000; Garzanti, 2008; Najman et al., 2010; Zhang, 2011). Further complicating matters this initial collision is also believed to be diachronous along the strike length of the orogen, however, the extent of the diachroneity is open to debate (Rowley et al., 1998; Najman et al., 2005).

Continuing convergence between India and Eurasia resulted in initial subduction of the Indian plate followed by underplating of the Indian crust beneath Eurasia producing doubly thick crust underneath the Himalaya and southern Tibet (Molnar, 1984). This crustal thickening was paired with a large-scale, dominantly southward-propagating thrust system (Searle et al., 1988, 1990, 1997; Rowley, 1996; Zhu et al., 2005) that has accommodated over 1400 km of post-initial collision shortening (Yin and Harrison, 2000).

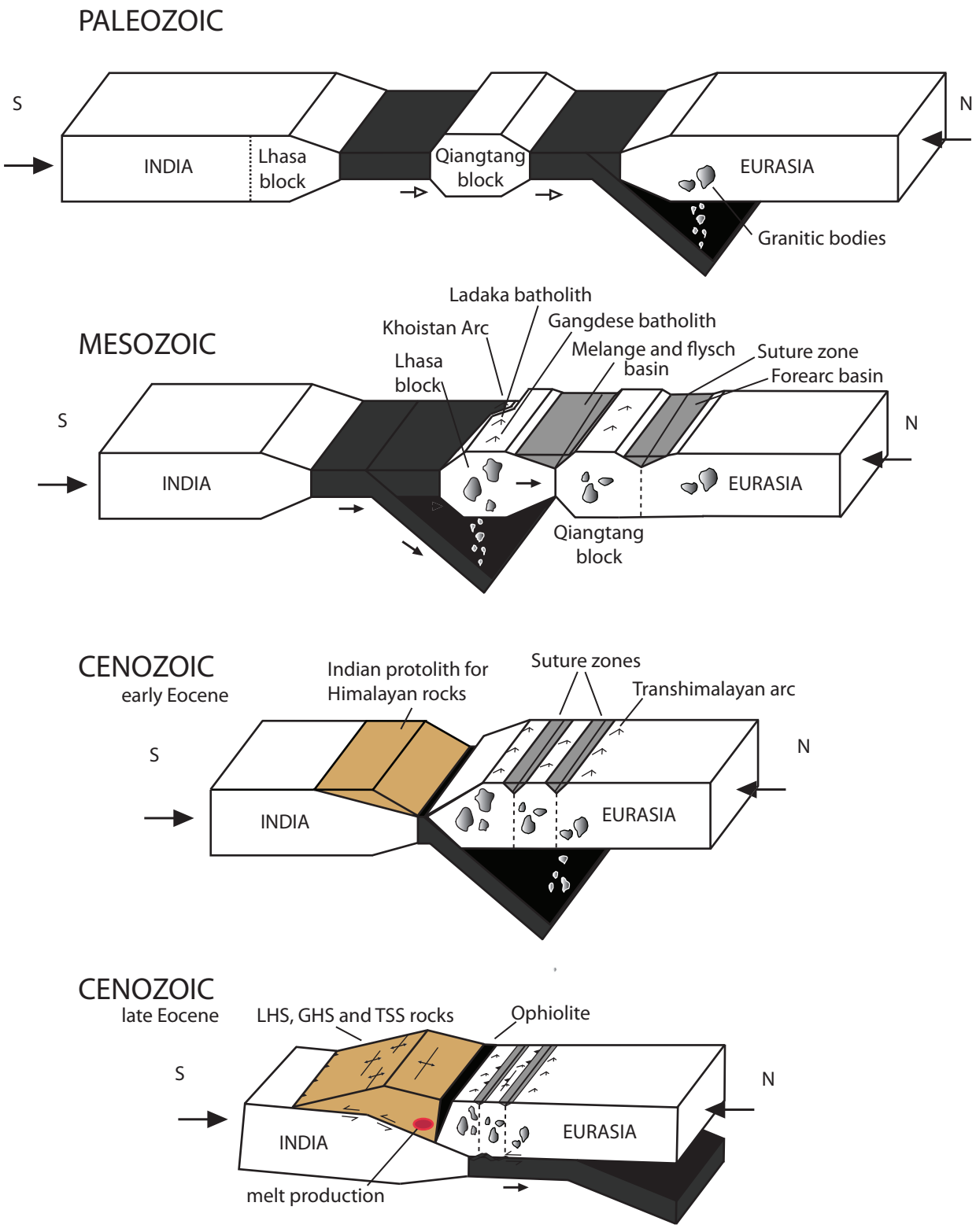

Figure 1.2 – Block diagram evolution of the convergence between Eurasia and India from accretion of exotic terranes during the Paleozoic to underplating of the Indian continent beneath Eurasia and potential melt production in the mid-crust during the late Eocene.

1.3 Lithotectonic units and structure

The structural framework of the Himalayan front is defined by four fault-bounded lithotectonic domains (Heim and Gasser, 1939). These lithotectonic domains are separated by major faults, have distinctly different tectonic characteristics and deformational histories, and can be traced along the entire length of the orogen (Hodges, 2000 and references therein). The faults that bound the different lithotectonic domains consist of dominantly shallow, mainly northward dipping structures (Figure 1.1C) that may merge at depth into a common basal detachment fault beneath the Tibetan plateau (e.g., Hauck et al., 1998). Alternatively the faults may simply continue into the hinterland as sub-parallel individual structures (e.g., Searle et al., 2003). The rocks exposed along the Himalayan front are dominantly metamorphosed sediments of Indian plate origin that were deposited on or to the north of the thinned continental margin of the Indian continent between the Proterozoic and Early Paleozoic (Brookfield, 1993; Parrish and Hodges, 1996).

The structurally highest tectonostratigraphic unit is the Tethyan sedimentary sequence (TSS; Figure 1.1C). It is composed of Upper Proterozoic to Middle Eocene unmetamorphosed to low-grade sedimentary rocks scraped off of the former Indian plate northern margin (Searle et al., 1987; Mascle et al., 2012). It is bounded to the north by the Indus suture zone (Hodges, 2000) and to the south by the Southern Tibetan detachment system (STDS). The STDS is a generally north dipping top-to-the-north sense high-strain zone that separates the TSS from the subjacent metamorphic core of the orogen, the Greater Himalayan sequence (GHS). The GHS is characterized by greenschist to granulite-grade metamorphic rocks of Indian plate affinity and associated anatectic melt. The supracrustal protoliths to GHS rocks were deposited on the northern Indian passive margin between the Proterozoic and Early Paleozoic (Brookfield, 1993; Parrish and Hodges, 1996; Mascle et al., 2012). The lower boundary of the GHS is marked by

the north dipping, top-to-the-south sense Main Central thrust (MCT), which separates it from the Lesser Himalayan sequence (LHS). The movement across the MCT was coeval with that across the STDS, but with opposite shear sense. The LHS, which occurs in the footwall of the MCT, consists of low metamorphic grade Proterozoic to Early Paleozoic metasedimentary rocks of Indian plate affinity. The lower boundary of the LHS is marked by the Main Boundary thrust, which carries the LHS over the unmetamorphosed Siwalik molasse in its footwall. The Siwalik molasse is the youngest and southernmost lithotectonic assemblage found along the Himalayan front. It is composed of Neogene to Quaternary foreland basin strata and is bounded by the Main Frontal thrust to the south (Burchfiel et al., 1992; Hodges, 2000; Mascle et al., 2012).

1.4 Metamorphism

There is cryptic evidence for regional metamorphism of the GHS and LHS during pre-Cenozoic time (Gehrels et al., 2006) before the present collision between Eurasia and India. Recently, Martin and Ducea (2011) used garnet crystallization, muscovite $^{40}Ar/^{39}Ar$ and monazite U-Pb ages from the LHS to suggest that peak metamorphic temperatures were reached in the Mesoproterozoic, during a previously unrecognized orogeny. Evidence for this older metamorphic episode is not yet recognized across the length of the Himalaya and additional research is required to delineate how Proterozoic deformation and metamorphism may have influenced the Cenozoic orogenic record.

The dominant metamorphic record appears to be related to the Cenozoic collision of India with Eurasia. Two distinct phases of metamorphism in the Himalaya have been identified associated with continental collision. Eohimalayan metamorphism, which occurred during the Eocene, was the result of initial crustal thickening due to the continental collision between Eurasia and India (Hodges et al., 1996; Godin et al., 2001). This was a Barrovian-type regional

metamorphic event that is recorded as kyanite grade mineral assemblages variably preserved in GHS rocks (Hodges et al., 1988a,b; Vannay and Hodges, 1996). The second, major pulse of metamorphic activity, the Neohimalayan phase (Hodges et al., 1988a,b; Pêcher, 1989; Guillot et al., 1999), occurred during the early to middle Miocene. This later episode was characterized by sillimanite-grade metamorphism (Hubbard and Harrison, 1989) and is interpreted to record isothermal decompression, paired crustal anatexis (Streule et al., 2010) and the extrusion of the GHS from beneath the Tibetan plateau (Vannay and Hodges, 1996; Hodges et al., 1996). The Neohimalayan and Eohimalayan phases have alternatively been interpreted as the result of a single prolonged, dynamic metamorphic event (Walker et al., 1999; Jamieson et al., 2004) with the time between them representing a lull or slowdown in tectonic activity or a gap in the preserved record. Recent work by Cottle et al. (2009) on the metamorphic history of the STDS in the Mt. Everest region has shown that deformation and metamorphism occurred over a protracted period from 38 Ma to 16-13 Ma. Regardless of which interpretation is correct, there is record of a protracted metamorphic history from across the Himalaya.

1.5 Evolution of the Greater Himalayan sequence

The GHS is the exhumed metamorphic core of the orogen bounded by coeval shear zones of opposite shear sense. The STDS bounds the top of the GHS and has been interpreted as a Miocene low angle normal-sense fault system, dipping 5-20° northward beneath the Tibetan Plateau (Burg 1983; Burg et al., 1984; Burchfiel et al., 1992; Searle et al., 1997; Kellett and Grujic, 2012). There is also local evidence, however, for south-southwest directed thrust movement across the STD in the Eocene (Vannay and Hodges, 1996). The MCT, which bounds the base of the GHS is interpreted as a north-dipping, thrust-sense high-strain zone. The thrust sense movement translated GHS rocks south over LHS rocks, which were largely unaffected by

Himalayan metamorphism (Gansser, 1964, 1983; Hodges 2000; Searle and Godin, 2003, Searle et al., 2006). The movement across the MCT was parallel to and contemporaneous with that across the STDS; the STDS is believed to have acted as a passive roof (stretching fault) enabling extrusion of the GHS from beneath the Tibetan plateau (Searle et al., 2003; Law et al., 2004). Focused and rapid erosional processes may have enhanced exhumation of the extruding GHS (Beaumont, 2001). Stratigraphic and thermochronometric data have been interpreted to indicate that the formation of the Tibetan plateau influenced strengthening of the Asian monsoon climate (Prell and Kutzbach, 1992; Molnar et al., 1993; Clift et al., 2008). Increased monsoonal rainfall may have increased and focused erosion on the southern edge of the Tibetan plateau removing significant amounts of material, advecting heat and significantly affecting the tectonic evolution of the Himalaya. This focused erosion on the Himalayan front paired with the excess gravitational potential energy of over-thickened Tibetan crust may have created a positive feedback loop (Willett, 1999; Clift et al., 2010), allowing the GHS to be exhumed at a faster than normal rate.

1.6 Problems in Himalayan Geology

1.6.1 Contrasting models for GHS evolution

Different models for the evolution of the GHS have been the topic of considerable ongoing debate among Himalayan researchers (e.g., Harrison, 2006; Grujic, 2006; Harris, 2007; Kohn, 2008). There are currently two main end-member models based on two different schools of thought. One end-member model is based on a critical taper wedge theory developed by Davis et al., (1983), which posits that an orogenic wedge propagated southward into the foreland during formation of a conventional thrust belt in response to continued crustal thickening during convergence while maintaining a critical taper angle (Figure 1.3A). The theory predicts in and

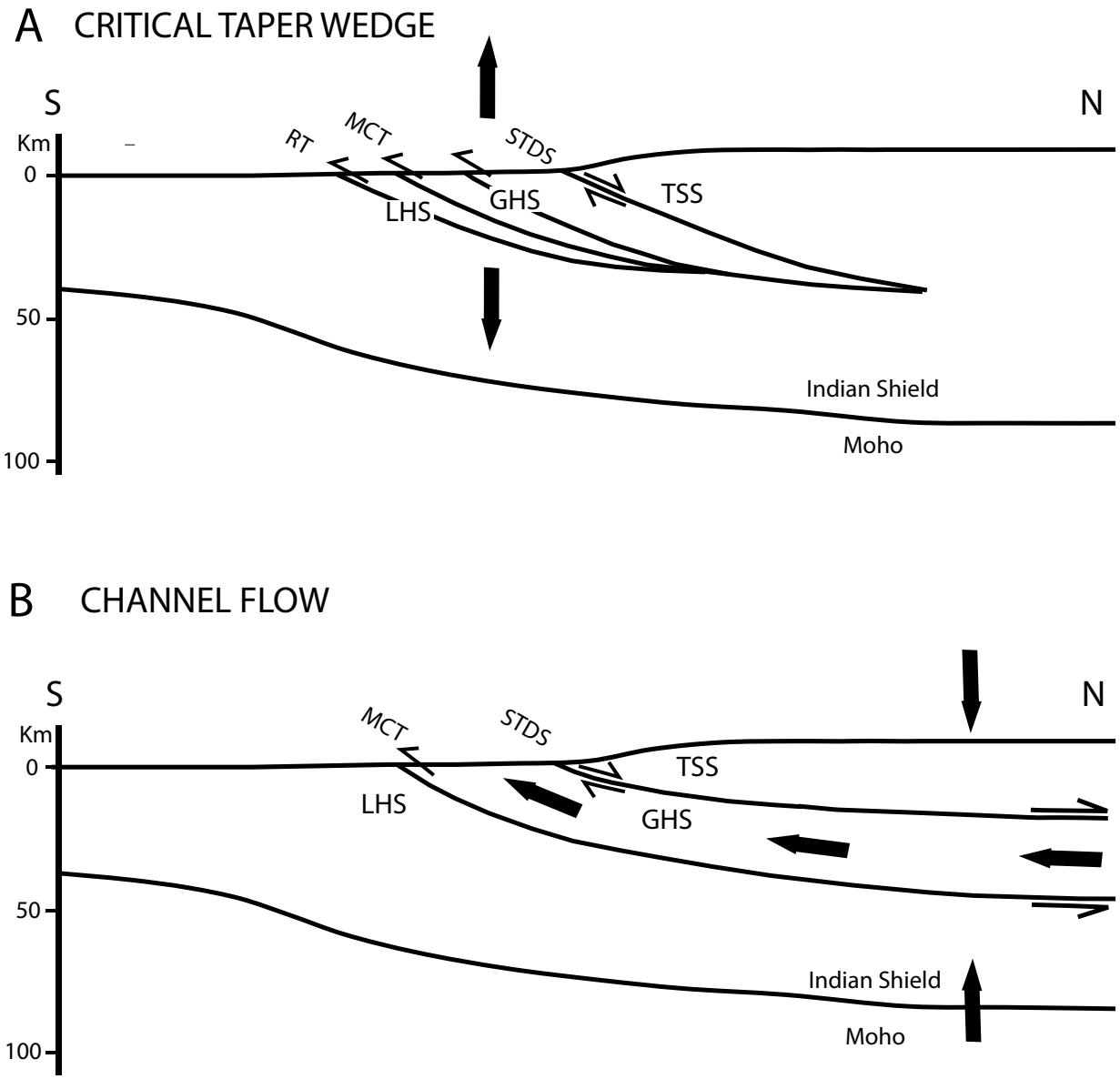

Figure 1.3 - Tectonic Models for the Himalayan Orogen (A) Critical Taper Wedge after Kohn et al. (2008) showing characteristic vertical extension that is paired with howizontal shortening. (B) Channel Flow after Beaumont et al. (2001) and Larson et al. (2010a) showing characteristic vertical shortening that is paired with horizontal extension. GHS: Greater Himalayan Sequence, LHS: Lesser Himalayan Sequence, MCT: Main Central Thrust, MFT: Main Frontal Thrust, STDS: South Tibetan Detachment System, TSS: Tethyan Sedimentary Sequence, RT: Ramgarh Thrust.

out-of-sequence thrusting and local normal faulting to maintain the critical angle between the topographic surface and basal detachment in order to continue propagation into the foreland (DeCelles et al., 2001; Robinson et al., 2006; Kohn, 2008; Robinson, 2008). The alternate end-member is the channel flow hypothesis, which suggests that partial melting of the GHS at mid-crustal levels lowered its viscosity enough to allow it to be extruded southward from beneath the Tibetan plateau due to a lateral pressure gradient between the doubly thickened crust of the Tibetan plateau and the normal crustal thickness of the Indian craton to the south (Figure 1.3B; Bird, 1991; Grujic et al., 1996; Beaumont et al., 2001; 2004; 2006). The ideas about crustal flow began with an initial conception by Dewey and Burke (1973) that the continent-continent collision increases crustal thickness resulting in partial melting of the lower crust. Bird (1991) expanded on their ideas and developed a model for crustal flow where the GHS was extruded from the mid-crust beneath the Tibetan Plateau.

1.6.2 Evidence supporting the models

Geophysical data has been interpreted to indicate a partial melt layer currently existing at mid-crustal levels just north of the Indus suture zone and extending north beneath the Tibetan plateau. The INDEPTH project, which was carried out in 1992 with results and interpretations published by Nelson et al. (1996), delineated a reflective horizon at 15-20 km depth that also coincides with low seismic velocities and anomalous electrical conductivity. These properties indicate the presence of fluids along that horizon. This project has added validity to the idea of partial melting at mid-crustal depths due to thickened crust and the formation of a semi-viscous channel (Nelson et al., 1996; Hodges, 2000; Searle et al., 2006). Alternatively, these findings could simply represent a present vapour phase (water or carbon dioxide) potentially related to hot spring activity throughout the area (Tong and Zhang, 1981). Moreover, the INDEPTH data only

indicates a fluid-rich layer in the immediate vicinity of the geophysical transect, within a few tens of kilometers of the northern Yadong-Gulu rift. This transect was chosen due to the relative ease of geophysical work, but because it is within a graben it may not be representative of the Tibetan Plateau as a whole (Nelson et al., 1996, Harrison, 2006). Geologic research, however, has also been interpreted to support the model of active crustal melting. Recently, Searle et al. (2010) published multi-system thermochronologic data from the Everest transect (Nepal-Tibet) that shows that mid-crustal melting, similar in scope to that potentially imaged at depth using geophysics, spanned from ~32 to 17 Ma, which may have triggered mid-crustal flow of the GHS coeval with movement across the MCT and STDS.

Alternatively, pressure, temperature and time (P-T-t) data presented by Kohn (2008) from the Langtang and Darondi areas of central Nepal differ significantly from values predicted in channel flow models. As opposed to long residence times of high heat, retrograde isothermal decompression pressure and temperature (P-T) paths and rapid cooling expected for GHS rocks in channel flow models, Kohn (2008) observes short residence times at high temperature, isobaric cooling of GHS rocks and slow cooling rates, more consistent with taper wedge models (Henry et al., 1997; Bollinger et al., 2006; Kohn, 2008). In addition, Robinson (2008) used forward modeling, reconstructed balanced cross-sections, and deformational timing data to construct a model that supports a conventional wedge model for the development of the central Himalayan thrust belt.

Recent research, however, has postulated a transition within the GHS between two end-members (e.g., Beaumont and Jamieson, 2010; Larson et al., 2010a). Larson et al. (2010a) interpreted the sillimanite-grade, migmatitic upper section of the GHS to record extension in the direction of flow associated with vertical thinning and horizontal extension, deformation

consistent with channel flow. In contrast, the lower section of the GHS is interpreted to record shortening in the direction of flow that is associated with vertical thickening and horizontal shortening, deformation consistent with critical wedge taper. Moreover, metamorphic P-T conditions and U-Th-Pb monazite ages from the base of the GHS are interpreted to represent the progressive downward migration of the MCT and associated subcretion of material to the base of the GHS (Larson et al., 2011). This work suggests that there is a continuum between channel flow processes operating in the upper GHS and critical taper thrust wedge processes in the lower GHS. This theory indicates that the two end-member models of channel flow and critical taper wedge are not mutually exclusive and the debate between these model end-members may be a false dichotomy (Beaumont and Jamieson, 2010, 2011; Larson et al., 2011).

1.7 The Likhu Khola Region

1.7.1 Previous work

The Likhu Khola river valley system is located in east-central Nepal northeast of Kathmandu and just west of the Everest region (Figure 1.1B). Parts of the Likhu Khola region were mapped at a basic reconnaissance scale during an expedition by Ishida (1969) in 1966. Ishida (1969) reported that this region consists mainly of sillimanite-garnet-biotite gneisses and tourmaline-biotite migmatite. Using structural and lithological observations, Ishida recognized the basic lithologic units in this region and subdivided them into formations or zones as they were termed in Ishida and Ohta (1973). These zones were then grouped into the Himalayan Gneisses and the Midland Metasediment group.

Schelling (1992) conducted a large-scale study of Eastern Nepal that included six years of geological field research ranging from the Sikkim border in the east to the Kathmandu Valley in the west and from the Everest region peaks in the north to the Ganges plain in the south. He

also recognized the different large-scale tectonostratigraphic units in the Likhu Khola region and classified them into the more customary GHS and LHS with the MCT that separates them in the southwestern part of the current map-area. This thesis will build on these previous studies through more detailed mapping complimented by new laboratory work. Ultimately this study was formulated to test the recently developed tectonic models for the Himalaya, namely the channel flow and extrusion hypothesis (e.g., Grujic et al., 1996; Beaumont et al., 2001), the critical taper wedge hypothesis (e.g., Kohn et al., 2008), and the continuum model proposed by Larson et al. (2010a)

1.7.2 Objectives

The purpose of this study is to contribute to the evolving knowledge of the formational processes of the Himalaya. More specifically, as explained above, this thesis is designed to test models of orogenic evolution that have been developed in recent years for the Himalayan belt. The key data that govern the different models for Himalayan evolution have largely been extracted from within the GHS and its bounding structures. Therefore, targeted mapping, sampling and petrological/geochronological study within the GHS will yield valuable information to evaluate these different models and elucidate the tectonometamorphic history for the GHS in this region.

To achieve this goal we must answer two questions regarding the development of the orogen in this region. *1) What are the tectonometamorphic characteristics and geologic history of the Likhu Khola region? 2) Are the findings from the Likhu Khola compatible with any of the currently proposed models for the formation and evolution of the Himalayas?*

Fieldwork was carried out over one three-week field season in east-central Nepal during the spring of 2011. Detailed mapping of structures and rock units in the Likhu Khola region was

completed and will serve as the basis for all interpretations and subsequent analytical data. Specimens were collected to form a representative suite of the different lithologies encountered and to allow for the first detailed metamorphic, microstructural, and geochronologic data analysis of rocks in this region.

The models discussed above provide testable criteria regarding the metamorphic and deformational histories expected throughout the GHS (e.g., Jamieson et al., 2004; Kohn, 2008; Yakymchuk and Godin, 2012). In this study multiple geothermobarmetric techniques were used to estimate metamorphic temperatures and pressures of equilibrium assemblages. Deformation characteristics such as shear sense and temperature during deformation were investigated through assessing the lattice preferred orientations of quartz *c*-axes in quartz rich rock types. U-Th-Pb monazite geochronology was used to constrain the timing of deformation, metamorphism and infer P-T-t paths. In addition, correlations of age to Y zonation and trace element concentrations in the monazite grains was used to link the monazite growth histories to conditions of metamorphism (e.g., Cottle, 2009; Kohn et al., 2011; Larson et al., 2011).

The results of this thesis are presented in two main chapters. Chapter 2 presents the geology of the study area including classification of lithological units, structural and metamorphic observations and the results of quartz microstructural analysis. Chapter 3 presents results of petrological and geochronological studies including, 1) classification of metamorphic zones based on mineral assemblage data, 2) evaluation of textural relationships of minerals and their chemical compositional and potential zonation for use in geothermobarometric estimates and, 3) constrains the timing of metamorphism with U-Th-Pb monazite geochronology. Chapter 4 summarizes the results of this study and makes suggestions for further work.

CHAPTER 2

GEOLOGY OF THE LIKHU KHOLA REGION, EAST-CENTRAL NEPAL

2.1 Introduction

This study examines the region along the Likhu Khola river valley from Tholo Priti in the south to Gyajo La in the north and adjacent areas of the Nupche and Khimti Kholas from Gyajo La in the north to Those in the south (Figure 2.1). Ishida carried out reconnaissance-scale mapping of the region in 1966 (Ishida, 1969; Ishida and Ohta, 1973) and more recently Schelling (1992) created a regional map of eastern Nepal including this region. Ishida (1968) and Ishida and Ohta (1973) mapped multiple discrete faults within the study area, whereas Schelling (1992) mapped only one large-scale thrust fault (the Main Central thrust). This study builds on this previous work and focuses on examining the area in more detail with supporting laboratory work in microstructural analysis, petrology and geochronology. A consistent interpretation of the structural regime of the Himalaya is essential in progressing our understanding of orogenic processes and potential changes in how the mountain belt is thought to have evolved (e.g., see summaries by Yin and Harrison, 2000; Law et al., 2004; and Hodges, 2000, 2006). With the flood of research on the Himalaya over the past two decades the previous work in the study area must be re-visited and re-evaluated within the current Himalayan paradigm.

2.2 Lithotectonic Units

2.2.1 Introduction

The geology of the study area consists of exhumed, pervasively ductily deformed metamorphic rocks. Metamorphic grade generally increases up structural section from upper greenschist in the southern part of the study area to upper amphibolite grade in the northern

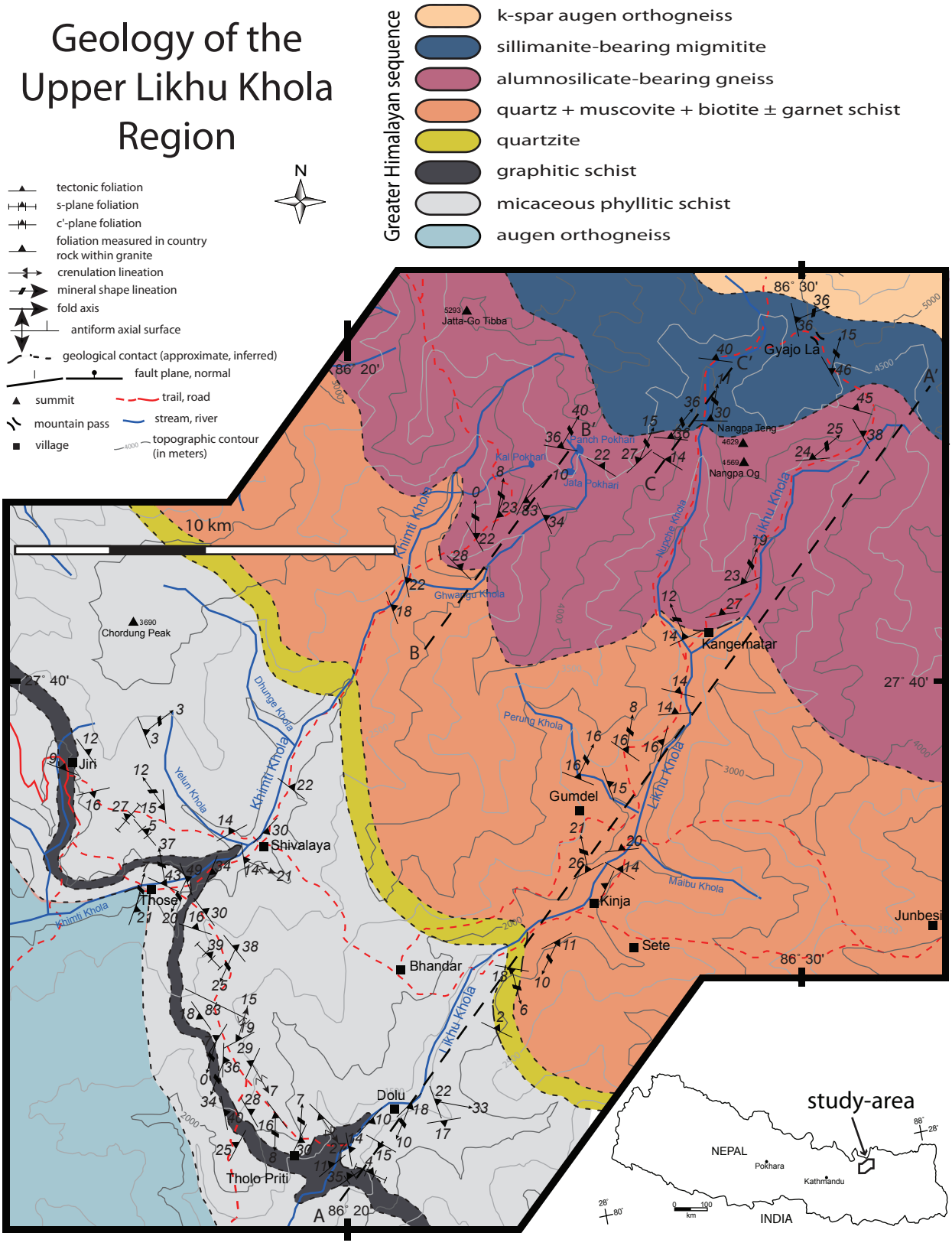

Figure 2.1 - Geologic map overview of the upper Likhu Khola study area showing the orientation and extent of a constructed cross section in Figure 2.2.

reaches (Figures 2.1 and 2.2). This is consistent with inverted metamorphic field gradients observed along the length Himalaya near the base of the GHS (e.g., Mallet, 1874; von Loczy, 1878; Oldham, 1883). The lithologies of the mapped area will be discussed in order from structurally lowest to highest.

2.2.2 Augen orthogneiss

An augen orthogneiss, which crops out just south of the town of Those (Figure 2.1), comprises the structurally lowest unit exposed in the study area (Figures 2.1, 2.2). The thickness of this unit is not constrained as it extends outside the map area to the southwest. It is composed of 35-40% quartz + 25-30% feldspar (plagioclase, perthite and minor K-spar) + 15% muscovite + 8% biotite ± 2% tourmaline. Anatexite comprises up to 10% of total rock volume and has a general composition of 50% quartz + 40% feldspar ± 10% biotite. The foliation is defined by micaceous partings of biotite and muscovite that also define a distinctive, well-developed mineral stretching lineation. This lineation is also expressed as quartz rods in the same orientation, plunging shallowly to the north (Figure 2.3A). The augen within this unit consist of variably fractured and slightly rotated perthitic feldspar crystals (Figure 2.3B). The quartz exhibits an inequigranular grain size due to grain boundary migration inhibition between micaceous partings (Figure 2.3C). Internal subgrain development throughout the quartz fabric with the formation of discrete, smaller quartz grains (Figure 2.3D) are the result of grain boundary migration recrystallization, correlative with Regime 3 of Hirth and Tullis (1992) and associated with deformational temperatures of 500-700°C (Stipp et al., 2002).

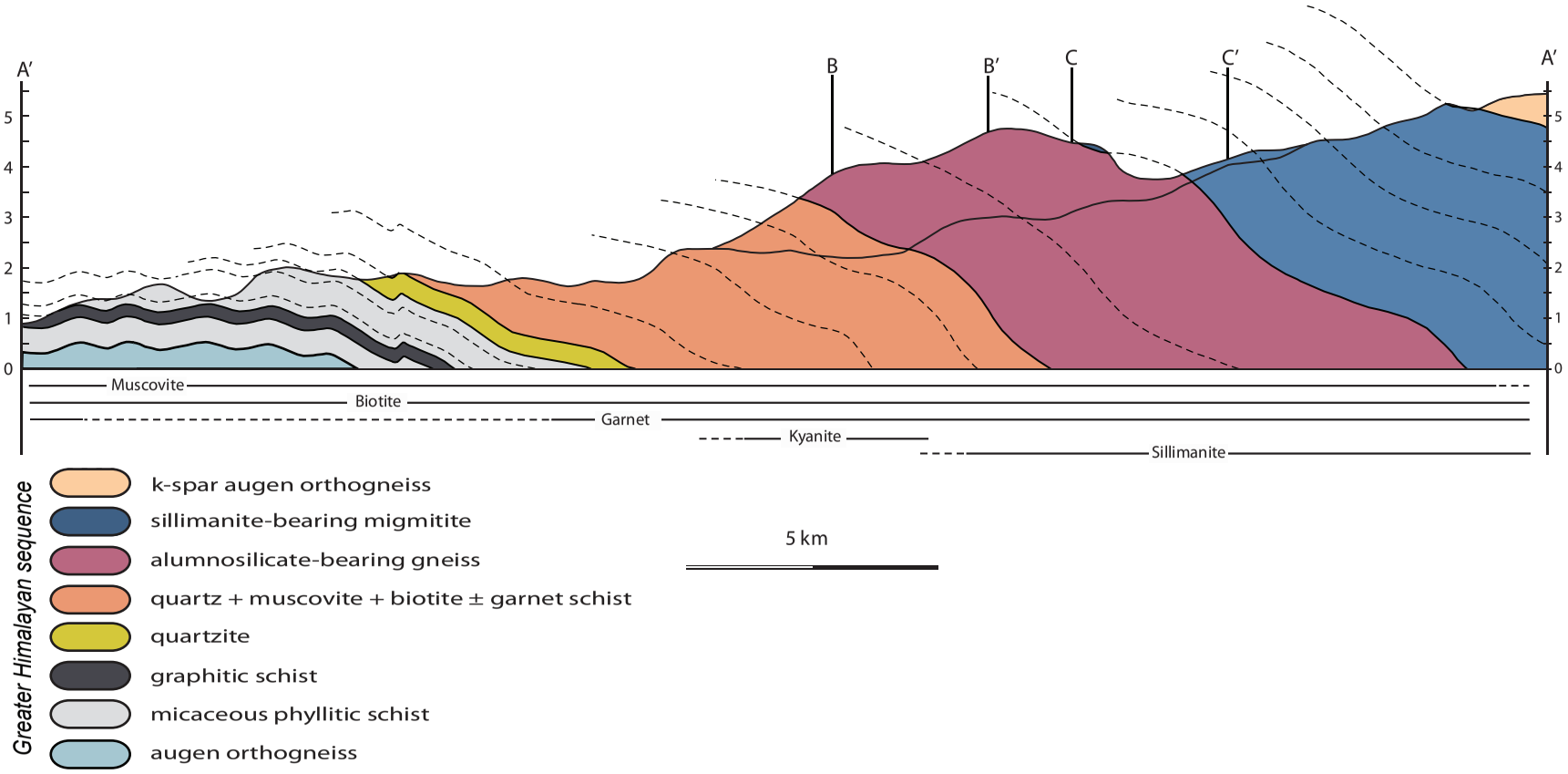

Figure 2.2 - Simplified cross section of the Likhu khola study area from A to A' as shown on Figure 2.1. Correlation of the rock units from transects B to B' and C to C' from the northwest side of the circuit traverse has enabled the stacking of three paralell cross ection segments and further extrapolation of the regional folding.

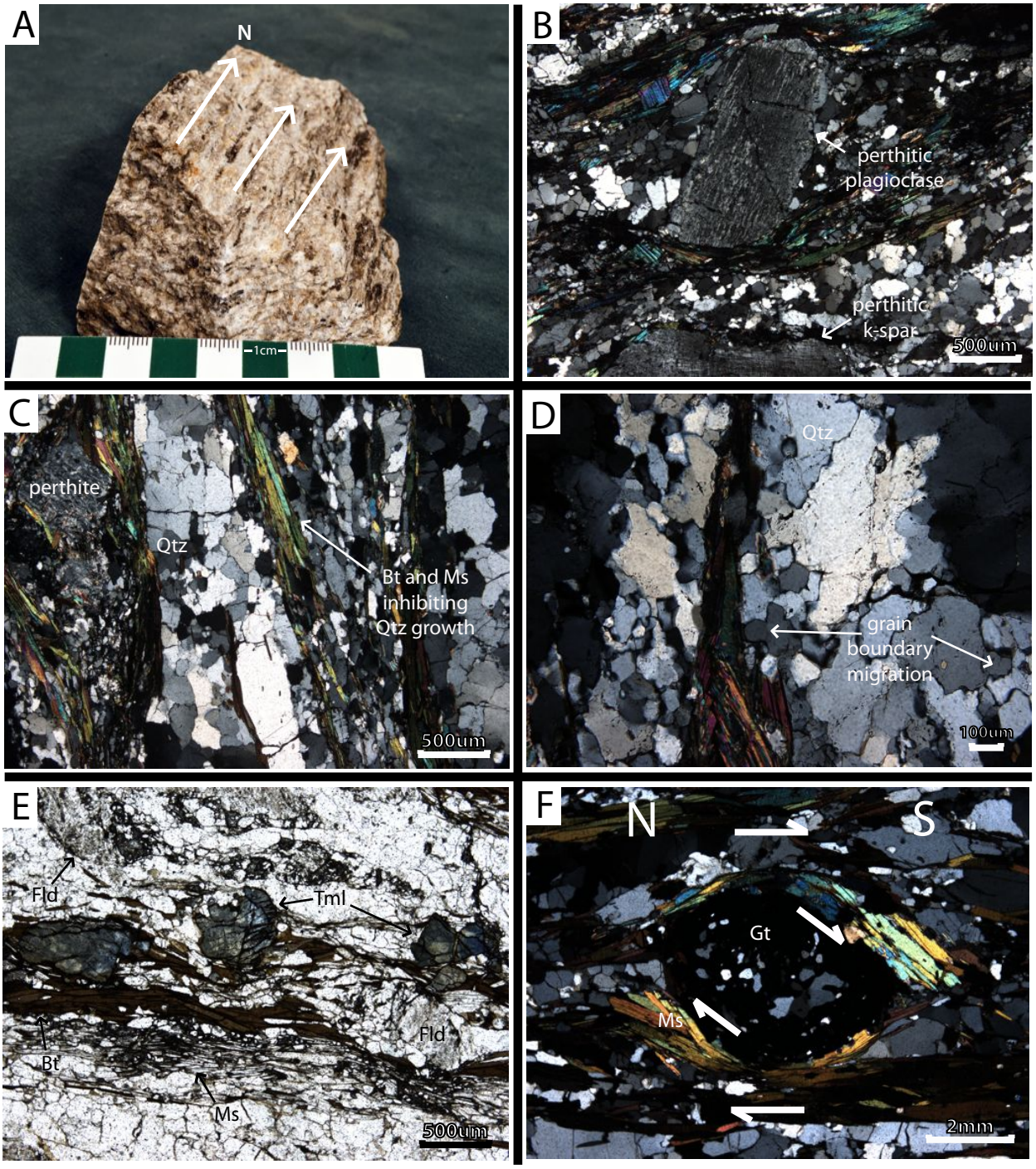

Figure 2.3 - Specimens from the Likhu Khola region. A) Hand specimen of augen orthogneiss showing a lineation defined by quartz rods, green tip of pencil for scale is 2cm. B) Augen orthogneiss showing a rotated perthite augen and a perthitic k-spar augen. C) Quartz textures within the augen orthogneiss showing inequigranular grain size and micaceous partings inhibiting quartz growth. D) Quartz within the augen orthogneiss showing grain boundary migration recrystallization. E) Micaceous schist showing thin, semi-continuous banding of biotite and muscovite, altered feldspar (to sericite) and tourmaline. F) Sigma-type garnet porphyroblast within micaceous schist showing top to the south sense of rotation with strain shadows allowing more muscovite growth to the bottom left and top right of the garnet porphyroblast. Qtz = quartz, Tml = tourmaline, Ms = muscovite, Bt = biotite, Fld = feldspar, Gt = garnet

2.2.3 Micaceous phyllitic schist with intercalations of marble and calc-silicate

Overlying the augen orthogneiss is a ~7500 m thick unit of micaceous phyllitic schist with intercalations of quartzite, marble and calc-silicate. The phyllitic schist has variable quartz and micaceous mineral content with a range in composition of 35-60% quartz + 10-20% feldspar + 5-15% muscovite + 5-20% biotite ± 1-10% garnet ± 5-10% carbonate. The accessory minerals present include tourmaline, zircon, monazite, epidote, apatite, rutile, magnetite and/or hematite. Anatexite comprises 5-15% of total rock volume within this unit and is composed of 50% quartz + 20% feldspar + 10-15% muscovite + 10% biotite ± 5-10% garnet ± 5% tourmaline. The foliation is defined by planar muscovite, biotite and local chlorite that also define a mineral lineation that plunges shallowly to the north. In rare situations the biotite alters completely to an orange colour on exposed surfaces, most likely due to relatively late-stage weathering. The plagioclase that is present has a dirty appearance due to sericitic alteration and is localized between semi-continuous bands of biotite in the micaceous schist (Figure 2.3E). Garnet within this unit ranges in size from 0.5 to 3 mm in diameter and sometimes occurs as sigma- and delta-type porphyroblasts (Figure 2.3F and 2.4A).

Marble layers are commonly subject to preferential weathering, aiding in their identification but creating a powdery texture that makes sampling virtually impossible. Marble directly overlies the graphitic marker unit in several outcrop locations and has a thickness on the order of 10-40 m.

Calc-silicate lithologies are composed of 50% carbonate + 40% quartz + 10% muscovite + 1-5% biotite. They have visible micaceous partings that define the foliation and locally are affected by a crenulation cleavage. These calc-silicate rocks contain pockets of fine-grained

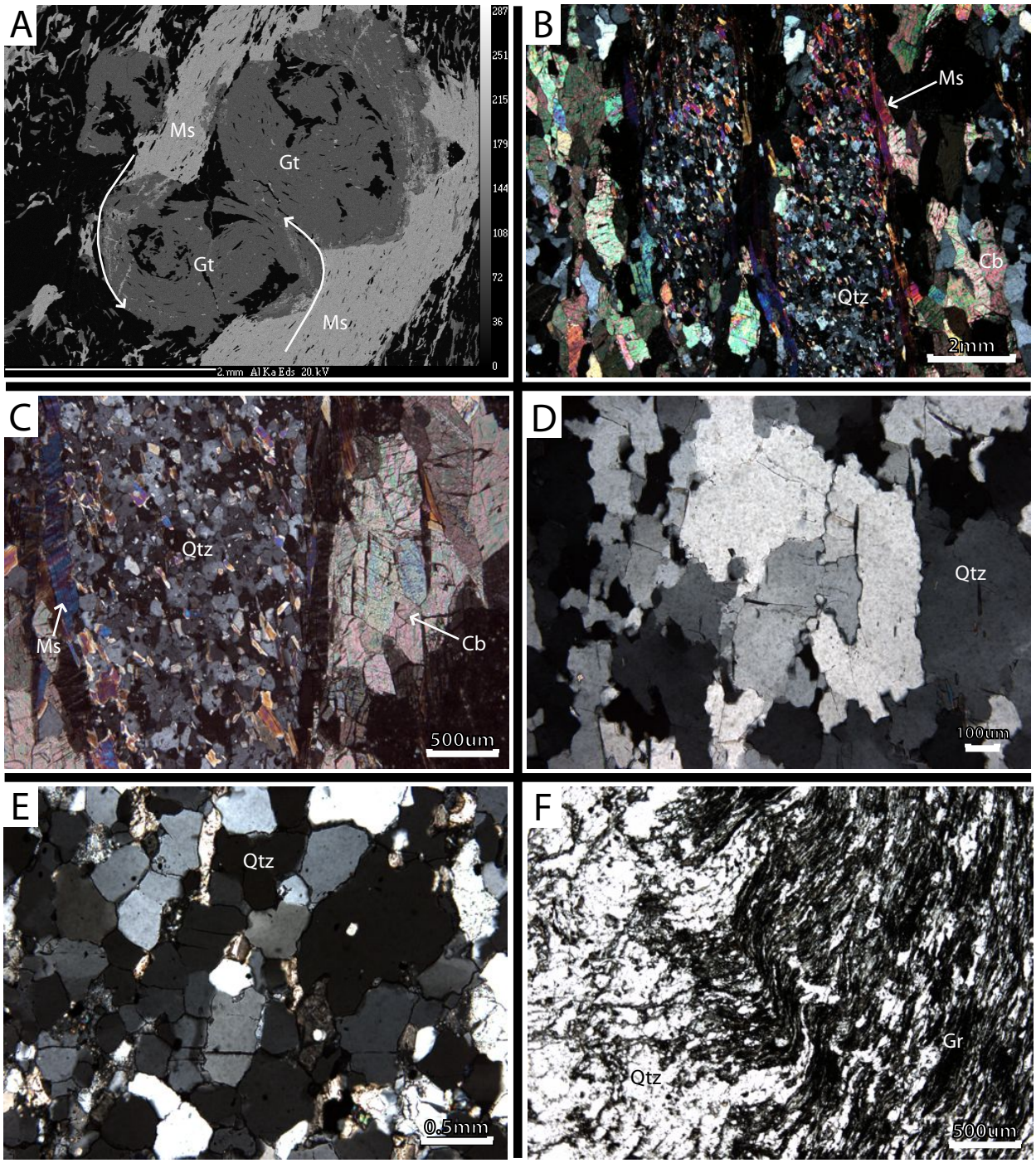

Figure 2.4 - Specimens from the Likhu Khola region. A) Delta-type garnet porphyroblast from structurally low part of the micaceous phyllitic schist unit (Al chemical map). B) Calc-silicate rock showing pockets of fine grained quartz (chert) rimmed with muscovite and ocurring within a coarser grained domain that is carbonate rich. C) Detailed view of a pocket of fine-grained quartz (chert) rimmed by muscovite and ocurring within a coarser grained fabric that is carbonate rich. D) Quartzite showing interlobate and irregular grain boundaries. E) Quartz-rich phyllite showing triple point junctions and polygonal texture indicative of post-deformational static "rebound" recrystallization. F) Graphitic schist showing the initial stages of crenulation cleavage development. Gt = garnet, Qtz = quartz, Gr = graphite, Ms = muscovite, Cb = carbonate

quartz aggregates rimmed by muscovite and partially surrounded by a coarser grained carbonate-rich fabric (Figure 2.4B and C).

Thin intercalations of quartzite lenses, mapped within the town of Those (Figure 2.1) are too small to depict at the scale of the map. Quartz grains in the quartzite have irregular and lobate grain boundaries with sweeping extinction (Figure 2.4D). These characteristics indicate that grain boundary migration is the dominant mechanism of recrystallization, which correlates to regime 3 of Hirth and Tullis (1992) and is associated with deformational temperatures of 500-700°C (Stipp et al., 2002).

Quartz throughout the rest of the unit is generally equigranular with minor sweeping extinction and polygonal triple point grain boundaries indicating static recrystallization due to the process of grain boundary area reduction (Figure 2.4E; Passchier and Trouw, 2005).

2.2.4 Graphitic schist

Contained within the micaceous phyllitic schist approximately 1000 m up-structural section from its lower contact is a 1500 to 2300 m thick unit of graphitic schist. It is easily identified and was observed in the same structural position in different locations within the mapped area. This graphitic unit is composed of 30-35% graphitic material + 30% quartz + 20% biotite + 15% muscovite + ~2% feldspar. The foliation is defined by micaceous partings of biotite and muscovite. No lineation was noted within this unit, however, a poorly developed crenulation cleavage is observed locally (Figure 2.4F). Rare quartz veins cross-cut the rock (up to 10% of rock by volume) and are characterized by dynamically recrystallized quartz that displays slightly irregular grain boundaries, inequigranular grain size distribution, undulose extinction and initial development of internal subgrain boundaries (Figure 2.5A). These textures indicate that dislocation glide and high temperature grain boundary migration recrystallization

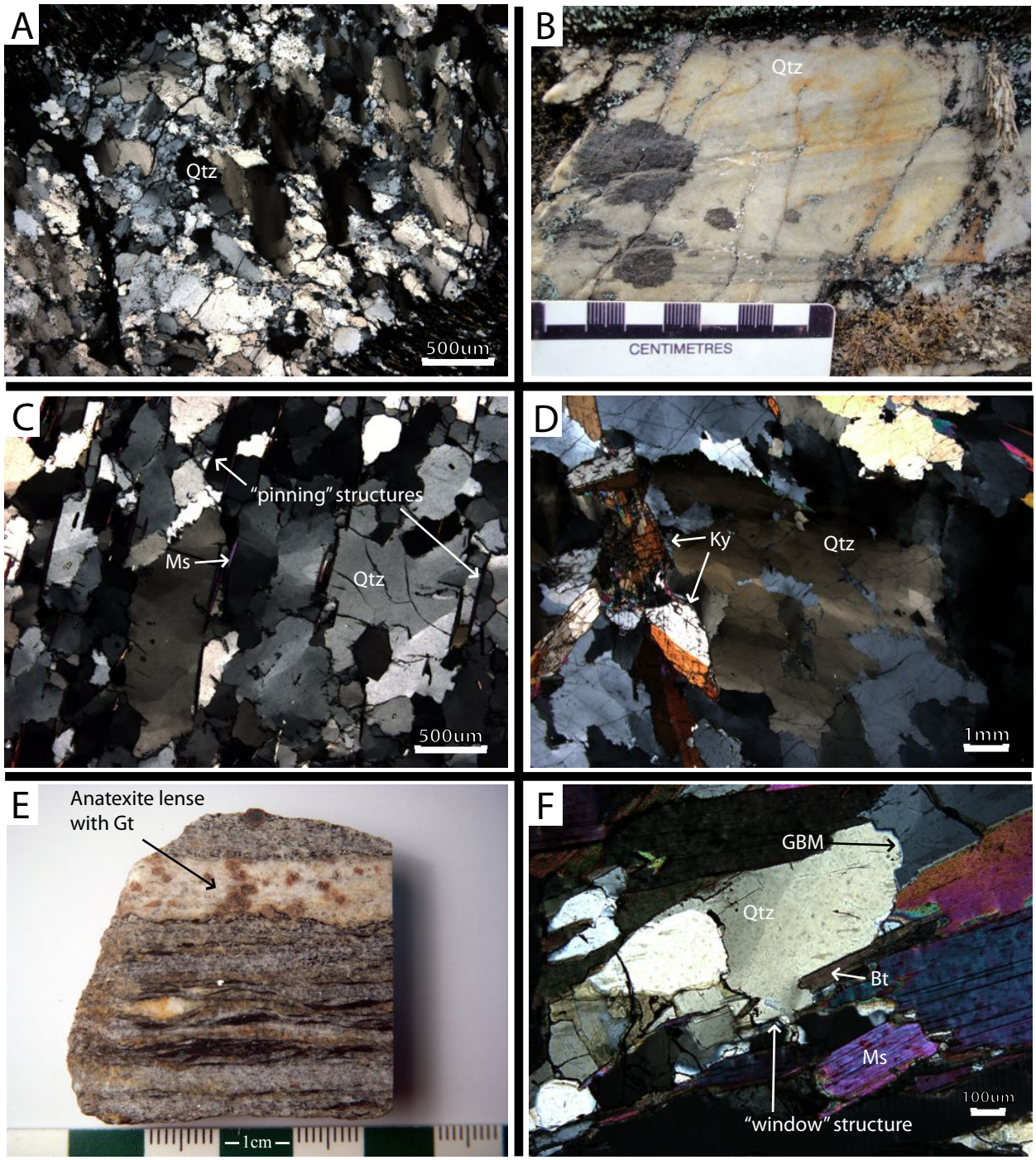

Figure 2.5 - Specimens from the Likhu Khola region. A) Quartz vein within graphitic schist showing inequigranular grain size and subgrain boundary development indicative of complete recrystallization. B) Quartzite with isoclinal folds. C) Quartzite showing irregular grain size and subgrain development in quartz grains and stretched muscovite grains. D) Anatexite specimen with kyanite showing irregular and interlobate quartz grain boundaries with well-developed subgrain boundaries. E) Pelitic schist showing large garnet porphyroblasts that are spatially related to the anatexite lenses. Rock slab is 4.4 cm wide. F) Quartz-rich schist displaying grain boundary migration (GBM) recrystallization and a "window structure" with the quartz grains growth being limited by biotite. In response, the recrystallizing quartz flows around the biotite grain. Qtz = quartz, Ms = muscovite, Ky = kyanite, Bt = biotite.

are the dominant deformation mechanisms recorded in the quartz veins. This corresponds with regime 3 of Hirth and Tullis (1992) and is associated with deformational temperatures of 500-700°C (Stipp et al., 2002).

2.2.5 Quartzite

Overlying the micaceous phyllitic schist is a ~400 m thick quartzite unit. The composition of the unit includes 95% quartz with 4% aligned muscovite ± 1% biotite ± 1% feldspar. The quartzite is inter-layered with quartz-dominated anatexite-bearing micaceous schist that is composed of 75% quartz + 10% feldspar + 10% muscovite + 5% biotite. The anatexite comprises 5-15% of total rock volume, is commonly boudinaged, and has the composition of 55% feldspar + 20-30% quartz + 10% mica + 5% tourmaline. The foliation in the quartzite is defined by muscovite and sparse biotite and is locally isoclinally folded (Figure 2.5B). Muscovite defines an aligned mineral lineation and is elongate plunging shallowly to the north. Relict primary sedimentary structures including cross bedding and poorly defined graded bedding were observed locally within thin laminations of quartzite intercalated with micaceous phyllitic schist.

The recrystallization textures displayed by the quartz in this unit include an inequigranular grain size distribution, interlobate grain boundaries and the development of internal subgrain boundaries. Pinning structures are observed where quartz growth is being limited by the presence of muscovite and rare biotite grains (Figure 2.5C). These textures are indicative of regime 3 of Hirth and Tullis (1992) and are associated with deformational temperatures of 500-700°C (Stipp et al., 2002).

2.2.6 Quartz + muscovite + feldspar + biotite ± garnet schist

The rocks structurally above the quartzite layer contain greater than 15% anatexite by volume. Overlying the quartzite is a quartz + muscovite + feldspar + biotite ± garnet pelitic to semi-pelitic schist which is the thickest unit in this study area, at ~10,200 m (Figure 2.2). The accessory minerals present in this unit include tourmaline, zircon, apatite, monazite and ilmenite. There is significant compositional variation within this unit, with the dominant pelitic to semi-pelitic schist interleaved with psammopelitic gneiss and local lenses of calc-silicate rocks. The composition of the dominant pelitic to semi-pelitic schist is 35-50% quartz + 10-25% feldspar + 15-30% muscovite + 15-20% biotite ± 5-10% garnet. Feldspar in the pelitic schist is locally perthitic. Anatexite comprises 15-25% of total rock volume within this unit and is composed of 50% quartz + 20% feldspar + 10-15% muscovite + 10% biotite ± 5-10% garnet ± 5% alumnosilicate. Kyanite occurs in the leucosome and immediate residuum towards the upper boundary of this unit (Figure 2.5D). Foliation in the schist is defined by semi-continuous partings of biotite that can contain inclusions of zircon. The biotite is locally altered to chlorite and clay minerals. The lineation is defined by elongate quartz grains that plunge shallowly to the north. The garnet in this unit is large (<2 x 2 mm) relative to other units and appears to be spatially associated with the anatexite lenses (Figure 2.5E).

The quartz within the micaceous schist exhibits inequigranular grain size distribution, interlobate grain boundaries, window structures and the development of internal subgrain boundaries (Figure 2.5F). These features are consistent with grain boundary migration and regime 3 of Hirth and Tullis (1992) and associated with deformational temperature estimates of 500-700°C (Stipp et al., 2002). Moreover, quartz within the kyanite bearing leucosome is generally coarse grained with an inequigranular grain size distribution, has interlobate to amoeboid grain boundaries and shows well-developed internal subgrain boundaries (Figure

2.5D). Following the criteria of Stipp et al. (2002) these characteristics are indicative of high-temperature grain boundary migration recrystallization (500-700°C) and classify within regime 3 of Hirth and Tullis (1992).

2.2.7 Alumnosilicate-bearing bearing migmatitic gneiss

The next structurally higher unit is a ~5000-7000 m thick alumnosilicate-bearing migmatitic gneiss. It is composed of 30-50% quartz + 10-30% feldspar + 15-25% biotite + 3-10% muscovite + 5-25% kyanite or sillimanite ± 5% garnet. The accessory minerals present in this unit include tourmaline, zircon, apatite, monazite and ilmenite. The appearance of kyanite in the paleosome, outside of association with anatexis (Figure 2.6A and B) marks the transition into this unit. Kyanite was indentified at two locations on opposite sides of the circuit traverse at similar structural levels (Figure 2.1). This kyanite-bearing migmatitic gneiss is characterized by a strongly developed tectonic lineation defined dominantly by kyanite and muscovite that plunges shallowly to the north. Linear features are dominant in the kyanite rich gneiss with no suitable planar features to take measurements.

Immediately up structural section kyanite is lost in favor of sillimanite. The sillimanite appears first as discrete mm-scale pods of fibrolite associated with biotite (Figure 2.6C) whereas farther up structural section the sillimanite occurs as microscopic, prismatic needles and discrete aggregates of needles termed “stringers” (Figure 2.6D and E). Sillimanite also occurs intergrown with quartz ± K-feldspar ± muscovite ± magnetite as ovoid nodules termed faserkiesel (Figure 2.6F). The long axes of these nodules are parallel to the north-south mineral lineation. The sillimanite in the paleosome can be seen growing at the expense of muscovite at the microscopic scale (Figure 2.7A and B). There are quartz-rich layers within this unit that contain large garnet porphyroblasts (<3.5 x 2.5 mm) whereas other parts of the unit contain much smaller garnet

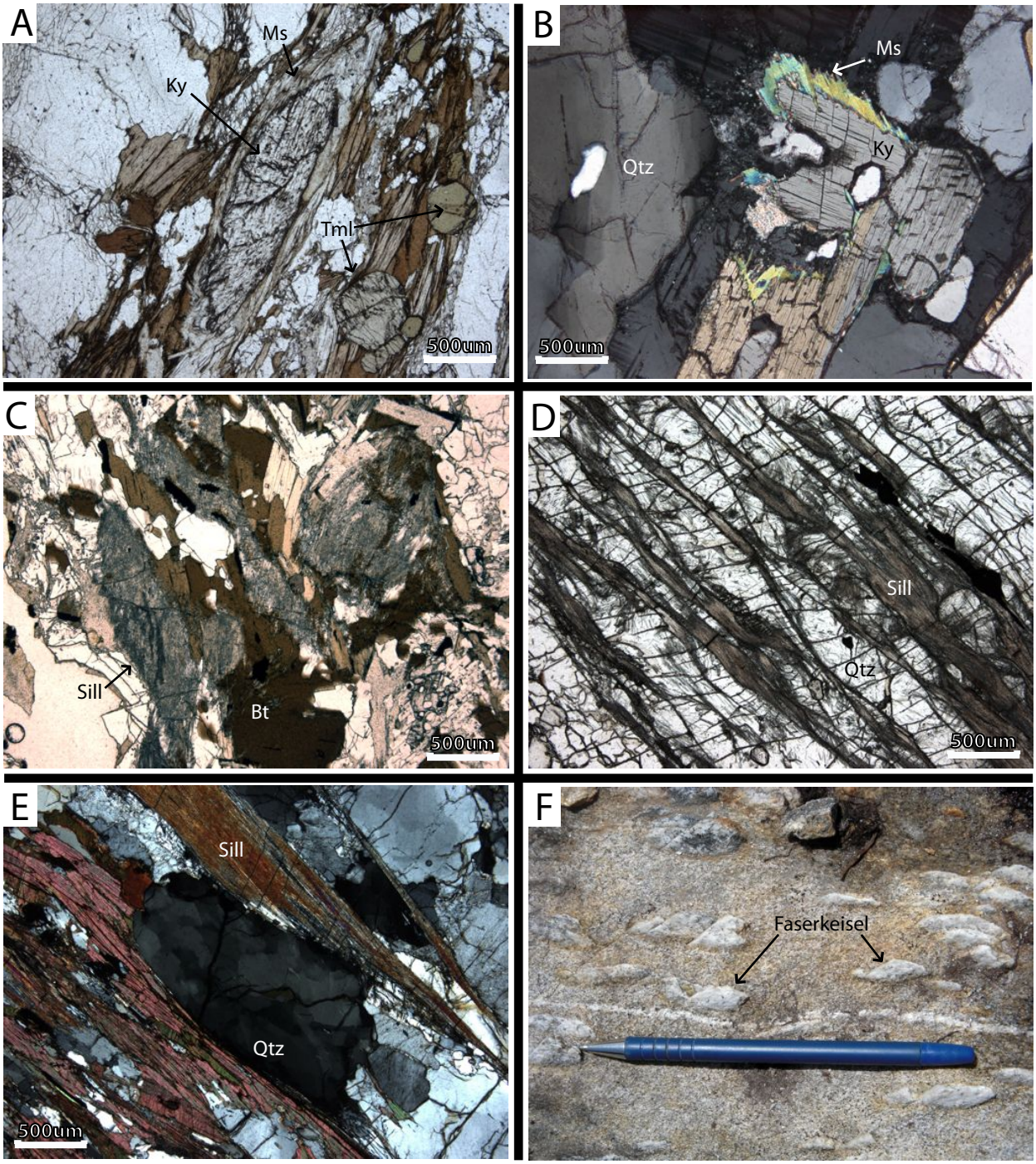

Figure 2.6 - Specimens from the Likhu Khola region. A) Kyanite-bearing gneiss showing kyanite rimmed by muscovite with tourmaline present nearby. B) Kyanite-bearing gneiss showing kyanite breaking down to muscovite. C) Sillimanite-bearing migmatitic gniess showing the sillimanite occuring as fibrolitic pods. D) Sillimanite-bearing gneiss showing the fibrolitic to prismatic sillamanite as sheared out stringers within small localised shear bands. E) Sillimanite-bearing gneiss showing prismatic needles of sillimanite and a quartz grain with well developed subgrain boundaries that can be referred to as “chessboard quartz” texture. F) Sillimanite-bearing gneiss showing sillimanite and quartz (± K-feldspar ± muscovite ± magnetite) intergrowths known as faserkiesel. Ky = kyanite, Ms = muscovite, Tml = tourmaline, Qtz = quartz, Sill = sillimanite, Bt = biotite. The pen for scale is 14.2 cm in length.

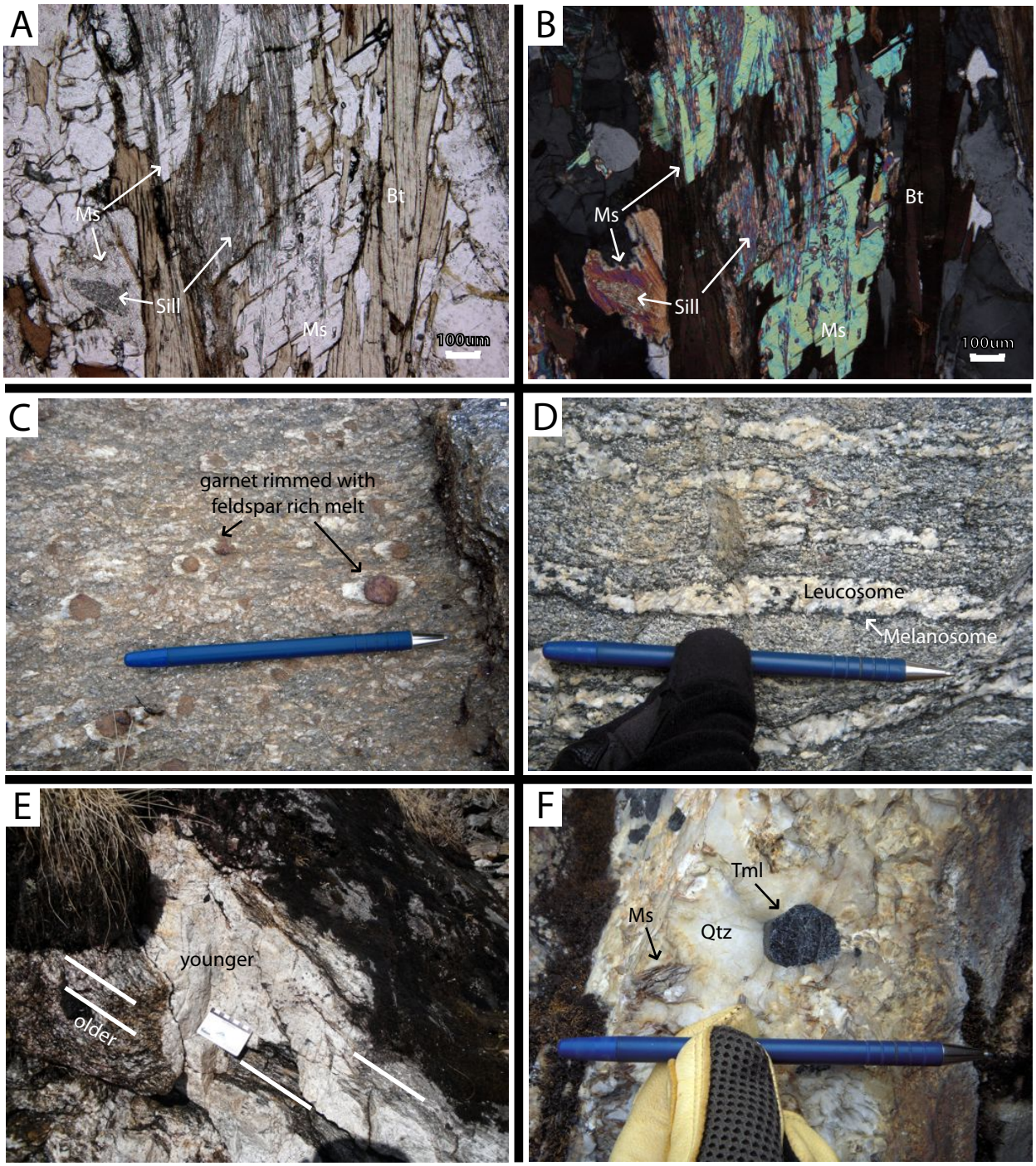

Figure 2.7 - Specimens from the Likhu Khola region. A) Sillimanite-bearing gneiss showing sillimanite growing inside and at the expense of muscovite. B) Equivalent to A, in XPL. C) Garnet with rims of quartz + feldspar melt that has collected in the strain shadows of the garnet. D) Psammopelitic gneiss showing a quartz + feldspar dominated leucosome and biotite-rich residuum. E) Psammopelitic gneiss with foliationplanes highlighted showing the cross-cutting nature of the younger anatexite phase. F) A cross-cutting pod of the younger anatexite composed of quartz + feldspar + biotite + muscovites (books) + tourmaline. Qtz = quartz, Tml = tourmaline, Ms = muscovite, Sill = silllimanite, Bt = biotite. The pen for scale is 14.2 cm in length; the scale card is 9 cm across in total.

porphyroblasts (<0.13 x 0.13 mm). Large garnet porphyroblasts were also observed with rims of feldspar-rich anatexite present in the strain shadows (Figure 2.7C). The sillimanite-bearing migmatitic gneiss gradually becomes more psammopelitic in nature up structural section; anatectic lenses and the micaceous minerals become increasingly segregated, defining the foliation. There are two distinct phases of anatexite at higher structural levels, which together comprise up to 45% of the total rock volume. One phase of the anatexite occurs as foliation parallel leucosomes with associated biotite-rich residuum (Figure 2.7D) whereas a second, younger pegmatitic phase cross-cuts both the foliation and the lit-par-lit anatexite (Figure 2.7E). The feldspar throughout this unit is locally altered to sericite.

The quartz within the migmatitic gneiss exhibits an inequigranular grain size distribution, interlobate to amoeboid grain boundaries and development of internal subgrain boundaries including "chessboard quartz" (Figure 2.6E; Passchier and Trouw, 2005). These recrystallization textures are indicative of high-temperature grain boundary migration recrystallization and dislocation glide both characteristic of regime 3 of Hirth and Tullis (1992) and associated with deformational temperatures of 500-700°C (Stipp et al., 2002). The chessboard extinction has been correlated to activation of the prism <c> glide plane (Passchier and Trouw, 2005), which occurs toward the upper end of the Stipp et al. (2002) temperature range (Law et al., 2004).

2.2.8 Sillimanite-bearing migmatite

Overlying the alumnosilicate bearing migmatitic gneiss is a 2800 m thick unit of sillimanite bearing migmatite. It is composed of 35-45% quartz + 10-35% feldspar + 10-25% biotite + 1-5% muscovite + 10-15% sillimanite + 2-10% garnet. This unit contains more than 45% stratiform anatexite by volume which itself is composed of 50% quartz + 45% feldspar + 5% biotite. The younger phase of pegmatitic anatexite is also present locally and is composed of

40% quartz + 35% feldspar + 10% biotite + 10% muscovite (in the form of books) ± 5-10% tourmaline (Figure 2.7F). The well-developed gneissosity in this unit (Figure 2.8A) is defined by quartz, biotite, sillimanite and leucosome layers. Sillimanite commonly defines a mineral alignment lineation that plunges shallowly to the north.

Quartz recrystallization textures observed in this migmatite are similar to those in the structurally subjacent unit. The "chessboard quartz", however, occurs more commonly and is better developed (Figure 2.8B). The dominant recrystallization mechanism is therefore inferred to be dislocation glide and is associated with deformational temperatures of 500-700°C (Stipp et al., 2002).

2.2.9 Augen Orthogneiss

An augen orthogneiss unit with distinct 10-15 cm k-feldspar augen overlies the sillimanite-bearing migmatite. The thickness of this unit is unknown as it continues northeastward out of the study area. In the adjacent Tama Kosi region, however, it is 1.5-2 km thick (Larson, 2012). The augen orthogneiss was seen only as float around Gyajo La at the northern most portion of the study area. It must have been sourced from the peaks adjacent to Gyajo La Pass and therefore must occur at structurally higher levels than the pass itself.

2.3 Structural observations

2.3.1 Field Observations

The rocks exposed in the mapped area have all been pervasively, ductily deformed and possess a well-developed tectonic foliation. The orientations of measured foliation planes show considerable variation and sub-horizontal to gentle dips throughout the structurally lower portion of the study area in the micaceous, graphitic and quartz-rich phyllitic schist units

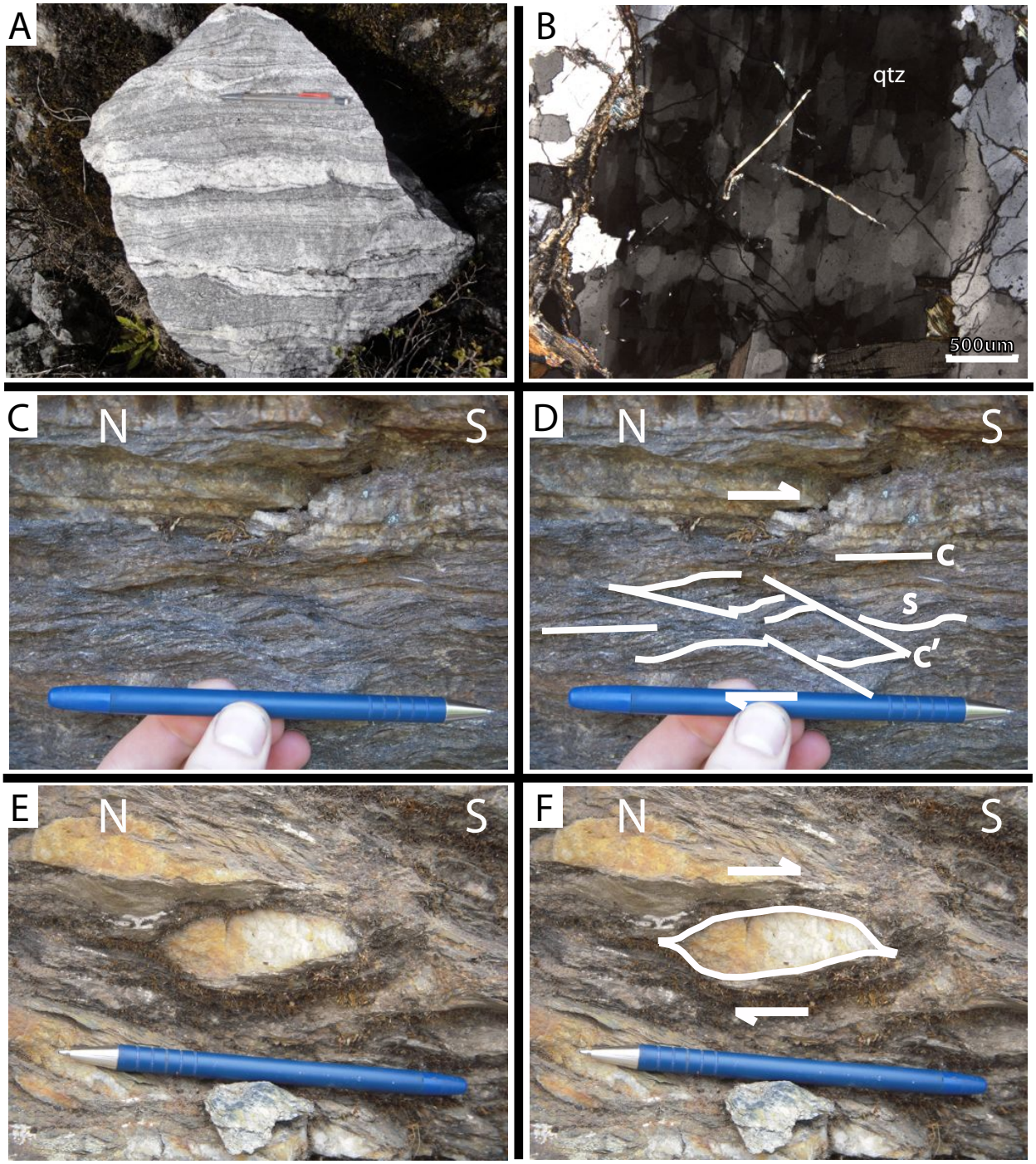

Figure 2.8 - Specimens from the Likhu Khola region. A) Well-segregated psammopelitic gneiss. B) Sillimanite-bearing gneiss showing diagnostic subgrain structure development in quartz termed "chess-board quartz" texture. This is indicative of high-grade recrystallization conditions (500-700°C). C) S and C' fabric within a micaceous phyllitic schist from a structurally low region of the map area.. D) S and C' fabric within a micaceous phyllitic schist from a structurally low region of the map area showing top-to-the-south shear sense. E) Mineral fish within a garnet-bearing micaceous phylllitic schist from a structurally low region of the map area. F) Mineral fish within a garnet-bearing micaceous phylllitic schist from a structurally low region of the map area showing top-to-the-south shear sense. Qtz = quartz, Bt = biotite. The pen for scale is 14.2 cm in length.

(Figure 2.9A). Up structural section the foliation planes moderately dip more consistently towards the north and northeast (Figure 2.9B). The tectonic foliation throughout the micaceous phyllitic schist unit commonly contains mineral elongation lineations defined by aligned biotite, muscovite, and locally, chlorite grains. Moreover, plastically deformed quartz defines the stretching lineation in the augen orthogneiss below the graphitic marker unit. Northwards, and structurally up section, mineral lineations are better developed. Plastically deformed quartz, as well as aligned micaceous and alumnosilicate, minerals define the lineation at these higher structural levels. These lineations generally trend north-northeast with a shallow to moderate plunge (Figure 2.9C). A variably developed crenulation cleavage occurs in some of the lower structural units. It is best developed in the graphitic schist and quartz-rich phyllitic schist. The trend of fold axes associated with the crenulation cleavage is variable but seems to be consistently NW-SE (Figure 2.9C)

Asymmetric secondary foliation planes including S and C' fabrics were identified in many of the quartz and mica-rich units. The geometry of these secondary foliation planes consistently indicates a top-to-the-south sense of shear (Figure 2.8C and D). Other shear sense indicators observed in outcrop include sigma-type clasts with geometry consistent with a top-to-the-south sense of shear (Figure 2.8E and F). Similar deformational features are observed at the microstructural scale (Figure 2.10A to D) and further support pervasive top-to-the-south shear sense throughout the entire section studied.

Small-scale isoclinal folding (1 cm to 1 m) is recorded in the quartzite unit with an axial plane and fold limbs parallel to the dominant tectonic foliation. Folding on a regional scale (100 m to >1 km) was observed in more southern units that underlie the quartzite layer. This folding is most evident in the rock units just east of Dolu (Figure 2.1) where the foliations on the north and

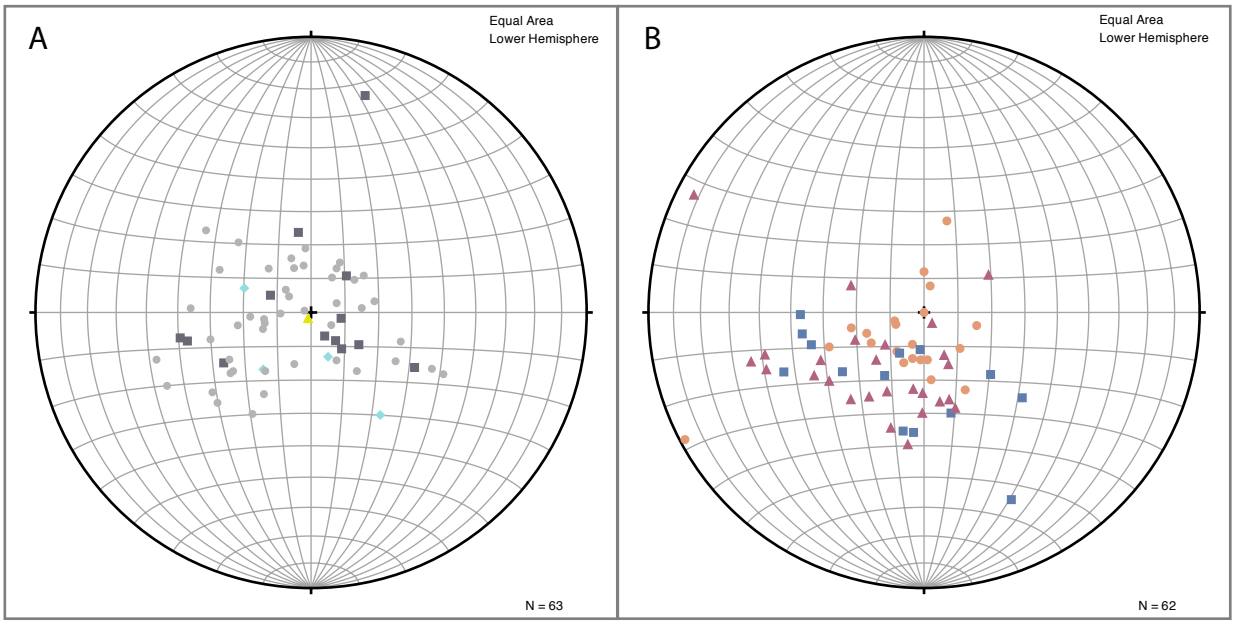

Foliation of lower units (plotted as poles)

Foliation of upper units (plotted as poles)

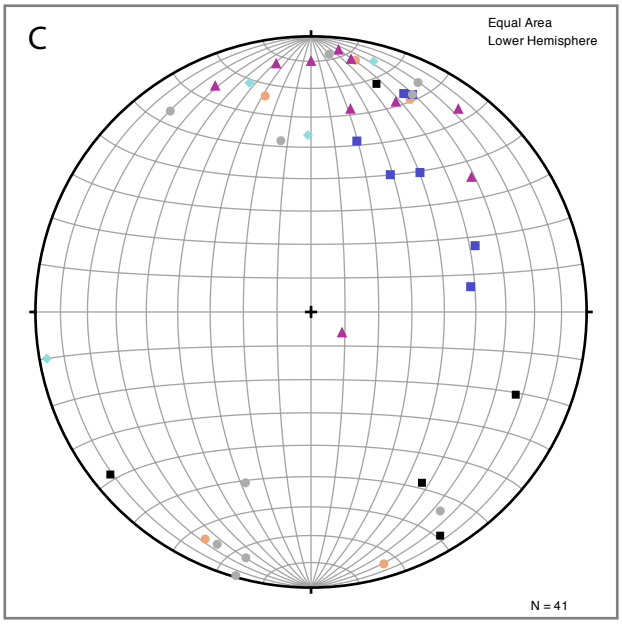

Lineation of all units

Legend

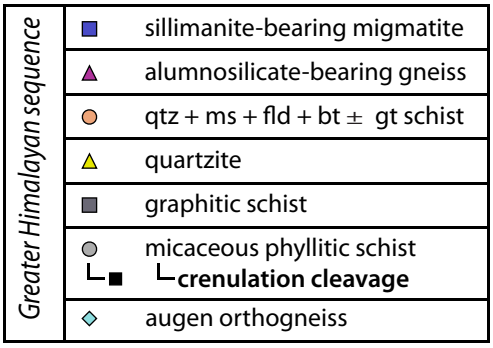

Figure 2.9 - Sterographic projection plots of the foliation and lineation mesurements from the Likhu Khola study area. Foliations are plotted as poles to the planes. A) Foliation measurements from the lower units structurally below (and including) the quartzite unit. B) Foliation measurements of the upper units structurally above the quartzite unit. The grouping here is slightly tigher and more consistently dipping towards the north and northeast compared to the structurally lower units. C) Lineation measurements from all units in the study area that show a general north-northeast trend with shallow to moderate plunge.

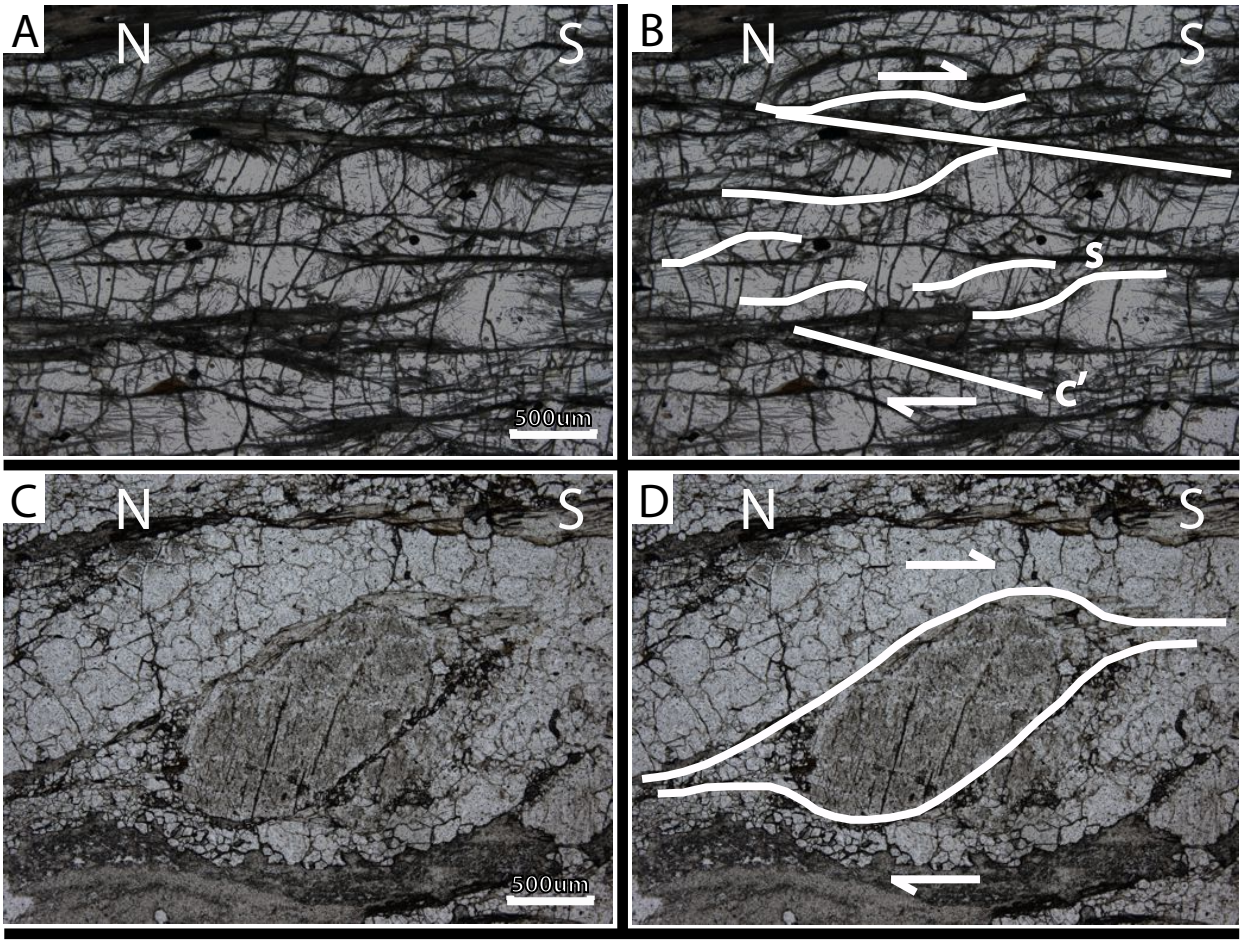

Figure 2.10 - Photomicrographs in plane polarized light of specimens from the Likhu Khola region. A) Sillimanite-bearing gneiss showing localised micro-shear bands. B) Sillimanite-bearing gneiss high-lighting localised micro-shear bands with S and C‘ fabrics that indicate top-to-the-south and dextral shear sense. C) Sillimanite-bearing gneiss showing an asymmetric mantled clast of feldspar surrounded by quartz. D) Sillimanite-bearing gneiss highlighting an asymmetric mantled clast of feldspar surrounded by quartz that indicates top-to-the-south and dextral shear sense.

south sides of a ridge dip in opposite directions (Figure 2.2). This regional folding has an open geometry and postdates the development of the pervasive foliation and associated top to the south deformation in these units. The observed crenulation cleavage is probably related to this deformation phase. Large-scale folding has also been recognized in the Tama Kosi valley to the west where a structural window has been interpreted to reflect interference folding of separate regional events with perpendicular vertical planes (Ishida and Ohta, 1973). All station and structural data can be found in APPENDIX A.

2.3.2 Quartz lattice preferred orientation (LPO) analyses

The lattice-preferred orientation (LPO) of quartz can be used to determine the dominant slip planes that were active during dynamic recrystallization, verify the sense of shear, and estimate temperatures of deformation (e.g., Law, 1991; Passchier and Trouw, 2005). Quartz LPO analysis techniques have been employed successfully throughout the Himalaya (e.g., Bouchez and Pêcher, 1976; Grasemann et al., 1999; Law et al., 2004; Larson and Godin, 2009; Larson et al., 2010a; Langille et al., 2010; Yakymchuk and Godin, 2012). As described in Yakymchuk and Godin (2012):

> The slip systems active in quartz are dependent upon deformation temperature, strain rate (Lister et al., 1978), and water content (Mainprice and Nicolas, 1989). Assuming that the glide system is dominantly controlled by temperature, quartz *c*-axis fabrics can act as a thermometer during deformation (Kruhl, 1998; Law et al., 2004). The opening angle of *c*-axes girdles in quartz fabrics has been experimentally (Tullis et al., 1973), numerically (Lister and Hobbs, 1980), and empirically (Kruhl, 1998; Law et al., 2004) calibrated with temperature during deformation. The opening angle of quartz *c*-axes girdles increases linearly with

temperature up to 650°C (Kruhl, 1998) and more rapidly from 650 to 800°C likely reflecting the low-high quartz transition and the increasing influence of prism <*c*> slip (Law et al., 2004). Deformation temperature has been calculated using the opening angles of *c*-axis girdles along the Himalayan front in central Nepal (Law et al., 2004; Larson and Godin, 2009; Larson et al., 2010a) and in the North Himalayan gneiss domes (Larson et al., 2010b; Langille et al., 2010). Opening angles are determined visually by measuring the angle between the two opposing arms of the fabric skeleton, which follows the region of the highest concentration of quartz *c*-axes. The accuracy of the opening angle is limited by the sharpness of the skeleton arms. Calibration of the opening angle 'thermometer' is based on empirical data and deformation temperatures are therefore assigned an error of ± 50°C (Law et al., 2004).

Quartz LPOs in this study were measured using a G50 automated fabric analyzer fabricated by Russell-Head Instruments in Australia (e.g., Peternell et al., 2010). All thin sections analyzed were cut perpendicular to the dominant foliation and parallel to lineation. The plane of projection for all equal area stereonets is setup looking west with a sinistral sense of shear representing a top to the south sense of shear. The specimen foliation lies vertically along the east-west axis while the lineation lies horizontal along the same axis.

Specimen 083 is a quartzite from the structurally lowest part of the study area immediately above the augen orthogneiss (Figure 2.11A). The quartz yields a single girdle LPO pattern with an asymmetry indicating top-to-the-south sense of shear (Figure 2.11B). The LPO appears to be dominated by glide along the rhomb crystal orientations.

Specimen 032 is a quartz rich schist collected just below the distinctive quartzite unit in the micaceous phyllitic schist (Figure 2.11A). The quartz LPO pattern yielded a type-II cross girdle pattern with a measurable opening angle that can be used to estimate temperature of

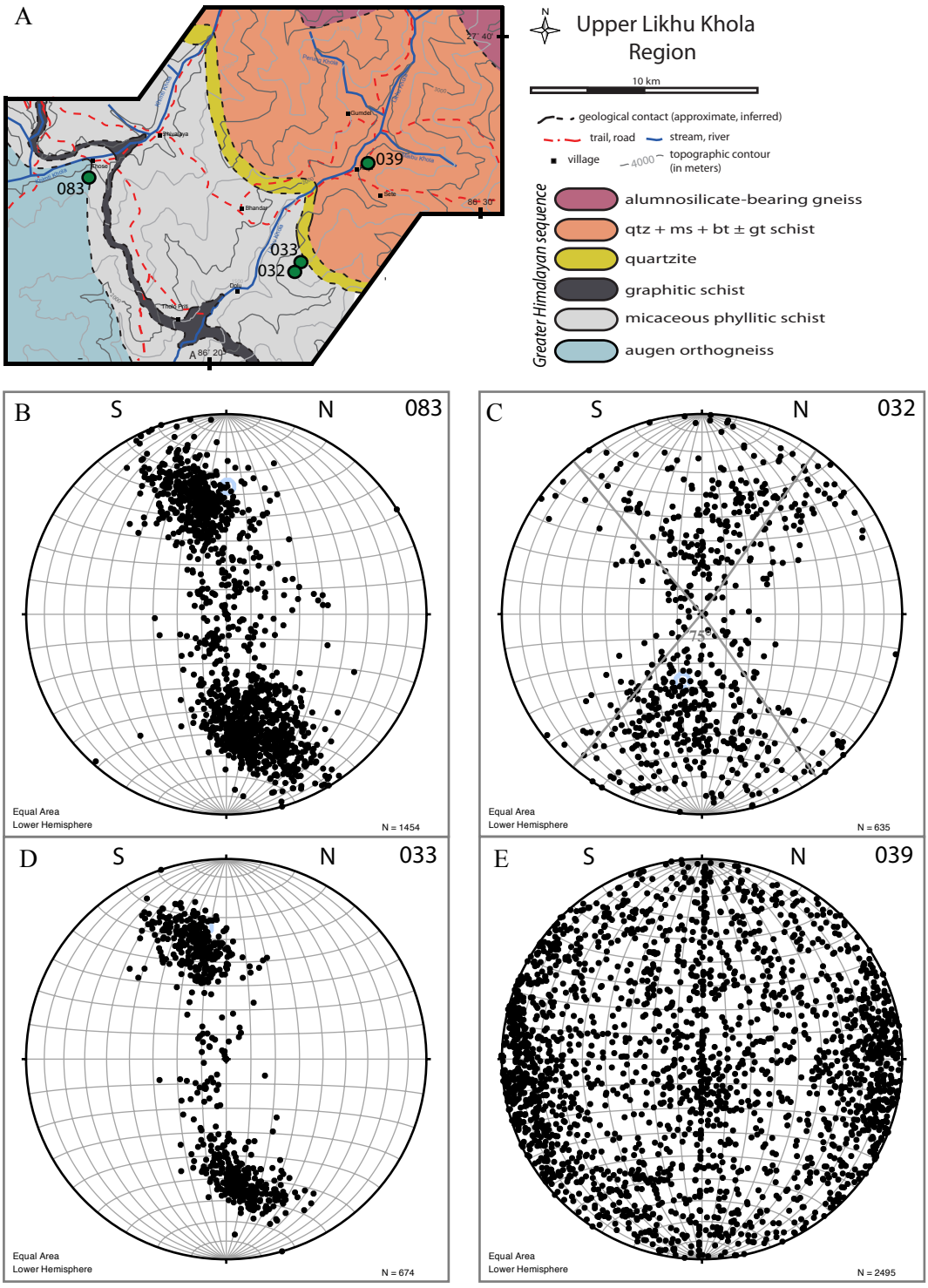

Figure 2.11 - Stereographic projections of quartz *c*-axis lattice preferred orientations of specimens from the Likhu Khola study area. A) Simplified Geologic map of the study area highlighting the sample locations. B) Quartzite specimen 083 exhibits top-to-the-south shear sense. C) Quartz-rich specimen 032 exhibits a distinctive type-1 crossed girdle pattern from which an opening angle of 75° is measured and a deformational temperature estimate derived. D) Quartzite specimens 033 exhibits top-to-the-south shear sense. E) Specimen 039 exhibits concentrations of LPOs along the lnorth and south rims of the stereonet indicating the activation of prism <*c*> slip in quartz.

deformation (Figure 2.11D). Based on an opening angle of ~75° the estimated temperature is 600 ± 50°C (Figure 2.12), which is consistent with deformational temperature estimates from quartz recrystallization textures for the same unit.

Specimen 033 is a quartzite collected from the distinctive quartzite unit in the micaceous phyllitic schist. The well-defined single girdle pattern is very similar to that of specimen 083 (Figure 2.11C). It too displays a sinistral asymmetry and therefore indicates top-to-the-south shear sense. Moreover, like specimen 083, slip is dominated by glide along the rhomb planes.

Specimen 039 is a quartz rich schist collected above the distinctive quartzite layer and does not yield a well-defined LPO pattern. It can, however, provide some information on the different slip systems that may have been operating in those rocks. The quartz LPO pattern shows concentrations of quartz *c*-axes near the east and west poles of the stereonet (Figure 2.11E). This pattern represents activation of prism [*c*] slip in quartz which generally initiates near temperatures of ~650˚C (Law et al., 2004).

All other specimens analyzed up-structural section from the distinctive quartzite unit yielded incoherent LPO patterns. However, there was consistent congregations of quartz *c*-axes near the east and west poles of the stereonet similar to specimen 039 indicating that prism [*c*] slip in quartz was activated and deformational temperatures were in excess of ~650˚C (Law et al., 2004).

2.4 Metamorphic observations

As previously mentioned, evidence for a classic Himalayan inverted metamorphic sequence (e.g., Mallet, 1874; von Loczy, 1878; Oldham, 1883) was observed in this study area. Starting with upper greenschist facies rocks in the structurally lowest unit of micaceous phyllitic schist, the metamorphic grade increases up structural section to upper sillimanite facies

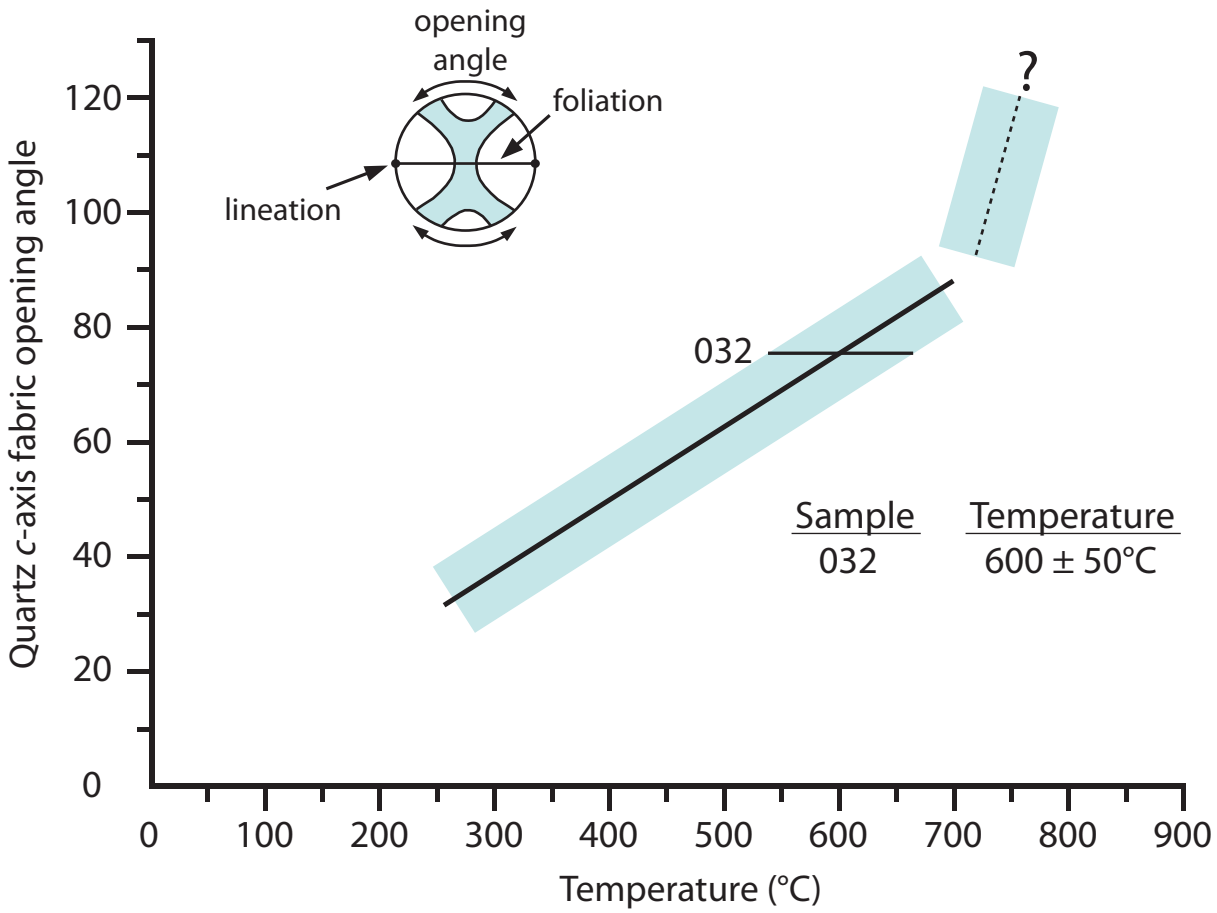

Figure 2.12 - Graph of quartz *c*-axis fabric opening angles plotted against experimentally calibrated estimates of deformation temperatures. Specimen 032 from the Likhu Khola study area has a measured opening angle of 75° that correlates to a deformational temperature of 600 ± 50°C. Modified after Law et al. (2004).

migmatitic rocks at the highest structural position reached in this study. The distribution of indicator minerals confirms the general increase in recorded metamorphism northward and up structural section (Figure 2.2). Upper greenschist facies rocks have a typical assemblage of biotite + muscovite ± chlorite as seen near the town of Tholo Priti (Figure 2.1). Garnet is first observed as part of this assemblage just above the graphitic marker unit in this map area, however, previous mapping in this region indicates that the first appearance of garnet may occur farther down structural section to the south of the study area (Ishida, 1969). A few kilometers above the graphitic schist market unit chlorite is no longer observed and the metamorphic assemblage here includes biotite + muscovite + garnet. Staurolite is not observed in the map area, though it does occur in a thin portion of the exhumed metamorphic core in adjacent areas (Larson, 2012). It is possible that it was not observed in the study region due to a bulk composition of the rocks non-conducive to its growth or lack of outcrop exposure. Kyanite occurs in an narrow range of exposure, first appearing within stratiform anatexite and then as part of the unaffected paleosome. This first occurrence of kyanite was mapped just south of the village Kangematar where the Likhu Khola meets the Nupche Khola (Figure 2.1). Sillimanite first appears in association with anatexite approximately 1900 m to the north along the Likhu Khola and then as part of the paleosome assemblage in immediately adjacent rocks. Kyanite and Sillimanite are observed to coexist in at least one rock specimen (048). There was no evidence to indicate that sillimanite is forming directly from kyanite, therefore two separate reactions of kyanite + quartz + K^+ + fluid = muscovite + H^+ and muscovite + H^+ = sillimanite + quartz + K^+ + fluid were taking place simultaneously in different domains of the rock (Carmichael, 1969). Sillimanite remains a constituent of the metamorphic assemblage northward until Gyajo La at the most northern, and structurally highest, point reached in the study area. Importantly, minor

amounts of muscovite remains (1-4%) in the rock up to the structurally highest point in the study area.

2.5 Crustal Melting

There are two distinct phases of anatexite within this region. The older phase occurs as quartz-rich boudins at lower structural levels and becomes more abundant and lit-par-lit in character, associated with residuum, at higher structural levels (Figure 2.7D). This phase of anatexite comprises approximately 1-15% of total rock volume at low structural levels with an increase up-structural section from 15-55% of total rock volume beginning to markedly increase above the distinctive quartzite layer mapped between Bhandar and Kenja (Figure 2.1). The anatexite is typically fine to medium grained with a general composition of 30-50% quartz + 30-45% feldspar + 10% muscovite ± 5-10% biotite ± 5-15% alumnosilicate.

The younger anatexite phase predominantly occurs as undeformed pods that cross-cut both the country rock and the stratiform anatexite. This phase is typically coarse grained to pegmatitic with a general composition of 40% quartz + 35% feldspar + 10% biotite + 10% muscovite (books) ± 5-10% tourmaline (Figure 2.7F). In localized occurrences this younger anatexite is partially deformed indicating it is very late-to-post tectonic.

2.6 Discussion

No discrete thrust faults or localized high strain zones were observed in the study area; there is evidence of pervasive ductile strain throughout the study area. The metamorphism and deformation recorded in these rocks are interpreted to indicate that the rocks in the study area represent the exhumed metamorphic core of the orogen, the GHS, in the hanging wall of the Main Central thrust. This interpretation differs from that of Ishida (1968) who mapped the rocks

in this area as several “formations”, each separated by a thrust fault. This also differs from the interpretations of Schelling (1992) who mapped the Main Central thrust through this study area just above the phyllitic schist unit (Figure 2.13).

The observed shear sense recorded in outcrop and at the microscopic scale indicates top-to-the-south sense deformation throughout the entire section studied. This is consistent with the shear sense commonly observed throughout the Himalaya at similar structural levels within GHS rocks in the hanging wall of the Main Central thrust (e.g., Heim and Gansser, 1939; Lefort, 1975; Burchfiel and Royden, 1985). The general north-northeast trend of lineations in the study area (Figure 2.9) indicates tectonic transport directions to the south and southwest. This is consistent with fabrics observed in other areas of Nepal (e.g., Larson and Godin, 2009)

Temperatures of deformation were estimated using, (1) quartz recrystallization textures and, (2) quartz LPO patterns. The quartz recrystallization textures indicate that high-temperature grain boundary migration (GBM) was the dominant mechanism of recrystallization across the study area. As noted above grain boundary migration recrystallization is consistent with regime 3 of Hirth and Tullis (1992) and associated with deformational temperatures of 500-700°C (Stipp et al., 2002). This is consistent with pervasive ductile shearing throughout the study area and all rocks belonging to GHS. Quartz recrystallization textures indicate a general increase in deformational temperatures up structural section. Rocks at lower structural positions exhibit slightly irregular grain boundaries, inequigranular grain size distribution, undulose extinction and initial development of internal subgrain boundaries indicative of deformational temperatures at the lower end of the 500-700°C range for regime 3 of Hirth and Tullis (1992). While closer to the top of the structural section in this study area the quartz exhibits distinct subgrain boundaries with “chessboard” quartz texture. This specific texture indicates deformation temperatures

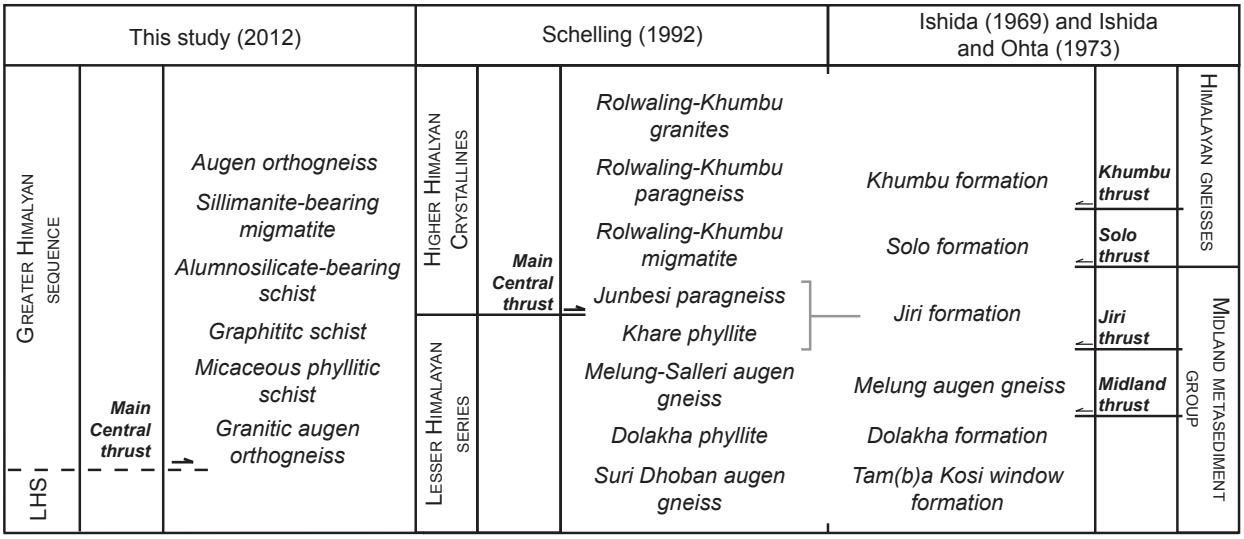

Figure 2.13 - Lithotectonic correlations between previous studies that have examined a portion of the Likhu Khola study area. Modified after Larson (2012). LHS = Lesser Himalayan sequence

greater than ~630°C (Stipp et al., 2002) or ranging between 650 and 750°C (Lister and Dornsiepen, 1982; Mainprice et al., 1986). The deformational temperatures indicated by quartz LPO patterns also appear to increase up-structural section with the disappearance of coherent cross-girdle patterns and the activation of prism <*c*> slip above the distinctive quartzite layer which generally initiates near temperatures of ~650˚C (Law et al., 2004). Moreover, quartz LPO patterns derived from quartzite specimens confirm other observations of top-to-the-south shear sense. The apparent deformation temperature gradient parallels the observed inverted metamorphic field gradient and indicates a contemporary relationship between deformation and metamorphism.

The first appearance of the alumnosilicates kyanite and sillimanite occur in association with anatectic pods before they are observed within the unaffected paleosome. Kyanite's initial appearance in anatexite indicates that either the anatexite formed under kyanite-grade conditions or that it was introduced and later metamorphosed to kyanite grade. In either case, the country rock may not have grown kyanite because, in contrast to the partial melt, it might not have had the free aluminum required to form it. Sillimanite's first appearance is also associated with anatexite. The surrounding country rock, however, contained kyanite. This is consistent with the interpretation that the alumnosilicate-bearing anatexite crystallizes directly at either kyanite or sillimanite grade rather than being taken to higher metamorphic conditions post-crystallization. This indicates that the anatexite was either emplaced by injection at slightly higher grade conditions or that the composition of in-situ anatexite was able to crystallize the alumnosilicate minerals at the current P-T conditions.

The sillimanite + quartz ± muscovite ± K-feldspar ± magnetite intergrowths occurring as nodules (faserkiesel) are observed at high structural levels in the study area. The formation of a

faserkiesel texture is believed to be controlled by a preferential composition of metasedimentary rocks although their origin is still considered enigmatic. Tippett (1984) suggested that the presence of faserkiesel indicates the former presence of a stable K-feldspar + sillimanite assemblage that has been subjected to retrograde metamorphism involving paired ionic equilibria. However, the preferential alignment of the faserkiesel with the regional foliation indicates that the formation of these intergrowth nodules must have been pre-to syn-tectonic consistent with their formation early in the protracted metamorphic history of the mid-crust.

Although the variations throughout the lithological units described above are interpreted to be reflections of the protoliths of metasedimentary rocks it is possible that the thickness of some units and potential duplication of similar units could be achieved through folding or ductile duplex formation. The absence of a repetition of the graphitic marker bed, however, argues against significant structural duplication. Outcrop-scale isoclinal folding with an associated horizontal fold axial plane was observed in the intercalated micaceous schist and within the quartzite layer (Figure 2.5B) so although large-scale duplication is unlikely, smaller scale duplication certainly occurs. This recumbent folding is typical of high-grade metamorphic zones and is consistent with vertical thinning and horizontal extension (Price, 1972; Larson et al., 2010a).

In the adjacent Tama Kosi valley to the west, Larson (2012) proposes a boundary between differing structural styles of extending flow (extension in the direction of flow) in the upper portion of the GHS and compressing flow (shortening in the direction of flow) in the lower portion of the GHS (e.g., Larson et al., 2010; Yakymchuk and Godin, 2012). The transition between these two distinct flow types would correspond approximately with the distinctive quartzite layer if extrapolated into the current study area. This quartzite layer could potentially

represent a similar boundary between these different flow types. The following chapter will assess the presence or absence of this lithologic and structural boundary in the study area and use detailed analytical data derived from the GHS to assess the validity of the different models proposed for its evolution.

CHAPTER 3

MINERAL CHEMISTRY, GEOTHERMOBAROMETRY AND U-TH-PB GEOCHRONOLOGY OF ROCKS IN THE LIKHU KHOLA REGION, EAST CENTRAL NEPAL

3.1 Introduction

The evolution of the mid-crustal core of the Himalayan orogen, the Greater Himalayan sequence (GHS), is currently one of the most contentious issues in Himalayan geologic research. Debate over which of the different models currently proposed for the evolution of the Himalaya, such as critical taper wedge (e.g., Kohn, 2008) and extrusion of a ductile mid-crust termed "channel flow" (Beaumont et al., 2001; Grujic et al., 2002; Beaumont et al., 2004; Jamieson et al., 2004, 2006; Jamieson & Beaumont, 2011) best describes or explains the geologic data is on going (e.g., Grujic, 2006; Harrison, 2006; Harris, 2007; Kohn, 2008; Larson et al., 2011; Corrie et al., 2012). Moreover, the models of Larson et al. (2010a) and Yakymchuk and Godin (2012) predict a combination of the two separated by a discontinuity. The majority of the data incorporated into the evolutionary models proposed have largely been extracted from the GHS. Detailed study of the GHS in the Likhu Khola region of east-central Nepal (Figure 1.1) has been undertaken in order to compare and contrast the viability of these models (see section 1.2.3 of this thesis for an overview of the models)

As outlined by Gervais and Brown (2011) critical taper wedge models predict an increase in temperature and pressure up structural section with short crustal residence times at high temperatures, syn-kinematic metamorphism and systematically younger timing of exhumation towards the foreland involving discrete ductile to brittle thrusts that may induce stratigraphic

repetition. In contrast, mid-crustal channel flow models predict protracted crustal residence times at high temperatures and broadly synchronous exhumation that is coeval with burial of footwall material. In this chapter, the GHS in the study area is divided into metamorphic zones, garnet chemistry and zonation is determined and metamorphic pressure-temperature (P-T) estimates are made to evaluate any possible metamorphic and structural discontinuities across this section of the GHS. In situ monazite geochronology with concomitant trace element data is incorporated with both the metamorphic and structural data to constrain the timing of deformation and metamorphism. The time-constrained P-T conditions along with the presence or absence of metamorphic or structural discontinuities can be used to discern between the models proposed for the GHS.

3.2 Metamorphic Zonation

As reported in Chapter 2, metamorphic grade and anatexite content increases up-structural section in the study area from upper greenschist to upper sillimanite grade with the appearance of key index minerals. Petrography was conducted on thirty-one specimens collected from the Likhu Khola region and the related mineral assemblage data allows definition of four metamorphic zones, described below.

3.2.1 Garnet Zone I

Garnet zone I extends over a horizontal distance of 8.2 km from the southernmost portion of the study area to a distinctive quartzite layer northeast of Bhandar (Figure 3.1). This zone contains micaceous phyllitic schist, a distinctive graphitic marker unit, localized calc-silicate intercalations and a quartzite layer to mark the structurally highest boundary. The interpreted peak assemblage of this zone is quartz + feldspar + muscovite + biotite + garnet with locally

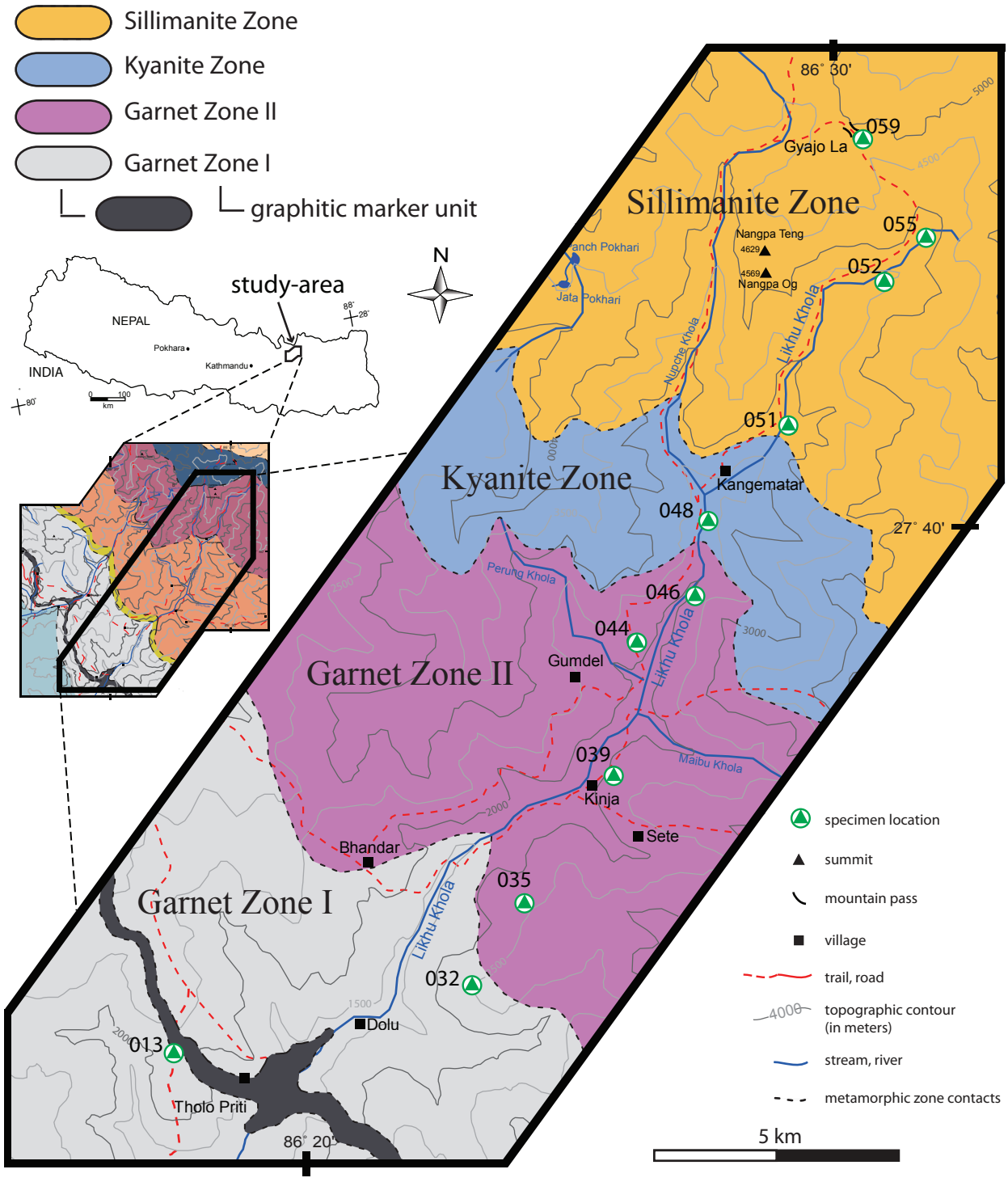

Figure 3.1 - Simplified map of the upper Likhu Khola study area showing the metamorphic zones and locations of specimens used for P-T geothermobarometry and U-(Th)-Pb geochronology. An outline of Nepal showing the study area and location of this map within the overall study area is included. The graphitic marker unit is shown for reference to the map of the entire study area.

present accessory phases of tourmaline ± ilmenite ± zircon ± monazite ± epidote ± apatite. Garnet is seen throughout this zone as porphyroblasts ranging in size from 0.5 mm to 3 mm in diameter and sometimes occurs as sigma and delta-type porphyroblasts (Figure 2.4F). The anatexite content of this zone typically ranges from 1-15%. It is locally chaotic and quartz dominated with subsidiary components of feldspar and biotite.

3.2.2 Garnet Zone II

Garnet zone II extends over a horizontal distance of approximately 7.4 km from the top of the quartzite layer to the first appearance of alumnosilicate minerals in paleosome (Figure 3.1). This zone contains quartz + muscovite + biotite ± garnet schist with intercalated psammopelitic metasedimentary rocks and local lenses of calc-silicate rocks. The interpreted peak assemblage of this unit is quartz + feldspar + muscovite + biotite + garnet with locally present accessory phases of tourmaline ± zircon ± apatite ± monazite ± ilmenite. The garnet throughout this zone is large (<2.25 x 2 mm) and is commonly spatially related to the anatexite lenses (Figure 2.5E). Anatexite comprises 15-25% of total rock volume within this zone and is composed of quartz + feldspar + muscovite + biotite ± garnet.

3.2.3 Kyanite Zone

The kyanite zone extends over a horizontal distance of approximately 2.8 km from the first appearance of kyanite in the country rock until it gives way to sillimanite at higher structural levels (Figure 3.1). This zone contains kyanite-bearing schistose gneiss. The interpreted peak assemblage of this zone is quartz + feldspar + biotite + muscovite + garnet + kyanite with locally present accessory phases of tourmaline ± zircon ± apatite ± monazite ± ilmenite. The garnet grains throughout this zone fluctuate in size with localized quartz-rich layers containing large

grains (<3.5 x 2.5 mm) and other portions of this zone containing much smaller grains (>0.13 x 0.13 mm). The anatexite at this level occurs as two distinct phases, which together comprise up to 45% of the total rock volume. One phase of the anatexite occurs as foliation parallel leucosomes (Figure 2.7D whereas a younger pod-like phase crosscuts both the foliation and the stromatic anatexite locally (Figure 2.7E).

3.2.4 Sillimanite Zone

The sillimanite zone extends over a horizontal distance of greater than 10 km from the complete disappearance of kyanite in favour of sillimanite to the structurally highest location reached in the study area at Gyajo La (Figure 3.1). This zone contains sillimanite-bearing gneiss and migmatite (rock with >45% of total rock volume composed of anatexite) with an interpreted peak assemblage of quartz + feldspar + sillimanite + biotite + muscovite with locally present accessory phases of zircon ± monazite. The garnet grains throughout this zone vary greatly in size and distribution similar to that observed in the kyanite zone. Both phases of the anatexite occur commonly, which together comprise >45% of the total rock volume. The older, foliation-parallel phase of the anatexite comprises quartz + feldspar + minor biotite. The younger phase that crosscuts both the foliation and the older anatexite phase is composed of quartz + feldspar + biotite + muscovite (in the form of books) ± tourmaline.

3.3 Mineral chemistry and texture

3.3.1 Methodology

Ten specimens were selected for a detailed geothermobarometric study in order to constrain the P-T evolution of this section of the GHS exposed in the Likhu Khola. A Cameca SX100 electron microprobe housed at the Saskatchewan Research Council in Saskatoon was

utilized for qualitative and quantitative analyses. Multiple garnet, biotite, muscovite and plagioclase grains from selected specimens were analyzed for quantitative compositional data. In order to estimate the peak temperature and pressure conditions recorded by these minerals the chemical zonation was investigated to determine whether they posses prograde, retrograde or homogeneous zoning (e.g., Jessup, 2008; Yakymchuck and Godin, 2012). Qualitative chemical maps were acquired for garnet grains representative of each metamorphic zone in order to investigate their potential compositional zonation. Garnet grains were selected based on their proximity and textural relationship to biotite, muscovite and plagioclase and the potential of the grains to represent sections through their core. The representative garnet grains were imaged using backscattered electron microscopy (BSE) and mapped for Fe, Ca, Mg, Mn, Al, K, Na, Th and Y by wavelength dispersive spectrometry with an accelerating voltage of 15kV and a beam current of ~200 nA.

Quantitative major element concentrations were obtained with the Cameca SX100 operating at 15-20 kV with a beam size of ~10nm and current of 20nA. Line transects and single point data taken along garnet, biotite, muscovite and feldspar grains were performed on multiple grains per specimen. This compositional transect data paired with the chemical maps were used to determine what data to use in geothermobarometric calculations (see below). The geothermobarometric methods employed generally rely on garnet chemistry to estimate both pressure and temperatures. As such detailed examination of garnet is a necessary first step, the results of which are presented below.

almandine (Fe2+) along the secondary y-axis on the right side and spessartine (Mn), pyrope (Mg) and grossular (Ca) along the primary y-axis on the left side. The x-axis is the distance across the garnet grain, which

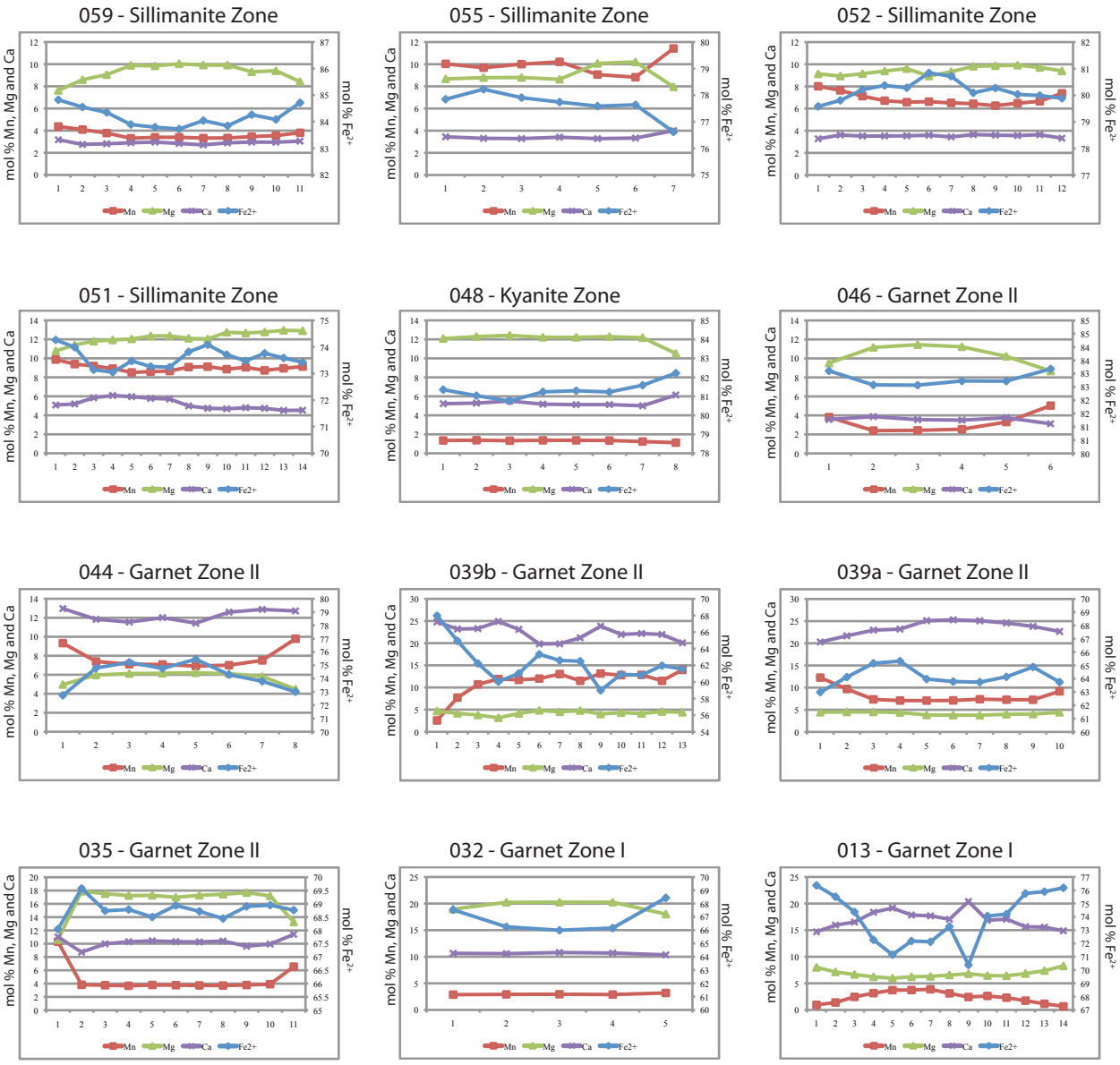

Figure 3.2 - Composition charts of one representative garnet grain from each specimen analyzed with geothermobarometry. The data is from rim to core to rim and presented in mol% with almandine (Fe^{2+}) along the secondary y-axis on the right side and spessartine (Mn), pyrope (Mg) and grossular (Ca) along the primary y-axis on the left side. The x-axis is the distance across the garnet grain, which is approximately 10 *u*m between each spot location. The graphs are read like a book from the structurally highest specimen 059 down to the structurally lowest specimen 013. See text for full descriptions.

3.3.2 Results

One representative transect of garnet per specimen is presented in Figure 3.2 as mol% for Almandine (Fe^{2+}), Spessartine (Mn), Pyrope (Mg), and Grossular (Ca). Detailed descriptions of the garnet grains from specimens utilized for geothermobarometric analyses will be discussed from structurally lowest to highest.

The structurally lowest specimen, 013, is within Garnet Zone I. Garnet grains record Mn and Ca decreasing from core to rim and Mg and Fe increasing from core to rim (Figure 3.2). This trend is typical of prograde garnet growth at medium grade metamorphism (Yardley, 1977; Spear et al., 1990; Kohn and Spear, 2000) The chemical map of a representative grain confirms this distinct prograde growth zonation (Figure 3.3A). In this case the chemistry at the rims of the garnet is interpreted to represent peak or near-peak conditions (Hollister, 1966).

Specimen 032 is structurally higher within the Garnet zone I. The transect of garnet in this specimen shows minor zonation with Mg decreasing from core to rim, Fe increasing from core to rim and Mn and Ca remaining consistent (Figure 3.2). The Fe trend is suggestive of relict prograde zonation with the Mg trend suggestive of diffusional zonation (Yardley, 1977; Spear, 1993). The chemical mapping of a representative garnet grain from this sample reveals additional information. There is an inclusion-rich core retaining very slightly elevated Mn and Ca relative to the large inclusion-free rim that indicates preservation of relict prograde growth zonation (Figure 3.3B, Yardley, 1977; Spear, 1993). There is also a sharp increase in Mn along the rim of the garnet that may be attributed to garnet resorption and the preferential retention of Mn as a resorption rind (Florence and Spear, 1991; Kohn and Spear, 2000). The transect data did not reflect this feature due to its very thin profile along the rim only (Figure 3.3B). The rim of the garnet in specimen 032 is locally embayed with those embayments cutting through the Mn-rich

A - 013, Garnet Zone I

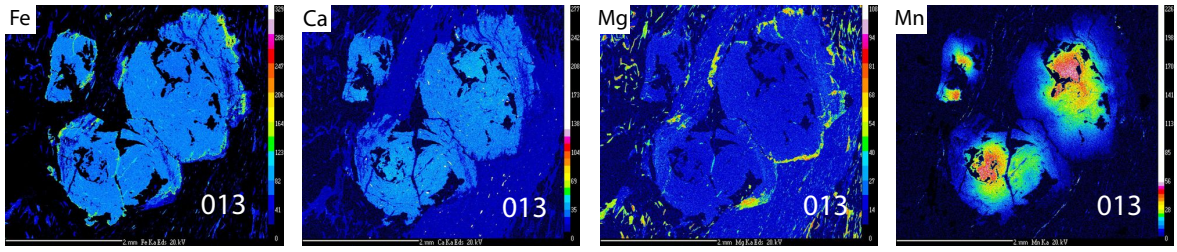

B - 032, Garnet Zone I

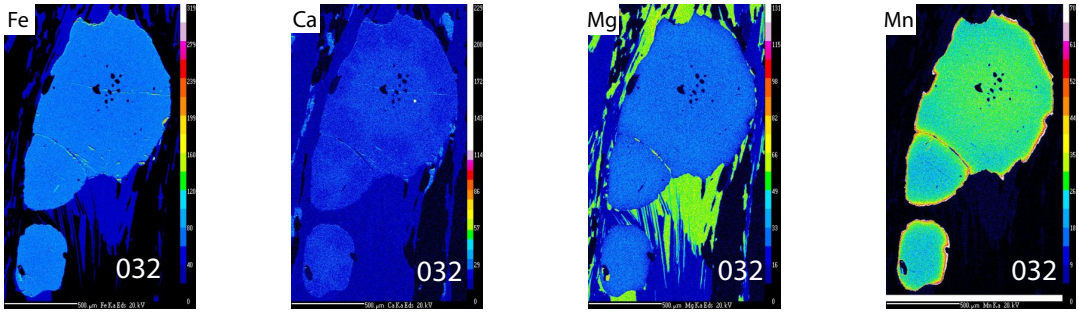

C - 039, Garnet Zone II

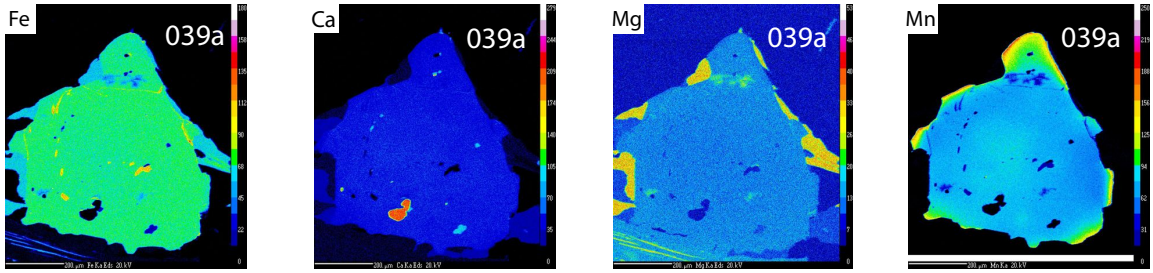

D - 039b, Garnet Zone II

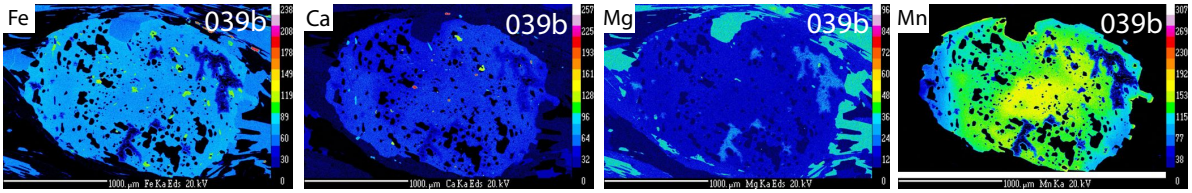

E - 048, Kyanite zone

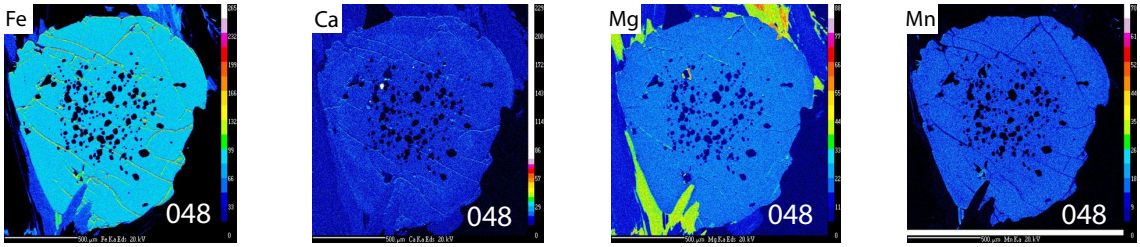

Figure 3.3 - Chemical maps of garnet representative of each type of chemical zonation present throughout the Likhu Khola study area. Compositional maps for Fe, Ca, Mg and Mn were obtained by Electron Microprobe housed at SRC labortories, Saskatoon operated at 15 Kv and 200 nA. See text for full descriptions. In specimens 013, 032 and 048 the color scales have been altered, creating a relative scale for Mn and Ca in order to accentuate the chemical zonation.

rind (Figure 3.3B). In this case, compositional data from the large inclusion free rim, but carefully avoiding the Mn-rich resorption rind, is taken to best represent the peak or near-peak metamorphic conditions.

Specimen 035 represents entry into Garnet zone II. The transect data records relatively flat trends of Mn, Mg, Ca and Fe in the core with rim compositions recording large increases of Mn and decreases of Mg and to a lesser degree Fe (Figure 3.2). In this case the Mn rich resorption rind attributed to garnet resorption and the preferential retention of Mn (Florence and Spear, 1991; Kohn and Spear, 2000) is recorded in the transect data. Compositional data from the core of grains, avoiding the Mn-rich resorption rind, is used to best represent the peak or near-peak metamorphic conditions.

Specimen 039 is within the Garnet zone II and contains garnet grains with different zonation patterns. The smaller garnet grains within this specimen 039a (~560 um in diameter) have little to no inclusions, Mn increasing from core to rim, Ca decreasing from core to rim and consistent Mg that likely represents diffusional zoning (Figures 3.2 and 3.3C; Yardley, 1977; Kohn and Spear, 2000). The larger garnet grains from specimen 039b (>1000 μm in diameter) have the opposite trend with numerous inclusions throughout, Mn decreasing from core to rim, and Ca increasing from core to rim, more consistent with preserved prograde growth zoning (Figures 3.2 and 3.3D). The preserved prograde growth zoning of these garnet may be attributed to the large size of the garnet where chemical diffusion would take significantly longer to reach the core compared to smaller grains. The chemical map shows significant embayment and therefore resorption of the garnet (Figure 3.3C and D). The cores of the smaller diffusional zoned garnet grains, avoiding the Mn resorption rind, and the rims of the larger prograde growth garnet grains are taken to represent peak or near-peak metamorphic conditions.

Specimens 044 and 046 are from structurally higher in Garnet zone II and display classic diffusional zonation commonly seen in the core of the GHS (e.g., Catlos et al., 2002; Simpson, 2002; Searle et al., 2003; Jessup et al., 2008). Mn is close to homogeneous throughout the core with a pronounced increase close to the rims. Mg and Ca decrease from core to rim (Figure 3.2) with Mg again showing the more pronounced decrease in concentration close to the rims. These trends indicate the presence of an Mn-rich resorption rind as seen in specimens 032, 035 and 039. Specimen 044 also shows a higher Mn concentration relative to 046 (Figure 3.2). The Fe trends in these specimens differ from each other with specimen 044 showing a decrease from core to rim and 046 increasing from core to rim. In both cases the core composition of the garnet were used to represent the peak or near-peak metamorphic conditions.

Specimen 048 represents entry into the kyanite zone and shows negligible variations in Mn, Mg, and Ca, with minor irregularities in the Fe (Figure 3.2). The chemical map also shows no zonation with an inclusion rich core, inclusion free rim and locally embayed grain boundary (Figure 3.3E). This lack of zonation may represent homogenization of the grain's elemental composition due to diffusional processes at the high temperatures experienced at this structural level (e.g., Jessup et al., 2008; Larson et al., 2010a). Subsequent creation of the Mn-rich resorption rind can be associated with similar retrograde net transfer reactions (Kohn and Spear, 2000) that are observed in most samples. In this case the average of the transect data (excluding the rims) is used to represent the closest approximation of peak metamorphic conditions.

Specimens 051, 052 and 055 are within the sillimanite zone. The rocks in this zone are sillimanite-rich with no kyanite remaining. Garnet grains in these rocks show minor but appreciable variation in zoning representing diffusional retrograde exchange. Mn increases slightly from the core to rim, with a large spike in increased Mn content along in the rim in

specimen 055 (Figure 3.2) indicating the presence of an Mn-rich resorption rind. Garnet grains in all three specimens have inclusion-rich cores with inclusion-free rims, irregular shapes and locally embayed grain boundaries. The inclusions are dominantly quartz with local biotite, muscovite and rare feldspar. Specimen 055 appears to record an earlier fabric orientation delineated by quartz inclusions within garnet. For these specimens, the core composition of the garnet is taken to represent peak or near-peak metamorphic conditions.

The structurally highest specimen 059 is within the sillimanite zone. It appears to preserve diffusional zonation, specifically with Mg decreasing distinctly from core to rim (Figure 3.2; Spear, 1993). Mn and Fe slightly increase in concentration from core to rim but cannot be definitive to assess the presence of an Mn-rich resorption rind diffusional zonation. The garnet grains in this specimen are full of inclusions with no distinct inclusion-free rims and embayed grain boundaries. The core composition of garnet in this specimen is taken to represent peak or near-peak metamorphic conditions.

3.4 Metamorphic P-T estimates

3.4.1 Methodology

Temperatures and pressures were estimated using a combination of geothermobarometric methods. Method 1 utilized THERMOCALC v.3.26 in average-PT mode with the internally consistent data set of Holland and Powell (1998). The fluid content was assumed to be pure H_2O in equilibrium with the peak metamorphic assemblage (e.g., Kellet et al., 2010) as no graphite or carbonate was identified in any of the specimens analyzed. The THERMOCALC calculations can be sensitive to the fluid composition (Yakymchuk and Godin, 2012) therefore a second method was employed to compare the calculated temperatures and pressures. For method 2, temperatures and pressures were calculated using the garnet-biotite-plagioclase

geothermobarometer of Wu et al. (2006), which is calibrated against the 5AV garnet-biotite geothermometer of Holdaway (2000) and the garnet-aluminosilicate-plagioclase (GASP) geobarometer of Holdaway (2001). For the structurally lowest specimen, 013, only the Wu et al. (2006) method were used to estimate temperature due to the absence of plagioclase. No suitable geobarometer was found for the assemblage of specimen 013.

Examining the chemical zonation of the garnet, plagioclase, biotite and muscovite is essential in selecting the data that best represents the peak P-T estimates as discussed above (see section 3.3.1). Garnet compositions with the lowest Fe# (Fe/Fe+Mg) and Mn were generally chosen to use for P-T calculations. This is the closest approximation of the garnet composition prior to resorption and diffusion effects during a high-grade metamorphic overprint (e.g., Spear and Peacock, 1989, Jessup et al., 2008). This Fe# and Mn criteria associates well with the core of garnet grains that exhibit diffusional zonation and the near-rim data for garnet that preserved prograde growth zonation as discussed above. In specimens exhibiting diffusional zonation any excessively large increase in Mn directly at the rim was carefully avoided because this represents a diffusional resorption process that postdates the peak metamorphic conditions.

Biotite was investigated with line transects across large grains and grain clusters with negligible zonation found. For specimens that showed diffusional growth zonation in garnet the average compositions of matrix biotite were exclusively used because the retrogressive diffusion reactions would affect the biotite that is in contact or close proximity to garnet. In the specimens that preserved growth zoning, the average of biotite both in the matrix and in close proximity of garnet was used. Muscovite analyses were also conducted as line transects across small grains and large sheaths with negligible zonation found. Compositions used for geothermobarometry follow the same principles as the selection for biotite. Transects of plagioclase feldspar also

revealed negligible zonation and therefore the same procedure of data selection for biotite and muscovite was used.

The one exception to the above-mentioned selection technique was specimen 013; it contains a lack of available near-rim biotite. Therefore, because of specimen 013's distinctive prograde growth zonation, the rim compositions of garnet were used with near-rim muscovite and matrix biotite. Certain garnet grains were observed to have retrograde biotite pervasively disseminated throughout fractures within the garnet therefore data from these garnet were excluded from P-T calculations.

3.4.2 Results

The compositional data used during THERMOCALC P-T calculations is presented in Table 1 with results in Table 2. Compositional data and results from the garnet-biotite-plagioclase geothermobarometer of Wu et al. (2006) are presented in Table 3. All compositional data can be found in APPENDIX B. All calculated pressure and temperatures are presented in Table 1. The same P-T trend is evident in the results from both methods, however, we will focus on the THERMOCALC results due to the garnet-biotite-plagioclase geothermometer of Wu et al. (2006) returning temperature values that are too low to be associated with the high degree of partial melting observed in the structurally highest portions of the study area. A petrogenetic grid in the KFMASH system, suitable for these metapelitic rocks (e.g., Yakymchuk and Godin, 2012), predicts vapour-saturated melting at temperatures >700°C (Figure 3.4); however, all P-T estimates calculated with the Wu et al. (2006) geothermobarometer plot on the solidus side of the muscovite dehydration-melting curve on the KFMASH petrogenetic grid (Figure 3.4). THERMOCALC P-T estimates plot on the liquidus side of the muscovite dehydration-melting curve and each specimen plots within error of P-T space that is reasonable for the mineral phases

Table 1. Mineral compostions used for P-T calculations in THERMOCALC

Sample	Mineral	SiO_2	TiO_2	Al_2O_3	Cr_2O_3	Fe_2O_3	FeO	MnO	MgO	CaO	Na_2O	K_2O
013	bt	34.49	1.34	18.59	0.00	0.00	17.74	0.01	9.67	0.27	0.16	7.67
013	gt	35.89	0.05	21.87	0.00	0.00	35.45	0.10	2.32	5.13	0.01	0.08
013	ms	43.31	0.26	34.72	0.00	0.00	1.33	0.00	0.78	0.03	0.84	8.48
032	bt	37.03	1.49	19.53	0.00	0.00	16.16	0.06	12.44	0.03	0.32	8.56
032	gt	37.60	0.00	21.18	0.00	0.00	31.43	0.99	5.20	3.85	0.01	0.00
032	ms	47.06	0.52	36.80	0.00	0.00	1.29	0.00	0.93	0.03	1.20	9.08
032	plag	61.07	0.00	24.90	0.00	0.00	0.02	0.00	0.00	5.65	8.76	0.09
035	bt	36.57	1.74	18.34	0.00	0.00	18.74	0.17	10.34	0.12	0.28	8.67
035	gt	37.35	0.01	21.97	0.00	0.00	31.29	1.80	4.29	3.85	0.01	0.00
035	ms	48.26	0.70	34.20	0.00	0.00	3.23	0.02	1.00	0.03	0.77	8.36
035	plag	63.02	0.00	23.96	0.00	0.00	0.05	0.01	0.00	4.81	8.48	0.13
039	bt	34.32	3.32	17.98	0.00	0.00	24.02	0.29	5.90	0.01	0.07	9.40
039	gt	36.64	0.04	21.66	0.00	0.00	29.53	1.28	1.34	10.33	0.01	0.00
039	ms	47.60	0.89	34.36	0.00	0.00	2.71	0.03	1.11	0.00	0.26	9.63
039	plag	60.24	0.00	24.86	0.00	0.00	0.06	0.01	0.01	5.44	8.41	0.23
044	bt	33.52	3.57	17.90	0.00	0.00	25.48	0.20	4.65	0.11	0.08	8.89
044	gt	35.60	0.00	21.40	0.00	0.00	34.83	2.89	1.64	4.16	0.00	0.00
044	ms	45.88	1.09	34.91	0.00	0.00	2.30	0.01	0.75	0.11	0.29	9.58
044	plag	59.19	0.00	25.45	0.00	0.00	0.04	0.01	0.00	6.31	7.95	0.23
046	bt	34.84	2.43	19.21	0.00	0.00	22.51	0.04	7.93	0.02	0.22	8.77
046	gt	36.18	0.00	20.94	0.00	0.00	37.50	1.38	2.73	1.36	0.00	0.01
046	ms	46.17	0.97	36.08	0.00	0.00	1.59	0.00	0.75	0.02	0.86	9.36
046	plag	64.72	0.00	23.06	0.00	0.00	0.04	0.00	0.00	3.20	9.82	0.08
048	bt	33.18	2.89	18.80	0.00	0.00	19.35	0.01	8.26	0.02	0.24	9.04
048	gt	35.20	0.00	21.88	0.00	0.00	36.87	0.55	2.90	1.95	0.00	0.01
048	ms	46.18	1.12	35.91	0.00	0.00	1.27	0.00	0.70	0.04	0.72	8.34
048	plag	62.45	0.00	23.88	0.00	0.00	0.02	0.00	0.00	4.74	8.22	0.19
051	bt	33.65	3.33	19.67	0.00	0.00	20.36	0.15	7.26	0.04	0.13	9.44
051	gt	36.39	0.01	21.42	0.00	0.00	33.77	4.02	3.24	1.83	0.01	0.00
051	ms	45.75	0.95	37.06	0.00	0.00	1.31	0.01	0.64	0.04	0.31	9.43
051	plag	59.82	0.00	24.64	0.00	0.00	0.01	0.01	0.00	5.36	8.50	0.37
052	bt	34.11	3.71	18.32	0.00	0.00	21.51	0.12	6.34	0.03	0.15	9.61
052	gt	35.13	0.00	21.46	0.00	0.00	36.10	2.85	2.45	1.28	0.00	0.00
052	ms	48.12	0.92	35.99	0.00	0.00	1.38	0.02	0.56	0.02	0.45	9.18
052	plag	62.04	0.00	24.08	0.00	0.00	0.27	0.02	0.00	4.84	8.33	0.21
055	bt	34.31	3.46	19.58	0.00	0.00	22.17	0.13	6.58	0.05	0.16	9.34
055	gt	35.67	0.00	20.73	0.00	0.00	34.80	4.87	2.18	1.19	0.00	0.00
055	ms	45.73	1.19	36.80	0.00	0.00	1.34	0.01	0.53	0.01	0.47	10.03
055	plag	60.47	0.00	24.34	0.00	0.00	0.09	0.01	0.00	5.19	8.83	0.24
059	bt	32.73	3.14	19.11	0.00	0.00	22.88	0.05	5.72	0.05	0.14	9.69
059	gt	34.45	0.00	21.50	0.00	0.00	37.94	1.40	2.50	1.14	0.00	0.01

Table 1. Mineral compostions used for P-T calculations in THERMOCALC continued

Sample	Mineral	SiO_2	TiO_2	Al_2O_3	Cr_2O_3	Fe_2O_3	FeO	MnO	MgO	CaO	Na_2O	K_2O
059	ms	45.52	0.60	35.95	0.00	0.00	1.45	0.00	0.51	0.01	0.43	9.33
059	plag	60.55	0.00	23.73	0.00	0.00	0.19	0.01	0.00	4.87	8.61	0.20

Table 2. Results from THERMOCALC v3.26 in average-PT mode

Sample	T (°C)	± 2σ	P (Kbar)	± 2σ	cor	sigfit
032	772	37	10.8	1.2	0.764	0.58
035	845	51	11.6	1.4	0.75	0.7
039	851	61	11.8	1.4	0.808	1.04
044	888	245	10.4	3.2	0.947	0.1
046	817	56	8.5	1.9	0.755	1.27
048	852	53	8.9	1.5	0.816	0.72
051	828	51	7.8	1.4	0.808	0.51
052	804	50	6.7	1.3	0.812	0.41
055	796	50	6.5	1.3	0.82	0.34
059	853	58	7.0	1.4	0.804	0.42

Table 3. P-T calculations using a Gt-Bt-Plag geothermobarometer from Wu et al., (2006)

Specimen	Bt Fe(tot)	Bt Mg	Bt Al(VI)	Bt Ti	Plag Ca	Plag Nal	Plag K	Gt Fet	Gt Mg	Gt Ca	Gt Mn
013	1.179	1.145	1.741	0.800				2.383	0.278	0.442	0.007
032	0.999	1.371	1.701	0.083	0.272	0.740	0.005	2.073	0.618	0.344	0.056
035	1.187	1.167	1.636	0.099	0.227	0.722	0.007	2.069	0.506	0.327	0.121
039	1.571	0.688	1.658	0.195	0.261	0.730	0.013	1.969	0.160	0.882	0.087
044	1.695	0.551	1.678	0.214	0.304	0.693	0.013	2.369	0.199	0.363	0.199
046	1.450	0.893	1.743	0.133	0.129	0.855	0.006	2.564	0.335	0.105	0.082
048	1.287	0.978	1.761	0.172	0.248	0.769	0.012	2.523	0.353	1.171	0.038
051	1.326	0.843	1.805	0.195	0.259	0.743	0.021	2.273	0.388	0.158	0.274
052	1.942	1.018	2.615	0.383	0.230	0.716	0.012	2.484	0.300	0.113	0.199
055	1.427	0.754	1.773	0.200	0.245	0.754	0.017	2.416	0.294	0.107	0.318
059	1.525	0.679	1.795	0.188	0.236	0.755	0.012	2.630	0.309	0.101	0.098

Specimen	**Results T (ºC)**	**Results P (bars)**
013	**566**	
032	**640**	**9390**
035	**658**	**10120**
039	**627**	**11016**
044	**653**	**8131**
046	**621**	**6808**
048	**632**	**11992**
051	**650**	**6261**
052	**625**	**4262**
055	**629**	**3975**
059	**639**	**4234**

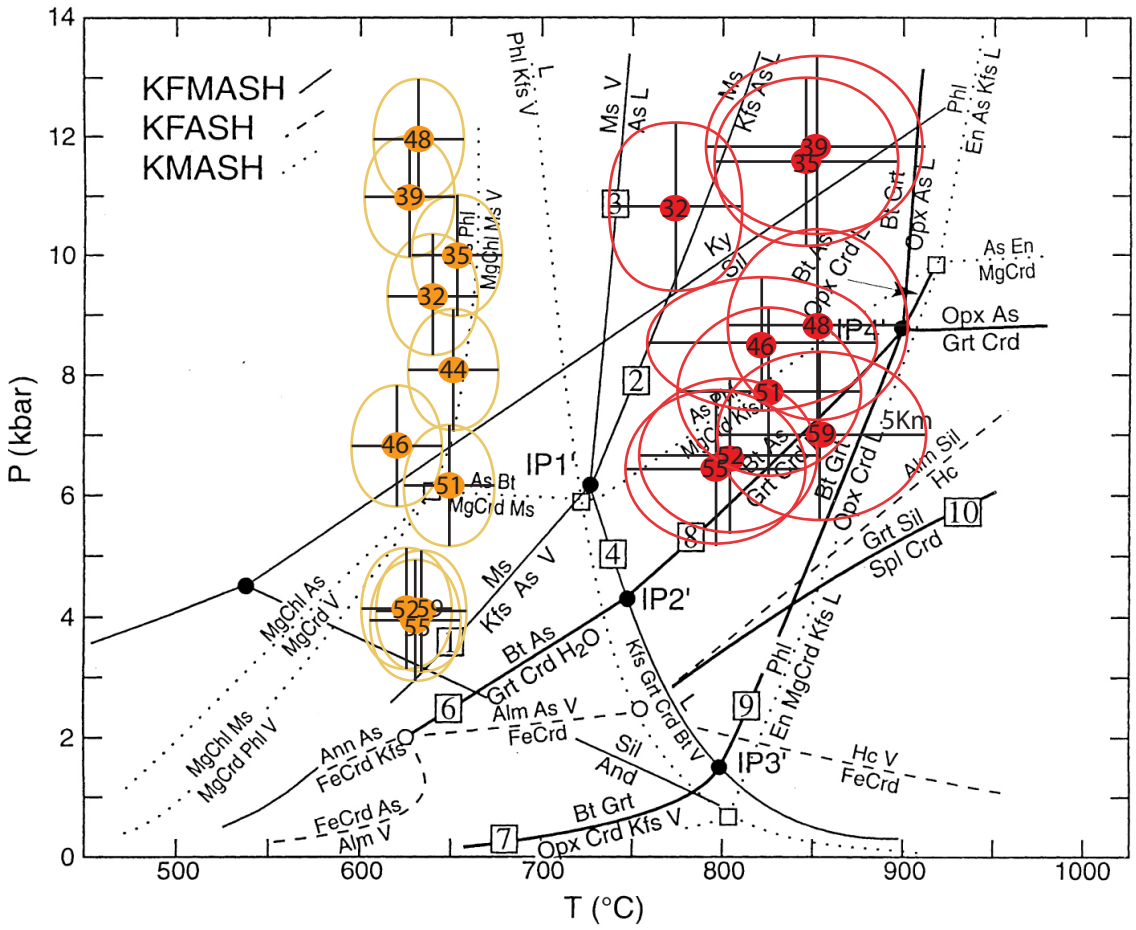

1 Muscovite + quartz = Al_2SiO_5 + K-feldspar + H2O
2 Muscovite + quartz = Al_2SiO_5 + K-feldspar + liquid
3 Muscovite + quartz + H2O = Al_2SiO_5 + liquid
4 K-Feldspar + Al_2SiO_5 + quartz + H2O = liquid
5 Muscovite + K-feldspar + quartz + H2O = liquid

P-T estimates from Gt-Bt-Plag geothermobarometer of Wu et al. (2006)

P-T estimates from THERMOCALC v.3.26 in average P-T mode

Figure 3.4 - P/T estimates using multiple methods plotted on a KFMASH petrogenetic grid modified after Spear et al. (1999) in order to compare geothermobarometers. Results from the Wu et al. (2006) Gt-Bt-Plag geothermobarometer calibrated against the geothermometer of Holdaway (2000) and the geobarometer of Holdaway (2001) are in yellow. Associated error bars are ± 25 °C and ± 1 kbar. All of these temperature estimates plot on the solidus side of reactions 3 and 4. Results from THERMOCALC v.3.26 in average-PT mode are in red and plot on the liquidus side of reactions 3 and 4. Associated error bars are ± one standard deviation assigned by THERMOCALC. These results are more consisten with the P-T conditions associated with the observed mineral phases and partial melt textures in these specimens from the Likhu Khola study.

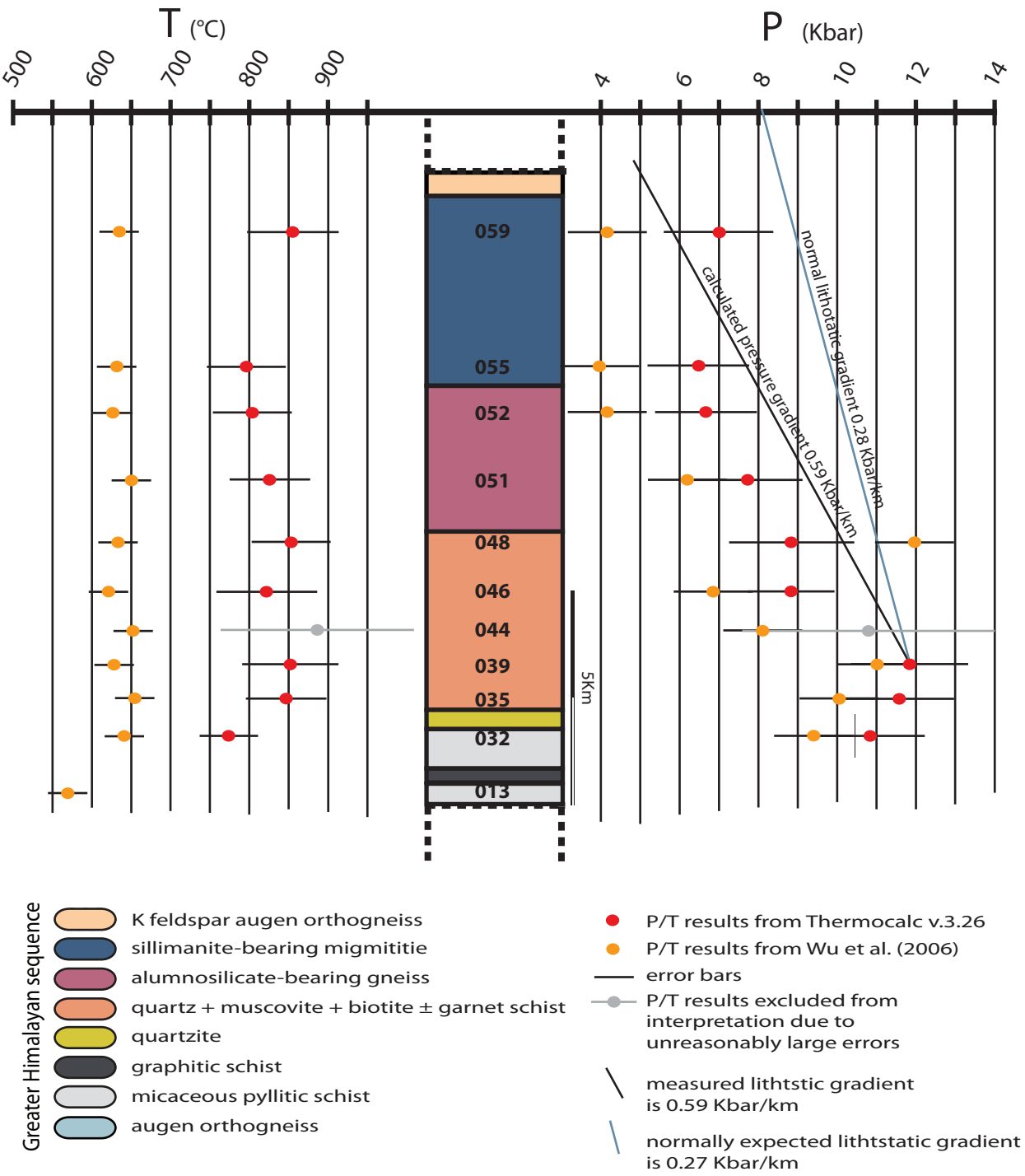

Figure 3.5 - Metamorphic pressure and temperature estimates using multiple methods plotted next to a structural section of the Likhu Khola study area in true thickness. Results from the Wu et al. (2006) Gt-Bt-Plag geothermobarometer calibrated against the geothermometer of Holdaway (2000) and the geobarometer of Holdaway (2001) are in yellow. Associated error bars are ± 25 °C and ± 1 kbar. Results from THERMOCALC v.3.26 in average-PT mode are in red. Associated error bars are one standard deviation assigned by THERMOCALC. A caculated lithostatic gradient of 0.59 Kbar/km is plotted next to a normal lithostatic gradient of 0.27 kbar/km (assuming a bulk crustal density of 2700 kg/m^3).

present (Figure 3.4). P-T results are also plotted next to a structural section with true thickness calculated from the cross section of the study area (Figure 3.5).

Peak temperatures increase up structural section from specimen 013 at 566 ± 25 °C to 039 at 851 ± 51 °C. The temperature subsequently ranges between ~800-850 °C from 046 to the structurally highest specimen 059 (Figure 3.5). The calculated temperature values within this range are within error of each other. The initial up-structural section increase in temperature is in agreement with the inverted metamorphic sequence found commonly throughout the Himalaya (e.g., Mallet, 1874; von Loczy, 1878; Oldham, 1883, Hodges, 2000; Searle et al., 2008).

Calculated pressures also generally appear to increase up structural section from specimen 032 at 10.8 ± 1.2 kbar to 039 at 11.8 ± 1.4 kbar though they are actually within error of each other. The calculated pressures decrease significantly after specimen 039 from 11.8 ± 1.4 kbar to 8.6 ± 1.4 kbar at specimen 046 and continues to drop to 6.5 ± 1.3 kbar at specimen 055, which is indistinguishable within error from the structurally highest pressure of 7.0 ± 1.4 kbar calculated from 059 (Figure 3.5).

The errors associated with P-T estimates from specimen 044 are exceptionally large. A calculated temperature estimates of 888 ± 288 °C and pressure of 10.4 ± 3.2 kbar conform to the general P-T trend discussed above but have associated errors excessive enough to warrant further discussion. The small size and amount of garnet available for quantitative analysis in specimen 044 is thought to be the main reason for the inaccuracy of the calculated P-T data. Only two garnets were large enough to use for geothermobarometric analysis and they appear to be significantly embayed, resorped and contain biotite disseminated in fractures indicating that the garnet may not be in equilibrium with the rest of the assemblage. Therefore P-T data calculated from this specimen is largely excluded.

The THERMOCALC temperature estimates for the upper portion of the GHS in the study area are all within error of each other and agree with the observations across the Himalaya of consistently high temperatures across the upper part of the GHS (e.g., Fraser et al., 2000; Larson et al., 2010a; Searle et al., 1999). This has been interpreted to indicate the effect of thermal buffering due to the pervasive in situ melt production (Hodges et al., 1988a). The calculated pressure estimates, however, are not within error of each other and delineate an apparent field gradient of decreasing pressures up-structural section. A regression line has been plotted through the apparent field gradient in order to compare it to a lithostatic gradient expected from normal mid-crust of similar composition (Figure 3.5). The calculated lithostatic pressure gradient across the decreasing up structural section of the Likhu Khola study area is 0.59 kbar/km, approximately twice the amount of a normal lithostatic gradient of 0.27 kbar/km (assuming a bulk crustal density of 2700 km/m^3).

3.5 U-Th-Pb monazite geochronology and Trace element analysis

3.5.1 Methodology

Monazite grains were indentified in six specimens from the suite of rocks analyzed for geothermobarometry using chemical mapping of thin sections for cerium, and phosphorus. A Cameca SX100 electron microprobe housed at the Saskatchewan Research Council in Saskatoon was utilized to construct these elemental maps with an accelerating voltage of 15 kV, a beam current of ~200 nA and a step size of ~ 30 microns. Suitable monazite grains were then mapped individually at high resolution to characterize the spatial proportions of U, Th, and Y in each grain. Zonation of Th, and Y within a monazite grain can be used to interpret the relative amounts of different elements available during crystallization events. Dating these different compositional domains may provide insight into the evolution of monazite growth and therefore

the rocks as a whole. Zonation of Y, a proxy for heavy rare earth elements (HREE), has specifically been shown to correlate with age domains within single monazite grains (Foster et al., 2002; Gibson et al., 2004; Kellett et al., 2010; Larson et al., 2011). An age-range within different domains of a single monazite grain may represent recrystallization, protracted or episodic growth. In previous studies, monazite growth in the presence of stable garnet is found to be relatively low in Y since garnet has a higher partition coefficient for Y and other HREE than monazite (Foster et al., 2002) whereas monazite growth prior to garnet growth and during garnet breakdown has been found to be high in Y and HREE (Kohn et al., 2005; Kellett et al., 2010). The Y zonation was closely monitored during the selection of U-Th-Pb spot analyses in order to provide age data entirely within distinct domains and avoid the overlap of different domains of ages that may be present in a single grain.

These monazite grains were dated using a split stream LA-MC-ICP-MS system at the University of Santa Barbara, California (UCSB) that collects U-Th-Pb ratios for geochronology and trace element data concurrently. The system consists of a Nu Plasma MC-ICP-MA (Nu Instruments, Wrexham, UK) and a 193nm ArF laser-ablation system equipped with a two-volume "HelEx" ablation cell that facilitates rapid transfer and washout of ablated material (Photon Machines, San Diego, USA). Analytical protocol is similar to that described by Cottle et al. (2009) with the modification that the collector arrangement on the Nu Plasma at UCSB allows for simultaneous determination of ^{232}Th and ^{238}U on highmass side Faraday cups equipped with 1011 ohm resistors and ^{208}Pb, ^{207}Pb, ^{206}Pb, and ^{204}Pb on four low-mass side ETP discrete dynode secondary electron multipliers. U-Th-Pb analyses were conducted for 30s each using spot diameters ranging from 7 to 20 *u*m in diameter, a frequency of 3 Hz, and 0.75 J/cm^2 fluence (equating to crater depths of ~7–8 *u*m). U-Th-Pb data from five samples were collected over four

analytical sessions. A primary reference material, "Managotry" monazite (554 Ma Pb/U isotope dilution–thermal ionization mass spectrometry [ID-TIMS] age; Paquette et al., 1994), was employed to monitor and correct for mass bias, as well as Pb/U and Pb/Th down-hole fractionation. To monitor data accuracy, two secondary reference monazites "FC-1" (55.7 Ma Pb/U ID-TIMS age; Horstwood et al., 2003) and "44096" (424 Pb/U Ma ID-TIMS age; Aleinikoff et al., 2006) were analyzed concurrently (once every 3-5 unknowns) and mass bias– and fractionation-corrected based on measured isotopic ratios of the primary reference material. During the analytical period, repeat analyses of FC-1 gave a weighted mean $^{206}Pb/^{238}U$ age of 54.9 ± 0.4 Ma, mean square of weighted deviates (MSWD) = 0.9, and a weighted mean $^{208}Pb/^{232}Th$ age of 57.2 ± 0.5 Ma, MSWD = 1.4 (2σ). Data reduction was performed with IgorPro and Iolite software at UCSB. All uncertainties are quoted at 2σ and include contributions from the external reproducibility of the primary reference material for the $^{207}Pb/^{206}Pb$, $^{206}Pb/^{238}U$, and $^{208}Pb/^{232}Th$ ratios.

Because of the young age of the monazite investigated in this study the radiogenic Pb signals are low. This results in relatively imprecise $^{207}Pb/^{235}U$ ages and difficulty in applying accurate ^{204}Pb corrections. The data presented in this study are therefore presented as $^{206}Pb/^{238}U$ vs. $^{208}Pb/^{232}Th$ concordia diagrams. The monazite ages are also presented as $^{208}Pb/^{232}Th$ ages to avoid problems with excess ^{206}Pb from unsupported ^{230}Th causing slight reverse discordance (excess ^{206}Pb) in the concordia diagrams. Data reduction of age and trace element data, including corrections for baseline, instrumental drift, mass bias, down-hole fractionation and uncorrected age calculations were carried out using Iolite version 2.1.2 (www.iolite.org.au). Full details of the data reduction methodology can be found in Paton et al (2011). Age data were plotted using Isoplot v.3.7 (Ludwig, 2003).

3.5.2 Results

The complete U-Th-Pb age data are presented in Table 4 with complete trace element data presented in APPENDIX C. Concordia diagrams plotting $^{206}Pb/^{238}U$ vs. $^{208}Pb/^{232}Th$ and age distribution histogram plots are shown in Figure 3.6. The textural context of representative monazite grains are shown in Figure 3.7 with embedded Y maps showing age spot locations. Trace element data plots with $^{208}Pb/^{232}Th$ age vs. total HREE and $^{208}Pb/^{232}Th$ age vs. Gd/Yb for each specimen are shown in Figure 3.8. Most of the specimens analyzed show distinct domains of different Y concentrations. These domains within monazite grains correspond to a trend with the concentrations of HREE very similar to the noted Y zonation. The interior cores of most monazite grains contain significantly lower Y concentrations, lower total HREE and higher Gd/Yb ratios than the exterior rims. In contrast, U and Th elemental maps and the light rare earth elements do not display any consistent, coherent pattern. Calculated ages from the study area the range from 27.4 ± 0.4 Ma to 15.3 ± 0.2 Ma with older ages always found in the low Y cores of the monazites. Each specimen analyzed will be discussed from structurally lowest to highest position.

Specimen 046, from the top of Garnet II Zone (Figure 3.1), yielded ages of 24.7 ± 0.4 Ma (cores) to 15.7 ± 0.2 Ma (rims) from a total of 19 spot analyses within seven individual monazite grains (Figure 3.6A). A representative monazite grain from this specimen yielded the widest age range of 24.7 ± 0.4 to 15.7 ± 0.2 Ma is located in the matrix with close proximity to biotite, garnet and plagioclase (Figure 3.7A). Ages show an inverse relationship with Y and HREE concentrations (Figure 3.8A) while they show a positive correlation with Gd/Yb ratios (Figure 3.8A).

Table 4. Complete age data from LA-ICP-MS analyses

Specimen	Pb (ppm)	U (ppm)	Th (ppm)	Th/U	208/232	2σ (%)	207/206	2σ (%)	206/238	2σ (%)	208/232 age	2σ (abs)
046_Gt1_1	64	7820	50900	6.5	0.00091	2.32	0.1096	2.55	0.00289	2.21	18.4	0.4
046_Gt1_2	67	7710	51400	6.7	0.00092	1.52	0.1108	2.71	0.00297	2.38	18.6	0.3
046_Gt5_1	85	5610	50100	8.9	0.00119	1.59	0.1387	2.09	0.00398	2.81	24.1	0.4
046_Gt5_2	89	9310	53300	5.7	0.00119	2.02	0.1402	2.00	0.00382	2.94	24.0	0.5
046_Gt5_3	88	9340	53300	5.7	0.00117	1.79	0.1376	2.11	0.00375	2.55	23.7	0.4
046_Gt5_4	75	7860	54600	6.9	0.00100	2.20	0.1463	2.19	0.00325	3.58	20.2	0.4
046_Gt5_5	83	8440	55800	6.6	0.00107	1.88	0.1594	1.88	0.00351	2.94	21.5	0.4
046_Gt6_2	72	6490	47000	7.2	0.00110	1.46	0.1358	2.21	0.00355	2.75	22.2	0.3
046_Gt6_3	101	6370	60000	9.4	0.00121	1.57	0.1361	2.50	0.00403	2.69	24.4	0.4
046_Gt8_1	70	7230	48900	6.8	0.00102	1.57	0.1246	2.41	0.00325	2.69	20.5	0.3
046_Gt9_1	94	7660	59800	7.8	0.00112	1.79	0.1345	2.16	0.00366	2.78	22.6	0.4
046_Gt14_1	92	5780	53800	9.3	0.00122	1.47	0.1495	2.21	0.00410	2.54	24.7	0.4
046_Gt14_3	90	5830	55500	9.5	0.00116	1.82	0.1581	2.53	0.00399	2.85	23.4	0.4
046_Gt14_4	58	6080	53400	8.8	0.00078	1.41	0.1412	2.69	0.00260	2.54	15.7	0.2
046_Gt16_1	93	6920	56500	8.2	0.00117	2.40	0.1337	2.17	0.00385	3.41	23.6	0.6
046_Gt16_2	62	7000	50500	7.2	0.00087	1.61	0.1220	3.03	0.00277	2.70	17.6	0.3
046_Gt16_3	97	10010	57300	5.7	0.00121	1.99	0.1562	1.66	0.00387	2.81	24.3	0.5
046_Gt16_4	95	6370	57300	9.0	0.00119	1.93	0.1357	2.21	0.00395	3.08	24.1	0.5
046_Gt16_5	95	6230	56700	9.1	0.00119	1.60	0.1397	2.22	0.00399	2.80	24.0	0.4
048_Gt1_1	46	2989	37250	12.0	0.00087	1.72	0.1060	2.92	0.00289	2.83	17.6	0.3
048_Gt1_2	56	4160	39700	9.2	0.00101	1.29	0.1003	2.09	0.00322	2.12	20.3	0.3
048_Gt1_3	54	3381	40170	11.6	0.00094	1.70	0.1183	2.11	0.00311	2.71	19.0	0.3
048_Gt1_4	57	4230	40200	9.3	0.00102	1.67	0.1203	1.58	0.00329	2.73	20.6	0.3
048_Gt1_5	61	4210	42600	10.0	0.00101	1.38	0.1220	1.48	0.00328	2.28	20.5	0.3
048_Gt1_6	52	3389	37550	11.0	0.00097	1.34	0.1093	2.10	0.00315	2.30	19.6	0.3
048_Gt1_7	52	3473	38220	11.1	0.00096	1.14	0.1017	1.87	0.00311	2.19	19.4	0.2
048_Gt1_8	57	3870	39800	10.5	0.00101	1.29	0.1089	1.74	0.00323	2.46	20.4	0.3
048_Gt1_9	64	3613	47000	13.2	0.00098	1.33	0.1165	2.06	0.00316	2.36	19.7	0.3
048_Gt1_10	60	3145	47400	15.3	0.00090	1.45	0.1265	1.74	0.00298	2.58	18.1	0.3
048_Gt1_11	73	3517	52900	15.5	0.00099	1.51	0.1253	1.68	0.00334	2.41	20.1	0.3
048_Gt1_12	53	3520	37600	11.0	0.00100	1.59	0.1073	1.96	0.00321	2.56	20.3	0.3
048_Gt6_1	86	5210	64800	12.7	0.00097	1.45	0.1044	1.72	0.00318	2.60	19.5	0.3
048_Gt6_2	88	5880	67000	11.6	0.00096	1.56	0.1086	1.66	0.00319	2.44	19.4	0.3
048_Gt6_3	98	6390	72800	11.6	0.00096	1.36	0.0994	1.61	0.00316	2.36	19.3	0.3
048_Gt6_4	71	4470	53400	12.3	0.00096	1.25	0.1028	2.14	0.00321	2.37	19.3	0.2
048_Gt6_5	101	6780	77400	11.6	0.00094	1.17	0.0995	1.61	0.00313	2.25	19.1	0.2
048_Gt6_6	72	4640	54000	11.8	0.00096	1.35	0.1029	1.75	0.00316	2.33	19.5	0.3
048_Gt7_1	67	4342	52900	12.0	0.00092	1.53	0.1039	2.31	0.00310	2.45	18.5	0.3
048_Gt7_2	72	5110	55500	10.9	0.00093	1.08	0.1008	1.98	0.00311	2.16	18.7	0.2
048_Gt7_3	69	6300	55500	8.7	0.00090	1.22	0.0907	1.76	0.00302	1.96	18.1	0.2
048_Gt7_4	58	4760	55000	11.4	0.00076	1.20	0.0939	2.24	0.00251	2.24	15.4	0.2
048_Gt7_5	66	5110	49400	9.5	0.00097	1.24	0.0977	1.54	0.00315	2.24	19.5	0.2
048_Gt7_6	60	3850	55400	14.1	0.00078	1.41	0.1042	2.40	0.00264	2.48	15.7	0.2
048_Gt9_1	101	6810	70700	10.1	0.00103	1.16	0.1606	1.56	0.00352	2.28	20.9	0.2
048_Gt9_2	62	5690	46700	8.1	0.00097	1.45	0.0898	1.78	0.00315	2.40	19.5	0.3
048_Gt9_3	68	5850	51700	8.8	0.00094	1.38	0.0935	1.60	0.00318	2.39	19.0	0.3
048_Gt9_4	89	7140	66600	9.2	0.00095	1.16	0.0950	1.47	0.00313	2.25	19.2	0.2
048_Gt9_5	71	7340	52400	7.1	0.00096	1.46	0.0882	1.25	0.00313	2.41	19.3	0.3
048_Gt9_6	99	7630	72200	9.4	0.00098	1.54	0.0996	1.31	0.00319	2.57	19.7	0.3

Table 4. Complete age data from LA-ICP-MS analyses continued

Specimen	Pb (ppm)	U (ppm)	Th (ppm)	Th/U	208/232	2σ (%)	207/206	2σ (%)	206/238	2σ (%)	208/232 age	2σ (abs)
048_Gt9_7	62	5050	44900	8.9	0.00099	1.22	0.0957	1.99	0.00322	2.21	19.9	0.2
048_Gt9_8	71	6260	50800	8.1	0.00099	1.42	0.1062	1.60	0.00322	2.46	20.0	0.3
048_Gt9_9	78	6280	55000	8.7	0.00100	1.60	0.1173	1.11	0.00332	2.48	20.2	0.3
048_Gt9_10	103	7410	74700	9.9	0.00096	1.25	0.1019	1.57	0.00319	2.41	19.4	0.2
048_Gt9_11	100	6400	70900	11.0	0.00098	1.33	0.1089	1.29	0.00328	2.34	19.7	0.3
048_Gt9_12	93	6060	66700	10.8	0.00098	1.74	0.1113	1.62	0.00326	2.75	19.8	0.3
048_Gt9_13	64	5760	45700	7.8	0.00099	1.52	0.0898	2.12	0.00319	2.44	19.9	0.3
048_Gt9_14	64	6550	46900	7.1	0.00096	1.35	0.0885	1.69	0.00313	2.28	19.5	0.3
048_Gt9_15	70	5430	50000	9.2	0.00099	1.21	0.0959	1.56	0.00324	2.21	20.1	0.2
048_Gt9_16	74	5610	52400	9.5	0.00098	1.33	0.0994	1.51	0.00322	2.40	19.7	0.3
048_Gt9_17	72	5200	51700	10.1	0.00097	1.44	0.0996	1.51	0.00325	2.32	19.7	0.3
048_Gt9_18	78	5790	56800	9.9	0.00097	1.34	0.0984	1.42	0.00317	2.48	19.6	0.3
048_Gt9_19	56	5910	46700	8.0	0.00085	1.42	0.0865	1.73	0.00274	2.42	17.1	0.2
048_Gt9_20	58	4960	48300	10.0	0.00085	1.41	0.0951	1.79	0.00283	2.38	17.3	0.2
048_Gt9_21	55	5660	45500	8.2	0.00085	1.42	0.0862	1.97	0.00278	2.30	17.1	0.2
048_Gt9_22	59	6020	49300	8.3	0.00085	1.53	0.0841	1.66	0.00276	2.67	17.2	0.3
048_Gt9_23	54	5790	45900	8.0	0.00084	1.43	0.0857	1.75	0.00274	2.39	16.9	0.2
048_Gt9_24	55	5760	46400	8.2	0.00085	1.54	0.0853	1.64	0.00278	2.47	17.1	0.3
048_Gt9_25	55	5420	46500	8.6	0.00084	1.43	0.0864	1.85	0.00269	2.37	17.0	0.2
048_Gt9_26	55	5480	46000	8.5	0.00085	1.64	0.0859	1.75	0.00279	2.58	17.3	0.3
048_Gt9_27	53	5170	45100	8.8	0.00083	1.45	0.0862	2.20	0.00268	2.42	16.7	0.2
048_Gt9_28	89	6100	65300	10.7	0.00098	1.54	0.0977	1.64	0.00321	2.53	19.7	0.3
048_Gt9_29	97	6920	71200	10.3	0.00096	1.45	0.1002	1.50	0.00318	2.45	19.5	0.3
048_Gt9_30	99	7010	72600	10.3	0.00097	1.76	0.0983	1.22	0.00320	2.91	19.6	0.3
048_Gt9_31	66	5500	52900	9.5	0.00090	1.45	0.0917	1.74	0.00297	2.35	18.1	0.3
048_Gt9_32	82	6710	61100	9.1	0.00094	1.28	0.0935	1.39	0.00313	2.21	19.0	0.2
048_Gt9_33	71	6580	52800	8.0	0.00096	1.66	0.0892	1.68	0.00314	2.66	19.4	0.3
048_Gt9_34	87	6820	64300	9.4	0.00098	1.53	0.0937	1.49	0.00318	2.64	19.8	0.3
048_Gt9_35	74	5750	54100	9.3	0.00098	1.33	0.0950	1.79	0.00321	2.37	19.8	0.3
048_Gt9_36	77	5890	57400	9.7	0.00096	1.46	0.0957	1.78	0.00320	2.53	19.4	0.3
048_Gt9_37	71	5950	50800	8.5	0.00101	1.29	0.1039	1.54	0.00329	2.52	20.4	0.3
048_Gt9_38	74	6200	52900	8.4	0.00100	1.49	0.1073	1.30	0.00327	2.44	20.3	0.3
048_Gt9_39	74	6360	53700	8.4	0.00100	1.40	0.1103	1.54	0.00327	2.53	20.2	0.3
048_Gt9_40	78	6300	56100	8.9	0.00101	1.49	0.1184	1.35	0.00333	2.47	20.3	0.3
048_Gt9_41	80	6380	57200	8.9	0.00101	1.38	0.1188	1.35	0.00333	2.29	20.5	0.3
048_Gt9_42	99	8530	73200	8.6	0.00098	1.32	0.0988	1.21	0.00323	2.48	19.8	0.3
048_Gt9_43	97	6510	70700	10.8	0.00100	1.60	0.1028	1.65	0.00328	2.62	20.1	0.3
048_Gt9_44	85	5970	63200	10.5	0.00098	1.33	0.0998	1.80	0.00326	2.38	19.8	0.3
048_Gt9_45	73	5680	53800	9.4	0.00098	1.53	0.0958	1.57	0.00321	2.28	19.8	0.3
048_Gt9_46	72	5450	52600	9.6	0.00098	1.73	0.0954	1.78	0.00321	2.68	19.9	0.3
048_Gt9_47	102	6190	74000	11.9	0.00099	1.61	0.1105	1.54	0.00331	2.51	20.0	0.3
048_Gt9_48	109	6480	78200	12.0	0.00100	1.60	0.1105	1.45	0.00332	2.60	20.1	0.3
048_Gt9_49	90	6500	63400	9.7	0.00100	1.29	0.1183	1.35	0.00332	2.39	20.3	0.3
048_Gt12_1	88	5440	63600	11.5	0.00098	1.32	0.1050	1.62	0.00324	2.39	19.9	0.3
048_Gt12_2	104	6810	76600	11.0	0.00098	1.43	0.1049	1.62	0.00327	2.35	19.8	0.3
048_Gt12_3	61	5940	58600	9.7	0.00076	1.72	0.0889	2.36	0.00246	2.79	15.3	0.3
048_Gt12_4	71	4700	56600	11.8	0.00090	1.67	0.1015	2.27	0.00300	2.83	18.1	0.3
048_Gt12_5	70	4500	57500	12.5	0.00087	1.73	0.1018	1.77	0.00293	2.53	17.5	0.3
051_Gt1_1	56	3893	48600	12.3	0.00083	2.76	0.0723	4.98	0.00266	4.34	16.8	0.5

Table 4. Complete age data from LA-ICP-MS analyses continued

Specimen	Pb (ppm)	U (ppm)	Th (ppm)	Th/U	208/232	2σ (%)	207/206	2σ (%)	206/238	2σ (%)	208/232 age	2σ (abs)
051_Gt1_2	53	3310	47260	14.3	0.00080	1.75	0.0804	6.72	0.00256	3.27	16.2	0.3
051_Gt1_3	51	3840	48500	12.6	0.00075	1.74	0.0661	5.90	0.00235	2.74	15.1	0.3
051_Gt5_1	55	3584	50000	14.0	0.00079	1.40	0.0702	5.70	0.00255	3.08	15.9	0.2
051_Gt5_2	64	3360	52500	15.9	0.00087	1.95	0.0701	6.13	0.00292	3.05	17.7	0.3
051_Gt5_3	72	4840	52900	11.1	0.00097	1.55	0.0828	4.11	0.00317	2.95	19.5	0.3
051_Gt6_1	62	3470	46400	13.8	0.00095	1.89	0.0822	5.11	0.00303	3.21	19.2	0.4
051_Gt6_2	81	6360	58300	9.3	0.00097	2.06	0.0784	3.70	0.00314	3.14	19.6	0.4
051_Gt6_3	75	5312	55700	10.5	0.00096	1.66	0.0823	3.77	0.00310	2.84	19.5	0.3
051_Gt6_5	80	6910	56800	8.3	0.00101	1.49	0.0833	3.12	0.00324	2.54	20.3	0.3
051_Gt10_1	78	5860	57400	9.7	0.00096	1.57	0.0831	4.21	0.00315	2.68	19.3	0.3
051_Gt10_2	76	5830	56500	9.5	0.00095	1.80	0.0819	4.03	0.00315	3.13	19.1	0.3
051_Gt10_3	69	3530	59300	16.5	0.00084	1.66	0.0646	6.97	0.00277	3.17	17.0	0.3
051_Gt10_4	72	3133	60200	18.7	0.00085	1.41	0.0719	6.95	0.00287	2.95	17.2	0.2
051_Gt11_1	91	7140	62400	8.5	0.00105	1.72	0.0882	3.17	0.00345	2.74	21.2	0.4
051_Gt11_2	96	6750	65600	9.4	0.00104	1.83	0.0897	2.90	0.00345	2.94	21.0	0.4
051_Gt11_3	105	6750	69900	10.1	0.00108	1.57	0.0905	3.09	0.00360	2.83	21.8	0.3
051_Gt11_4	103	6900	69200	9.8	0.00108	1.76	0.0867	2.88	0.00353	2.81	21.8	0.4
051_Gt11_5	84	6210	59000	9.4	0.00103	1.66	0.0851	2.70	0.00337	2.66	20.7	0.3
051_Gt11_6	83	5810	60300	10.2	0.00099	1.93	0.0836	3.59	0.00326	3.18	19.9	0.4
051_Gt11_7	77	4200	57400	13.6	0.00097	1.44	0.0840	4.40	0.00328	2.92	19.7	0.3
051_Gt11_8	105	6080	70400	11.6	0.00105	1.80	0.0955	3.04	0.00350	2.89	21.3	0.4
051_Gt11_9	101	5990	67200	11.5	0.00106	1.69	0.0864	3.24	0.00345	2.83	21.5	0.4
051_Gt11_10	96	5550	63900	11.9	0.00109	1.93	0.0988	3.34	0.00361	3.02	22.0	0.4
051_Gt11_11	99	5810	67800	12.1	0.00107	1.69	0.0886	3.05	0.00351	2.76	21.6	0.4
051_Gt11_12	91	5850	61100	10.9	0.00107	1.96	0.0865	3.01	0.00350	3.12	21.7	0.4
051_Gt11_13	82	5540	57000	10.8	0.00103	1.36	0.0863	3.24	0.00338	2.72	20.8	0.3
051_Gt11_14	91	5750	61300	11.2	0.00106	2.17	0.0942	3.08	0.00349	3.12	21.4	0.5
051_Gt11_15	73	4880	54700	11.5	0.00095	2.01	0.0790	4.43	0.00312	2.96	19.1	0.4
051_Gt11_16	70	3098	57700	19.1	0.00086	1.97	0.0659	6.22	0.00282	3.20	17.5	0.3
051_Gt11_17	80	4420	59800	13.4	0.00096	2.92	0.0854	5.27	0.00317	3.84	19.4	0.6
052_Gt1_1	31	3027	23400	7.6	0.00097	1.75	0.0626	7.67	0.00303	3.21	19.7	0.3
052_Gt1_2	45	2528	32460	12.8	0.00098	2.15	0.0664	7.23	0.00303	3.04	19.7	0.4
052_Gt1_3	36	2618	25050	9.6	0.00100	1.81	0.0687	5.97	0.00302	3.05	20.1	0.4
052_Gt3_2	51	3369	42000	12.4	0.00088	1.60	0.0608	6.25	0.00284	2.90	17.7	0.3
052_Gt3_3	41	3606	31300	8.7	0.00090	1.78	0.0593	5.40	0.00291	3.02	18.2	0.3
052_Gt3_4	66	5360	49000	9.1	0.00096	1.56	0.0786	4.07	0.00307	2.73	19.4	0.3
052_Gt3_5	39	5010	29530	5.9	0.00094	1.80	0.0588	4.42	0.00292	2.71	19.0	0.3
052_Gt3_7	64	5460	47600	8.7	0.00097	1.65	0.0833	3.24	0.00312	2.79	19.6	0.3
052_Gt3_8	29	2220	24100	10.6	0.00088	2.17	0.0799	8.39	0.00258	3.37	17.7	0.4
052_Gt3_10	48	2460	41420	16.7	0.00083	1.58	0.0754	6.90	0.00271	3.14	16.7	0.3
052_Gt5_1	110	12280	58400	4.8	0.00135	1.78	0.1810	1.33	0.00406	2.75	27.2	0.5
052_Gt5_2	87	4650	63900	13.8	0.00096	1.46	0.0939	3.51	0.00312	2.73	19.3	0.3
052_Gt5_3	78	4810	58000	12.0	0.00096	1.67	0.0902	3.99	0.00311	2.57	19.4	0.3
052_Gt5_4	86	5180	60300	11.1	0.00101	2.08	0.1341	6.11	0.00339	3.27	20.4	0.4
052_Gt6_1	77	4000	59800	15.1	0.00091	1.86	0.0983	3.87	0.00310	2.94	18.4	0.3
052_Gt6_2	70	2150	53900	25.3	0.00092	1.84	0.0761	8.02	0.00305	3.17	18.7	0.3
052_Gt6_3	80	4440	59000	13.3	0.00096	1.45	0.1147	3.75	0.00324	2.76	19.5	0.3
052_Gt8_1	94	4410	59900	13.6	0.00112	1.52	0.1270	3.07	0.00374	2.58	22.5	0.3
052_Gt8_2	87	8290	55300	6.7	0.00111	1.62	0.1557	1.73	0.00359	2.78	22.5	0.4

Table 4. Complete age data from LA-ICP-MS analyses continued

Specimen	Pb (ppm)	U (ppm)	Th (ppm)	Th/U	208/232	2σ (%)	207/206	2σ (%)	206/238	2σ (%)	208/232 age	2σ (abs)
052_Gt12_2	69	6610	47100	7.1	0.00104	1.63	0.1052	2.66	0.00330	2.85	21.1	0.3
052_Gt12_3	58	4080	43300	10.6	0.00095	1.47	0.0719	5.01	0.00306	2.86	19.2	0.3
052_Gt14_1	84	9720	50000	5.1	0.00120	1.83	0.1655	1.57	0.00371	2.65	24.3	0.4
052_Gt17_1	116	13830	62900	4.5	0.00132	1.67	0.1787	1.29	0.00391	2.74	26.7	0.4
052_Gt17_2	87	3450	66500	19.2	0.00094	1.38	0.1053	4.46	0.00318	2.64	19.0	0.3
052_Gt17_3	116	6710	70200	10.4	0.00118	1.70	0.1535	1.82	0.00395	3.00	23.8	0.4
052_Gt18_1	108	10670	57200	5.4	0.00134	1.34	0.1878	1.44	0.00404	2.51	27.1	0.4
052_Gt18_2	111	10940	61100	5.6	0.00129	1.71	0.2040	1.32	0.00392	2.71	26.0	0.4
052_Gt18_3	80	1949	61000	31.3	0.00093	1.51	0.0876	5.94	0.00313	3.20	18.8	0.3
052_Gt18_4	82	1723	63100	36.6	0.00093	1.62	0.1001	7.29	0.00314	3.39	18.7	0.3
055_Gt1_1	99	9370	83900	9.0	0.00084	2.15	0.0559	3.58	0.00281	3.35	16.9	0.4
055_Gt1_2	104	2910	84200	29.1	0.00089	2.15	0.0826	5.45	0.00314	3.39	17.9	0.4
055_Gt1_4	111	3290	89300	27.1	0.00089	2.47	0.1016	5.22	0.00311	3.70	18.0	0.4
055_Gt1_5	113	2985	90200	30.0	0.00090	2.01	0.1088	5.06	0.00326	3.30	18.1	0.4
055_Gt1_6	104	3670	83600	22.8	0.00089	2.25	0.0878	5.24	0.00304	3.47	17.9	0.4
055_Gt1_7	103	3260	82200	25.5	0.00088	1.93	0.0880	6.25	0.00306	2.89	17.8	0.3
055_Gt1_8	100	3690	80400	22.0	0.00088	1.81	0.0936	5.24	0.00305	3.06	17.8	0.3
055_Gt1_9	108	6310	81000	12.9	0.00093	2.15	0.1080	2.96	0.00319	3.32	18.8	0.4
055_Gt1_10	108	3733	87100	23.6	0.00088	2.15	0.0927	4.42	0.00305	3.30	17.8	0.4
055_Gt1_11	109	3507	84800	24.7	0.00090	1.78	0.1080	4.44	0.00317	3.02	18.1	0.3
055_Gt1_12	99	2437	79700	33.4	0.00087	1.72	0.0958	6.16	0.00305	3.49	17.6	0.3
055_Gt1_13	110	7600	81400	10.9	0.00096	2.29	0.1050	3.14	0.00317	3.34	19.4	0.4
055_Gt1_14	132	2322	107000	46.3	0.00089	2.25	0.1298	5.01	0.00321	3.55	18.0	0.4
055_Gt18_1	110	3120	88100	28.5	0.00089	2.13	0.1044	5.17	0.00329	3.43	18.0	0.4
055_Gt18_2	127	2800	102600	36.8	0.00089	1.91	0.0977	5.32	0.00318	3.17	17.9	0.3
055_Gt18_3	118	3169	95900	30.2	0.00089	2.03	0.0830	5.42	0.00304	3.11	17.9	0.4
055_Gt18_4	120	2990	99850	33.2	0.00085	2.00	0.0957	5.54	0.00299	3.71	17.1	0.3
055_Gt8_1	83	5500	66900	12.1	0.00091	2.10	0.0803	4.23	0.00294	3.45	18.3	0.4
055_Gt8_2	82	5140	65300	12.7	0.00091	2.52	0.0773	4.92	0.00304	3.37	18.4	0.5
055_Gt8_3	78	5050	62100	12.4	0.00090	2.00	0.0789	4.82	0.00301	3.39	18.2	0.4
055_Gt8_4	52	3890	45900	11.8	0.00080	1.89	0.0929	5.06	0.00254	3.17	16.1	0.3
055_Gt9_1	97	3699	77600	20.9	0.00089	2.37	0.0913	5.81	0.00299	3.58	17.9	0.4
055_Gt9_2	93	4510	71900	16.3	0.00092	2.92	0.0947	4.33	0.00310	3.71	18.7	0.5
055_Gt9_3	92	2317	73100	31.7	0.00090	2.56	0.1045	5.84	0.00315	4.12	18.1	0.5
055_Gt9_4	117	5760	90800	16.2	0.00092	1.75	0.1181	3.64	0.00320	2.81	18.5	0.3
055_Gt9_5	96	2378	81400	33.6	0.00087	2.31	0.0928	6.47	0.00303	3.61	17.5	0.4
055_Gt9_6	95	4310	77600	16.6	0.00089	2.13	0.0693	5.92	0.00294	3.42	18.0	0.4
055_Gt9_7	98	2787	79100	27.7	0.00089	2.26	0.0984	5.59	0.00307	3.51	17.9	0.4
055_Gt9_8	89	2423	70500	28.5	0.00090	2.56	0.1005	5.57	0.00309	3.65	18.1	0.5
055_Gt9_9	95	5820	72200	12.1	0.00096	2.08	0.0993	3.22	0.00320	3.00	19.4	0.4
055_Gt9_10	97	2380	77600	31.8	0.00091	2.54	0.0970	6.49	0.00320	4.00	18.3	0.5
059_Gt6_1	47	2700	3.26E+04	12.0	0.00099	1.31	0.0837	3.11	0.00320	2.47	20.0	0.3
059_Gt9-1	36	2220	2.44E+04	11.1	0.00102	1.38	0.0762	4.07	0.00319	2.50	20.5	0.3
059_Gt9-2	32	3270	2.29E+04	7.1	0.00098	1.33	0.0605	3.64	0.00295	2.29	19.8	0.3
059_Gt19_1	51	2270	3.90E+04	17.0	0.00092	1.31	0.0716	4.61	0.00302	2.46	18.6	0.2
059_Gt19_2	47	2913	3.44E+04	11.0	0.00095	1.26	0.0744	3.49	0.00313	2.25	19.3	0.2

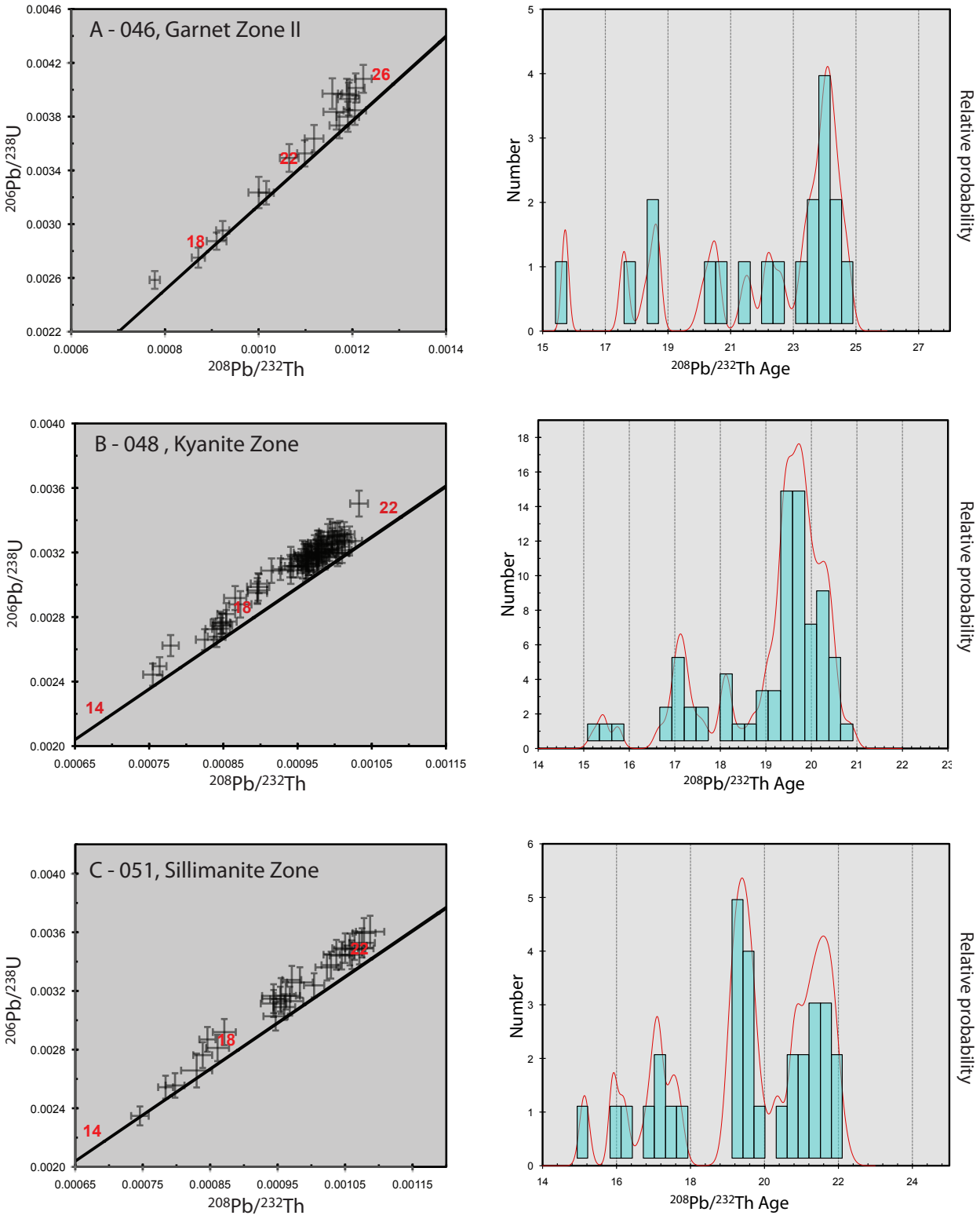

Figure 3.6 - Concordia plots of monazite age data plotting the $^{208}Pb/^{232}Th$ and $^{206}Pb/^{238}U$ ratios in order to avoid complications from $^{206}Pb/^{238}U$ disequilibrium. Age distribution histogram plots using the $^{208}Pb/^{232}Th$ ages are shown to enhance the visibility of different age domains within a single specimen.

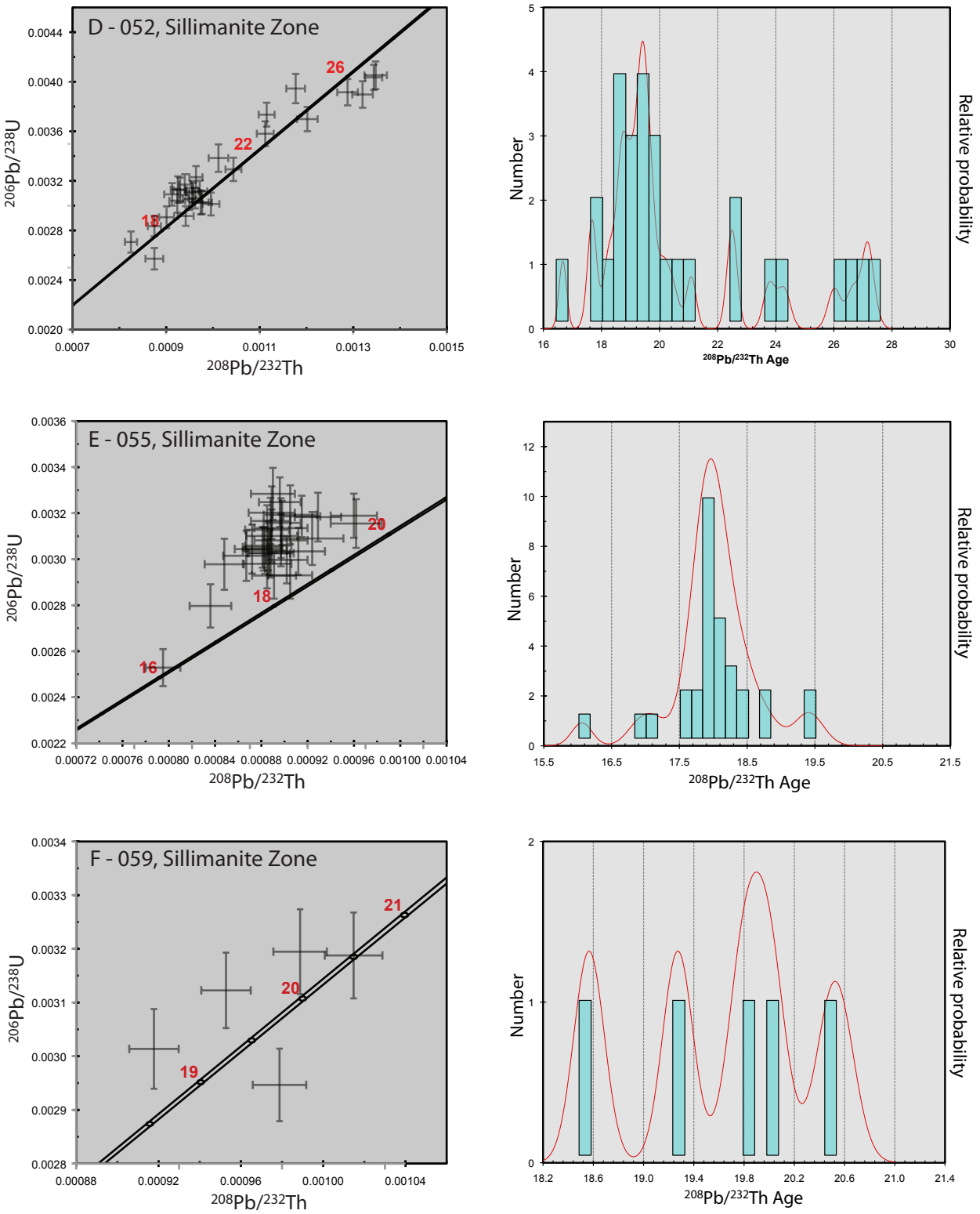

Figure 3.6 continued - Concordia plots of monazite age data plotting the $^{208}Pb/^{232}Th$ and $^{206}Pb/^{238}U$ ratios in order to avoid complications from $^{206}Pb/^{238}U$ disequilibrium. Age distribution histogram plots using the $^{208}Pb/^{232}Th$ ages are shown to enhance the visibility of different age domains within a single specimen.

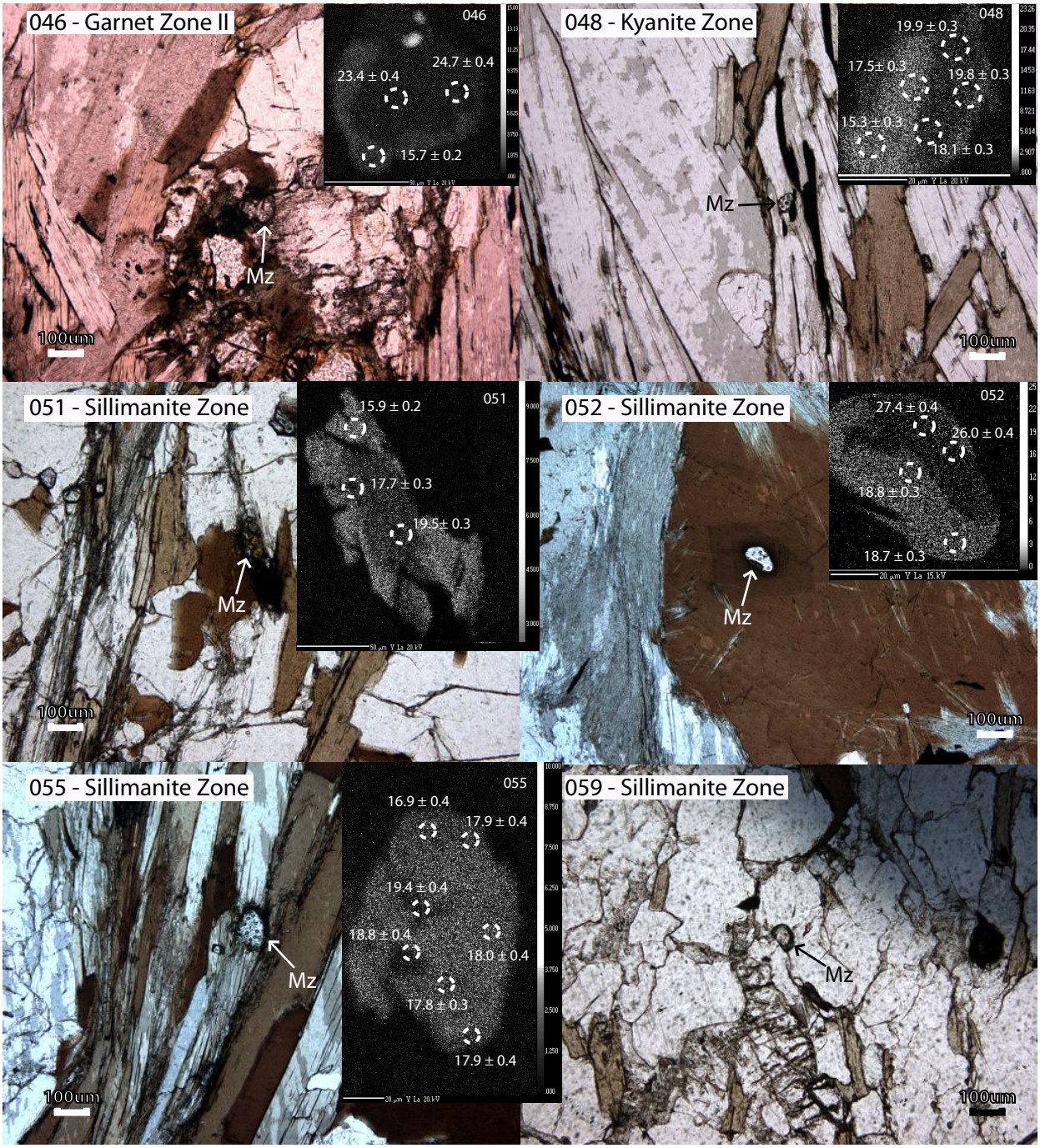

Figure 3.7 - Textural setting and location of spot analyses in representative monazite grains from each specimen analyzed for U-Th-Pb Geochronology. Yttrium maps of the monazite grains are embedded to show the relationship of older, Yttrium depleted cores to younger, Yttrium enriched overgrowth rims. The monazite grains observed in specimen 059 did not exhibit any Yttrium zonation and were relatively small, yielding a maximum of two spot analyses per grain with a narrow age range.

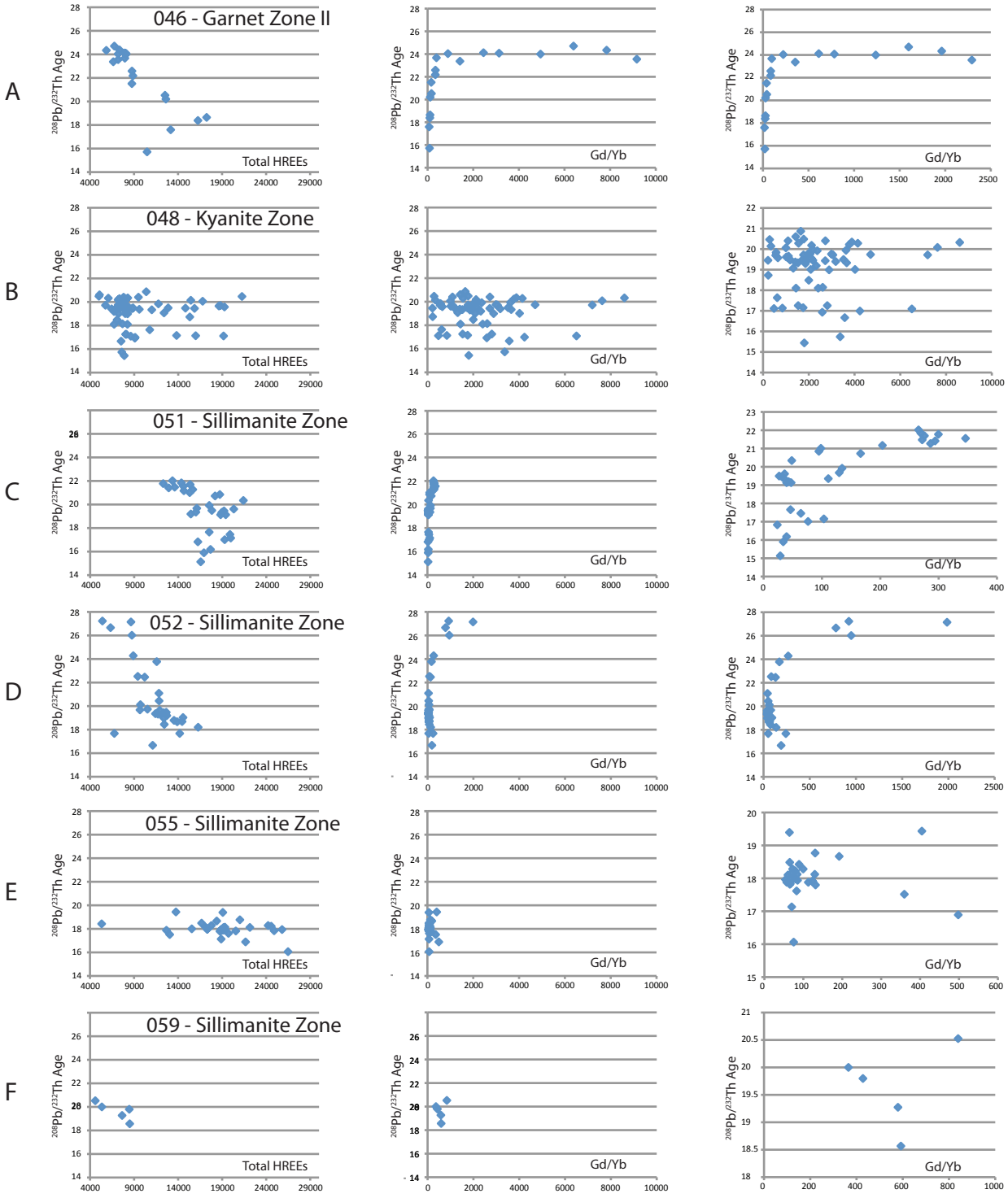

Figure 3.8 - Plots of trace element data taken concomitant with each monazite U-(Th)-Pb data point used for geochronology. $^{208}Pb/^{232}Th$ Ages are plotted against the total sum of heavy rare earth elements (HREE) and against Gd/Yb at an absolute scale. The second plots of $^{208}Pb/^{232}Th$ Ages vs. Gd/Yb have different scales in order to show a more detailed trend relative to the rare earth element concentrations of each specimen.

Specimen 048, from the Kyanite Zone (Figure 3.1), yields ages of 20.9 ± 0.2 Ma (cores) to 15.3 ± 0.2 Ma (rims) from a total of 78 spot analyses within five individual monazite grains (Figure 3.6B). A representative monazite grain from this specimen yielded the widest age range of 19.9 ± 0.3 to 15.3 ± 0.3 Ma (Figure 3.6) is in the matrix with close proximity to biotite (Figure 3.7B). Within this grain there are also three ages of 18.1 ± 0.3 and 17.5 ± 0.3 Ma that appear to have spots overlapping the distinctive Y domains and as such likely represent mixing of different age domains (Figure 3.7B). The total HREE concentrations and Gd/Yb ratios in this specimen do not show any discernable pattern (Figure 3.8B).

Specimen 051, from the Sillimanite Zone (Figure 3.1), yields ages of 21.8 ± 0.3 Ma (cores) to 15.1 ± 0.3 Ma (rims) from a total of 31 spot analyses within five individual monazite grains (Figure 3.6C). A representative monazite grain from this specimen that displays distinctive Y zonation has spot ages of 19.5 ± 0.3, 17.7 ± 0.3 and 15.9 ± 0.2 Ma (Figure 3.7C). The middle age of 17.7 ± 0.3 Ma appears to be overlapping the two distinct Y domains and likely represents mixing of the other two metamorphic age domains (Figure 3.7C). This monazite grain is in the matrix with close proximity to biotite, sillimanite and quartz (Figure 3.7C). The younger ages from this specimen are consistent with greater Y concentrations, higher total HREE concentrations and generally lower Gd/Yb ratios (Figure 3.8C).

Specimen 052, up-structural section from the Sillimanite Zone (Figure 3.1), yields ages of 27.4 ± 0.4 Ma (cores) to 16.7 ± 0.3 Ma (rims) from 29 spot analyses within nine individual grains (Figure 3.6D). A representative monazite grain from this specimen that displays distinctive Y zonation has spot ages of 27.1 ±0.4, 26.0 ± 0.4, 18.8 ± 0.3 and 18.7 ± 0.3 Ma that all occur within separate Y domains (Figure 3.7D). The monazite grain occurs as an inclusion

within a large biotite grain (Figure 3.7D). Younger ages are generally consistent with greater Y concentrations, higher total HREE concentrations and lower Gd/Yb ratios (Figure 3.8D).

Specimen 055, up-structural section from the Sillimanite Zone (Figure 3.1), yields ages of 19.4 ± 0.4 Ma (cores) to 16.4 ±0.4 Ma (rims) from 31 spot analyses within four individual grains (Figure 3.6E). The Y zonation of monazites in this specimen is not as distinct as the other specimens. A representative grain contains ages from 19.4 ± 0.4 to 16.9 ± 0.4 Ma and a concentration of ages within error of each other at 17.9 ± 0.4 Ma (Figure 3.7E). This monazite grain occurs in the matrix surrounded by large biotite laths (Figure 3.7E). The oldest ages of 19.4 ± 0.4 and 18.8 ± 0.4Ma were derived from spots within lower relative Y, however these lower Y zones are irregular and small (Figure 3.7E). Younger ages are generally consistent with greater Y concentrations, higher total HREE concentrations and lower Gd/Yb ratios (Figure 3.8E).

Specimen 059, from the structurally highest position reached in the Sillimanite Zone (Figure 3.1), contained only three monazites suitable for analyses and yielded ages ranging from 18.6 ± 0.2 to 20.5 ± 0.3 Ma (Figure 3.6F). Monazite in this specimen are rare, relatively small size (<50 *u*m) and found in the matrix (Figure 3.7F). No distinct Y domains were observed. The total HREE concentrations follow the same generally trend of the other specimens of increasing with younger ages. The Gd/Yb ratios, however, do not show a recognizable trend (Figure 3.8F). The range of ages found in this specimen is very limited therefore the trace element data may not particularly useful for interpreting monazite growth.

3.6 Discussion

Peak or near-peak metamorphic temperature estimates from geothermobarometry calculations show distinctive trends and allow for the subdivision of the GHS in lower ($GHS_{L)}$ and upper (GHS_U) portions (e.g., Larson et al., 2010a; Yakymchuk and Godin, 2012). There is a

distinct trend in the GHS_L of increasing temperature and pressure. A maximum pressure estimate is achieved just above the quartzite unit at specimen 039 and thereafter the trend changes up-structural section to temperatures within error of each other and decreasing pressures. This inflection in pressure trends is noted elsewhere in the Himalaya to represent the base of the GHS_U (Yakymchuk and Godin, 2012). This pressure trend inversion is consistent with different domains that have experienced unique tectonometamorphic histories and may represent a tectonometamorphic discontinuity that separates two distinct domains that have different structural, thermal and metamorphic histories. Similar tectonometamorphic discontinuities have been observed in recent studies throughout the length of the Himalaya and occur at very similar structural levels within the GHS (e.g., Groppo et al., 2009; Larson et al, 2010a; Carosi et al., 2010; Martin et al., 2010; Rubatto et al., 2012; Yakymchuk and Godin, 2012).

Although this general trend of upward-decreasing pressure estimates in the GHS_U is consistent with decreasing material on top of structurally higher rocks the preserved field gradient in this region at 0.59 kbar/km (assuming a bulk crustal density of 2800 kg m^{-3}) is approximately twice the expected gradient of 0.27 kbar/km (Figure 3.5). Similar field gradients have been noted elsewhere in the Himalaya including 1.2-1.6 kbar/km from east Nepal (Imayama et al., 2010), 0.54 kbar/km from the Langtang valley (Fraser et al., 2000), 0.62 kbar/km from the Budhi Gandaki valley of central Nepal (Larson et al., 2010a), and 0.45 ± 0.11 kbar/km from northwest Nepal (Yakymchuk and Godin, 2012). This steeper than expected pressure gradient may reflect tectonic thinning of the crust during deformation after metamorphism or the juxtaposition of post-peak metamorphic slices that reached peak metamorphic conditions at different times (Yakymchuk and Godin, 2012). Significant components of pure shear identified throughout Himalaya in the GHS (e.g., 35-62% pure shear

in Rongbuk valley from Jessup et al., 2006; 34-47% stretch parallel to flow in Kali Gandaki valley from Larson and Godin, 2009) are consistent with the type of strain necessary for tectonic thinning of the crust. Deformational temperature estimates from quartz recrystallization textures and <*c*> axis orientations are within error of metamorphic equilibrium temperatures in the lower positions of the GHS_L (as discussed in section 2.3.2) interpreted to reflect deformation contemporaneous with peak metamorphism and southward extrusion of the GHS. In contrast, the metamorphic equilibrium temperatures from the upper positions of the GHS_L and the entire GHS_U are significantly higher that the estimated deformational temperatures for quartz indicating post-peak metamorphic deformation that is consistent with tectonic thinning of the crust.

Combining the trace element data with the ages from different domains of Y concentration present in the monazite grains provides insight into the conditions of monazite crystallization. Trends in the HREE and Y content of monazite may be linked to the formation or breakdown of garnet (Yang and Pattison, 2006). During prograde growth, garnet preferentially acquires the bulk of the HREE and Y budget resulting in low concentrations of HREE and Y in monazite (Pyle et al., 2001; Foster et al., 2002; Buick et al., 2006; Rubatto et al., 2006). The monazite grains with low concentrations of HREE and therefore higher Gd/Yb ratios are interpreted to have crystallized during prograde metamorphism synchronous with garnet growth and are dated in multiple specimens from ca. 27 to 23 Ma. Subsequent Y-rich overgrowth rims around the initial prograde monazite grains record separate, distinct, crystallization events from ca. 22 to 15 Ma. These Y-poor overgrowth rims are moderate to highly enriched in HREEs. This enrichment of HREEs is likely sourced from the breakdown of garnet, and likely the monazite too, perhaps during partial melting (e.g., Spear, 1993). Therefore, partial melting of these rocks, and development of significant anatexite occurs sometime after ca. 23 Ma during which the

garnet, and likely the monazite too, resorb at least partially into the melt (e.g., Larson et al., 2011). At ca. 22 Ma the high Y overgrowth rims form on monazite potentially sourced from a melt associated with garnet breakdown that is now rich in HREEs. Observation of garnet at the microscopic level shows embayed grain boundaries in multiple specimens that most likely resulted from resorption. Monazite ages with associated high HREE concentrations and low Gd/Yb ratios indicates melt crystallization, or at least monazite growth in the absence of garnet growth appears to have continued until the middle Miocene. A summary diagram showing the evolution of monazite growth for the Likhu Khola study area is presented in Figure 3.9.

These timing constraints allow the interpretation of the data presented herein in the context of the currently proposed models for evolution of the Himalaya: critical taper wedge and mid-crustal channel flow. Limited data from the GHS_L in the Likhu Khola region agrees with the criteria of critical taper wedge processes. This includes an increase in temperature and pressure up structural section and syn-kinematic metamorphism. While data from the upper portion of the study area (GHS_U) agree with mid-crustal channel flow processes, which includes protracted crustal residence times at high temperatures and broadly post-peak metamorphism deformation.

Recent work by Larson et al. (2010a, 2011, 2012) and Yakymchuk and Godin (2012) have suggested that there is a continuum between channel flow processes operating in the upper GHS and critical taper wedge processes in the lower GHS. Thermo-mechanical models have also implicitly predicted this transition between channel flow processes in the ductile regime of the hinterland and critical taper wedge processes in the shallower and brittle regime of the foreland (e.g., Jamieson et al., 2004). The data from the GHS_L and GHS_U in the Likhu Khola region fit with the foreland-hinterland transition documented by Larson et al. (2010a) in the Manaslu-Himal Chuli region of west-central Nepal. The pervasively sheared foreland (GHS_L) in the Likhu

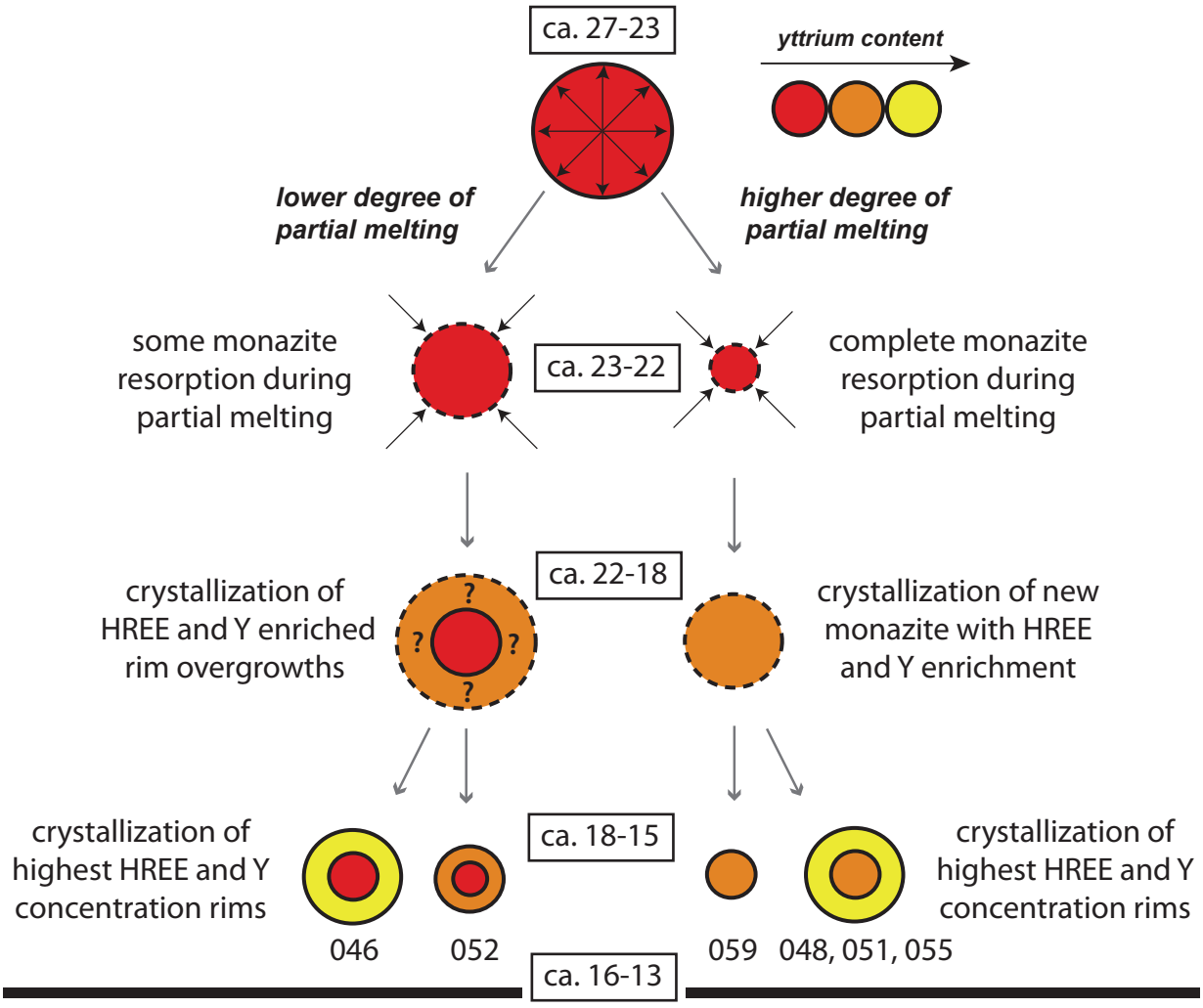

Figure 3.9 - Summary diagram of monazite growth in the Likhu Khola study area incorporating geochronologic and trace element data. Initial monazite growth of Y poor cores synchronous with prograde garnet growth from ca. 28 to 23 Ma was followed by a resorption event from ca. 23 to 22 Ma. Subsequent overgrowth rims sourced from this enriched melt crystallized from ca. 22 to 18 Ma likely in the absence of garnet growth with continued resorption of garnet and likely monazite as well possible during this time. Crystallization of the youngest monazite overgrowth rim ages with the highest enrichments of HREE and Y lasted from ca. 18 to 15 Ma. A leucogranite correlative to the adjacent valley to the west of the Likhu Khola study area constrains the cessation of pervasive deformation and migmatite development to before ca. 16-13 Ma (Larson, 2012).

Khola region is characterized by increased metamorphic temperatures and pressures up structural section going from 566 ± 25 °C at specimen 013 to 851 ± 61 °C at specimen 039 and from 10.8 ± 1.2 kbar at specimen 032 to 11.8 ± 1.4 kbar at specimen 039. No suitable monazite grains were found within the GHS_L to test for diachronous exhumation. Apatite was observed, however attempts to date the apatite with U-Th-Pb techniques were unsuccessful due to irreconcilably large errors due to anomalous common Pb content. However, the P-T data are within error of the deformational temperatures for the GHS_L indicating that deformation was synchronous with metamorphism at this structural level. In addition, distinct delta-type syn-kinematic garnets observed in specimen 013 were the only ones observed throughout the entire study area with the other garnet observed appearing to be more pre-to late syn-kinematic. In contrast to the GHS_L the pervasively sheared migmatitic hinterland (GHS_U) shows metamorphic pressures at peak temperatures that decrease up-section from 11.8 ± 1.4 kbar at specimens 039 to 6.5 ± 1.3 and 7.0 ± 1.4 kbar at specimens 055 and 059 respectively. Timing constraints from U-Th-Pb monazite geochronology provide evidence for protracted metamorphism and/or anatexis from ca. 27 to 15 Ma in the GHS_U.

The location of the proposed discontinuity between the GHS_L and GHS_U occurs just up structural section from specimen 039. A related structure was not readily apparent in the field but the discontinuity may be associated with the increase of anatexite volume recorded up-structural section from station 035. This association between a distinctive quartzite unit, an increase in anatexite content of total rock volume and a metamorphic discontinuity has been noted in the Kali Gandaki region (Larson et al., 2010a; personal observation) in addition to the tama kosi region adjacent to the west of the current study area (Larson, 2012).

These results from the GHS_L and GHS_U in the Likhu Khola region do not entirely agree with either the mid-crustal channel flow or critical taper wedge models. These results are consistent with the foreland/hinterland transition model conceptualized by Price (1972) and applied to the Budhi Gandaki and Tama Kosi regions by Larson et al. (2010a, 2011, 2012) and to the Karnali region by Yakymchuk and Godin (2012). This hybrid model demonstrates that a continuum of vertical thinning and horizontal elongation in the deep hinterland of orogens (mid-crustal channel flow processes) to vertical thickening and horizontal shortening (critical taper wedge processes) in the shallower foreland takes place. This illustrates that viewing mid-crustal flow and critical taper wedge models as end-member processes is a false dichotomy (Beaumont and Jamieson, 2010; Larson et al., 2010a, 2011, 2012; Yakymchuk and Godin, 2012).

CHAPTER 4

CONCLUSIONS AND FUTURE RESEARCH

The lithological, deformational and metamorphic characteristics of the GHS in the Likhu Khola map area, east-central Nepal, have been investigated in order to answer the two main questions posited in first chapter of this thesis: *1) What are the tectonometamorphic characteristics and geologic history of the Likhu Khola region? 2) Are the findings from the Likhu Khola compatible with any of the currently proposed models for the formation and evolution of the Himalayas?*

4.1 Lithologic, deformational and metamorphic framework

Lithological observations and classification of metamorphic zones that increase in grade up-structural section have delineated the inverted metamorphic field gradient that is commonly found in the GHS throughout the Himalaya (e.g., Mallet, 1874; von Loczy, 1878; Oldham, 1883, Hodges, 2000; Searle et al., 2008). The pervasive deformation and high metamorphic grades found throughout the entire study area indicate that all the rocks in this region are part of the GHS and that the Main Central thrust should be placed to the south of the current study area at the base of the pervasive top-to the-south sense of shear. This differs from the most recent field mapping of this region (Schelling, 1992) where the Main Central thrust was placed near the southern extent of the study area structurally above the graphitic schist marker unit. Top-to-the-south shear sense indicators observed throughout the region, especially in the southern portions, include delta-type garnet porphyroblasts, S and C' fabrics and quartz (LPO) fabric analyses. This documented shear sense direction is consistent with shear sense observed within the GHS along

the length of the Himalaya (e.g., Heim and Gansser, 1939; Le Fort, 1975; Burchfiel and Royden, 1985).

4.2 Pressure and temperature (P-T) estimates

P-T estimates from THERMOCALC v.3.26 yield a distinctive pattern enabling division of the GHS in the study area into GHS_L and GHS_U. From specimen 013 in the southernmost portion of the study area, temperatures and pressures increase up-structural section delineating the GHS_L. From maximum pressures at specimen 039, decreasing pressures up-structural section and consistently high temperatures within error of one another outline the GHS_U. A similar pattern has been documented elsewhere in the Himalaya by Larson et al. (2010a) in the Budhi Gandaki region and by Yakymchuk and Godin (2012) in the Karnali region.

4.3 Geochronology and Trace element constraints

Timing constraints from U-Th-Pb monazite geochronology provide evidence for protracted metamorphism in the GHS_U from ca. 27 Ma to 15 Ma. The HREE concentrations and Gd/Yb ratios tied to monazite age data point to initial crystallization of monazite during prograde metamorphism, synchronous with garnet growth, from ca. 27 to 23 Ma. Partial melting of these rocks occurs sometime after ca. 23 Ma during which the garnet, and likely the monazite too, resorb at least partially into the melt (e.g., Larson et al., 2011). At ca. 22 Ma monazite overgrowth rims, and likely new grains, began to form from a melt partially sourced from garnet breakdown that was enriched in HREE; this growth continued until at least ca. 15 Ma. Melt crystallization appears to have continued until the middle Miocene, with cessation of south-directed deformation and migmatite development in this region by ca. 16-13 Ma (Larson, 2012). This span of monazite ages likely represents the effects of a single prolonged metamorphic

event, possibly related to Eohimalayan metamorphism during southward extrusion of the GHS from mid-crustal depths.

4.4 Which model fits?

Since neither of the currently proposed end-member models of critical taper wedge or mid-crustal channel flow fit the complete data for the Likhu Khola region a proposed hybrid model with a continuum between these commonly though end-member modes must be considered. This hybrid model initially conceptualized by Price (1972) and applied to the Budhi Gandaki and Tama Kosi regions by Larson et al. (2010a, 2011, 2012) and to the Karnali region by Yakymchuk and Godin (2012) demonstrates a continuum of vertical thinning and horizontal elongation in the mid-crustal hinterland of orogens (mid-crustal channel flow processes) to vertical thickening and horizontal shortening (critical taper wedge processes) in the shallower foreland illustrating that viewing mid-crustal flow and critical taper wedge models as end-member processes is a false dichotomy (Beaumont and Jamieson, 2010; Larson et al., 2010a, 2011, 2012; Yakymchuk and Godin, 2012).

In the GHS_L of the Likhu Khola region P-T data documents an increase in temperature and pressure up-structural section from specimen 013 to 039. Syn-kinematic metamorphism was observed distinctly within specimen 013 as large delta-type garnet porphyroblasts to indicate syn-kinematic deformation. These characteristics are consistent with accreted slices of material being incorporated into the GHS from younger and lower grade rocks from structurally below the GHS during downward migration of the MCT shear zone during critical taper wedge processes.

In the GHS_U of the Likhu Khola region P-T data documents decreasing pressure up-structural section from specimen 039 to 059 immediately after the increasing pressure up-

structural section in the GHS_L. Timing constraints from U-Th-Pb monazite geochronology provide evidence for protracted crustal residence times with metamorphism occurring from ca. 27 Ma to ca. 15 Ma with cessation of south directed deformation in this region by 16-13 Ma (Larson, 2012). These characteristics are consistent with mid-crustal channel flow processes.

The location of the proposed discontinuity between the GHS_L and GHS_U occurs just up structural section from specimen 039 to as far as specimen 046. The research conducted for this study within the GHS best fits the models of Larson et al. (2010a) and Yakymchuk and Godin (2012) that predict a combination of critical taper wedge and mid-crustal channel flow separated by a discontinuity.

4.5 Future work

This research within the GHS of the Likhu Khola region in east-central Nepal contributes to the expanding database of P-T and geochronology data from the exhumed mid-crustal core of the Himalaya. As this study represents the first analytical data from the Likhu Khola region it would be complemented by an expansion of the map area to the south where more constraints of P-T and geochronology could be used to further quantify the characteristics of the GHS_L in this region. Geochronologic data from GHS_L in this region would allow for the evaluation of potentially diachronous metamorphism and deformation of the GHS_L rocks as predicted by critical taper wedge processes. Moreover, thermochronologic data, such as $^{40}Ar/^{39}Ar$ techniques would be useful for constraining the exhumation history of the area. Finally, phase equilibria modeling is also recommended for selected specimens throughout the study area in order to delineate pressure-temperature-time-deformation (P-T-t-D) paths. Reconstruction of P-T-t-D paths can provide a more detailed tectonometamorphic history and insight into the tectonic processes responsible for the P-T-t-D pathways of selected specimens.

REFERENCES

Allegre, C.J., Courtillot, V., Tapponnier, P., Hirn, A., Mattauer, M., Coulon, C., Jaeger, J.J., Achache, J., Schärer, U., and Marcoux, J. 1984. Structure and evolution of the Himalaya–Tibet orogenic belt. *Nature,* 307: 17-22.

Beaumont, C., Jamieson, R.A., Nguyen, M.H., and Lee, B. 2001. Himalayan tectonics explained by extrusion of a low-viscosity crustal channel coupled to focused surface denudation. *Nature*, 414: 738-742.

Beaumont, C., and Jamieson, R.A., 2010. Himalayan-Tibetan orogeny: Channel flow versus (critical) wedge models, a false dichotomy?, in Leech, M.L., et al., eds., *Proceedings for the 25th Himalaya-Karakoram-Tibet Workshop*: U.S. Geological Survey Open-File Report 2010-1099, 2 p., http://pubs.usgs.gov/of/2010/1099/beaumont/.

Beaumont, C and Jamieson, R., A. 2011. "channel flow vs. critical taper wedge: a false dichotomy?". *26th Himalaya-Karakoram-Tibet Workshop*, Canmore, Canada, July 12-13, 2011.

Besse, J., Courtillot, V., Pozzi, J.P., Westphal, M., and Zhou, Y.X. 1984. Palaeomagnetic estimates of crustal shortening in the Himalayan thrusts and Zangbo suture. *Nature,* 311: 621-626.

Bird, P. 1991. Lateral extrusion of the lower crust from under high topography, in the isostatic limit. *Journal of Geophysical Research, B, Solid Earth and Planets*, 96: 10,275-10,286.

Bollinger, L., Henry, P., and Avouac, J.P., 2006, Mountain building in the Nepal Himalaya: Thermal and kine- matic model. *Earth and Planetary Science Letters*, 244: 58–71, doi: 10.1016/j.epsl.2006.01.045.

Bordet, P. 1961. Researches geologiques dens L* Himalaya du Nepal region, du Makalu. *Cent. Nat. De La Re.*

Bouchez, J. L., and Pêcher, A. 1976. Microstructures and quartz preferred orientations in quartzites of the Annapurna area (central Nepal), in the proximity of the main central thrust. *Himalayan geology*, *6*: 118-131.

Buick, I. S., Allen, C., Pandit, M., Rubatto, D., and Hermann, J. 2006. The Proterozoic magmatic and metamorphic history of the Banded Gneiss Complex, central Rajasthan, India: LA-ICP-MS U–Pb zircon constraints. *Precambrian Research*, 151: 119-142.

Burbank, D.W., Derry, L.A., and France-Lanord, C. 1993. Reduced Himalayan sediment production 8 Myr ago despite an intensified monsoon. *Nature,* 364: 48-50.

Burchfiel, B.C., Zhiliang, C., Hodges, K.V., Yuping, L., Royden, L.H., Changrong, D., and Jiene, X., 1992. The South Tibetan detachment system, Himalaya orogen: extension contemporaneous with and parallel to shortening in a collisional mountain belt. *Geological Society of America Special Paper*, 269: 1-41.

Burchfiel, B. C., and Royden, L. H. 1985. North-south extension within the convergent Himalayan region, Geology, 13: 679-682.

Burg, J.P., and Chen, G.M., 1984. Tectonics and structural zonation of southern Tibet, China. *Nature*, 311: 219-223.

Burg, J.P., Brunel, M., Gapais, D., Chen, G.M., and Liu, G.H., 1984. Deformation of leucogranites of the crystalline Main Central Sheet in southern Tibet (China). *Journal of Structural Geology*, 6(5): 535-542.

Carmichael, D. M. 1969. On the mechanism of prograde metamorphic reactions in quartz-bearing pelitic rocks. *Contributions to Mineralogy and Petrology*, 20: 244-267.

Carosi, R., Montomoli, C., Rubatto, D., and Visonà, D. 2010. Late Oligocene high-temperature shear zones in the core of the Higher Himalayan Crystallines (Lower Dolpo, western Nepal). *Tectonics*, 29: TC4029.

Catlos, E.J., Harrison T.M., Manning C.E., Grove M., Rai S.M., Hubbard M.S., and Upreti B.N. 2002. Records of the evolution of the Himalayan orogen from in situ Th-Pb ion microprobe dating of monazite: Eastern Nepal and western Garhwal. *Journal of Asian Earth Sciences,* 20: 459-479.

Catlos, E.J., Harrison, T.M., Kohn, M.J., Grove, M., Ryerson, F.J., Manning, C.E., and Upreti, B.N. 2001. Geochronologic and thermobarometric constraints on the evolution of the Main Central Thrust, central Nepal Himalaya. *Journal of Geophysical Research*, 106: 16,177-16,204.

Catlos, E.J., Harrison, T.M., Manning, C.E., Grove, M., Rai, S.M., Hubbard, M.S., and Upreti, B.N. 2002. Records of the evolution of the Himalayan orogen from in situ Th-Pb ion microprobe dating of monazite: Eastern Nepal and western Garhwal. *Journal of Asian Earth Sciences,* 20: 459-479.

Cattin, R., and Avouac, J.P. 2000. Modeling mountain building and the seismic cycle in the Himalaya of Nepal. *Journal of Geophysical Research,* 105: 13389-13407.

Clift, P., D., Hodges, K., V. 2008. Correlation of Himalayan exhumation rates and Asian monsoon intensity. *Nature Geoscience,* 351: 875-880

Clift, P.D., Tada, R., and Zheng, H. 2010. Monsoon evolution and tectonics-climate linkage in Asia: an introduction. *Geological Society, London, Special Publications,* 342: 1-4.

Colchen, M., Mascle, G., and Van Haver, T. 1986. Some aspects of collision tectonics in the Indus suture zone, Ladakh. *Geological Society, London, Special Publications* 19: 173-184.

Corrie, S. L., Kohn, M. J., McQuarrie, N., and Long, S. P. 2012. Flattening the Bhutan Himalaya. *Earth and Planetary Science Letters*, *349*: 67-74.

Cottle, J.M., Searle, M.P., Horstwood, M.S.A., and Waters, D.J. 2009. Timing of midcrustal metamorphism, melting, and deformation in the Mount Everest region of southern Tibet revealed by U (-Th)-Pb geochronology. *The Journal of Geology,* 117: 643-664.

Cottle, J.M., Waters, D.J., Riley, D., Beyssac, O., Jessup, M.J. 2011. Metamorphic history of the South Tibetan Detachment System, Mt. Everest Region, Revealed by RSCM Thermometry and Phase Equilibria Modeling. *Journal of Metamorphic Geology*, doi: 10.1111/j.1525-1314.2011.00930

Coward, M.P., Butler, R.W.H., Khan, M.A., and Knipe, R.J., 1987. The tectonic history of Kohistan and its implications for Himalayan structure. *Journal of the Geological Society, London*, 144: 377-391.

Davis, D., Suppe, J., and Dahlen, F.A. 1983. Mechanics of fold-and-thrust belts and accretionary wedges. *Journal of Geophysical research,* 88: 1153-1172.

Dahlen, F.A. 1990. Critical taper model of fold-and-thrust belts and accretionary wedges. *Annual Review of Earth and Planetary Sciences*, 18: 55-99.

Daniel, C.G., Hollister, L.S., Parrish, R.R., and Grujic, D. 2003. Exhumation of the Main Central Thrust from lower crustal depths, eastern Bhutan Himalaya. *Journal of Metamorphic Geology,* 21: 317-334.

DeCelles, P.G., Gehrels, G.E., Quade, J., LaReau, B., and Spurlin, M., 2000, Tectonic implications of U-Pb, zircon ages of the Himalayan orogenic belt in Nepal: *Science*, 288: 497–499.

DeCelles, P.G., Robinson, D.M., Quade, J., Ojha, T.P., Garzione, C.N., Copeland, P., and Upreti, B.N. 2001. Stratigraphy, structure, and tectonic evolution of the Himalayan fold-thrust belt in western Nepal. *Tectonics,* 20: 487-509.

Dewey, J.F., and Burke, K. 1974. Hot spots and continental break-up: implications for collisional orogeny. *Geology,* 2: 57-60.

Dewey, J.F., and Burke, K.C.A. 1973. Tibetan, Variscan, and Precambrian basement reactivation: products of continental collision. *The Journal of Geology, 81:* 683-692.

Florence, F.P., and Spear, F.S. 1991. Effects of diffusional modification of garnet growth zoning on P-T path calculations. *Contributions to Mineralogy and Petrology*, 107, 487-500.

Foster, G., Gibson, H. D., Parrish, R., Horstwood, M., Fraser, J., and Tindle, A. 2002. Textural, chemical and isotopic insights into the nature and behaviour of metamorphic monazite. *Chemical Geology*, 191: 183-207.

Fraser, G. Worley B., Sandiford M. 2000. High-precision geothermobarometry across the High Himalayan metamorphic sequence, Langtang Calley, Nepal. *Journal of Metamorphic Geology*, *18*: 665-681.

Gansser, A. 1964. Geology of the Himalayas. *Interscience Publishers London*.

Gansser, A. 1983. The Wilder Himalaya, a Model for Scientific Research. *Kommissionaer: Munksgaard*.

Garzanti, E. 2008. Comment on "When and where did India and Asia collide?" by Jonathan C. Aitchison, Jason R. Ali, and Aileen M. Davis. *Journal of Geophysical Research,* 113: B04411.

Gehrels, G.E., DeCelles, P.G., Ojha, T.P., and Upreti, B.N. 2006. Geologic and U-Th-Pb geochronologic evidence for early Paleozoic tectonism in the Kathmandu thrust sheet, central Nepal Himalaya. *Geological Society of America Bulletin,* 118: 185-198.

Gervais, F., and Brown, R. L. 2011. Testing modes of exhumation in collisional orogens: Synconvergent channel flow in the southeastern Canadian Cordillera. *Lithosphere*, 3: 55-75.

Gibson, H. D., Carr, S. D., Brown, R. L., and Hamilton, M. A. 2004. Correlations between chemical and age domains in monazite, and metamorphic reactions involving major pelitic phases: an integration of ID-TIMS and SHRIMP geochronology with Y–Th–U X-ray mapping. *Chemical Geology*, 211: 237-260.

Godin, L., Parrish, R.R., Brown, R.L., and Hodges, K.V., 2001. Crustal thickening leading to exhumation of the Himalayan metamorphic core of central Nepal: insight from U-Pb geochronology and 40Ar/39Ar thermochronology. *Tectonics*, 20(5): 729-747.

Godin, L., Grujic, D., Law, R.D., and Searle, M.P. 2006a. Channel flow, ductile extrusion and exhumation in continental collision zones: an introduction. In Law, R.D., Searle, M.P., and Godin, L. (eds). Channel Flow, Ductile Extrusion and Exhumation in Continental Collision Zones. *Geological Society of London Special Publications*, 268: 1-23.

Godin, L., Gleeson, T.P., Searle, M.P., Ullrich, T.D., and Parrish, R.R. 2006b. Locking of the southward extrusion in favour of rapid crustal-scale buckling of the Greater Himalayan sequence, Nar valley, central Nepal. In Law, R.D., Searle, M.P., and Godin, L. (eds). Channel Flow, Ductile Extrusion and Exhumation in Continental Collision Zones. *Geological Society of London Special Publications*, 268: 269- 292.

Grujic, D. 2006. Channel flow and continental collision tectonics: an overview. In Law, R.D., Searle, M.P., and Godin, L. (eds). Channel Flow, Ductile Extrusion and Exhumation in Continental Collision Zones. *Geological Society of London Special Publications*, 268: 25-37.

Grujic, D., Casey, M., Davidson, C., Hollister, L.S., Kündig, R., Pavlis, T., and Schmid, S. 1996. Ductile extrusion of the Higher Himalayan Crystalline in Bhutan: evidence from quartz microfabrics. *Tectonophysics*, 260: 21-43.

Grujic, D. Hollister, L.S., and Parrish, R.R. 2002. Himalayan metamorphic sequence as an orogenic channel: Insight from Bhutan. *Earth and Planetary Science Letters,* 198: 177-191.

Guillot, S., Cosca, M., Allemand, P., and Le Fort, P., 1999. Contrasting metamorphic and geochronologic evolution along the Himalayan belt, *in* Macfarlane, A., Sorkhabi, R. B., and Quade, J., eds., Himalaya and Tibet: Mountain roots to mountain tops: *Geological Society of America Special Paper,* 328: 117–128.

Harris, N. 2007. Channel flow and the Himalayan–Tibetan orogen: a critical review. *Journal of the Geological Society,* 164: 511-523.

Harris, N. 2007. Channel flow and the Himalayan-Tibetan orogen: a critical review. *Journal of the Geological Society of London,* 164: 511-523.

Harrison, T.M., Ryerson, F.J., Le Fort, P., Yin, A., Lovera, O.M., and Catlos, E.J. 1997. A Late Miocene-Pliocene origin for the Central Himalayan inverted metamorphism. *Earth and Planetary Science Letters*, 146: E1-E7.

Harrison, T.M. 2006. Did the Himalayan Crystallines extrude partially molten from beneath the Tibetan Plateau? *Geological Society, London, Special Publications,* 268: 237-254.

Hauck, M.L., Nelson, K.D., Brown, L.D., Zhao, Wenjin and Ross, A.R. 1998. Crustal structure of the Himalayan orogen at ~90 east longitude from Project INDEPTH deep reflection profiles. *Tectonics*, 17(4): 481-500.

Hébert R., Bezard R., Guilmette C., Dostal, J., and Wang, C. 2011. The Indus-Yarlung Zangbo ophiolites belt: A Mariana arc-backarc system analog. *26th Himalaya-Karakoram-Tibet Workshop*, Canmore, Canada, July 12-13, 2011.

Heim, A.A., and Gansser, A. 1939. Central Himalaya: geological observations of the Swiss expedition, 1936. *Hindustan Pub. Corp.(India).*

Tippett, C. R. 1984. Geology of a transect through the southern margin of the Foxe fold belt (mainly NTS 27B), central Baffin Island, District of Franklin. Geological Survey of Canada, Open File 1110.

Henry, P., LePichon, X., and Goffé, B., 1997, Kinematic, thermal and petrological model of the Himalayas: Constraints related to metamorphism within the underthrust Indian crust and topographic evolution. *Tectonophysics*, 273: 31–56, doi: 10.1016/S0040- 1951(96)00287-9.

Hirth, G., and Tullis, J., 1992, Dislocation creep regimes in quartz aggregates: *Journal of Structural Geology*, 14: 145-160.

Hodges, K.V. 2000. Tectonics of the Himalaya and southern Tibet from two perspectives. *Geological Society of America Bulletin,* 112: 324-350.

Hodges, K.V. 2006. A synthesis of the Channel Flow-Extrusion hypothesis as developed for the Himalayan-Tibetan orogenic system. *Geological Society, London, Special Publications,* 268: 71-90.

Hodges, K.V., and Silverberg, D.S. 1988a. Thermal evolution of the Greater Himalaya, Garhwal, India. *Tectonics*, 7: 583-600.

Hodges, K. V., Hubbard, M. S., and Silverberg, D. S., 1988b, Metamorphic constraints on the thermal evolution of the central Himalayan orogen. *Royal Society of London Philosophical Transactions*, A-326: 257–280.

Hodges, K.V., Parrish, R., Housch, T., Lux, D., Burchfiel, B.C., Royden, L., and Chen, Z. 1992. Simultaneous Miocene extension and shortening in the Himalayan orogen. *Science*, 258: 1466-1470.

Hodges, K.V., Parrish, R.R., and Searle, M.P. 1996. Tectonic evolution of the central Annapurna range, Nepalese Himalaya. *Tectonics*, 15: 1264-1291.

Hodges, K.V., Hurtado, J.M., and Whipple, K.X. 2001. Southward extrusion of Tibetan crust and its effect on Himalayan. *Tectonics* 20: 799-809.

Holdaway, M.J., 2000. Application of new experimental and garnet Margules data to the garnet–biotite geothermometer. *American Mineralogist.* 85: 881–892.

Holdaway, M.J., 2001. Recalibration of the GASP geobarometer in light of recent garnet and plagioclase activity models and versions of the garnet–biotite geothermometer. *American Mineralogist*. 86: 1117–1129.

Holland, T.J.B., and Powell, R. 1998. An internally-consistent thermodynamic dataset for phases of petrological interest. *Journal of Metamorphic Geology, 16*: 309-344.

Horstwood, M. S., Foster, G. L., Parrish, R. R., Noble, S. R., and Nowell, G. M. 2003. Common-Pb corrected in situ U–Pb accessory mineral geochronology by LA-MC-ICP-MS. *Journal of Analytical Atomic Spectrometry*, 18: 837-846.

Hubbard, M.S., and Harrison, T.M. 1989. 40Ar/39Ar age constraints on deformation and metamorphism in the Main Central Thrust zone and Tibetan Slab, eastern Nepal Himalaya. *Tectonics*, 8: 865-880.

Hurtado Jr, J.M., Hodges, K.V., and Whipple, K.X. 2001. Neotectonics of the Thakkhola graben and implications for recent activity on the South Tibetan fault system in the central Nepal Himalaya. *Geological Society of America Bulletin,* 113: 222-240.

Iacopini, D., Carosi R., Montomoli C., and Passchier C.W. 2008. Strain analysis and vorticity of flow in the Northern Sardinian Variscan Belt: Recognition of a partitioned oblique deformation

event. *Tectonophysics,* 446: 77-96.

Iacopini, D., Frassi, C., and Carosi, R., and Montomoli C. 2011. Biases in three-dimensional vorticity analysis using porphyroclast system: limits and application to natural examples. *Geological Society Special Publications, London,* 360: 301-318.

Ishida, T. 1969. Petrography and structure of the area between the Dudh Kosi and the Tamba Kosi, east Nepal. *Journal of the Geological Society of Japan,* 75: 115-125.

Ishida, T., and Ohta Y. 1973. Ramechhap-Okhaldhunga region. *Hashimota, S., Himalayan Committee of Hokkaido Univ.(Supervisor), Geology of the Nepal Himalayas. Sapporo (Hokkaido Univ.), Japan, Saikon Publishing Company.* 35-67.

Jamieson, R.A., Beaumont, C., Medvedev, S., and Nguyen, M.H. 2004. Crustal channel flows: 2. Numerical models with implications for metamorphism in the Himalayan-Tibetan orogen. *Journal of Geophysical Research*, 109: doi: 10.1029/2003JB002811.

Jamieson, R.A., Beaumont, C., Nguyen, M.H., and Grujic, D. 2006. Provenance of the Greater Himalayan Sequence and associated rocks: predictions of channel flow models. In Law, R.D., Searle, M.P., Godin, L. (eds). Channel Flow, Ductile Extrusion and Exhumation in Continental Collision Zones. *Geological Society of London Special Publications*, 268: 165-182.

Jessup, M.J., Law, R.D., Searle, M.P., and Hubbard, M.S. 2006. Structural evolution and vorticity of flow during extrusion and exhumation of the Greater Himalayan Slab, Mount Everest Massif, Tibet/Nepal: implications for orogen-scale flow partitioning. In Law, R.D., Searle, M.P., and Godin, L. (eds). Channel Flow, Ductile Extrusion and Exhumation in Continental Collision Zones. *Geological Society of London Special Publications,* 268: 379-413.

Jessup, M. J., Cottle, J. M., Searle, M. P., Law, R. D., Newell, D. L., Tracy, R. J., and Waters, D. J. 2008. P–T–t–D paths of Everest Series schist, Nepal. *Journal of Metamorphic Geology*, 26: 717-739.

Jessup, M.J., and Cottle, J.M. 2010. Progression from South-Directed Extrusion to Orogen-Parallel Extension in the Southern Margin of the Tibetan Plateau, Mount Everest Region, Tibet. *The Journal of Geology,* 118: 467-486.

Kellett, D. A., Grujic, D., Warren, C., Cottle, J., Jamieson, R., and Tenzin, T. 2010. Metamorphic history of a syn-convergent orogen-parallel detachment: The South Tibetan detachment system, Bhutan Himalaya. *Journal of Metamorphic Geology*, *28:* 785-808.

Kerrick, D. M., 1990. The Al2SiO5 Polymorphs. Ed. Series ed. Paul H. Ribbe. Mineralogical Society of America, 22: 1-406

Kohn, M. J., Wieland, M. S., Parkinson, C. D., and Upreti, B. N. 2005. Five generations of monazite in Langtang gneisses: implications for chronology of the Himalayan metamorphic core. *Journal of Metamorphic Geology*, 23: 399-406.

Kohn, M.J. 2008. P-T-t data from central Nepal support critical taper and repudiate large- scale channel flow of the Greater Himalayan Sequence. *Geological Society of America Bulletin*, 120: 259-273.

Kohn, M.J., and Spear, F.S. 2000. Retrograde Net Transfer Reaction (ReNTR) Insurance for P-T Estimates. Geology, 28, 1127-1130.

Kruhl, J.H. 1998. Reply: Prism- and basal-plane parallel subgrain boundaries in quartz: a microstructural geothermobarometer. Journal of Metamorphic Geology, 16: 142-146.

Langille, J., Lee, J., Hacker, B., and Seward, G. 2010. Middle crustal ductile deformation patterns in southern Tibet: Insights from vorticity studies in Mabja Dome. *Journal of Structural Geology*, *32*: 70-85.

Larson, K.P. 2012. The geology of the Tama Kosi and Rolwaling Valley Region, East-Central Nepal. Geosphere, 8: doi:10.1130/GES00711.1.

Larson, K.P., Cottle, J., and Godin, L. 2011. Petrochronologic record of metamorphism and melting in the upper Greater Himalayan sequence, Manaslu– Himal Chuli Himalaya, west-central Nepal *Lithosphere*, 3: 379-392

Larson, K.P., and Godin, L. 2009. Kinematics of the Greater Himalayan sequence, Dhaulagiri Himal: implications for the structural framework of central Nepal. *Journal of the Geological Society, London*, 166: 25-43.

Larson, K.P., Godin, L., and Price, R.A. 2010a. Relationships between displacement and distortion in orogens: Linking the Himalayan foreland and hinterland in central Nepal. *GSA Bulletin*, 122: 1116-1134.

Larson, K.P., Godin, L., Davis, W.J., and Davis, D.W. 2010b. Out-of-sequence deformation and expansion of the Himalayan orogenic wedge: insight from the Changgo culmination, south-central Tibet. *Tectonics*, 29: TC4013.

Law, R. D., Searle, M. P., and Simpson, R. L. 2004. Strain, deformation temperatures and vorticity of flow at the top of the Greater Himalayan Slab, Everest Massif, Tibet. *Journal of the Geological Society of London,* 161: 305-320.

Law, R.D. 1991. Crystallographic fabrics: a selective review of their applications to research in structural geology. In Knipe, R.J., and Rutter, E.H. (eds). Deformation Mechanisms, Rheology, and Tectonics. *Geological Society of London Special Publications,* 54: 335-352.

Le Fort, P., 1975. Himalayas: the collided range. Present knowledge of the continental arc. *American Journal of Science*, 275-A, 1-44.

Lister, G. S., Paterson, M. S., and Hobbs, B. E. 1978. The simulation of fabric development in plastic deformation and its application to quartzite: the model. *Tectonophysics*, 45: 107-158.

Lister, G. S., and Hobbs, B. E. 1980. The simulation of fabric development during plastic deformation and its application to quartzite: the influence of deformation history. *Journal of Structural Geology*, 2: 355-370.

Lister, G. S., and Dornsiepen, U. F. 1982. Fabric transitions in the Saxony granulite terrain. *Journal of Structural Geology*, *4:* 81-92.

Ludwig, K. R. 2003. Isoplot/Ex Version 3.00: a geological toolkit for Microsoft Excel. *Berkeley Geochronology Center Special Publication, 70pp*.

Mallet, F.R. 1874. *On the Geology and Mineral Resources of the Dárjíling District and the Western Duára*. Printed for the Government of India.

Mainprice, D., Bouchez, J. L., Blumenfeld, P., and Tubià, J. M. 1986. Dominant c slip in naturally deformed quartz: implications for dramatic plastic softening at high temperature. *Geology*, 14: 819-822.

Mainprice, D., and Nicolas, A. 1989. Development of shape and lattice preferred orientations: application to the seismic anisotropy of the lower crust. *Journal of Structural Geology*, 11: 175-189.

Martin, A.J., DeCelles, P.G., Gehrels, G.E., Patchett, P.J., and Isachsen, C. 2005. Isotopic and structural constraints on the location of the Main Central thrust in the Annapurna Range, central Nepal Himalaya. *Geological Society of America Bulletin*, 117: 926-944.

Martin, A. J., Ganguly, J., and DeCelles, P. G. 2010. Metamorphism of Greater and Lesser Himalayan rocks exposed in the Modi Khola valley, central Nepal. *Contributions to Mineralogy and Petrology*, 159: 203-223.

Martin, A.J., and Ducea, M.N. 2011. Pre-Cenozoic peak metamorphism and deformation of Lesser Himalayan rocks in Nepal. *Journal of Himalayan Earth Sceinces,* 44: 56.

Molnar, P., 1984. Structure and tectonics of the Himalaya: constraints and implications of geophysical data. *Annual Review of Earth and Planetary Sciences*, 12: 489- 518.

Molnar P., and England P. 1990. Temperatures, heat flux, and frictional stress near major thrust faults. *Journal of geophysical Research,* 95: 4833-4856.

Molnar, P., England, P., and Martinod, J. 1993. Mantle dynamics, uplift of the Tibetan Plateau, and the Indian Monsoon*. Reviews of Geophysics*, 31: 357–396.

Mukherjee, S., and Koyi, H.A. 2010. Higher Himalayan Shear Zone, Zanskar Indian Himalaya: microstructural studies and extrusion mechanism by a combination of simple shear and channel flow. *International Journal of Earth Sciences,* 99: 1083-1110.

Najman, Y., Appel, E., Boudagher-Fadel, M., Bown, P., Carter, A., Garzanti, E., Godin, L., Han, J., Liebke, U., Oliver, G., Parrish, R., and Vezzoli, G. 2010. The timing of India-Asia collision: geological, biostratigraphic and palaeomagnetic constraints. *Journal of Geophysical Research*, 115, B12416, doi:10.1029/2010JB007673.

Najman, Y., Carter, A., Oliver, G., and Garzanti, E., 2005. Provenance of Eocene foreland basin sediments, Nepal: Constraints to the timing and diachroneity of early Himalayan orogenesis. *Geology*, 33(4): 309-312.

Nelson, K.D., Zhao, W., Brown, L.D., Kuo, J., Che, J., Liu, X., Klemperer, S.L., Makovsky, Y., Meissner, R., and Mechie, J. 1996. Partially molten middle crust beneath southern Tibet: synthesis of project INDEPTH results. *Science,* 274: 1684-1688.

Oldham, R.D. 1883. *Note on the geology of Jaunsar and the Lower Himalayas*.

Owen, L. A. 2006. Tectonic uplift and continental configurations. In: Scott, E. (ed.) *Encyclopedia of Quaternary Science,* Vol. 2. Elsevier, Oxford, 1011–1016.

Paquette, J. L., Nédélec, A., Moine, B., and Rakotondrazafy, M. 1994. U-Pb, single zircon Pb-evaporation, and Sm-Nd isotopic study of a granulite domain in SE Madagascar. *The Journal of Geology*, 523-538.

Passchier, C.W., and R.A.J. Trouw. 2005. *Microtectonics*. Springer Verlag.

Parrish, R.R., and Hodges, K.V. 1996. Isotopic constraints on the age and provenance of the Lesser and Greater Himalayan sequences, Nepalese Himalaya. *Geological Society of America Bulletin*, 108: 904-911.

Patriat, P., and Achache, J. 1984. India–Eurasia collision chronology has implications for crustal shortening and driving mechanism of plates. *Nature,* 311: 615-621.

Pêcher, A. 1989. The metamorphism in the Central Himalaya. *Journal of Metamorphic Geology*, 7: 31-41.

Peternell, M., Hasalová, P., Wilson, C. J. L., Piazolo, S., and Schulmann, K., 2010. Evaluating quartz crystallographic preferred orientations and the role of deformation partitioning using EBSD and Fabric Analyser techniques. *Journal of Structural Geology* 32: 803-817. doi:10.1016/j.jsg.2010.05.007

Petterson, M.G., and Windley, B.F. 1985. RbSr dating of the Kohistan arc-batholith in the Trans-Himalaya of north Pakistan, and tectonic implications. *Earth and Planetary Science Letters,* 74: 45-57.

Prell, W. L., and Kutzbach, J. E. 1992. Sensitivity of the Indian Monsoon to forcing parameters and implications for its evolution. *Nature,* 360: 647–652.

Price, R.A. 1972. The distinction between displacement and distortion in flow, and the origin of diachronism in tectonic overprinting in orogenic belts: *Proceedings, 24th International Geological Congress*, Montreal, Canada, Section 3: 545–551.

Priestley, K., Jackson, J., and McKenzie, D. 2008. Lithospheric structure and deep earthquakes beneath India, the Himalaya and southern Tibet. *Geophysical Journal International,* 172: 345-362.

Pyle, J.M., Spear, F.S., Rudnick, R.L., and McDonough, W.F. 2001. Monazite-xenotime and monazite-garnet equilibrium in a prograde pelite sequence. Journal of Petrology, 42, 2083-2107.

Pyle, J. M., and Spear, F. S. 1999. Yttrium zoning in garnet: coupling of major and accessory phases during metamorphic reactions. Geological Materials Research (http://gmr.minsocam.org), 1, 1-49.

Richards, A., Argles, T., Harris, N., Parrish, R., Ahmad, T., Darbyshire, F., and Draganits, E. 2005. Himalayan architecture constrained by isotopic tracers from clastic sediments. *Earth and Planetary Science Letters,* 236: 773-796.

Richards, A., Parrish, R., Harris, N., Argles, T., and Zhang, L. 2006. Correlation of lithotectonic units across the eastern Himalaya, Bhutan. *Geology,* 34: 341.

Robinson, D.M. 2008. Forward modeling the kinematic sequence of the central Himalaya thrust belt, western Nepal. *Geosphere*, 4: 785-801.

Robinson, D.M., DeCelles, P.G., Patchett, P.J., Garzione, C.N. 2001. The kinematic evolution of the Nepalese Himalaya interpreted from Nd isotopes. *Earth and Planetary Science Letters*, 192: 507-521.

Robinson, D.M., DeCelles, P.G., and Copeland, P. 2006. Tectonic evolution of the Himalayan thrust belt in western Nepal: Implications for channel flow models. *Geological Society of America Bulletin*, 118: 865-885.

Rowley, D.B., 1996. Age of initiation of collision between India and Asia: a review of stratigraphic data. *Earth and Planetary Science Letters*, 145: 1-13.

Rowley, D.B., 1998. Minimum age of initiation of collision between India and Asia north of Everest based on the subsidence history of the Zhepure mountain section. *The Journal of Geology*, 106: 229-235.

Rubatto D., Hermann J., Buick I.S. 2006. Temperature and bulk composition control on the growth of monazite and zircon during low-pressure anatexis (Mount Stafford, central Australia). *Journal of Petrology*. 47: 1973-1996.

Rubatto, D., Chakraborty, S., and Dasgupta, S. 2012. Timescales of crustal melting in the Higher Himalayan Crystallines (Sikkim, Eastern Himalaya) inferred from trace element-constrained monazite and zircon chronology. *Contributions to Mineralogy and Petrology*, 1-24.

Ruddiman W.F. 1997. *Tectonic uplift and climate change*. New York, Plenum Publishing Corporation.

Schelling D. 1992. The tectonostratigraphy and structure of the eastern Nepal Himalaya. *Tectonics,* 11: 925-943.

Searle, M.P., Cooper, D.J.W., Rex, A.J., Herren, E., Rex, A.J., and Colchen, M. 1988. Collision Tectonics of the Ladakh--Zanskar Himalaya [and Discussion]. *Philosophical Transactions of the Royal Society of London,* Series A, Mathematical and Physical Sciences: 117-150.

Searle, M.P., Pickering, K.T., and Cooper, D.J.W. 1990. Restoration and evolution of the intermontane Indus molasse basin, Ladakh Himalaya, India. *Tectonophysics,* 174: 301-314.

Searle, M., Corfield, R.I., Stephenson, B., and McCarron, J. 1997. Structure of the North Indian continental margin in the Ladakh-Zanskar Himalayas: implications for the timing of obduction of the Spontang ophiolite, India-Asia collision and deformation events in the Himalaya. *Geological Magazine*, 134: 297-316.

Searle, M. P., Noble, S. R., Hurford, A. J., and Rex, D. C. 1999. Age of crustal melting, emplacement and exhumation history of the Shivling leucogranite, Garhwal Himalaya. *Geological Magazine*, 136: 513-525.

Searle, M., and Godin, L., 2003. The South Tibetan Detachment and the Manaslu Leucogranite: a structural reinterpretation and restoration of the Annapurna- Manaslu Himalaya, Nepal. *The Journal of Geology,* 111: 505-523.

Searle, M.P., Simpson, R.L., Law, R.D., Parrish, R.R., and Waters, D.J. 2003. The structural geometry, metamorphic and magmatic evolution of the Everest massif, High Himalaya of Nepal–South Tibet. *Journal of the Geological Society* 160: 345-366.

Searle, M.P., Law, R.D., and Jessup, M. 2006. Crustal structure, restoration and evolution of the Greater Himalaya in Nepal-South Tibet: implications for channel flow and ductile extrusion of the middle crust. In Law, R.D., Searle, M.P., and Godin, L. 201(eds). Channel Flow, Ductile Extrusion and Exhumation in Continental Collision Zones. *Geological Society of London Special Publications*, 268: 355-378.

Searle, M.P., Law, R.D., Godin, L., Larson, K.P., Streule, M.J., Cottle, J.M., and Jessup, M.J. 2008. Defining the Himalayan Main Central Thrust in Nepal. *Journal of the Geological Society*, 165: 523-534.

Searle, M.P., Cottle, J.M., Streule, M.J., and Waters, D.J. 2010. Crustal melt granites and migmatites along the Himalaya: melt source, segregation, transport and granite emplacement

mechanisms. *Transactions of the Royal Society of Edinburgh,* 100: 219-233.

Simpson, R. L. 2002. *Metamorphism, melting and extension at the top of the High Himalayan slab, Mount Everest region, Nepal and Tibet* (Doctoral dissertation, University of Oxford).

Spear, F.S., 1993. Metamorphic phase equilibria and pressure-temperature-time paths. *MineralogicalSocietyofAmerica,* 799pp.

Spear, F.S., Kohn, M.J., and Cheney, J.T. 1999. P-T paths from anatectic pelites. Contributions to Mineralogy and Petrology, 134, 17-32.

Spear, F.S., Peacock, S.M., 1989. In: Metamorphic pressure-temperature time paths. *American Geophysical Union,* Short Course in Geology, 7: 102pp.

Stephenson, B.J., Waters, D.J., and Searle, M.P. 2000. Inverted metamorphism and the Main Central Thrust: field relations and thermobarometric constraints from the Kishtwar Window, NW Indian Himalaya. *Journal of Metamorphic Geology,* 18: 571-590.

Stephenson, B.J., Searle, M.P., Waters, D.J., and Rex, D.C. 2001. Structure of the Main Central Thrust zone and extrusion of the High Himalayan deep crustal wedge, Kishtwar-Zanskar Himalaya. *Journal of the Geological Society,* 158: 637.

Streule, M.J., Searle, M.P., Waters, D.J., and Horstwood, M.S.A. 2010. Metamorphism, melting, and channel flow in the Greater Himalayan Sequence and Makalu leucogranite: Constraints from thermobarometry, metamorphic modeling, and U-Pb geochronology. *Tectonics,* 29: TC5011.

Stipp, M., Stünitz, H., Heilbronner, R., and Schmid, S.M. 2002. The eastern Tonale fault zone: a natural laboratory'for crystal plastic deformation of quartz over a temperature range from 250 to 700° C. *Journal of Structural Geology* 24: 1861-1884.

Tong, W., and Zhang, J. 1981. Characteristics of geothermal activities in Xizang Plateau and their controlling influence on Plateau's tectonic model. *Geological and Ecological Studies of the Quinghai-Xizang Plateau,* 841-846.

Tullis, J., Christie, J. M., and Grigs, D. T. 1973. Microstructures and preferred orientations of experimentally deformed quartzites. *Geological Society of America Bulletin*, 84: 297-314.

Vannay, J.C., and Hodges, K.V. 1996. Tectonometamorphic evolution of the Himalayan metamorphic core between the Annapurna and Dhaulagiri, central Nepal. *Journal of Metamorphic Geology*, 14: 635-656.

Von Loczy, L. 1878. Beobachtungen im östichen Himalaya. *Földr Közlem* 35: 1-24.

Walker, J.D., Martin, M.W., Bowring, S.A., Searle, M.P., Waters, D.J., and Hodges, K.V. 1999. Metamorphism, Melting, and Extension: Age Constraints from the High Himalayan Slab of Southeast Zanskar and Northwest Lahaul. *Journal of Geology*, 107: 473-495.

Willett, S. D. 1999. Orogeny and orography: the effects of erosion on the structure of mountain belts. *Journal of Geophysical Research*, 104: 28 957–28 981.

Windley, B.F. 1983. Metamorphism and tectonics of the Himalaya. *Journal of the Geological Society,* 140: 849-865.

Wu, C.M., Zhao, G.C., 2006. Recalibration of the garnet–muscovite (GM) geothermometer and the garnet–muscovite–plagioclase– quartz (GMPQ) geobarometer for metapelitic assemblages. *Journal of Petrology.* 47: 2357–2368.

Yakymchuk and Godin. 2012. Coupled role of deformation and metamorphism in the construction of the inverted metamorphic sequences: an example from far-northwest Nepal. *Journal of Metamorphic Geology,* unknown volume: 1-76.

Yang, P., and Pattison, D.R.M. 2006. Genesis of monazite and Y-zoning in garnet from the Black Hills, South Dakota. *Lithosphere.* 88: 233-253.

Yardley, B.W.D. 1977. An empirical study of diffusion in garnet. *American Mineralogist*, 62: 793-800.

Yin, A., and Harrison, T.M. 2000. Geologic Evolution of the Himalayan-Tibetan Orogen. *Annual Reviews in Earth and Planetary Science*, 28: 211-280.

Zeng, L., Gao, L.E., and Dong, C and Tang, S. 2011. High-pressure melting of metapelite and the formation of Ca-rich granitic melts in the Namche Barwa Massif, Southern Tibet. *Gondwana Research*, 21: 138-151.

Zhang, Q., Willems, H., Ding, L., Grafe, K., Appel, E. 2011. The initial India-Asia continental collision and foreland basin evolution in the Tethyan Himalaya of Tibet: Evidences from straatigraphy and palaeontology. *26th Himalaya-Karakoram-Tibet Workshop*, Canmore, Canada, July 12-13, 2011.

Zhu, B., Kidd, W.S.F., Rowley, D.B., Currie, B.S., and Shafique, N. 2005. Age of initiation of the India-Asia collision in the east-central Himalaya. *The Journal of Geology,* 113: 265-285.

APPENDIX A: Station and structural data

Station	Structure	Azimuth	Dip/Plunge	Latitude	Longitude	Elevation (m)
001	foliation	323	30	27.58580156	86.28414357	2322
002	foliation	288	16	27.58645635	86.28141032	2393
003	foliation	321	38	27.57414325	86.28146463	2698
	foliation	345	31			
	foliation	316	39			
	lineation	025	9			
004				27.57038648	86.2824055	2755
005	foliation	120	17	27.55698809	86.28088217	2902
	foliation	170	19			
	fault	115	83			
006	foliation	212	7	27.55275741	86.28222529	2868
	lineation	197	0			
007	foliation	160	8	27.54491556	86.28484187	2794
008	foliation	242	16	27.54140144	86.28536875	2794
	foliation	232	22			
	lineation	016	15			
009	foliation	002	36	27.53428948	86.28862387	2717
	lineation	201	34			
010	foliation	205	40	27.53381339	86.2892681	2688
	foliation	205	44			
	contact	300	44			
011				27.53250397	86.2901316	2672
012	foliation	210	29	27.53072935	86.2912681	2667
	lineation	231	7			
013	foliation	300	28	27.52304591	86.29260946	2529
014	foliation	349	40	27.51658925	86.28976833	2405
015				27.51336129	86.29234744	2259
016	foliation	230	14	27.5142823	86.29206832	2268
	foliation	208	35			
	foliation	104	70			
017	foliation	341	15	27.51936022	86.29587044	2288
	foliation	330	28			
018	foliation	121	12	27.52018953	86.29969284	2247
	foliation	143	16			
	foliation	145	19			
	lineation	150	7			
	lineation	196	8			
019	foliation	025	30	27.51234951	86.3145537	1921
	lineation	004	7			
020	foliation	134	15	27.5124485	86.31877818	1772
	foliation	147	27			
021	foliation	081	24	27.50855871	86.3239463	1395
022	foliation	229	11	27.5042018	86.32504868	1225
	foliation	214	17			
	foliation	240	8			
023	foliation	036	8	27.50548935	86.32891609	1279
024	foliation	356	18	27.50676013	86.33090403	1427
	foliation	347	14			
	lineation	147	15			
025	foliation	358	9	27.50837322	86.33315197	1437
026	foliation	120	15	27.51386697	86.3384065	1438

027	foliation	042	10	27.50649149	86.33841665	1438
028	foliation	046	18	27.51835808	86.35373332	1695
	lineation	202	10			
029	foliation	081	14	27.52025985	86.36571349	1438
	foliation	070	17			
030	foliation	350	22	27.52139652	86.36524863	1463
	lineation	100	33			
031				27.53914101	86.36897723	1869
032	foliation	015	2	27.5450298	86.38147373	1908
033	foliation	296	2	27.55029146	86.38343333	1816
034	foliation	104	28	27.5670758	86.39233676	1868
	foliation	103	8			
	foliation	090	12			
	lineation	165	6			
035	foliation			27.56794123	86.39573595	1836
036	foliation			27.57468279	86.39621272	1793
	lineation	205	10			
037	foliation	225	15	27.59078351	86.41612301	1663
038	foliation	274	14	27.59677171	86.41826701	1677
	foliation	242	26			
	lineation	348	21			
039	foliation	305	14	27.59859963	86.41923487	1698
	foliation	290	10			
040	foliation	264	20	27.60216001	86.42452419	1693
041	foliation	292	16	27.63038792	86.41913454	2155
	lineation	025	16			
042	foliation	344	9	27.63124924	86.42089332	2264
	foliation	340	30			
	foliation	337	9			
043				27.63482848	86.43140255	2338
044	foliation	330	18	27.6397759	86.43125787	2321
	foliation	304	14			
	foliation	332	88			
	lineation	010	8			
045	foliation	194	16	27.6490954	86.4489602	2244
046	foliation	266	14	27.6566915	86.452017	2221
047	foliation	284	14	27.66086829	86.4533597	2190
048	foliation	150	22	27.6666373	86.45442219	2198
049	foliation	245	14	27.67333805	86.45467138	2256
	lineation	337	12			
050	foliation	260	27	27.68310321	86.46349736	2660
051	foliation	245	17	27.69510912	86.47721275	2832
	foliation	252	30			
	foliation	278	23			
	lineation	022	19			
052	foliation	271	24	27.73326346	86.51092091	3694
	foliation	254	27			
	lineation	050	25			
053				27.7406418	86.51820084	3801
054	foliation	330	38	27.74224441	86.51649479	3928
	joint set	124	79			
055	foliation	234	4	27.74721924	86.51755803	4002
	foliation	340	51			

	foliation	303	30			
056	foliation	286	36	27.74844308	86.51207124	4331
057	foliation	324	35	27.75040068	86.51074522	4368
	foliation	344	55			
	foliation	345	50			
058	foliation	324	30	27.76190551	86.50246281	4584
	foliation	337	46			
	lineation	015	36			
	2° lineation	081	41			
059	foliation	344	35	27.76741695	86.4944757	4891
	foliation	350	37			
	foliation	359	37			
	lineation	068	36			
060	foliation	277	40	27.76133202	86.45954319	3999
	joint	141	85			
061	foliation	295	26	27.74233578	86.45772859	3718
062	foliation	271	30	27.74171275	86.4563253	3740
	lineation	011	26			
063	foliation	275	36	27.73970478	86.44325154	4186
	foliation	038	36			
064	foliation	255	31	27.73877791	86.44266967	4244
	foliation	245	64			
065	foliation	223	27	27.73382605	86.44154306	4318
	foliation	301	14			
	foliation	276	11			
	lineation	023	15			
	lineation	025	14			
066	foliation	221	39	27.7297931	86.42700146	4526
	foliation	302	22			
067	foliation	280	36	27.7302717	86.41745087	4522
	lineation	030	42			
068	foliation	335	34	27.71853562	86.40581251	3908
069	foliation	027	83	27.71833587	86.40208047	3905
	lineation	036	10			
070	foliation	020	23	27.71637828	86.39235201	3933
	lineation	009	8			
071	foliation	315	20	27.7075513	86.37606489	3809
	foliation	338	22			
	lineation	000	10			
072	foliation	320	15	27.70526111	86.37373086	3704
	foliation	310	34			
	lineation	006	5			
	foliation	352	10			
073	foliation	348	22	27.69334883	86.34978913	2328
074	foliation	340	18	27.68985232	86.34890241	2304
		005	00			
075				27.63428274	86.31038245	1889
076	foliation	308	22	27.62764586	86.30673531	1858
077	foliation	044	30	27.60958672	86.29835324	1813
078	foliation	352	14	27.60532963	86.29313014	1787
	lineation	112	21			
079	foliation	038	40	27.60246386	86.28860341	1784
	foliation	198	28			

080	foliation	023	13	27.60019756	86.28072417	1779
081	foliation	347	38	27.59869175	86.27654663	1773
	foliation	330	30			
082	foliation	343	49	27.59510195	86.26705924	1749
	foliation	333	49			
	lineation	025	14			
	2° lineation	178	25			
083	foliation	323	29	27.59629235	86.2610806	1724
	foliation	300	35			
	lineation	350	37			
084	foliation	020	21	27.59470674	86.25841255	1706
	foliation	310	22			
	lineation	014	7			
	lineation	345	15			
085	foliation	236	37	27.60853454	86.29224753	1826
	foliation	249	14			
	lineation	359	36			
	lineation	260	3			
086				27.61201009	86.28215664	1935
087	foliation	175	15	27.61416567	86.26030234	2418
	lineation	325	12			
088	foliation	069	14	27.62606403	86.24023841	2112
	foliation	085	19			
089	foliation	191	9	27.63490668	86.23236939	1960

APPENDIX B: Complete Microprobe analyses for biotite

Location	SiO2	TiO2	Al2O3	FeO	MnO	MgO	CaO	Na2O	K2O	Total
013 area 1	26.17	0.13	23.31	24.24	0.01	12.38	0.09	0.05	0.85	87.24
013 area 1	25.30	0.11	23.36	24.88	0.00	13.50	0.05	0.00	0.43	87.63
013 area 1	25.92	0.11	23.98	25.56	0.00	12.07	0.14	0.05	0.59	88.43
013 area 1	27.63	0.19	24.14	22.73	0.01	11.25	0.11	0.03	1.02	87.13
013 area 1	26.04	7.33	22.59	23.10	0.00	8.91	0.24	0.04	0.51	88.76
013 area 1	24.65	0.05	23.41	25.60	0.01	13.35	0.06	0.02	0.24	87.41
013 area 1	25.97	0.09	23.88	25.00	0.00	12.75	0.06	0.02	0.44	88.21
013 area 1	25.82	0.09	23.85	24.89	0.00	13.23	0.08	0.04	0.45	88.44
013 area 3	23.57	0.04	23.28	25.83	0.00	12.83	0.00	0.00	0.04	85.59
013 area 3	24.93	0.48	21.06	25.13	0.01	10.43	0.15	0.04	2.00	84.24
013 area 3	33.90	0.97	19.25	18.59	0.00	9.26	0.13	0.26	8.39	90.77
013 area 3	31.79	1.37	19.50	19.04	0.00	8.14	0.24	0.19	7.87	88.15
013 area 3	33.92	0.59	19.52	18.34	0.00	9.79	0.11	0.17	8.57	91.03
013 area 3	33.99	0.86	19.43	18.86	0.00	9.56	0.10	0.18	8.72	91.71
013 area 4	34.36	1.35	18.09	17.24	0.01	9.52	0.35	0.15	7.34	88.41
013 area 4	34.18	1.28	18.94	17.44	0.01	9.84	0.33	0.17	7.04	89.23
013 area 4	34.44	1.42	18.18	18.02	0.00	9.24	0.25	0.14	7.84	89.53
013 area 4	23.46	0.07	23.71	24.22	0.00	14.19	0.02	0.00	0.08	85.76
013 area 4	34.27	1.23	18.32	17.64	0.01	9.71	0.23	0.15	7.38	88.93
013 area 4	24.41	0.23	23.51	24.26	0.00	13.51	0.03	0.01	0.85	86.81
013 area 4	34.90	1.27	18.47	17.01	0.01	9.60	0.25	0.13	7.51	89.14
013 area 4	34.21	1.25	18.52	17.56	0.02	9.33	0.54	0.18	6.81	88.42
013 area 4	35.16	1.29	18.80	17.66	0.00	10.05	0.33	0.15	6.73	90.18
013 area 4	35.09	1.24	18.72	17.66	0.01	9.86	0.29	0.14	6.80	89.81
013 area 4	35.35	1.27	18.40	17.44	0.00	9.95	0.28	0.14	7.40	90.25
013 area 4	34.36	1.27	18.37	17.36	0.00	9.65	0.35	0.15	6.52	88.03
013 area 4	34.34	1.26	18.62	17.46	0.02	9.65	0.39	0.15	7.07	88.96
013 area 4	34.64	1.24	18.78	17.66	0.02	9.75	0.38	0.15	6.88	89.50
013 area 4	33.86	1.23	18.62	17.24	0.00	9.27	0.30	0.17	7.38	88.07
013 area 4	44.62	0.25	36.86	1.12	0.00	0.79	0.02	0.91	8.14	92.71
013 area 4	35.02	1.26	18.35	18.12	0.03	10.36	0.10	0.16	8.75	92.16
013 area 4	34.93	1.27	18.42	17.73	0.00	9.83	0.33	0.11	6.76	89.39
013 area 4	32.79	1.26	17.19	18.11	0.02	9.12	0.27	0.14	7.56	86.45
013 area 4	33.77	1.22	18.57	17.90	0.01	9.55	0.46	0.16	6.66	88.30
013 area 4	34.42	1.23	17.86	17.91	0.02	10.00	0.13	0.18	8.85	90.59
013 area 4	34.63	1.27	18.32	18.10	0.00	10.75	0.05	0.16	9.16	92.44
013 area 7	30.92	0.72	20.54	21.15	0.00	12.26	0.20	0.16	4.52	90.46
013 area 7	27.22	0.30	21.89	22.62	0.01	13.93	0.09	0.05	1.54	87.65
013 area 7	24.29	0.09	23.43	24.00	0.00	13.91	0.09	0.02	0.16	85.98
013 area 7	24.26	0.07	23.38	23.86	0.00	14.82	0.00	0.00	0.06	86.45
013 area 7	23.95	0.06	23.45	23.66	0.01	14.47	0.01	0.00	0.02	85.64
013 area 7	23.99	0.16	22.77	23.18	0.00	13.85	0.05	0.02	0.50	84.51
013 area 7	24.60	0.18	22.52	23.65	0.02	14.03	0.06	0.02	0.64	85.71
013 area 7	35.84	1.47	19.31	16.85	0.00	10.08	0.14	0.17	8.71	92.58
013 area 7	36.80	1.35	19.25	15.88	0.00	10.34	0.16	0.15	8.38	92.29
013 area 7	34.30	1.43	19.12	16.07	0.00	9.41	0.19	0.14	8.67	89.32
013 area 7	35.22	1.35	19.17	17.75	0.02	10.67	0.12	0.19	8.35	92.83
013 area 7	33.39	1.29	19.25	18.86	0.01	8.22	0.22	0.19	7.96	89.40
013 area 7	34.69	1.41	18.88	17.03	0.00	10.07	0.13	0.20	8.90	91.30
013 area 7	31.72	1.44	18.36	22.86	0.01	9.03	0.17	0.16	7.96	91.71
013 area 7	35.98	1.54	18.71	16.13	0.02	10.30	0.15	0.15	8.89	91.87

Location	SiO2	TiO2	Al2O3	FeO	MnO	MgO	CaO	Na2O	K2O	Total
013 area 7	34.90	1.48	19.18	17.76	0.03	10.05	0.16	0.20	8.89	92.64
013 area 7	35.76	1.46	18.49	17.88	0.01	10.44	0.11	0.17	8.76	93.08
013 area 8	46.03	0.22	37.33	2.34	0.00	0.68	0.12	0.68	7.14	94.53
013 area 8	45.10	0.25	36.70	2.02	0.02	0.60	0.08	0.81	8.91	94.48
013 area 8	26.30	0.08	24.40	23.97	0.01	10.13	0.11	0.01	0.30	85.31
013 area 8	33.62	1.06	19.06	20.60	0.01	8.51	0.13	0.17	8.04	91.21
013 area 8	23.58	0.04	23.54	24.17	0.01	14.11	0.00	0.00	0.02	85.47
013 area 8	24.74	0.04	22.86	25.01	0.01	13.84	0.01	0.00	0.00	86.50
013 area 8	25.40	0.05	22.64	26.62	0.01	13.04	0.03	0.01	0.28	88.09
013 area 8	23.63	0.05	23.00	27.45	0.01	12.56	0.01	0.00	0.01	86.73
013 area 8	25.80	0.11	22.90	25.76	0.01	12.26	0.06	0.02	0.67	87.59
013 area 8	25.46	0.04	22.47	26.46	0.01	13.25	0.07	0.04	0.18	87.99
032 area 1	37.02	1.69	18.96	15.79	0.07	12.44	0.02	0.28	8.18	94.45
032 area 1	37.19	1.69	19.75	16.13	0.07	12.42	0.03	0.34	8.44	96.05
032 area 1	37.38	1.66	19.18	15.67	0.05	12.67	0.00	0.31	8.77	95.71
032 area 2	37.57	1.38	19.51	16.37	0.05	12.32	0.00	0.31	8.52	96.03
032 area 2	37.34	1.43	19.63	16.62	0.07	12.30	0.00	0.34	8.67	96.38
032 area 2	37.34	1.47	19.80	16.55	0.05	12.51	0.00	0.34	8.50	96.56
032 area 2	37.28	1.53	19.60	16.30	0.05	12.55	0.00	0.32	8.62	96.26
032 area 2	36.88	1.42	19.54	16.99	0.05	12.45	0.01	0.34	8.60	96.27
032 area 4	36.04	1.43	20.36	15.90	0.06	12.66	0.03	0.35	8.69	95.53
032 area 4	37.76	1.45	19.51	15.78	0.07	12.89	0.06	0.34	8.56	96.43
032 area 4	36.93	1.55	19.88	15.86	0.06	12.67	0.00	0.30	8.81	96.07
032 area 4	36.64	1.48	19.78	15.81	0.05	12.55	0.00	0.31	8.75	95.37
032 area 4	36.88	1.49	19.73	16.29	0.06	12.77	0.00	0.29	8.77	96.28
032 area 4	46.91	0.69	36.37	1.51	0.00	1.05	0.00	1.09	9.01	96.63
032 area 4	46.68	0.64	36.64	1.35	0.00	0.94	0.01	1.13	9.09	96.49
032 area 4	46.45	0.41	37.86	1.25	0.01	0.66	0.01	1.19	8.80	96.64
032 area 6	37.51	1.50	19.44	16.04	0.07	12.66	0.04	0.27	8.64	96.18
032 area 6	36.63	1.52	18.71	16.10	0.06	12.07	0.05	0.26	8.72	94.12
032 area 6	35.85	1.40	17.74	15.76	0.07	10.98	0.24	0.32	7.90	90.25
032 area 6	37.27	1.41	19.89	16.65	0.03	12.62	0.02	0.32	8.66	96.88
032 area 6	37.59	1.37	20.51	16.26	0.06	12.42	0.07	0.36	8.33	96.96
032 area 7	47.08	0.94	34.98	1.41	0.00	1.38	0.00	0.97	9.22	95.98
032 area 7	47.79	0.99	34.72	1.34	0.02	1.45	0.00	0.95	9.19	96.44
032 area 7	47.48	1.00	34.95	1.30	0.00	1.47	0.00	0.94	9.25	96.40
032 area 7	47.14	0.95	35.30	1.28	0.00	1.31	0.00	0.98	9.15	96.10
032 area 7	46.54	0.89	35.75	1.34	0.00	1.23	0.01	1.04	9.32	96.13
032 area 7	46.92	0.84	36.02	1.32	0.00	1.12	0.00	1.06	9.17	96.45
032 area 7	46.93	0.82	35.50	1.26	0.01	1.23	0.01	1.04	9.11	95.90
032 area 7	46.65	0.74	35.34	1.39	0.00	1.18	0.00	1.02	9.35	95.68
035 area 1	48.37	0.64	34.16	3.10	0.01	1.00	0.01	0.75	8.33	96.38
035 area 1	37.30	1.80	18.20	18.22	0.12	10.12	0.12	0.25	7.66	93.78
035 area 1	35.50	1.88	17.11	18.53	0.14	10.15	0.12	0.22	8.33	91.99
035 area 1	43.88	0.87	29.42	8.90	0.05	3.96	0.02	0.57	8.71	96.37
035 area 1	48.51	0.64	34.19	3.39	0.00	1.10	0.00	0.73	8.36	96.93
035 area 1	48.69	0.61	34.33	3.16	0.01	1.01	0.00	0.72	8.42	96.96
035 area 1	36.36	1.89	18.82	17.89	0.12	10.44	0.14	0.38	8.97	95.01
035 area 1	36.46	1.99	18.28	18.53	0.10	10.72	0.00	0.28	9.30	95.66
035 area 1	37.53	1.62	19.90	18.69	0.18	9.38	0.04	0.31	8.86	96.51
035 area 1	38.88	1.88	17.26	18.91	0.18	11.19	0.09	0.20	9.33	97.92
035 area 1	38.54	1.29	20.90	16.76	0.41	8.31	0.43	0.40	6.70	93.73

Location	SiO2	TiO2	Al2O3	FeO	MnO	MgO	CaO	Na2O	K2O	Total
035 area 4	35.31	1.34	18.66	18.98	0.28	10.31	0.40	0.34	8.38	94.00
035 area 4	37.91	0.01	13.61	29.93	2.91	3.42	3.96	0.02	0.08	91.83
035 area 4	8.05	1.03	20.24	21.38	0.73	1.08	0.88	0.33	5.36	59.08
035 area 4	36.69	0.01	22.01	30.88	2.74	3.02	4.54	0.02	0.03	99.94
035 area 4	17.35	0.08	17.93	24.89	7.25	1.20	3.34	0.16	0.55	72.76
035 area 4	45.29	0.65	33.32	3.64	0.02	1.21	0.09	0.64	8.42	93.27
035 area 4	34.88	1.72	18.81	19.33	0.13	11.06	0.08	0.29	8.14	94.44
035 area 4	36.15	1.75	18.44	19.25	0.15	10.77	0.04	0.27	9.07	95.89
035 area 4	36.08	1.76	18.46	19.35	0.13	10.89	0.01	0.24	8.87	95.78
035 area 4	35.96	1.77	18.72	18.93	0.15	10.64	0.03	0.24	8.93	95.36
035 area 4	35.91	1.81	18.21	19.73	0.14	10.79	0.01	0.24	8.94	95.78
035 area 5	47.79	0.56	35.48	3.39	0.00	0.98	0.03	0.81	8.15	97.18
035 area 5	37.16	1.22	18.40	18.84	0.13	11.00	0.02	0.25	9.11	96.12
035 area 5	35.30	1.07	19.40	17.19	0.11	10.65	0.05	0.31	8.87	92.96
035 area 5	36.72	1.23	18.82	18.93	0.11	10.90	0.01	0.22	9.26	96.20
035 area 5	47.10	0.58	32.04	4.47	0.03	2.04	0.00	0.57	8.59	95.42
035 area 5	48.02	0.68	33.92	3.32	0.00	1.00	0.00	0.69	8.43	96.07
035 area 5	35.75	1.24	19.42	18.54	0.11	10.38	0.12	0.26	8.27	94.10
035 area 5	36.86	1.29	18.45	18.72	0.11	10.64	0.06	0.22	8.84	95.19
035 area 5	36.08	0.88	18.57	19.06	0.13	11.39	0.16	0.24	7.55	94.07
035 area 5	35.96	0.49	18.99	18.48	0.12	9.82	0.16	0.22	7.87	92.11
035 area 5	36.68	0.40	20.37	19.03	0.11	10.32	0.18	0.21	7.94	95.24
035 area 6	37.26	1.68	17.75	18.29	0.14	10.56	0.21	0.27	8.65	94.82
035 area 6	33.82	1.61	17.41	17.64	0.13	8.88	0.27	0.32	8.34	88.41
035 area 6	36.77	1.69	18.05	18.18	0.14	10.53	0.23	0.30	8.57	94.47
035 area 6	46.62	0.71	29.33	5.19	0.03	2.79	0.09	0.51	8.33	93.60
035 area 6	37.82	1.52	15.69	17.69	0.14	10.48	0.22	0.21	8.56	92.34
035 area 6	38.83	1.57	15.51	18.96	0.21	10.67	0.24	0.22	8.77	94.96
035 area 6	34.12	1.81	17.54	19.27	0.18	8.90	0.12	0.28	8.77	90.98
035 area 6	38.83	1.81	17.68	18.83	0.14	11.24	0.10	0.28	9.10	98.02
035 area 6	36.39	1.78	17.88	18.71	0.14	10.37	0.06	0.24	9.04	94.61
035 area 6	36.80	1.73	17.42	19.09	0.16	10.30	0.13	0.24	9.07	94.93
035 area 6	37.68	2.24	18.34	18.09	0.16	10.52	0.09	0.27	9.21	96.60
039 area 1	33.10	3.13	18.64	24.25	0.36	5.20	0.17	0.08	7.95	92.87
039 area 1	33.56	3.18	18.20	24.71	0.35	5.36	0.10	0.06	8.75	94.27
039 area 1	33.78	2.73	18.52	24.98	0.34	5.66	0.03	0.06	9.42	95.51
039 area 1	34.06	2.92	18.37	25.18	0.31	5.56	0.03	0.05	9.53	96.01
039 area 1	34.14	3.00	18.18	24.90	0.34	5.54	0.05	0.06	9.27	95.48
039 area 1	34.43	3.18	17.97	25.04	0.30	5.66	0.03	0.07	9.36	96.04
039 area 2	35.23	2.55	18.02	24.42	0.30	6.34	0.00	0.04	9.41	96.33
039 area 2	35.02	2.62	17.70	24.24	0.27	6.38	0.03	0.05	9.17	95.48
039 area 2	34.98	2.66	18.09	24.51	0.31	6.27	0.01	0.05	9.35	96.22
039 area 2	35.01	2.92	17.72	24.47	0.30	6.13	0.02	0.04	9.22	95.83
039 area 2	34.64	2.90	17.87	24.91	0.30	6.16	0.00	0.06	9.27	96.10
039 area 2	34.78	3.00	17.80	24.90	0.29	5.96	0.00	0.05	9.35	96.13
039 area 2	34.95	3.11	17.86	24.47	0.29	6.15	0.00	0.07	9.46	96.36
039 area 3	34.99	2.94	17.18	24.71	0.31	6.13	0.01	0.05	9.39	95.70
039 area 3	33.79	2.88	17.68	24.08	0.27	5.65	0.02	0.07	9.31	93.74
039 area 3	34.05	2.92	18.65	23.81	0.30	5.77	0.00	0.06	9.46	95.01
039 area 3	34.99	2.73	18.72	23.50	0.32	5.90	0.01	0.08	9.30	95.55
039 area 3	35.42	2.61	18.59	23.70	0.31	5.97	0.01	0.07	9.39	96.07
039 area 3	35.05	2.57	18.18	23.39	0.31	5.99	0.02	0.06	9.49	95.06

Location	SiO2	TiO2	Al2O3	FeO	MnO	MgO	CaO	Na2O	K2O	Total
039 area 3	35.05	2.54	17.89	23.49	0.30	6.06	0.04	0.06	9.48	94.90
039 area 3	33.72	3.10	18.35	24.16	0.30	5.56	0.00	0.06	9.40	94.65
039 area 3	34.25	3.79	17.49	24.88	0.29	5.56	0.00	0.05	9.49	95.80
039 area 3	33.70	3.53	17.80	24.90	0.31	5.51	0.00	0.06	9.48	95.28
039 area 4	33.75	3.31	17.66	24.01	0.28	5.76	0.03	0.10	9.34	94.26
039 area 4	33.91	2.87	17.98	24.40	0.30	5.77	0.00	0.07	9.40	94.71
039 area 4	32.99	2.79	17.81	24.46	0.30	5.88	0.01	0.07	9.36	93.66
039 area 4	33.08	3.44	17.52	24.37	0.28	5.76	0.01	0.08	9.30	93.84
039 area 4	32.71	3.44	17.85	25.02	0.30	5.58	0.00	0.06	9.50	94.45
039 area 4	34.64	3.28	18.11	24.31	0.31	5.76	0.00	0.08	9.45	95.93
039 area 4	34.94	3.33	17.82	23.99	0.28	5.69	0.01	0.05	9.33	95.43
039 area 4	34.97	3.33	18.03	24.46	0.26	5.77	0.00	0.07	9.29	96.17
039 area 4	35.09	3.27	17.97	24.23	0.25	5.70	0.01	0.07	9.39	95.96
039 area 4	35.13	3.17	17.96	24.26	0.29	5.84	0.02	0.06	9.41	96.15
039 area 4	33.76	3.23	18.95	23.32	0.30	5.32	0.01	0.08	9.39	94.34
039 area 4	33.39	3.21	18.42	23.35	0.28	5.54	0.15	0.06	9.37	93.77
039 area 4	33.52	3.22	18.67	23.24	0.24	5.61	0.00	0.09	9.43	94.01
039 area 4	33.48	3.24	18.40	23.41	0.26	5.75	0.00	0.09	9.44	94.05
039 area 4	33.91	2.94	18.55	23.24	0.30	5.59	0.01	0.08	9.46	94.08
039 area 4	34.80	3.49	18.39	23.60	0.28	5.64	0.01	0.10	9.35	95.64
039 area 4	34.80	3.63	18.10	23.51	0.26	5.52	0.00	0.09	9.40	95.32
039 area 4	33.76	3.61	18.13	23.69	0.26	5.49	0.00	0.07	9.43	94.44
039 area 4	33.84	3.60	18.03	23.78	0.24	5.35	0.00	0.08	9.47	94.38
039 area 4	33.55	3.20	18.02	24.43	0.29	5.48	0.00	0.04	9.59	94.60
039 area 5	33.92	3.27	17.81	24.06	0.28	5.88	0.02	0.05	9.18	94.47
039 area 5	35.09	3.77	19.32	23.67	0.28	5.50	0.00	0.07	9.46	97.16
039 area 5	34.04	3.47	17.75	24.92	0.30	5.76	0.00	0.06	9.45	95.75
039 area 5	33.95	3.49	17.98	24.66	0.28	5.85	0.00	0.05	9.49	95.74
039 area 5	34.10	3.70	17.90	24.41	0.29	5.89	0.00	0.08	9.43	95.79
039 area 5	34.47	3.45	18.25	24.16	0.29	5.92	0.00	0.07	9.53	96.14
039 area 5	34.57	3.41	18.13	24.43	0.27	5.97	0.00	0.08	9.42	96.27
039 area 5	34.48	3.40	18.09	23.91	0.26	5.70	0.00	0.07	9.46	95.37
039 area 5	34.06	3.46	17.96	24.76	0.30	5.77	0.01	0.06	9.24	95.60
039 area 5	33.96	3.50	18.20	24.35	0.29	5.75	0.00	0.06	9.46	95.57
039 area 5	34.21	3.52	18.06	24.41	0.28	5.87	0.00	0.06	9.57	95.98
039 area 5	33.90	3.46	17.85	24.42	0.27	5.86	0.00	0.06	9.55	95.37
039 area 5	34.14	3.55	17.87	24.09	0.27	5.98	0.00	0.06	9.57	95.53
039 area 5	34.33	3.60	17.53	24.29	0.31	5.85	0.00	0.06	9.46	95.45
039 area 6	35.32	3.66	17.52	23.83	0.26	6.25	0.00	0.06	9.41	96.31
039 area 6	35.37	3.69	17.51	23.86	0.27	6.39	0.00	0.06	9.34	96.49
039 area 6	35.56	3.71	17.46	23.88	0.27	6.31	0.00	0.06	9.34	96.58
039 area 6	35.42	3.68	17.47	23.75	0.26	6.20	0.00	0.05	9.35	96.17
039 area 6	35.28	3.89	17.15	23.88	0.26	6.17	0.00	0.06	9.39	96.08
039 area 6	33.66	0.18	23.10	8.68	0.33	0.30	16.69	0.04	0.02	82.99
039 area 6	34.93	0.21	23.83	8.44	0.07	0.17	18.46	0.00	0.02	86.14
039 area 6	34.58	0.18	0.04	0.82	0.15	0.07	0.07	0.06	0.06	36.03
039 area 7	34.42	3.46	17.98	23.26	0.33	6.10	0.01	0.08	9.43	95.06
039 area 7	34.43	3.41	17.98	23.45	0.34	6.23	0.00	0.07	9.44	95.37
039 area 7	34.70	3.06	19.11	22.60	0.30	5.72	0.01	0.04	8.93	94.45
039 area 7	33.97	3.06	17.70	22.80	0.32	6.58	0.01	0.07	9.32	93.81
039 area 7	34.47	3.18	17.72	23.15	0.32	6.51	0.02	0.05	9.40	94.80
039 area 7	34.11	3.28	17.76	23.36	0.34	6.27	0.00	0.07	9.44	94.63

Location	SiO2	TiO2	Al2O3	FeO	MnO	MgO	CaO	Na2O	K2O	Total
039 area 7	34.06	3.26	17.80	23.14	0.35	6.34	0.00	0.07	9.48	94.50
039 area 7	33.63	3.26	18.12	23.63	0.31	6.30	0.00	0.07	9.39	94.71
039 area 7	34.33	2.98	17.95	23.05	0.33	6.50	0.01	0.07	9.42	94.65
039 area 7	33.36	2.44	18.84	21.27	0.27	5.85	0.02	0.08	8.49	90.61
039 area 7	34.24	2.90	18.19	23.37	0.27	6.47	0.00	0.09	9.27	94.80
039 area 7	29.52	35.66	2.23	0.32	0.10	0.02	27.97	0.01	0.00	95.84
039 area 7	29.56	36.57	1.88	0.28	0.07	0.00	28.64	0.02	0.00	97.04
039 area 8	30.71	0.45	22.90	26.70	0.56	5.51	0.16	0.05	3.03	90.08
039 area 8	47.55	2.30	31.18	3.79	0.05	1.39	0.02	0.10	9.32	95.71
039 area 8	28.66	8.61	18.08	24.52	0.42	5.09	0.18	0.05	3.67	89.27
039 area 8	23.91	0.14	21.68	33.22	0.90	7.34	0.03	0.00	0.18	87.39
039 area 8	34.26	1.07	19.42	23.52	0.34	5.76	0.16	0.09	5.62	90.24
039 area 8	35.56	4.58	22.60	16.76	0.26	3.29	0.18	0.04	2.14	85.41
039 area 8	23.37	0.09	21.44	34.09	0.92	7.72	0.03	0.00	0.06	87.72
039 area 8	24.69	0.16	21.30	32.52	0.81	7.02	0.06	0.01	0.43	87.00
039 area 8	23.18	0.08	22.18	33.92	0.93	7.48	0.03	0.01	0.01	87.82
039 area 8	34.46	2.17	19.09	23.37	0.36	5.52	0.06	0.08	8.08	93.18
039 area 8	25.22	0.22	21.57	33.23	0.90	6.75	0.09	0.01	0.46	88.45
039 area 8	34.86	3.13	17.99	23.87	0.36	5.99	0.00	0.06	9.41	95.66
044 area 1	33.31	3.99	17.17	25.22	0.24	4.92	0.05	0.07	9.33	94.31
044 area 1	31.79	3.42	18.48	24.95	0.18	4.46	0.10	0.09	8.94	92.40
044 area 1	30.04	1.64	19.70	29.98	0.12	4.53	0.27	0.10	3.66	90.04
044 area 1	46.69	0.94	36.01	2.35	0.00	0.79	0.02	0.32	9.45	96.56
044 area 1	46.33	0.96	35.49	2.42	0.02	0.78	0.04	0.27	9.35	95.66
044 area 1	32.63	3.22	17.79	25.24	0.20	4.68	0.17	0.10	8.75	92.78
044 area 2	33.52	3.27	19.03	25.18	0.18	4.99	0.08	0.09	8.91	95.24
044 area 2	33.56	2.49	18.66	25.59	0.17	4.73	0.19	0.07	7.32	92.79
044 area 2	34.14	3.04	18.12	25.52	0.20	5.09	0.14	0.08	8.80	95.12
044 area 2	36.08	3.17	18.33	25.27	0.19	5.69	0.10	0.07	9.11	98.01
044 area 2	33.60	3.23	18.79	26.08	0.20	5.02	0.09	0.08	8.87	95.97
044 area 2	46.24	0.90	34.34	2.52	0.01	0.75	0.09	0.31	9.59	94.75
044 area 3	34.89	2.63	18.89	26.05	0.25	4.90	0.16	0.09	8.55	96.42
044 area 3	31.37	3.11	19.16	26.42	0.27	4.38	0.13	0.08	7.64	92.57
044 area 3	32.03	3.15	17.39	25.74	0.23	4.19	0.11	0.07	8.92	91.84
044 area 3	33.85	3.15	17.16	25.60	0.22	4.60	0.13	0.09	8.98	93.78
044 area 3	34.17	3.10	18.28	25.62	0.24	4.84	0.07	0.09	9.07	95.47
044 area 3	34.01	3.12	18.53	25.76	0.23	4.78	0.05	0.08	9.22	95.78
044 area 3	34.68	2.98	18.71	25.89	0.24	4.96	0.07	0.09	9.05	96.67
044 area 3	34.91	2.79	19.26	25.44	0.37	4.79	0.24	0.13	8.49	96.42
044 area 3	35.59	2.80	18.18	25.84	0.27	4.90	0.15	0.10	8.84	96.68
044 area 3	34.26	2.85	18.59	25.22	0.27	4.83	0.18	0.11	8.20	94.51
044 area 3	33.17	3.06	18.79	25.76	0.23	4.49	0.14	0.10	8.71	94.45
044 area 5	34.43	4.09	16.82	25.47	0.23	4.84	0.13	0.06	9.06	95.13
044 area 5	33.41	3.85	17.47	25.39	0.17	4.76	0.14	0.07	8.92	94.18
044 area 5	34.55	3.88	18.58	25.39	0.17	4.87	0.11	0.09	9.00	96.64
044 area 5	33.74	4.08	17.22	25.56	0.18	4.69	0.05	0.06	9.30	94.89
044 area 5	25.52	0.17	19.60	36.79	1.06	5.72	0.17	0.03	0.33	89.40
044 area 5	31.58	1.20	18.01	27.09	0.52	3.62	0.14	0.05	8.04	90.24
044 area 5	25.92	0.54	20.75	33.52	0.66	5.44	0.09	0.04	2.20	89.15
044 area 5	27.62	0.76	18.99	32.96	0.41	4.69	0.18	0.11	3.45	89.18
044 area 6	33.01	3.88	17.53	25.42	0.21	4.56	0.13	0.07	8.93	93.75
044 area 6	33.86	3.95	18.04	25.33	0.18	4.73	0.10	0.07	8.96	95.24

Location	SiO2	TiO2	Al2O3	FeO	MnO	MgO	CaO	Na2O	K2O	Total
044 area 6	32.51	3.93	17.17	25.03	0.18	4.17	0.16	0.08	8.77	92.01
044 area 6	33.74	3.89	17.99	24.99	0.16	4.58	0.12	0.09	8.95	94.50
044 area 6	32.45	3.74	18.00	24.87	0.18	4.27	0.14	0.10	8.68	92.43
044 area 8	33.78	2.49	19.41	24.89	0.31	4.66	0.15	0.11	8.76	94.56
044 area 8	33.28	2.72	18.83	24.55	0.22	4.63	0.19	0.11	8.61	93.15
044 area 8	33.46	2.77	18.04	24.64	0.23	4.72	0.17	0.10	8.75	92.88
044 area 8	34.78	2.74	17.82	25.16	0.25	5.10	0.14	0.10	8.83	94.92
044 area 8	33.99	2.00	17.87	25.24	0.25	5.18	0.12	0.07	8.68	93.41
044 area 8	34.71	2.95	18.20	24.97	0.26	4.99	0.06	0.07	9.19	95.39
044 area 8	32.84	2.74	19.07	26.12	0.38	4.38	0.13	0.08	8.72	94.47
044 area 8	45.73	0.66	36.38	2.42	0.01	0.73	0.03	0.26	9.46	95.69
044 area 8	33.45	1.76	19.37	25.29	0.42	4.96	0.19	0.10	8.04	93.58
044 area 8	32.88	2.19	17.70	25.63	0.36	4.78	0.16	0.07	8.86	92.62
044 area 8	32.83	2.23	18.39	25.54	0.33	4.77	0.17	0.08	8.39	92.72
046 area 2	35.56	2.24	19.26	19.86	0.03	9.55	0.00	0.25	8.89	95.65
046 area 2	35.11	2.19	19.77	20.25	0.05	9.29	0.04	0.26	8.72	95.69
046 area 2	35.41	2.22	19.48	19.77	0.01	9.87	0.00	0.26	8.69	95.70
046 area 2	35.46	2.25	19.47	19.80	0.03	9.51	0.00	0.26	8.87	95.65
046 area 2	35.41	2.25	19.56	20.18	0.02	9.62	0.01	0.28	8.71	96.04
046 area 2	35.70	2.22	19.43	19.87	0.02	9.74	0.00	0.24	8.78	96.01
046 area 2	35.20	2.14	19.57	20.44	0.03	9.21	0.01	0.22	8.75	95.58
046 area 2	35.57	0.07	20.51	21.76	0.03	9.24	0.06	0.19	8.40	95.83
046 area 2	34.25	1.38	20.19	23.85	0.07	7.31	0.00	0.16	9.08	96.30
046 area 2	34.76	1.43	19.77	23.54	0.06	7.41	0.00	0.18	8.97	96.12
046 area 2	34.71	1.70	19.71	23.48	0.06	7.21	0.00	0.14	9.04	96.05
046 area 2	34.09	1.42	20.20	23.40	0.09	7.17	0.00	0.13	9.01	95.52
046 area 2	23.73	0.76	14.98	41.02	0.04	4.88	0.06	0.20	5.45	91.12
046 area 2	33.71	2.11	19.55	24.71	0.09	7.10	0.01	0.12	8.69	96.10
046 area 2	34.43	2.47	18.90	24.21	0.09	6.93	0.00	0.14	8.90	96.08
046 area 2	34.71	2.39	18.77	24.12	0.11	7.07	0.01	0.13	8.96	96.28
046 area 2	34.47	2.28	19.06	24.01	0.05	7.36	0.00	0.16	8.94	96.33
046 area 3	33.67	1.62	19.62	21.91	0.03	7.02	0.18	0.27	8.20	92.51
046 area 3	33.92	2.42	19.11	23.35	0.05	7.09	0.03	0.21	8.80	94.98
046 area 3	33.62	2.25	19.01	23.56	0.06	7.22	0.01	0.22	8.80	94.75
046 area 3	34.00	2.21	19.30	23.06	0.05	7.32	0.00	0.21	8.87	95.01
046 area 3	35.01	2.08	19.28	23.34	0.04	7.48	0.02	0.23	8.70	96.17
046 area 3	34.09	2.35	19.12	23.54	0.04	7.17	0.01	0.22	8.83	95.36
046 area 3	34.26	2.71	19.26	23.65	0.05	7.17	0.02	0.21	8.82	96.15
046 area 4	34.81	2.95	18.97	24.46	0.04	6.65	0.02	0.18	8.82	96.89
046 area 4	35.04	2.86	18.87	24.65	0.06	6.83	0.01	0.17	8.80	97.28
046 area 4	35.02	2.96	18.77	24.22	0.06	6.94	0.02	0.21	8.82	97.01
046 area 4	34.47	2.92	18.49	23.91	0.06	6.80	0.06	0.24	8.69	95.63
046 area 4	34.94	2.97	18.84	24.10	0.05	6.84	0.01	0.22	8.82	96.79
046 area 4	34.74	2.80	18.84	23.77	0.04	6.84	0.01	0.19	8.80	96.03
046 area 4	34.71	2.42	19.34	23.51	0.04	7.03	0.01	0.19	8.95	96.19
046 area 4	34.64	2.69	18.77	23.44	0.03	6.97	0.03	0.24	8.78	95.60
046 area 4	34.48	2.65	18.79	23.69	0.05	6.97	0.03	0.23	8.84	95.73
046 area 4	34.85	2.60	19.21	23.93	0.05	6.96	0.01	0.19	8.91	96.71
046 area 5	35.56	2.22	19.64	19.90	0.04	9.60	0.05	0.30	8.66	95.97
046 area 5	36.25	2.21	19.98	19.85	0.03	9.77	0.08	0.33	8.50	96.99
046 area 5	35.01	2.16	20.18	20.11	0.03	9.36	0.08	0.35	8.29	95.59
046 area 5	35.60	2.20	18.95	20.58	0.03	9.49	0.07	0.29	8.52	95.73

Location	SiO2	TiO2	Al2O3	FeO	MnO	MgO	CaO	Na2O	K2O	Total
046 area 5	22.84	0.31	22.17	36.93	0.39	4.95	0.17	0.07	0.07	87.89
046 area 5	20.73	0.31	21.92	38.79	0.36	3.37	0.13	0.06	0.05	85.72
046 area 5	22.97	0.00	24.06	39.67	0.80	3.10	0.07	0.06	0.05	90.78
046 area 5	22.42	0.00	23.57	39.52	0.81	3.03	0.08	0.04	0.05	89.51
046 area 5	33.80	1.95	19.72	24.42	0.08	6.58	0.04	0.19	8.74	95.51
046 area 5	34.15	1.84	19.69	23.94	0.07	6.73	0.04	0.21	8.74	95.42
046 area 5	33.78	1.84	20.15	25.07	0.07	6.47	0.03	0.15	8.44	96.00
046 area 5	34.13	1.76	19.62	24.57	0.09	6.57	0.01	0.13	8.78	95.65
046 area 5	34.36	1.80	19.60	24.75	0.06	6.67	0.03	0.13	8.88	96.29
046 area 5	33.93	1.69	20.00	24.16	0.09	6.55	0.03	0.11	8.17	94.71
046 area 5	34.41	1.45	19.95	24.28	0.06	6.72	0.01	0.16	8.67	95.72
048 area 2	33.10	2.95	19.04	19.09	0.01	8.23	0.03	0.24	9.52	92.21
048 area 2	33.90	3.07	19.26	19.46	0.01	8.27	0.02	0.26	9.47	93.72
048 area 2	32.82	3.07	19.56	19.11	0.02	7.95	0.04	0.29	9.35	92.21
048 area 2	32.42	2.96	19.14	18.69	0.01	7.95	0.05	0.31	9.27	90.80
048 area 2	33.06	2.95	18.62	18.99	0.01	8.38	0.03	0.25	9.50	91.78
048 area 2	32.97	2.92	18.57	19.38	0.01	8.27	0.00	0.23	9.57	91.91
048 area 2	33.17	2.85	18.79	19.38	0.03	8.47	0.00	0.21	9.34	92.25
048 area 2	34.21	2.75	18.62	19.39	0.00	9.05	0.03	0.22	9.37	93.64
048 area 2	31.70	2.67	18.52	18.66	0.01	7.92	0.04	0.24	9.22	88.99
048 area 2	32.14	2.96	18.47	19.01	0.00	8.32	0.02	0.29	9.37	90.58
048 area 2	32.48	2.58	19.35	18.64	0.02	8.58	0.00	0.26	9.45	91.36
048 area 2	33.21	2.57	19.53	18.60	0.01	8.67	0.00	0.28	9.48	92.34
048 area 2	32.01	2.64	18.82	19.05	0.01	8.38	0.00	0.25	9.51	90.67
048 area 2	29.41	2.54	20.32	17.87	0.01	7.10	0.10	0.48	8.69	86.53
048 area 2	33.98	2.55	18.75	20.59	0.02	8.76	0.02	0.20	9.36	94.24
048 area 2	32.60	2.71	17.57	22.20	0.01	7.77	0.02	0.20	9.03	92.11
048 area 2	33.38	2.71	18.25	20.43	0.03	8.15	0.04	0.24	9.03	92.25
048 area 2	32.97	2.82	19.03	19.84	0.01	8.31	0.01	0.33	9.20	92.52
048 area 2	33.55	2.48	18.93	19.45	0.03	8.64	0.00	0.25	9.39	92.73
048 area 2	33.92	2.73	18.58	20.37	0.00	8.38	0.00	0.24	9.32	93.54
048 area 3	30.43	2.90	16.82	17.97	0.02	7.13	0.11	0.26	8.90	84.54
048 area 3	32.16	2.88	15.89	18.61	0.02	7.79	0.07	0.20	8.75	86.37
048 area 3	29.58	2.31	13.06	17.97	0.01	6.53	0.09	0.06	8.88	78.48
048 area 3	34.01	3.09	17.88	18.39	0.01	8.12	0.09	0.25	8.96	90.78
048 area 3	32.66	2.87	19.39	18.42	0.00	7.68	0.09	0.31	8.68	90.10
048 area 3	36.52	2.82	16.67	17.76	0.02	9.34	0.12	0.21	8.93	92.38
048 area 3	31.90	3.01	17.53	18.29	0.00	7.78	0.05	0.25	8.61	87.41
048 area 3	32.01	3.00	18.36	17.96	0.00	8.02	0.03	0.30	8.63	88.32
048 area 3	34.03	2.89	19.20	18.13	0.01	8.99	0.03	0.31	8.88	92.47
048 area 3	34.05	1.94	20.16	18.44	0.00	9.16	0.01	0.26	8.68	92.72
048 area 3	34.10	2.84	18.64	19.57	0.03	8.65	0.03	0.21	9.09	93.16
048 area 3	44.52	1.27	34.24	1.49	0.01	0.77	0.04	0.62	8.68	91.63
048 area 3	44.41	1.10	34.20	1.54	0.01	0.67	0.04	0.58	8.57	91.10
048 area 3	43.01	1.17	35.04	1.51	0.00	0.73	0.08	0.67	8.40	90.61
048 area 3	46.18	1.07	34.84	1.41	0.00	0.66	0.05	0.61	8.44	93.27
048 area 3	46.35	1.18	35.28	1.50	0.01	0.83	0.04	0.62	8.29	94.10
048 area 3	46.55	1.19	35.38	1.48	0.01	0.86	0.03	0.64	8.25	94.39
048 area 4	33.34	3.13	18.95	19.85	0.04	7.78	0.00	0.18	9.01	92.26
048 area 4	34.27	3.07	18.35	19.51	0.02	8.69	0.01	0.13	8.54	92.59
048 area 4	33.92	3.17	19.35	18.94	0.02	8.42	0.00	0.23	8.85	92.91
048 area 4	34.08	3.22	19.56	18.64	0.01	8.55	0.00	0.26	8.74	93.05

Location	SiO2	TiO2	Al2O3	FeO	MnO	MgO	CaO	Na2O	K2O	Total
048 area 4	35.27	3.23	19.26	18.79	0.01	8.88	0.00	0.25	8.85	94.55
048 area 4	34.48	3.25	19.28	19.13	0.02	8.75	0.00	0.20	8.72	93.83
048 area 4	34.76	3.19	19.15	18.63	0.01	8.42	0.01	0.24	8.84	93.24
048 area 4	33.53	3.13	19.34	19.55	0.01	8.04	0.01	0.19	8.71	92.50
048 area 4	34.61	3.21	19.21	19.60	0.02	8.35	0.00	0.20	8.80	94.01
048 area 4	34.18	3.19	18.93	19.58	0.01	8.14	0.00	0.17	8.80	93.00
048 area 4	20.45	0.06	22.20	31.63	0.06	6.20	0.14	0.10	0.25	81.08
048 area 4	34.74	1.21	22.22	22.54	0.04	5.73	0.09	0.19	9.12	95.87
048 area 4	46.24	0.72	35.77	1.16	0.00	0.52	0.03	0.55	8.69	93.68
048 area 4	45.52	1.08	35.88	1.29	0.00	0.64	0.03	0.63	8.44	93.52
048 area 4	46.41	1.13	34.77	1.31	0.00	0.70	0.09	0.55	8.22	93.18
048 area 4	46.35	1.13	34.81	1.42	0.00	0.89	0.03	0.58	8.15	93.37
048 area 4	44.84	1.07	34.81	1.39	0.00	0.89	0.10	0.71	8.50	92.31
048 area 6	31.06	0.99	19.92	21.92	0.02	7.01	0.10	0.19	8.88	90.08
048 area 6	31.77	0.56	20.15	23.14	0.02	8.33	0.14	0.14	7.41	91.67
048 area 6	29.80	0.52	19.19	25.45	0.03	8.88	0.08	0.05	6.22	90.23
048 area 6	33.48	2.73	16.87	21.91	0.03	7.86	0.06	0.11	9.01	92.06
048 area 6	32.93	2.30	18.95	22.30	0.01	7.47	0.08	0.19	8.73	92.96
048 area 6	32.49	2.18	18.47	22.95	0.01	7.96	0.05	0.11	8.65	92.89
048 area 6	32.36	2.41	18.38	22.55	0.03	8.03	0.03	0.12	9.11	93.02
048 area 6	32.93	2.51	18.12	21.41	0.04	7.65	0.05	0.13	9.39	92.23
048 area 9	32.85	1.74	17.75	20.17	0.03	6.84	0.08	0.17	8.97	88.60
048 area 9	34.01	1.81	17.92	20.64	0.02	7.87	0.14	0.17	9.05	91.63
048 area 9	32.82	1.77	18.65	20.55	0.03	7.03	0.11	0.18	8.73	89.87
048 area 9	34.81	2.11	18.02	20.58	0.02	8.06	0.09	0.18	9.13	93.00
048 area 9	33.07	2.24	16.54	21.65	0.02	7.51	0.07	0.09	8.79	89.99
048 area 9	33.62	1.77	19.22	20.00	0.02	7.80	0.12	0.22	8.87	91.63
048 area 9	34.02	1.77	19.96	20.27	0.01	7.91	0.09	0.21	9.26	93.50
048 area 9	33.67	2.43	18.22	21.28	0.03	8.38	0.03	0.15	9.55	93.75
048 area 9	33.18	2.50	18.64	21.27	0.02	8.27	0.05	0.18	9.30	93.40
048 area 9	33.05	2.58	17.94	20.53	0.01	8.23	0.03	0.22	9.28	91.87
048 area 9	33.14	2.57	18.82	20.06	0.04	7.96	0.07	0.29	9.11	92.07
048 area 9	33.82	2.60	17.52	20.18	0.01	8.63	0.22	0.29	8.95	92.21
048 area 9	32.82	2.63	18.01	20.48	0.02	8.18	0.06	0.26	9.13	91.58
048 area 9	31.32	2.61	17.91	20.35	0.03	7.65	0.05	0.31	9.04	89.28
048 area 9	32.22	2.52	18.24	20.50	0.03	8.08	0.00	0.25	9.28	91.12
048 area 9	31.26	2.55	18.34	20.35	0.02	7.57	0.05	0.22	7.84	88.20
048 area 9	30.37	2.50	18.61	21.25	0.02	7.13	0.05	0.22	7.79	87.94
051 area 1	34.11	2.95	20.15	19.56	0.15	7.46	0.05	0.15	9.37	93.93
051 area 1	33.35	2.98	19.67	19.37	0.15	6.93	0.14	0.22	9.00	91.83
051 area 1	34.77	3.00	19.90	19.77	0.18	7.79	0.06	0.16	9.41	95.03
051 area 1	33.50	3.07	19.73	20.47	0.15	7.22	0.04	0.13	9.37	93.69
051 area 1	31.52	3.11	19.30	20.31	0.16	6.60	0.07	0.16	9.02	90.24
051 area 1	34.20	3.24	19.86	20.09	0.18	7.33	0.01	0.11	9.57	94.59
051 area 1	32.89	3.19	19.95	19.90	0.16	7.01	0.05	0.15	9.34	92.65
051 area 1	29.26	1.02	20.84	26.43	0.20	8.55	0.08	0.14	3.70	90.22
051 area 1	32.64	3.75	18.52	20.22	0.20	6.64	0.07	0.13	9.32	91.49
051 area 1	34.61	3.46	20.02	20.44	0.15	7.29	0.02	0.11	9.61	95.71
051 area 1	34.77	3.27	20.39	19.23	0.14	6.89	0.11	0.13	8.74	93.67
051 area 1	34.13	2.50	20.98	19.77	0.14	7.08	0.07	0.15	9.00	93.84
051 area 1	33.23	2.67	17.86	20.14	0.15	7.39	0.07	0.11	9.27	90.90
051 area 1	33.94	2.48	20.38	20.37	0.16	7.73	0.04	0.13	9.06	94.29

Location	SiO2	TiO2	Al2O3	FeO	MnO	MgO	CaO	Na2O	K2O	Total
051 area 2	35.36	0.93	20.57	20.20	0.11	9.19	0.00	0.07	9.11	95.55
051 area 2	35.14	0.98	20.66	19.40	0.13	9.22	0.01	0.10	9.08	94.74
051 area 2	29.93	0.67	20.91	23.53	0.18	7.06	0.03	0.09	7.01	89.41
051 area 2	34.55	0.87	20.25	20.18	0.14	8.58	0.02	0.08	8.86	93.53
051 area 2	35.75	1.03	21.12	18.64	0.14	7.98	0.02	0.08	8.63	93.39
051 area 2	34.34	1.07	20.60	20.01	0.10	8.64	0.02	0.08	9.20	94.06
051 area 2	34.46	1.37	20.06	20.39	0.09	8.45	0.00	0.07	9.30	94.19
051 area 3	33.86	3.40	19.51	20.71	0.15	7.47	0.06	0.13	9.53	94.83
051 area 3	33.92	3.44	19.59	20.69	0.14	7.36	0.04	0.14	9.60	94.93
051 area 3	33.84	3.41	19.76	20.46	0.15	7.19	0.05	0.13	9.52	94.50
051 area 3	33.47	3.41	19.75	20.39	0.18	7.28	0.02	0.11	9.64	94.25
051 area 3	32.80	3.28	20.34	20.46	0.16	6.95	0.07	0.18	9.16	93.40
051 area 3	33.45	3.22	20.31	20.40	0.16	7.19	0.03	0.14	9.58	94.48
051 area 3	33.57	3.13	20.10	20.13	0.13	7.01	0.15	0.20	9.09	93.51
051 area 3	34.12	3.09	20.05	19.32	0.15	6.96	0.08	0.21	9.05	93.02
051 area 3	33.29	3.09	21.01	19.47	0.14	6.85	0.06	0.16	9.16	93.21
051 area 3	32.19	2.97	19.15	19.42	0.13	6.81	0.04	0.13	9.29	90.13
051 area 3	33.71	3.13	19.45	20.41	0.16	7.25	0.10	0.13	9.37	93.70
051 area 3	33.80	3.15	19.33	20.71	0.16	7.36	0.04	0.11	9.55	94.21
051 area 4	34.47	3.54	20.06	19.74	0.15	7.47	0.02	0.10	9.59	95.13
051 area 4	32.75	3.34	18.48	20.70	0.15	7.08	0.02	0.10	9.18	91.80
051 area 4	33.90	3.36	19.31	20.63	0.14	7.64	0.00	0.11	9.50	94.60
051 area 4	33.77	3.41	19.47	20.80	0.15	7.35	0.00	0.11	9.44	94.50
051 area 4	33.76	3.36	19.77	20.47	0.14	7.43	0.00	0.11	9.54	94.56
051 area 4	33.78	3.43	19.51	20.32	0.15	7.30	0.00	0.09	9.41	93.98
051 area 4	34.09	3.51	19.71	20.23	0.16	7.37	0.02	0.11	9.37	94.57
051 area 4	33.79	3.29	20.13	20.74	0.17	7.35	0.03	0.15	9.55	95.20
051 area 4	33.55	3.36	19.07	20.75	0.18	7.29	0.04	0.13	9.60	93.97
051 area 4	33.86	3.43	19.11	20.78	0.17	7.39	0.00	0.12	9.52	94.37
051 area 4	34.21	3.46	19.57	20.82	0.17	7.45	0.00	0.10	9.70	95.49
051 area 4	33.75	3.61	19.48	20.13	0.14	7.43	0.00	0.11	9.74	94.39
052 area 1	33.02	3.74	18.23	22.24	0.14	6.06	0.00	0.12	9.87	93.42
052 area 1	33.82	3.80	19.08	21.58	0.13	6.06	0.00	0.12	10.04	94.62
052 area 1	32.97	3.77	18.14	22.65	0.11	6.21	0.00	0.12	9.96	93.92
052 area 1	32.67	3.65	18.17	23.06	0.13	5.99	0.01	0.11	9.42	93.21
052 area 1	33.05	3.76	18.09	22.37	0.15	5.98	0.03	0.15	9.79	93.38
052 area 1	33.08	3.71	18.45	22.35	0.14	6.05	0.00	0.14	9.90	93.81
052 area 1	33.24	3.77	18.26	22.10	0.13	6.07	0.02	0.18	9.70	93.47
052 area 1	32.99	3.78	18.62	21.83	0.15	6.00	0.00	0.14	10.05	93.56
052 area 2	64.69	0.00	18.62	0.17	0.01	0.00	0.02	1.44	14.93	99.89
052 area 2	64.94	0.00	18.55	0.16	0.00	0.00	0.00	0.93	15.67	100.25
052 area 2	64.39	0.01	18.51	0.17	0.01	0.00	0.01	0.99	15.65	99.74
052 area 2	64.60	0.01	18.55	0.15	0.02	0.00	0.03	1.46	15.14	99.96
052 area 2	64.83	0.00	18.58	0.13	0.02	0.00	0.02	1.47	14.86	99.93
052 area 2	65.02	0.01	18.50	0.11	0.00	0.00	0.03	1.47	15.13	100.28
052 area 2	34.54	2.83	19.49	20.80	0.07	7.39	0.01	0.14	9.88	95.15
052 area 2	34.19	2.82	19.88	20.67	0.07	7.32	0.01	0.12	9.85	94.93
052 area 2	34.73	2.73	19.57	20.33	0.06	7.11	0.01	0.14	9.94	94.62
052 area 2	33.96	2.70	20.03	20.48	0.08	6.99	0.02	0.15	9.81	94.23
052 area 2	33.50	2.72	19.69	20.34	0.09	6.54	0.05	0.17	9.86	92.95
052 area 2	34.55	2.73	19.63	20.49	0.05	7.12	0.00	0.13	9.98	94.69
052 area 2	34.74	2.74	19.51	20.73	0.06	6.97	0.01	0.14	9.99	94.89

Location	SiO2	TiO2	Al2O3	FeO	MnO	MgO	CaO	Na2O	K2O	Total
052 area 2	34.46	3.18	19.31	21.42	0.09	6.66	0.02	0.11	9.94	95.20
052 area 2	34.24	3.23	19.46	21.12	0.07	6.66	0.00	0.13	10.07	94.99
052 area 2	33.90	3.23	18.87	21.10	0.09	6.60	0.02	0.14	9.99	93.94
052 area 3	34.80	3.58	18.34	21.59	0.12	6.67	0.00	0.11	9.76	94.97
052 area 3	33.39	3.53	18.77	21.76	0.13	6.25	0.00	0.11	9.74	93.68
052 area 3	32.67	3.61	17.79	21.71	0.13	5.98	0.00	0.09	9.50	91.49
052 area 3	33.91	3.67	17.77	22.00	0.14	6.38	0.00	0.10	9.68	93.65
052 area 3	34.00	3.68	18.15	21.68	0.13	6.32	0.00	0.12	9.75	93.84
052 area 3	33.70	3.82	18.26	21.79	0.13	6.24	0.00	0.13	9.77	93.83
052 area 3	33.03	3.68	17.98	21.81	0.13	6.12	0.00	0.13	9.66	92.53
052 area 4	34.78	3.47	19.59	20.01	0.06	6.72	0.05	0.21	9.69	94.59
052 area 4	35.52	2.96	19.23	20.25	0.04	7.22	0.07	0.19	9.66	95.14
052 area 4	35.15	2.85	19.25	19.37	0.06	7.27	0.10	0.22	9.33	93.58
052 area 4	34.55	2.95	20.19	19.79	0.07	6.66	0.08	0.25	9.25	93.79
052 area 4	35.46	3.14	18.33	19.63	0.09	6.78	0.07	0.16	9.37	93.03
052 area 4	34.30	2.60	17.49	20.24	0.10	6.23	0.09	0.11	9.40	90.56
052 area 4	36.87	3.66	17.37	20.46	0.11	6.96	0.09	0.16	9.38	95.07
052 area 4	33.88	3.67	18.73	20.67	0.08	6.45	0.07	0.19	9.56	93.31
052 area 4	24.41	0.15	21.33	31.38	0.07	8.87	0.04	0.04	0.09	86.39
052 area 4	33.69	3.45	18.27	22.86	0.12	6.39	0.05	0.14	9.08	94.05
052 area 4	27.18	1.12	18.38	30.18	0.06	7.95	0.05	0.05	2.88	87.86
052 area 4	32.53	3.40	17.47	22.73	0.11	6.02	0.11	0.16	8.41	90.96
052 area 4	33.83	3.66	18.19	22.03	0.12	6.19	0.05	0.15	9.72	93.94
052 area 4	34.34	3.92	18.75	18.38	0.06	7.98	0.07	0.22	9.66	93.37
052 area 4	32.85	3.86	17.71	18.14	0.06	7.23	0.30	0.19	9.50	89.85
052 area 4	32.43	3.90	19.07	18.56	0.08	7.24	0.07	0.24	9.61	91.19
052 area 5	33.46	3.78	18.36	21.65	0.11	6.39	0.00	0.11	9.57	93.43
052 area 5	33.84	3.77	18.08	21.87	0.12	6.56	0.00	0.11	9.69	94.04
052 area 5	33.87	3.79	19.06	21.70	0.13	6.37	0.00	0.12	9.53	94.57
052 area 5	34.18	3.78	18.27	21.61	0.13	6.50	0.00	0.13	9.42	94.03
052 area 5	33.66	3.76	18.19	22.10	0.11	6.46	0.00	0.10	9.61	94.00
052 area 5	32.93	3.76	18.65	21.85	0.12	6.22	0.00	0.11	9.44	93.09
052 area 5	33.16	3.89	18.57	21.92	0.13	6.33	0.00	0.10	9.52	93.62
052 area 5	35.02	2.73	19.92	20.01	0.07	5.31	0.06	0.10	8.17	91.38
052 area 5	24.09	0.31	20.84	30.83	0.05	8.22	0.08	0.06	0.21	84.69
052 area 5	33.13	4.13	17.62	22.35	0.13	6.24	0.03	0.14	9.10	92.86
052 area 5	31.74	3.54	18.15	23.58	0.10	6.53	0.00	0.10	7.92	91.67
052 area 6	34.51	4.17	18.69	21.10	0.15	6.29	0.06	0.20	9.61	94.78
052 area 6	32.76	3.95	18.82	21.59	0.13	5.66	0.05	0.19	9.51	92.66
052 area 6	34.40	3.97	18.70	21.72	0.14	6.32	0.04	0.17	9.67	95.14
052 area 6	33.60	3.96	18.92	21.56	0.15	5.82	0.04	0.17	9.54	93.76
052 area 6	32.49	3.93	17.28	21.30	0.14	5.70	0.05	0.15	9.41	90.44
052 area 6	34.47	4.01	17.54	21.33	0.12	6.25	0.05	0.18	9.44	93.37
052 area 6	35.33	4.04	17.98	21.72	0.12	6.47	0.04	0.16	9.73	95.59
052 area 6	30.93	4.02	17.57	21.23	0.12	5.27	0.05	0.17	9.47	88.84
052 area 6	34.23	4.03	18.46	21.27	0.13	6.07	0.07	0.20	9.45	93.91
052 area 6	35.00	3.84	18.93	20.53	0.11	6.10	0.12	0.25	8.93	93.82
052 area 7	47.91	3.13	13.12	18.96	0.17	4.85	0.10	0.16	7.92	96.31
052 area 7	34.87	3.52	19.06	21.92	0.18	7.03	0.06	0.19	9.49	96.34
052 area 7	34.15	3.67	17.91	21.58	0.12	6.63	0.08	0.17	9.44	93.74
052 area 7	35.54	3.56	18.89	21.81	0.12	6.85	0.10	0.21	9.34	96.43
052 area 7	36.11	3.57	17.41	21.01	0.12	6.96	0.14	0.23	9.16	94.71

Location	SiO2	TiO2	Al2O3	FeO	MnO	MgO	CaO	Na2O	K2O	Total
052 area 7	36.85	3.41	19.63	17.98	0.08	5.43	0.07	0.12	8.07	91.64
052 area 7	33.79	2.60	16.89	24.64	0.12	7.55	0.06	0.13	7.48	93.26
052 area 7	35.16	3.39	16.74	21.59	0.16	7.06	0.10	0.18	9.45	93.84
052 area 7	51.32	2.54	12.67	16.03	0.15	4.12	0.09	0.10	7.52	94.53
052 area 7	33.89	3.29	17.09	21.63	0.15	6.78	0.12	0.22	9.13	92.30
052 area 7	35.59	3.25	17.86	22.02	0.16	7.06	0.10	0.22	9.25	95.51
052 area 7	34.02	3.09	18.00	22.64	0.14	6.81	0.10	0.22	8.84	93.87
052 area 7	38.44	3.01	19.19	21.18	0.41	5.93	0.11	0.13	8.38	96.79
052 area 7	47.76	1.12	22.90	8.78	0.13	3.09	0.12	0.12	8.22	92.25
052 area 7	22.70	0.02	22.16	31.86	5.86	0.52	1.01	0.07	0.06	84.26
052 area 7	32.87	4.02	16.72	22.34	0.12	5.90	0.02	0.11	9.61	91.70
055 area 1	34.78	3.55	19.92	22.38	0.16	6.78	0.03	0.17	9.52	97.29
055 area 1	34.33	3.50	20.09	21.89	0.16	6.65	0.01	0.15	9.59	96.38
055 area 1	34.23	3.49	19.74	22.21	0.12	6.72	0.01	0.17	9.54	96.25
055 area 1	33.73	3.55	19.81	21.80	0.14	6.71	0.00	0.14	9.51	95.41
055 area 1	38.19	3.37	25.62	12.74	0.09	3.87	0.06	0.11	8.71	92.75
055 area 1	33.39	3.60	19.48	22.76	0.16	6.68	0.00	0.14	9.55	95.77
055 area 1	34.42	3.59	19.90	22.44	0.15	6.62	0.00	0.15	9.66	96.92
055 area 2	34.43	3.37	20.17	22.04	0.10	6.88	0.00	0.14	9.65	96.78
055 area 2	34.26	3.45	20.21	22.53	0.13	6.79	0.00	0.16	9.62	97.15
055 area 2	34.25	3.42	19.80	22.20	0.10	6.87	0.00	0.14	9.66	96.45
055 area 2	34.51	3.21	20.39	21.75	0.08	6.85	0.00	0.16	9.56	96.51
055 area 2	34.43	3.05	20.37	22.60	0.09	6.86	0.00	0.16	9.32	96.87
055 area 3	31.27	3.30	19.21	22.12	0.11	5.43	0.11	0.17	8.81	90.52
055 area 3	34.33	1.87	20.37	21.87	0.14	7.59	0.08	0.19	9.35	95.80
055 area 3	34.08	3.28	20.51	22.50	0.11	6.20	0.14	0.22	9.07	96.11
055 area 3	35.29	3.13	20.18	21.96	0.09	6.66	0.16	0.19	9.04	96.70
055 area 3	34.36	2.91	20.32	21.41	0.08	6.60	0.17	0.23	8.89	94.97
055 area 3	34.40	2.76	16.78	21.02	0.09	6.84	0.22	0.17	9.14	91.41
055 area 3	35.28	2.81	20.64	21.27	0.06	7.05	0.15	0.21	9.09	96.56
055 area 3	34.09	2.84	21.23	20.97	0.08	6.55	0.19	0.27	8.82	95.04
055 area 3	35.75	2.94	20.33	21.65	0.07	7.21	0.17	0.22	9.02	97.36
055 area 3	34.43	3.21	20.63	22.59	0.12	6.55	0.17	0.21	8.89	96.80
055 area 3	32.89	3.28	20.11	22.03	0.09	6.06	0.13	0.20	8.76	93.54
055 area 3	33.18	3.38	19.39	22.54	0.13	6.45	0.07	0.16	9.27	94.57
055 area 3	31.89	3.40	17.27	22.51	0.13	6.03	0.03	0.10	9.35	90.72
055 area 3	33.40	3.43	19.48	21.31	0.12	6.19	0.09	0.20	9.21	93.44
055 area 3	33.87	3.07	18.69	23.94	0.11	7.25	0.09	0.12	8.01	95.15
055 area 3	34.08	3.34	18.31	21.81	0.14	6.71	0.10	0.15	9.34	93.98
055 area 3	31.36	3.40	17.64	21.98	0.11	6.02	0.12	0.15	9.32	90.10
055 area 4	34.63	4.08	18.87	22.73	0.13	6.58	0.00	0.17	9.50	96.69
055 area 4	34.68	3.86	18.90	23.00	0.17	6.78	0.00	0.16	9.53	97.08
055 area 4	34.80	3.89	18.72	22.77	0.14	6.88	0.00	0.16	9.60	96.96
055 area 4	34.45	3.84	19.17	23.09	0.15	6.86	0.01	0.15	9.44	97.14
055 area 4	34.57	3.96	19.12	22.57	0.13	6.66	0.00	0.13	9.58	96.73
055 area 4	34.22	3.83	18.86	23.19	0.14	6.70	0.00	0.13	9.37	96.45
055 area 4	34.40	3.88	18.55	23.67	0.15	6.66	0.00	0.15	9.44	96.89
055 area 4	34.85	3.97	19.26	22.25	0.13	6.68	0.00	0.14	9.62	96.90
055 area 4	34.59	3.80	19.27	22.15	0.12	6.99	0.01	0.15	9.51	96.59
055 area 4	34.57	3.81	19.19	22.92	0.14	6.66	0.01	0.17	9.45	96.92
055 area 4	34.65	3.71	19.12	22.82	0.23	6.70	0.00	0.15	9.37	96.76
055 area 4	34.72	3.86	19.37	22.89	0.15	6.54	0.00	0.16	9.43	97.12

Location	SiO2	TiO2	Al2O3	FeO	MnO	MgO	CaO	Na2O	K2O	Total
055 area 5	34.90	3.51	19.66	22.75	0.15	6.41	0.00	0.13	9.55	97.07
055 area 5	34.68	3.54	19.60	22.81	0.15	6.50	0.00	0.15	9.55	96.97
055 area 5	34.63	3.51	19.72	22.78	0.16	6.39	0.01	0.13	9.50	96.82
055 area 5	34.34	3.54	19.40	22.36	0.17	6.55	0.00	0.14	9.47	95.95
055 area 5	34.90	3.50	19.08	22.36	0.15	6.75	0.01	0.15	9.49	96.39
055 area 5	34.48	3.50	19.39	22.82	0.17	6.59	0.00	0.13	9.54	96.62
055 area 5	34.50	3.49	19.30	22.25	0.16	6.81	0.02	0.13	9.59	96.24
055 area 5	34.31	3.50	19.27	22.23	0.16	6.58	0.02	0.15	9.46	95.67
055 area 5	34.37	3.45	19.50	22.78	0.14	6.85	0.00	0.14	9.63	96.87
055 area 5	34.67	3.40	19.27	22.52	0.14	6.73	0.00	0.14	9.60	96.47
055 area 2	13.98	1.85	12.08	12.49	0.08	4.62	0.00	0.12	7.23	52.44
055 area 2	13.91	1.91	11.99	12.19	0.08	4.54	0.00	0.12	7.13	51.87
055 area 2	13.99	1.94	11.89	12.23	0.10	4.59	0.00	0.10	7.12	51.96
055 area 2	13.83	1.95	11.73	12.28	0.09	4.56	0.00	0.12	7.09	51.64
059 area 1	33.56	1.95	19.47	23.01	0.08	6.22	0.03	0.11	9.71	94.14
059 area 1	32.69	2.36	20.25	23.40	0.08	5.43	0.08	0.19	9.36	93.85
059 area 1	32.58	2.16	19.09	24.30	0.08	6.00	0.02	0.08	9.53	93.84
059 area 1	33.01	2.22	18.46	23.25	0.06	6.20	0.05	0.11	9.75	93.10
059 area 1	33.57	2.14	19.45	23.68	0.05	6.07	0.02	0.13	9.85	94.95
059 area 1	32.12	2.23	18.94	23.88	0.08	5.99	0.00	0.10	9.93	93.27
059 area 1	32.07	2.16	19.18	23.48	0.05	5.80	0.00	0.10	9.98	92.82
059 area 1	32.70	2.52	19.01	23.41	0.06	5.90	0.00	0.07	10.03	93.70
059 area 1	33.18	2.58	18.93	23.51	0.04	5.91	0.00	0.07	9.90	94.13
059 area 1	39.07	1.74	24.34	13.49	0.04	3.00	0.02	0.06	9.09	90.84
059 area 1	95.20	0.00	0.03	0.39	0.00	0.00	0.00	0.00	0.04	95.66
059 area 1	35.63	2.29	18.25	19.05	0.05	8.80	0.08	0.16	9.32	93.62
059 area 1	25.31	0.31	15.01	30.98	1.12	2.01	1.21	0.07	1.48	77.50
059 area 3	33.51	0.39	19.59	21.73	0.04	8.57	0.06	0.17	9.46	93.52
059 area 3	32.48	0.40	20.04	20.98	0.05	8.15	0.03	0.18	9.67	91.98
059 area 3	34.91	0.31	18.46	20.65	0.04	8.42	0.12	0.18	9.49	92.58
059 area 3	32.33	0.38	19.14	20.72	0.04	7.67	0.08	0.17	9.54	90.07
059 area 3	33.29	0.41	20.57	20.85	0.03	8.46	0.04	0.20	9.57	93.42
059 area 3	32.67	3.20	19.17	22.77	0.06	5.38	0.08	0.17	9.53	93.03
059 area 3	31.87	2.99	19.77	23.40	0.09	5.28	0.07	0.16	9.40	93.04
059 area 3	31.07	2.96	19.76	23.01	0.06	4.90	0.10	0.18	9.34	91.37
059 area 3	31.97	3.02	20.23	21.97	0.06	4.80	0.20	0.27	8.95	91.47
059 area 3	31.29	1.01	20.29	23.85	0.08	5.42	0.07	0.14	9.50	91.66
059 area 3	32.23	1.06	19.28	25.09	0.09	5.85	0.02	0.12	9.79	93.53
059 area 3	32.10	1.07	19.34	25.00	0.08	5.82	0.02	0.12	9.65	93.20
059 area 3	32.39	1.08	18.66	24.78	0.10	6.07	0.04	0.12	9.67	92.90
059 area 3	31.60	1.09	19.52	24.46	0.06	5.82	0.04	0.15	9.64	92.39
059 area 3	31.61	1.08	19.30	24.17	0.06	5.92	0.05	0.14	9.57	91.90
059 area 3	32.26	1.62	20.64	23.60	0.07	5.08	0.01	0.07	9.19	92.54
059 area 3	31.60	1.87	18.95	24.09	0.07	5.78	0.00	0.09	9.83	92.28
059 area 3	32.96	3.23	18.60	23.87	0.06	5.63	0.07	0.13	9.61	94.16
059 area 3	31.73	3.48	17.99	23.60	0.06	5.12	0.11	0.19	9.40	91.68
059 area 3	34.25	3.46	18.36	23.30	0.07	5.91	0.06	0.14	9.66	95.20
059 area 3	33.41	3.39	19.37	23.53	0.07	5.44	0.05	0.17	9.61	95.03
059 area 3	33.19	3.18	20.24	22.97	0.05	5.46	0.05	0.17	9.56	94.87
059 area 3	33.64	3.24	19.52	23.43	0.05	5.45	0.05	0.17	9.61	95.17
059 area 3	33.81	2.34	19.77	24.48	0.07	5.87	0.06	0.18	9.49	96.06
059 area 3	32.26	2.31	18.90	24.44	0.09	5.74	0.01	0.10	9.63	93.49

Location	SiO2	TiO2	Al2O3	FeO	MnO	MgO	CaO	Na2O	K2O	Total
059 area 3	32.94	2.41	18.98	23.82	0.05	5.67	0.00	0.11	9.85	93.84
059 area 3	32.88	2.47	19.32	24.08	0.06	5.66	0.00	0.12	9.84	94.43
059 area 3	33.38	2.31	19.11	24.37	0.09	5.94	0.00	0.12	9.79	95.11
059 area 4	35.28	0.00	21.05	37.62	1.88	1.84	0.92	0.00	0.03	98.62
059 area 4	35.28	0.00	20.86	37.49	1.88	2.12	0.96	0.00	0.00	98.60
059 area 4	35.43	0.00	20.89	37.93	1.78	2.20	0.99	0.00	0.01	99.24
059 area 4	35.37	0.00	21.15	37.84	1.80	2.18	0.98	0.00	0.00	99.32
059 area 4	35.46	0.00	21.00	37.83	1.79	2.15	0.99	0.00	0.00	99.22
059 area 4	35.53	0.00	21.20	37.52	1.75	2.14	1.02	0.00	0.00	99.16
059 area 4	35.44	0.00	20.97	38.10	1.75	1.96	0.96	0.00	0.00	99.18
059 area 4	35.55	0.00	21.08	38.10	1.71	2.16	0.98	0.00	0.01	99.58
059 area 4	24.68	0.25	20.83	31.59	0.13	6.63	0.06	0.10	1.03	85.32
059 area 4	24.39	0.83	19.81	28.36	0.14	5.37	0.05	0.10	3.39	82.44
059 area 4	30.04	1.90	20.01	22.26	0.04	4.95	0.05	0.16	9.43	88.85
059 area 4	31.85	1.87	20.07	22.61	0.05	5.60	0.04	0.16	9.59	91.85
059 area 4	35.11	1.81	20.30	21.93	0.05	6.50	0.07	0.17	9.28	95.22
059 area 4	33.96	1.85	17.69	22.44	0.06	6.20	0.11	0.14	9.40	91.86
059 area 4	34.41	1.97	19.06	22.88	0.06	6.24	0.04	0.15	9.67	94.47
059 area 4	34.13	1.68	19.92	22.61	0.06	6.75	0.04	0.15	9.57	94.92
059 area 4	31.30	2.32	18.87	22.03	0.05	5.78	0.05	0.12	9.84	90.38
059 area 4	30.98	2.16	19.01	22.40	0.03	5.80	0.06	0.12	9.80	90.36
059 area 4	33.33	2.21	19.01	22.07	0.06	6.40	0.08	0.14	9.75	93.04
059 area 4	30.91	1.97	18.40	21.51	0.06	5.90	0.10	0.15	9.59	88.59
059 area 4	30.71	2.02	18.35	21.79	0.05	6.05	0.08	0.15	9.78	88.98
059 area 4	32.04	2.13	18.10	22.39	0.05	6.38	0.06	0.10	9.93	91.18
059 area 6	31.61	2.69	19.91	23.24	0.10	5.83	0.10	0.17	9.37	93.02
059 area 6	30.74	2.68	18.35	22.51	0.06	5.56	0.07	0.12	9.72	89.81
059 area 6	32.64	2.78	18.66	22.95	0.06	6.16	0.02	0.11	9.92	93.30
059 area 6	32.84	2.59	19.09	23.24	0.07	6.28	0.07	0.13	9.67	93.98
059 area 6	32.63	2.66	19.36	23.41	0.05	6.15	0.04	0.14	9.87	94.30
059 area 6	32.41	2.60	18.06	22.81	0.08	6.21	0.07	0.13	9.70	92.07
059 area 6	32.64	3.10	18.71	22.88	0.04	6.04	0.02	0.11	9.96	93.48
059 area 6	32.69	3.07	18.89	22.68	0.05	6.13	0.00	0.10	10.03	93.65
059 area 6	32.75	3.36	18.70	23.01	0.04	6.00	0.00	0.09	9.98	93.93
059 area 6	32.33	2.52	19.18	22.87	0.06	5.99	0.03	0.12	9.94	93.04
059 area 6	31.65	2.59	19.03	22.28	0.05	5.85	0.08	0.11	9.72	91.35
059 area 6	32.83	2.58	19.16	22.61	0.06	6.15	0.06	0.12	9.74	93.31
059 area 6	32.66	2.72	18.68	23.55	0.08	6.16	0.01	0.07	9.98	93.91
059 area 6	32.69	2.52	19.03	23.47	0.06	6.02	0.05	0.08	9.90	93.82
059 area 6	33.09	2.72	18.65	23.44	0.05	6.19	0.02	0.11	9.99	94.26
059 area 6	33.18	2.49	18.69	23.49	0.08	6.32	0.04	0.10	9.85	94.25
059 area 6	32.62	2.63	18.73	23.64	0.04	5.98	0.01	0.10	9.84	93.57
059 area 6	33.90	1.36	19.45	21.96	0.02	8.04	0.02	0.13	9.75	94.63
059 area 6	33.29	1.34	19.64	21.58	0.02	7.95	0.00	0.11	9.87	93.80
059 area 6	33.57	1.40	19.60	21.42	0.03	7.82	0.00	0.12	9.93	93.89
059 area 6	33.36	1.39	19.79	21.63	0.04	7.92	0.00	0.12	9.90	94.15
059 area 6	33.58	1.41	19.86	21.51	0.03	7.83	0.00	0.12	9.97	94.30
059 area 6	33.76	1.42	19.92	21.40	0.02	7.81	0.01	0.12	9.93	94.38
059 area 6	33.91	1.38	20.21	20.72	0.03	8.05	0.01	0.13	9.87	94.31
059 area 6	32.77	3.34	19.01	22.04	0.04	6.12	0.08	0.12	9.72	93.26
059 area 6	39.86	1.59	27.97	11.89	0.01	3.26	0.09	0.09	4.93	89.68
059 area 6	33.42	3.17	19.32	21.93	0.03	6.42	0.00	0.09	9.96	94.35

Location	SiO2	TiO2	Al2O3	FeO	MnO	MgO	CaO	Na2O	K2O	Total
059 area 6	33.88	3.51	19.40	22.15	0.03	6.43	0.03	0.13	9.80	95.35

APPENDIX B: Complete Microprobe analyses for garnet

Location	SiO2	TiO2	Al2O3	FeO	MnO	MgO	CaO	Na2O	K2O	Total
013 area 1	36.94	0.11	21.84	35.63	0.19	2.33	4.79	0.00	0.00	101.83
013 area 1	36.01	0.06	21.78	35.25	0.37	2.05	5.42	0.02	0.00	100.95
013 area 1	36.57	0.03	21.58	34.79	0.51	1.96	5.42	0.01	0.00	100.88
013 area 1	35.98	0.04	21.74	35.23	0.42	2.00	5.38	0.00	0.00	100.79
013 area 1	36.26	0.05	21.79	35.78	0.33	2.07	5.20	0.02	0.00	101.50
013 area 1	35.63	0.03	21.29	34.48	0.18	2.09	5.25	0.01	0.00	98.97
013 area 1	35.75	0.08	21.72	36.07	0.15	2.23	4.72	0.02	0.00	100.74
013 area 1	36.28	0.02	21.74	35.75	0.09	2.38	5.15	0.02	0.00	101.44
013 area 3	36.69	0.05	21.81	35.48	0.10	2.29	5.26	0.00	0.00	101.69
013 area 3	57.06	0.55	12.54	13.17	0.01	3.57	0.67	0.08	4.27	91.93
013 area 3	58.05	0.12	25.22	2.73	0.01	1.24	0.06	0.30	6.67	94.41
013 area 3	37.03	0.55	22.51	19.89	0.13	4.92	1.56	0.10	7.09	93.77
013 area 3	34.94	0.06	21.92	35.34	0.18	2.18	5.22	0.01	0.04	99.89
013 area 3	35.90	0.51	21.19	26.10	0.10	4.15	2.49	0.03	3.84	94.31
013 area 3	47.52	0.91	20.23	15.98	0.02	6.34	0.19	0.12	8.00	99.32
013 area 3	35.91	0.09	21.71	35.23	0.40	1.96	5.48	0.01	0.00	100.79
013 area 3	36.19	0.06	21.75	35.42	0.45	1.98	5.45	0.02	0.00	101.32
013 area 3	36.67	0.06	21.79	35.35	0.61	1.86	5.40	0.00	0.01	101.75
013 area 3	35.19	0.06	21.83	35.38	0.43	2.08	5.31	0.01	0.00	100.30
013 area 3	35.24	0.06	21.70	34.57	0.63	1.83	5.70	0.00	0.00	99.74
013 area 3	36.44	0.08	21.65	34.38	1.12	1.73	5.96	0.02	0.00	101.37
013 area 3	35.01	0.07	21.92	33.50	1.44	1.62	6.64	0.01	0.00	100.23
013 area 3	35.77	0.05	21.71	32.81	1.70	1.54	6.89	0.01	0.00	100.48
013 area 3	35.39	0.07	21.77	33.61	1.72	1.63	6.48	0.02	0.00	100.69
013 area 3	35.56	0.18	21.80	33.14	1.76	1.62	6.35	0.02	0.01	100.44
013 area 3	35.34	0.08	21.81	33.63	1.41	1.69	6.11	0.01	0.00	100.08
013 area 3	35.64	0.08	21.83	32.45	1.10	1.76	7.33	0.01	0.01	100.22
013 area 3	31.83	0.02	20.37	33.12	1.12	1.37	4.66	0.05	0.17	92.71
013 area 3	35.16	0.05	21.80	34.09	1.19	1.66	6.06	0.01	0.00	100.02
013 area 3	35.08	0.06	21.15	33.48	1.02	1.63	6.01	0.01	0.00	98.44
013 area 3	35.61	0.04	21.75	34.88	0.79	1.77	5.62	0.02	0.00	100.50
013 area 3	36.33	0.04	21.70	35.05	0.53	1.91	5.61	0.01	0.00	101.19
013 area 3	36.44	0.05	21.70	35.12	0.31	2.14	5.35	0.01	0.00	101.11
013 area 5	34.07	0.07	21.74	35.31	0.09	2.27	5.43	0.01	0.01	99.00
013 area 5	34.80	0.05	21.95	35.55	0.11	2.30	5.24	0.00	0.00	100.00
013 area 5	26.38	0.00	14.43	28.86	0.15	2.98	9.19	0.00	0.00	81.99
013 area 5	35.93	0.06	21.63	34.47	0.68	1.86	5.97	0.01	0.00	100.61
013 area 5	34.48	0.06	21.82	34.35	0.89	1.81	5.85	0.01	0.00	99.27
013 area 5	35.81	0.09	21.67	33.96	0.94	1.82	6.27	0.00	0.00	100.56
013 area 5	35.03	0.05	21.86	34.53	0.65	1.83	6.30	0.01	0.00	100.26
013 area 5	34.79	0.06	21.86	35.33	0.37	2.01	5.45	0.01	0.01	99.88
013 area 5	36.77	0.05	22.64	34.07	0.09	2.40	4.99	0.02	0.82	101.86
013 area 5	35.11	0.06	21.87	36.12	0.07	2.34	4.91	0.00	0.05	100.53
013 area 5	35.86	0.04	21.89	35.98	0.11	2.29	4.97	0.00	0.00	101.14
013 area 5	35.79	0.06	21.89	35.82	0.12	2.25	5.22	0.00	0.00	101.15
013 area 5	35.42	0.04	21.88	36.00	0.13	2.24	4.93	0.00	0.00	100.64
013 area 5	35.48	0.07	21.81	35.86	0.18	2.24	4.85	0.00	0.00	100.48
013 area 5	35.14	0.07	21.82	35.68	0.22	2.07	5.09	0.00	0.00	100.09

Location	SiO2	TiO2	Al2O3	FeO	MnO	MgO	CaO	Na2O	K2O	Total
013 area 5	35.15	0.07	21.82	35.09	0.34	2.18	5.37	0.01	0.01	100.03
013 area 5	34.71	0.07	21.81	34.74	0.45	2.03	5.74	0.00	0.00	99.55
013 area 5	35.08	0.06	21.77	34.32	0.81	1.91	6.14	0.01	0.00	100.11
013 area 5	34.57	0.04	21.79	34.80	0.87	1.77	5.84	0.00	0.00	99.70
013 area 5	35.20	0.05	21.87	34.95	0.67	1.84	5.78	0.00	0.00	100.37
013 area 5	35.85	0.04	21.82	35.03	0.59	1.92	5.56	0.01	0.00	100.82
013 area 5	35.49	0.07	21.87	35.67	0.32	2.05	5.24	0.01	0.00	100.71
013 area 5	33.15	0.22	20.29	32.44	0.14	2.06	5.04	0.01	0.00	93.36
013 area 5	35.43	0.06	21.93	34.84	0.09	2.30	5.45	0.00	0.03	100.12
013 area 8	36.68	0.06	21.49	34.86	0.12	2.13	6.06	0.00	0.00	101.42
013 area 8	35.90	0.04	21.67	35.96	0.15	2.17	5.05	0.00	0.00	100.95
013 area 8	35.77	0.05	21.85	35.57	0.20	2.12	5.60	0.00	0.00	101.16
013 area 8	36.14	0.06	21.75	35.17	0.24	2.11	5.83	0.00	0.00	101.30
013 area 8	35.08	0.09	21.84	35.41	0.24	2.03	5.62	0.00	0.00	100.31
013 area 8	36.00	0.04	21.73	35.47	0.27	2.05	5.58	0.00	0.00	101.16
013 area 8	35.53	0.04	21.89	35.50	0.30	2.08	5.39	0.00	0.01	100.73
013 area 8	36.34	0.05	21.94	35.51	0.19	2.18	5.23	0.00	0.00	101.44
013 area 8	36.85	0.02	21.67	35.43	0.07	2.37	5.28	0.00	0.00	101.69
013 area 8	36.19	0.03	21.67	35.20	0.07	2.36	5.36	0.00	0.00	100.89
013 area 8	36.23	0.06	21.70	36.14	0.13	2.19	4.86	0.00	0.01	101.32
013 area 8	33.46	0.02	19.51	32.46	0.39	1.92	4.98	0.00	0.00	92.74
013 area 8	36.19	0.07	21.82	34.85	0.57	1.84	5.91	0.01	0.00	101.25
032 area 2	38.04	0.00	20.93	32.62	1.01	5.17	2.95	0.00	0.00	100.73
032 area 2	38.22	0.00	21.11	31.11	1.11	5.32	3.64	0.01	0.00	100.51
032 area 2	37.92	0.00	21.05	31.35	1.23	5.25	3.66	0.01	0.00	100.47
032 area 2	38.24	0.00	20.88	31.23	1.26	5.23	3.66	0.01	0.00	100.50
032 area 2	37.98	0.00	20.88	32.74	1.27	4.72	3.20	0.01	0.01	100.81
032 area 2	37.81	0.00	21.01	32.51	1.12	4.93	3.10	0.00	0.00	100.49
032 area 2	38.35	0.00	20.93	32.29	0.98	5.37	3.19	0.01	0.01	101.14
032 area 2	38.03	0.00	21.01	32.68	1.63	4.53	2.98	0.00	0.03	100.87
032 area 2	37.96	0.01	20.86	31.85	1.25	4.72	3.56	0.01	0.01	100.24
032 area 2	37.90	0.00	21.05	32.63	1.63	4.51	3.27	0.01	0.00	101.01
032 area 2	37.96	0.00	20.60	32.40	1.16	4.91	3.22	0.00	0.00	100.25
032 area 2	37.69	0.00	20.88	32.55	1.33	4.67	3.04	0.00	0.01	100.18
032 area 4	37.58	0.00	21.09	31.53	1.33	4.96	3.88	0.00	0.01	100.38
032 area 4	37.74	0.00	21.08	30.93	1.35	5.30	3.86	0.01	0.00	100.27
032 area 4	37.87	0.00	21.18	30.80	1.36	5.30	3.93	0.02	0.00	100.46
032 area 4	37.94	0.00	21.06	30.79	1.33	5.29	3.89	0.01	0.00	100.30
032 area 4	37.82	0.00	21.07	31.72	1.46	4.69	3.75	0.00	0.02	100.53
032 area 4	37.61	0.00	21.10	31.75	1.31	4.72	3.71	0.00	0.01	100.22
032 area 4	37.48	0.00	21.00	32.03	1.33	4.64	3.77	0.00	0.01	100.26
032 area 4	38.00	0.00	21.10	31.97	1.22	4.74	3.32	0.00	0.00	100.35
032 area 4	37.85	0.00	21.29	31.96	1.24	4.98	3.24	0.00	0.01	100.56
032 area 4	37.91	0.00	21.24	31.33	1.15	4.99	3.82	0.00	0.00	100.44
032 area 6	37.30	0.00	21.45	32.10	1.04	5.04	3.50	0.01	0.00	100.44
032 area 6	37.31	0.00	21.42	31.43	0.90	5.32	3.79	0.01	0.00	100.19
032 area 6	37.36	0.00	21.24	31.34	0.84	5.41	4.07	0.01	0.00	100.27
032 area 6	37.34	0.00	21.34	31.12	0.78	5.24	4.06	0.02	0.00	99.91
032 area 6	37.54	0.00	21.23	31.36	0.79	5.20	4.06	0.01	0.00	100.20
032 area 6	37.76	0.00	21.22	31.36	0.78	5.26	4.07	0.00	0.00	100.46
032 area 6	37.65	0.00	21.32	31.25	0.80	5.27	4.07	0.02	0.01	100.38
032 area 6	37.68	0.00	21.16	30.90	0.79	5.24	4.01	0.01	0.00	99.80

Location	SiO2	TiO2	Al2O3	FeO	MnO	MgO	CaO	Na2O	K2O	Total
032 area 6	37.67	0.00	21.05	31.52	0.78	5.13	4.02	0.02	0.00	100.19
032 area 6	37.93	0.00	21.08	31.41	0.89	5.19	4.00	0.00	0.01	100.51
032 area 6	37.76	0.00	21.07	31.57	0.88	5.11	4.05	0.00	0.00	100.46
032 area 6	37.70	0.00	21.26	31.44	0.88	5.10	3.73	0.01	0.00	100.13
032 area 6	37.81	0.00	21.23	31.59	0.87	5.21	3.84	0.01	0.00	100.56
032 area 6	37.77	0.00	21.14	31.28	0.85	5.23	3.87	0.00	0.00	100.14
032 area 6	37.58	0.00	21.32	31.07	0.85	5.21	4.12	0.00	0.01	100.15
032 area 6	37.57	0.00	21.52	31.16	0.85	5.24	4.24	0.00	0.01	100.59
032 area 6	37.78	0.00	21.37	31.18	0.82	5.28	4.23	0.01	0.01	100.69
032 area 6	37.71	0.00	21.16	30.87	0.81	5.36	4.26	0.02	0.01	100.19
032 area 6	36.27	0.00	21.25	31.51	0.90	5.29	3.93	0.00	0.01	99.17
032 area 6	36.21	0.00	21.22	31.09	0.88	5.19	4.25	0.00	0.01	98.85
032 area 6	36.49	0.00	21.27	31.35	0.99	5.18	4.12	0.01	0.00	99.40
032 area 6	36.43	0.00	21.50	31.30	0.88	5.23	4.28	0.01	0.00	99.62
035 area 1	36.52	0.00	21.78	31.44	2.55	3.92	3.89	0.00	0.01	100.11
035 area 1	36.76	0.03	21.95	31.10	2.40	4.28	3.94	0.00	0.00	100.46
035 area 1	36.71	0.01	21.85	31.03	2.41	4.46	3.81	0.01	0.00	100.29
035 area 1	36.26	0.01	21.83	31.07	2.41	4.37	3.86	0.01	0.00	99.82
035 area 1	36.44	0.01	21.86	31.12	2.38	4.47	3.74	0.00	0.00	100.03
035 area 1	38.05	0.00	21.76	30.33	2.30	4.39	3.86	0.01	0.00	100.70
035 area 1	31.54	0.00	24.01	28.49	2.22	3.57	3.60	0.15	0.02	93.60
035 area 1	24.75	0.03	20.01	20.30	3.04	0.84	2.88	0.48	0.26	72.58
035 area 1	36.85	0.06	22.01	30.77	2.31	4.44	3.86	0.00	0.00	100.30
035 area 1	36.70	0.00	22.05	31.11	2.28	4.45	3.88	0.00	0.00	100.47
035 area 1	36.96	0.02	22.05	30.91	2.27	4.20	4.22	0.01	0.00	100.64
035 area 1	36.59	0.02	21.88	30.93	4.01	2.96	4.03	0.00	0.00	100.42
035 area 1	36.78	0.00	22.13	31.79	2.88	3.52	3.79	0.00	0.02	100.89
035 area 1	36.43	0.00	22.03	31.32	3.70	3.04	3.60	0.00	0.03	100.16
035 area 1	36.53	0.00	22.06	31.44	3.25	3.30	3.60	0.00	0.02	100.19
035 area 1	36.65	0.00	22.08	31.55	2.67	3.59	3.61	0.00	0.01	100.17
035 area 1	36.38	0.00	21.82	31.12	3.55	3.19	4.19	0.00	0.01	100.27
035 area 1	36.18	0.00	21.94	31.51	2.57	3.58	4.15	0.00	0.01	99.94
035 area 1	36.09	0.00	21.93	31.07	2.29	3.92	4.06	0.01	0.01	99.38
035 area 1	36.32	0.01	21.86	31.79	2.54	3.86	3.60	0.00	0.01	99.99
035 area 1	35.99	0.00	21.82	30.73	3.88	2.89	4.48	0.01	0.01	99.80
035 area 1	35.97	0.02	21.94	31.74	2.52	3.86	3.53	0.00	0.02	99.61
035 area 1	36.16	0.02	21.89	31.78	2.30	3.99	3.56	0.00	0.02	99.70
035 area 1	36.06	0.01	21.76	31.67	2.51	3.94	3.74	0.00	0.01	99.69
035 area 4	37.02	0.00	21.87	30.83	2.18	3.57	4.42	0.00	0.00	99.89
035 area 4	37.26	0.00	22.04	31.07	1.89	3.96	4.39	0.00	0.00	100.62
035 area 4	37.22	0.01	22.02	31.13	1.72	4.23	4.15	0.00	0.00	100.48
035 area 4	37.34	0.01	22.05	31.25	1.70	4.18	4.23	0.00	0.01	100.77
035 area 4	37.09	0.00	22.00	31.63	1.73	4.14	4.13	0.00	0.00	100.73
035 area 4	37.25	0.02	21.90	31.25	1.82	4.08	4.18	0.16	0.00	100.66
035 area 4	37.31	0.02	21.75	31.41	1.82	4.08	4.07	0.00	0.00	100.46
035 area 4	37.55	0.00	21.88	31.47	1.84	4.00	4.04	0.00	0.00	100.78
035 area 4	37.32	0.00	22.00	31.30	1.90	4.06	3.85	0.01	0.00	100.44
035 area 4	37.61	0.00	21.99	30.87	1.96	4.02	3.90	0.01	0.00	100.38
035 area 4	37.50	0.00	22.25	30.84	1.95	4.02	4.17	0.00	0.00	100.72
035 area 4	37.16	0.00	21.65	30.22	1.99	3.73	4.24	0.00	0.00	99.00
035 area 4	39.62	0.01	22.12	30.74	3.09	3.48	4.38	0.00	0.03	103.47
035 area 4	35.46	0.02	12.86	29.46	3.66	2.65	4.30	0.00	0.06	88.47

Location	SiO2	TiO2	Al2O3	FeO	MnO	MgO	CaO	Na2O	K2O	Total
035 area 4	40.82	0.03	21.61	28.58	4.92	2.94	4.25	0.03	0.10	103.28
035 area 4	37.41	0.00	21.84	29.94	4.03	2.76	4.48	0.04	0.01	100.50
035 area 4	38.52	0.00	21.70	31.09	2.45	3.66	4.43	0.01	0.00	101.85
035 area 4	37.13	0.02	21.84	30.83	3.45	2.95	4.43	0.01	0.02	100.67
035 area 4	37.02	0.00	21.95	31.33	2.48	3.41	4.27	0.00	0.01	100.47
035 area 4	37.63	0.00	22.07	31.35	2.20	3.77	4.10	0.00	0.00	101.11
035 area 4	37.32	0.00	22.04	31.23	2.08	3.89	4.08	0.00	0.00	100.65
035 area 4	37.22	0.00	22.06	31.24	1.97	3.98	4.07	0.00	0.00	100.54
035 area 4	37.33	0.00	22.05	31.13	1.83	4.16	4.13	0.00	0.00	100.64
035 area 4	37.39	0.00	21.89	31.07	1.74	4.14	4.06	0.00	0.00	100.31
035 area 4	37.22	0.00	21.88	31.48	1.74	4.15	4.03	0.00	0.00	100.51
035 area 4	37.46	0.02	21.75	31.39	1.80	4.17	4.12	0.00	0.00	100.72
035 area 4	37.88	0.00	22.05	31.21	1.82	4.15	4.06	0.00	0.01	101.18
035 area 4	37.20	0.00	22.05	30.70	2.57	3.35	4.67	0.00	0.00	100.54
035 area 4	37.03	0.00	21.94	30.69	2.49	3.34	4.71	0.00	0.00	100.21
035 area 4	37.30	0.00	22.03	30.83	2.47	3.41	4.78	0.00	0.00	100.81
035 area 5	37.12	0.02	21.83	30.36	4.54	2.66	3.84	0.02	0.03	100.41
035 area 5	9.52	0.00	23.05	26.76	1.68	0.41	3.08	0.17	0.07	64.74
035 area 5	37.71	0.01	22.12	31.88	1.73	4.59	3.12	0.00	0.00	101.16
035 area 5	37.59	0.00	21.91	31.31	1.69	4.48	3.55	0.00	0.00	100.53
035 area 5	37.39	0.03	21.23	31.42	1.66	4.42	3.67	0.01	0.01	99.83
035 area 5	37.36	0.02	21.83	31.52	1.72	4.46	3.74	0.01	0.00	100.67
035 area 5	37.38	0.02	21.78	31.59	1.70	4.37	3.69	0.01	0.00	100.53
035 area 5	37.53	0.00	21.81	31.55	1.69	4.45	3.68	0.00	0.01	100.70
035 area 5	37.47	0.01	22.03	31.17	1.67	4.46	3.70	0.01	0.00	100.50
035 area 5	37.46	0.01	22.12	31.51	1.71	4.54	3.43	0.00	0.01	100.79
035 area 5	37.60	0.00	22.06	31.52	1.77	4.41	3.55	0.00	0.00	100.92
035 area 5	36.99	0.08	21.83	30.65	2.88	3.32	3.97	0.44	0.00	100.15
035 area 5	37.22	0.09	21.91	30.92	3.02	3.20	4.14	0.00	0.00	100.50
035 area 5	37.23	0.08	21.96	31.34	3.03	3.26	3.98	0.00	0.00	100.88
035 area 5	36.88	0.06	21.37	31.15	2.98	3.24	4.14	0.00	0.00	99.83
035 area 5	37.07	0.08	22.00	31.47	2.94	3.40	3.98	0.00	0.00	100.94
035 area 5	37.37	0.12	22.17	31.16	2.99	3.38	3.88	0.00	0.00	101.08
035 area 5	37.22	0.11	21.93	31.23	2.63	3.59	4.01	0.00	0.00	100.73
035 area 5	37.57	0.02	21.87	31.54	2.67	3.60	3.47	0.01	0.02	100.75
035 area 5	36.29	0.01	24.85	27.11	6.21	1.80	2.52	0.17	0.24	99.22
035 area 5	36.97	0.01	22.02	31.66	3.06	3.20	3.17	0.01	0.03	100.12
035 area 5	37.40	0.00	21.93	30.48	3.92	2.90	3.89	0.00	0.05	100.57
035 area 5	38.94	0.03	21.31	28.59	3.89	2.65	3.81	0.09	0.15	99.46
035 area 5	41.93	0.00	19.69	30.22	3.41	3.74	3.75	0.01	0.05	102.81
035 area 6	37.41	0.00	22.35	30.99	2.51	3.55	4.28	0.01	0.00	101.11
035 area 6	40.42	0.00	8.31	30.29	1.82	4.45	3.35	0.04	0.00	88.67
035 area 6	38.70	0.00	22.06	31.61	2.05	4.49	3.75	0.00	0.00	102.66
035 area 6	37.36	0.00	22.08	31.11	2.05	4.33	3.68	0.01	0.00	100.64
035 area 6	37.13	0.00	22.07	31.34	1.93	4.37	3.88	0.01	0.00	100.72
035 area 6	37.63	0.00	22.13	31.17	1.89	4.35	3.87	0.00	0.00	101.03
035 area 6	36.38	0.00	21.84	30.52	1.86	4.13	4.08	0.00	0.00	98.82
035 area 6	37.58	0.01	21.93	31.05	1.90	4.35	4.10	0.00	0.00	100.93
035 area 6	36.60	0.01	24.36	30.78	1.88	4.17	3.90	0.04	0.00	101.75
035 area 6	36.43	0.00	20.30	31.30	1.86	4.14	3.93	0.00	0.01	97.97
035 area 6	37.52	0.00	22.01	31.19	1.94	4.35	3.87	0.00	0.01	100.89
035 area 6	37.76	0.00	22.07	31.10	1.93	4.36	3.74	0.00	0.00	100.97

Location	SiO2	TiO2	Al2O3	FeO	MnO	MgO	CaO	Na2O	K2O	Total
035 area 6	37.77	0.00	22.14	31.12	1.94	4.30	3.77	0.00	0.00	101.05
035 area 6	37.90	0.00	22.07	30.93	2.06	4.27	3.84	0.00	0.01	101.08
035 area 6	37.76	0.00	22.08	31.34	2.12	4.12	3.78	0.00	0.00	101.21
035 area 6	37.53	0.00	21.98	31.12	2.25	3.93	3.73	0.02	0.01	100.56
035 area 6	35.45	0.00	22.18	30.43	2.81	3.29	3.59	0.09	0.01	97.86
035 area 6	38.84	0.01	22.67	30.08	4.13	2.88	4.09	0.01	0.06	102.78
035 area 6	37.70	0.01	21.90	30.87	3.54	3.00	3.96	0.01	0.03	101.02
035 area 6	37.91	0.01	21.92	31.04	3.43	3.15	3.96	0.00	0.03	101.46
035 area 6	37.37	0.01	21.86	31.06	3.62	3.02	3.94	0.00	0.01	100.89
035 area 6	37.39	0.00	21.88	30.95	4.12	2.84	3.72	0.00	0.02	100.92
035 area 6	37.26	0.00	21.99	31.14	3.34	3.10	3.92	0.01	0.01	100.76
035 area 6	37.46	0.01	21.47	30.13	4.42	2.66	4.08	0.03	0.03	100.28
035 area 6	37.58	0.00	21.92	31.03	2.95	3.27	4.35	0.00	0.00	101.09
039 area 1	35.67	0.01	21.63	29.02	5.58	1.15	7.30	0.02	0.00	100.37
039 area 1	36.03	0.00	21.70	29.49	4.40	1.16	7.78	0.02	0.00	100.59
039 area 1	36.05	0.02	21.69	30.09	3.35	1.17	8.28	0.04	0.00	100.69
039 area 1	36.18	0.03	21.69	30.14	3.23	1.13	8.36	0.03	0.00	100.78
039 area 1	36.11	0.04	21.66	29.41	3.21	0.99	9.01	0.03	0.00	100.46
039 area 1	36.13	0.15	21.38	29.51	3.25	0.98	9.14	0.04	0.00	100.58
039 area 1	35.87	0.19	21.65	29.46	3.37	0.98	9.05	0.04	0.00	100.62
039 area 1	36.05	0.03	21.79	29.81	3.34	1.04	8.92	0.03	0.01	101.01
039 area 1	35.75	0.03	21.73	29.83	3.29	1.04	8.55	0.04	0.00	100.26
039 area 1	36.04	0.02	21.56	29.19	4.14	1.13	8.10	0.02	0.02	100.22
039 area 1	35.27	0.02	21.83	28.92	4.31	1.10	8.44	0.03	0.00	99.91
039 area 1	35.33	0.03	21.77	30.14	3.01	1.01	8.79	0.04	0.00	100.13
039 area 1	35.21	0.05	21.68	29.91	2.92	1.00	8.92	0.04	0.01	99.74
039 area 1	35.26	0.04	21.66	29.60	3.16	1.00	8.94	0.04	0.00	99.70
039 area 1	35.29	0.03	21.69	29.38	3.36	1.04	8.84	0.05	0.01	99.70
039 area 1	14.89	0.00	9.68	14.03	1.76	0.50	34.67	0.04	0.00	75.57
039 area 1	35.40	0.02	21.70	29.80	3.99	1.19	7.87	0.03	0.00	100.00
039 area 3	36.77	0.06	21.39	30.31	2.26	1.10	8.89	0.03	0.00	100.82
039 area 3	36.89	0.01	21.50	30.05	3.34	0.95	8.55	0.02	0.01	101.33
039 area 3	36.96	0.06	21.22	28.00	4.57	0.76	9.12	0.03	0.00	100.72
039 area 3	37.37	0.12	21.31	27.14	5.46	0.70	9.36	0.04	0.00	101.51
039 area 3	37.22	0.11	21.21	27.56	5.71	0.95	8.45	0.04	0.00	101.25
039 area 3	37.37	0.08	21.10	28.79	5.40	1.17	7.44	0.01	0.00	101.35
039 area 3	37.72	0.09	20.96	28.97	5.65	1.11	7.13	0.01	0.00	101.65
039 area 3	36.19	0.01	21.51	28.72	5.82	1.10	7.41	0.02	0.00	100.79
039 area 3	36.41	0.19	21.29	25.42	7.55	0.74	8.77	0.02	0.00	100.39
039 area 3	36.86	0.12	21.14	25.41	7.41	0.76	8.72	0.03	0.00	100.46
039 area 3	36.84	0.11	21.32	26.15	6.78	0.83	8.79	0.02	0.00	100.84
039 area 3	36.44	0.11	20.98	25.68	6.72	0.68	9.14	0.03	0.01	99.80
039 area 3	36.19	0.08	21.50	27.02	6.10	0.65	9.09	0.03	0.00	100.67
039 area 3	35.35	0.10	21.63	27.62	4.94	0.83	9.43	0.04	0.00	99.94
039 area 3	36.37	0.06	21.55	28.85	5.08	1.14	7.86	0.03	0.00	100.94
039 area 3	36.09	0.07	21.46	28.53	5.41	1.14	7.72	0.01	0.00	100.45
039 area 3	36.49	0.05	21.45	28.94	5.36	1.19	7.35	0.01	0.01	100.86
039 area 3	35.65	0.03	21.86	29.00	5.64	1.26	6.95	0.03	0.00	100.43
039 area 3	35.70	0.01	21.91	28.86	5.14	1.15	7.62	0.03	0.00	100.43
039 area 3	35.64	0.07	21.56	29.59	3.38	0.95	8.83	0.03	0.00	100.05
039 area 4	35.81	0.03	21.81	31.77	1.18	1.23	9.04	0.02	0.00	100.89
039 area 4	35.60	0.06	21.70	30.18	3.54	1.08	8.41	0.03	0.00	100.61

Location	SiO2	TiO2	Al2O3	FeO	MnO	MgO	CaO	Na2O	K2O	Total
039 area 4	35.62	0.09	21.57	28.74	4.88	0.98	8.40	0.02	0.00	100.30
039 area 4	35.71	0.10	21.58	27.77	5.44	0.82	8.98	0.02	0.00	100.41
039 area 4	35.20	0.07	21.63	28.24	5.36	1.07	8.34	0.02	0.00	99.94
039 area 4	35.65	0.04	21.35	29.36	5.49	1.26	7.18	0.01	0.00	100.35
039 area 4	35.27	0.09	21.37	28.65	5.89	1.16	7.10	0.01	0.00	99.54
039 area 4	35.21	0.09	21.53	28.94	5.26	1.24	7.66	0.01	0.00	99.94
039 area 4	35.20	0.06	21.77	27.16	5.98	1.04	8.57	0.01	0.00	99.78
039 area 4	34.85	0.12	21.44	27.91	5.78	1.11	7.86	0.01	0.00	99.08
039 area 4	34.89	0.11	21.49	28.18	5.88	1.07	8.02	0.02	0.00	99.66
039 area 4	35.14	0.11	21.60	28.78	5.28	1.19	7.96	0.02	0.00	100.08
039 area 4	35.28	0.07	21.29	28.16	6.31	1.13	7.17	0.02	0.00	99.43
039 area 4	35.63	0.11	21.44	27.55	6.31	1.01	8.14	0.02	0.00	100.20
039 area 4	36.04	0.06	21.57	29.24	5.32	1.17	7.37	0.02	0.00	100.80
039 area 4	35.74	0.02	21.69	28.74	5.34	1.22	7.57	0.01	0.00	100.34
039 area 4	35.94	0.12	21.34	26.83	6.23	1.01	8.40	0.01	0.00	99.88
039 area 4	35.88	0.11	21.36	27.32	5.89	0.98	8.45	0.02	0.00	100.02
039 area 4	35.59	0.14	21.56	27.07	5.66	1.04	8.75	0.02	0.00	99.84
039 area 4	35.38	0.08	21.59	28.72	4.94	1.22	7.99	0.03	0.00	99.97
039 area 4	35.12	0.06	21.60	29.18	4.76	1.25	7.65	0.02	0.00	99.65
039 area 4	35.81	0.07	21.42	28.81	4.91	1.27	7.55	0.02	0.00	99.88
039 area 8	37.40	0.04	21.59	28.22	1.72	1.57	10.81	0.00	0.00	101.35
039 area 8	36.84	0.05	21.67	29.09	1.12	1.44	10.84	0.01	0.00	101.07
039 area 8	36.66	0.03	21.62	29.31	1.01	1.36	10.47	0.01	0.00	100.47
039 area 8	36.60	0.03	21.68	29.64	1.10	1.40	10.33	0.01	0.00	100.80
039 area 8	36.58	0.04	21.63	29.70	1.07	1.36	10.33	0.02	0.00	100.73
039 area 8	36.60	0.04	21.68	29.91	1.13	1.29	10.30	0.02	0.00	100.96
039 area 8	36.61	0.06	21.61	29.88	1.14	1.24	10.18	0.02	0.00	100.74
039 area 8	36.88	0.03	21.59	29.83	1.16	1.35	10.34	0.01	0.00	101.19
039 area 8	36.69	0.04	21.64	29.59	1.18	1.28	10.31	0.02	0.00	100.75
039 area 8	36.60	0.04	21.65	29.37	1.38	1.24	10.32	0.01	0.00	100.61
039 area 8	36.79	0.06	21.53	29.91	1.17	1.26	10.24	0.02	0.00	100.97
039 area 8	36.65	0.03	21.67	30.37	1.22	1.25	9.89	0.01	0.00	101.09
039 area 8	36.98	0.03	21.51	29.66	1.30	1.34	10.09	0.01	0.00	100.93
039 area 8	37.68	0.04	21.56	29.88	1.23	1.31	10.09	0.00	0.00	101.80
039 area 8	37.36	0.04	21.52	29.95	1.18	1.34	9.99	0.02	0.00	101.38
039 area 8	37.71	0.03	21.39	29.55	1.16	1.41	10.19	0.01	0.00	101.46
039 area 8	35.83	0.02	21.89	28.41	1.83	1.44	10.69	0.00	0.00	100.11
039 area 8	36.32	0.03	21.82	27.79	2.21	1.52	10.97	0.02	0.00	100.67
039 area 8	35.91	0.01	21.89	25.29	4.14	1.22	11.40	0.02	0.00	99.89
039 area 8	36.29	0.04	21.91	28.82	1.13	1.47	10.92	0.01	0.00	100.60
039 area 8	36.28	0.03	21.88	27.80	1.59	1.36	11.49	0.02	0.01	100.46
039 area 8	35.53	0.02	21.97	28.93	1.11	1.45	10.90	0.01	0.01	99.93
039 area 8	35.67	0.05	21.84	29.20	1.13	1.40	10.91	0.01	0.00	100.20
039 area 8	37.23	0.01	21.56	24.94	4.29	0.97	11.95	0.00	0.00	100.95
039 area 8	36.55	0.06	21.73	23.91	3.05	1.15	13.78	0.00	0.00	100.22
039 area 8	36.41	0.03	21.82	27.18	1.58	1.61	12.09	0.01	0.00	100.74
039 area 8	36.10	0.06	21.63	26.18	1.95	1.52	12.12	0.00	0.01	99.55
039 area 8	37.92	0.05	21.95	21.98	1.87	1.99	14.80	0.00	0.01	100.57
039 area 8	36.44	0.06	22.06	20.91	2.86	1.87	15.80	0.00	0.00	100.00
039 area 8	36.94	0.08	21.77	20.21	2.81	2.00	16.03	0.00	0.00	99.85
039 area 8	36.92	0.07	21.83	22.27	2.87	1.38	15.05	0.00	0.02	100.40
039 area 8	36.89	0.08	21.99	20.73	2.43	2.06	15.85	0.00	0.00	100.04

Location	SiO2	TiO2	Al2O3	FeO	MnO	MgO	CaO	Na2O	K2O	Total
039 area 8	37.68	0.07	21.78	19.91	3.03	2.15	15.64	0.00	0.00	100.28
039 area 8	37.30	0.08	21.80	21.52	2.57	1.59	15.48	0.00	0.00	100.34
039 area 8	37.66	0.10	21.67	22.35	2.66	1.41	15.18	0.00	0.00	101.03
039 area 8	36.93	0.07	21.97	21.05	3.00	1.71	15.58	0.00	0.00	100.30
039 area 8	36.43	0.04	22.07	20.98	2.76	1.70	16.03	0.01	0.00	100.02
039 area 8	37.79	0.02	21.70	23.67	2.23	1.43	14.15	0.00	0.00	100.98
039 area 8	0.00	0.00	0.00	0.05	0.04	0.01	55.02	0.00	0.00	55.12
039 area 8	22.52	0.09	20.42	32.48	0.86	7.07	0.09	0.00	0.03	83.56
039 area 8	37.45	0.04	21.56	23.98	2.57	1.22	14.00	0.00	0.01	100.82
039 area 8	0.00	0.00	0.00	0.10	0.02	0.00	55.57	0.02	0.00	55.72
044 area 3	36.20	0.00	21.44	34.26	3.40	1.51	4.33	0.00	0.00	101.16
044 area 3	36.34	0.00	21.44	34.96	3.10	1.66	3.75	0.00	0.00	101.27
044 area 3	97.24	0.00	0.00	0.47	0.05	0.00	0.01	0.00	0.00	97.78
044 area 3	36.40	0.00	21.27	34.55	3.03	1.69	4.42	0.00	0.00	101.36
044 area 3	36.30	0.00	21.20	34.24	3.67	1.44	4.00	0.01	0.01	100.88
044 area 3	36.39	0.00	21.43	34.30	3.57	1.40	3.91	0.00	0.01	101.00
044 area 3	36.33	0.00	21.39	34.36	3.52	1.47	3.92	0.00	0.00	101.00
044 area 3	36.14	0.00	21.30	34.38	4.01	1.29	3.84	0.00	0.01	100.97
044 area 3	35.95	0.00	21.42	33.75	4.36	1.18	4.19	0.01	0.00	100.85
044 area 3	36.32	0.01	21.26	34.35	3.93	1.41	4.15	0.01	0.00	101.44
044 area 5	35.37	0.00	21.22	33.06	4.19	1.26	4.60	0.01	0.00	99.71
044 area 5	35.03	0.00	21.26	34.35	3.35	1.54	4.24	0.01	0.00	99.78
044 area 5	35.27	0.00	21.29	34.77	3.24	1.59	4.17	0.01	0.00	100.33
044 area 5	35.28	0.00	21.46	34.48	3.22	1.59	4.32	0.01	0.00	100.38
044 area 5	34.98	0.00	21.51	34.57	3.13	1.59	4.09	0.01	0.00	99.88
044 area 5	34.87	0.00	21.56	34.17	3.18	1.58	4.52	0.01	0.00	99.88
044 area 5	34.72	0.00	21.32	33.72	3.39	1.49	4.59	0.00	0.00	99.24
044 area 5	34.93	0.00	21.38	33.19	4.39	1.14	4.51	0.00	0.03	99.59
044 area 5	34.67	0.00	21.25	33.67	4.10	1.34	4.50	0.01	0.00	99.55
044 area 5	34.92	0.00	21.55	33.95	3.89	1.27	4.05	0.01	0.01	99.64
044 area 5	35.05	0.01	21.46	34.41	3.58	1.48	3.98	0.00	0.01	99.98
044 area 8	35.42	0.00	21.48	34.99	2.96	1.62	4.11	0.00	0.00	100.59
044 area 8	35.61	0.00	21.49	35.03	2.66	1.73	4.12	0.00	0.00	100.64
044 area 8	35.82	0.00	21.33	35.13	2.92	1.66	3.98	0.00	0.00	100.85
044 area 8	35.58	0.00	21.42	35.10	2.63	1.75	4.10	0.00	0.00	100.58
044 area 8	35.63	0.00	21.34	35.10	2.70	1.74	4.08	0.00	0.00	100.60
044 area 8	35.67	0.01	21.20	34.93	2.76	1.61	4.05	0.00	0.00	100.22
044 area 8	35.84	0.00	21.39	34.08	3.51	1.36	4.40	0.01	0.01	100.60
044 area 8	35.55	0.00	21.41	34.69	2.79	1.60	4.15	0.00	0.02	100.20
044 area 8	35.81	0.00	21.41	34.82	2.78	1.60	4.27	0.00	0.02	100.71
044 area 8	35.73	0.00	21.42	34.05	3.08	1.52	4.52	0.00	0.01	100.35
044 area 8	35.63	0.01	21.32	35.15	2.76	1.60	4.07	0.00	0.02	100.56
044 area 8	35.65	0.01	21.33	34.82	2.77	1.60	4.14	0.00	0.02	100.36
044 area 8	35.40	0.00	21.44	34.72	2.83	1.62	4.39	0.00	0.00	100.39
044 area 8	35.79	0.00	21.37	34.22	3.21	1.55	4.33	0.00	0.00	100.47
044 area 8	35.76	0.00	21.28	34.55	3.42	1.44	4.29	0.00	0.00	100.75
044 area 8	35.92	0.00	21.27	34.63	3.12	1.46	4.25	0.00	0.00	100.66
044 area 8	35.87	0.01	21.28	34.76	3.18	1.49	4.05	0.00	0.00	100.65
046 area 2	36.40	0.00	20.78	37.76	1.21	2.77	1.18	0.00	0.00	100.09
046 area 2	36.39	0.00	20.78	37.63	1.16	2.53	1.27	0.00	0.01	99.77
046 area 2	36.31	0.00	20.87	37.61	1.23	2.78	1.11	0.00	0.00	99.93
046 area 2	36.48	0.00	20.95	37.75	1.24	2.71	1.10	0.01	0.02	100.25

Location	SiO2	TiO2	Al2O3	FeO	MnO	MgO	CaO	Na2O	K2O	Total
046 area 2	36.43	0.00	20.82	37.80	1.27	2.70	1.19	0.00	0.01	100.23
046 area 2	36.49	0.00	20.85	37.52	1.25	2.82	1.12	0.00	0.00	100.05
046 area 2	36.76	0.00	20.76	37.66	1.20	2.82	1.21	0.00	0.01	100.42
046 area 2	36.59	0.00	21.41	37.89	1.23	2.70	1.11	0.01	0.01	100.96
046 area 2	36.15	0.00	20.74	37.83	1.22	2.67	1.31	0.00	0.00	99.93
046 area 2	35.70	0.00	20.95	37.58	1.70	2.41	1.26	0.00	0.01	99.62
046 area 2	35.72	0.00	21.04	37.56	1.08	2.85	1.37	0.00	0.00	99.62
046 area 2	35.56	0.00	21.01	37.44	1.09	2.91	1.26	0.00	0.00	99.27
046 area 2	35.71	0.00	21.00	37.55	1.14	2.86	1.24	0.00	0.00	99.50
046 area 2	35.69	0.00	20.95	37.41	1.48	2.59	1.33	0.00	0.00	99.45
046 area 2	38.08	0.00	22.10	37.64	2.25	2.20	1.10	0.02	0.04	103.43
046 area 2	36.11	0.00	20.83	37.09	3.44	1.38	1.20	0.00	0.04	100.07
046 area 2	36.16	0.00	20.91	37.83	1.64	2.44	1.29	0.01	0.01	100.29
046 area 2	36.11	0.02	20.67	37.57	1.99	2.22	1.44	0.01	0.01	100.03
046 area 2	35.96	0.01	20.58	37.88	1.81	2.14	1.34	0.00	0.01	99.73
046 area 2	35.90	0.09	21.03	37.77	2.14	2.04	1.26	0.00	0.00	100.24
046 area 2	36.30	0.00	20.76	37.65	1.47	2.54	1.32	0.01	0.00	100.06
046 area 2	36.37	0.00	20.93	37.74	1.60	2.33	1.35	0.01	0.02	100.36
046 area 3	35.60	0.00	20.79	37.32	2.01	2.18	1.31	0.00	0.01	99.22
046 area 3	35.83	0.00	20.83	37.39	1.87	2.36	1.15	0.00	0.00	99.43
046 area 3	36.07	0.00	20.74	37.57	1.86	2.34	1.21	0.00	0.01	99.80
046 area 3	36.52	0.00	20.77	37.82	1.94	2.29	1.19	0.01	0.00	100.54
046 area 3	36.16	0.00	20.90	37.48	2.21	2.05	1.12	0.01	0.01	99.93
046 area 3	38.32	0.00	19.85	37.14	2.22	2.39	1.17	0.02	0.03	101.12
046 area 3	35.66	0.00	20.90	37.73	2.10	2.14	1.08	0.00	0.00	99.61
046 area 3	35.75	0.00	20.87	37.75	2.10	2.07	1.21	0.01	0.00	99.75
046 area 3	35.97	0.00	20.65	38.10	2.30	2.04	1.15	0.00	0.00	100.22
046 area 5	36.38	0.00	20.88	37.27	1.46	2.67	1.52	0.00	0.01	100.19
046 area 5	36.34	0.01	20.81	37.58	1.47	2.62	1.54	0.00	0.03	100.40
046 area 5	36.41	0.00	20.96	37.41	1.48	2.71	1.56	0.00	0.01	100.55
046 area 5	36.60	0.00	20.93	37.56	1.45	2.73	1.50	0.00	0.01	100.79
046 area 5	36.48	0.00	20.70	37.29	1.47	2.69	1.69	0.00	0.01	100.33
046 area 5	36.65	0.00	20.99	37.48	1.43	2.71	1.58	0.00	0.01	100.86
046 area 5	35.57	0.00	20.79	37.25	1.62	2.58	1.41	0.00	0.00	99.23
046 area 5	35.82	0.01	20.96	37.24	1.51	2.79	1.46	0.00	0.00	99.80
046 area 5	35.59	0.00	21.08	37.03	1.43	2.89	1.57	0.00	0.00	99.58
046 area 5	35.56	0.00	21.03	37.05	1.57	2.79	1.50	0.00	0.00	99.50
046 area 5	35.72	0.00	21.07	37.19	1.58	2.86	1.46	0.00	0.00	99.88
046 area 5	36.13	0.00	20.99	36.98	1.53	2.81	1.54	0.00	0.00	99.97
046 area 5	36.11	0.00	20.92	37.07	1.40	2.89	1.47	0.01	0.00	99.87
046 area 5	36.55	0.00	20.98	37.56	1.47	2.86	1.30	0.00	0.01	100.74
046 area 5	36.39	0.00	21.12	37.47	1.41	2.85	1.47	0.00	0.01	100.72
046 area 5	36.69	0.00	21.21	37.93	1.41	2.67	1.37	0.00	0.00	101.28
046 area 5	35.89	0.00	20.92	37.62	1.92	2.20	1.55	0.00	0.00	100.11
046 area 5	35.99	0.00	20.99	37.49	1.70	2.34	1.46	0.01	0.01	99.99
046 area 5	36.20	0.00	21.01	37.66	1.61	2.45	1.55	0.00	0.00	100.49
046 area 5	35.50	0.00	21.08	37.66	1.90	2.29	1.44	0.00	0.02	99.87
046 area 5	35.79	0.00	21.44	37.79	1.70	2.41	1.52	0.01	0.02	100.68
046 area 5	35.81	0.00	20.76	37.68	2.34	1.99	1.39	0.00	0.03	100.00
048 area 1	8.86	0.06	3.36	2.88	0.03	0.39	0.05	0.13	0.66	16.43
048 area 1	36.37	0.01	21.84	36.26	0.50	2.87	1.83	0.00	0.00	99.69
048 area 1	27.35	0.00	25.00	34.50	0.48	1.67	1.60	0.06	0.07	90.73

Location	SiO2	TiO2	Al2O3	FeO	MnO	MgO	CaO	Na2O	K2O	Total
048 area 1	36.49	0.00	22.01	36.30	0.55	3.06	1.98	0.00	0.00	100.38
048 area 1	36.52	0.00	21.98	36.55	0.56	3.08	1.92	0.00	0.00	100.62
048 area 1	36.25	0.00	21.83	36.31	0.56	3.02	1.93	0.00	0.00	99.90
048 area 1	36.65	0.00	21.95	36.52	0.59	3.04	1.98	0.00	0.00	100.73
048 area 1	36.43	0.00	21.91	36.43	0.58	3.07	1.95	0.00	0.00	100.38
048 area 1	36.66	0.01	22.00	36.48	0.56	3.01	1.93	0.00	0.00	100.64
048 area 1	36.60	0.00	21.92	36.41	0.58	3.07	1.97	0.00	0.00	100.55
048 area 1	36.64	0.00	22.41	36.23	0.54	3.11	1.96	0.00	0.00	100.90
048 area 2	34.46	0.00	21.70	36.84	0.60	3.07	1.85	0.00	0.00	98.52
048 area 2	34.77	0.00	21.91	36.55	0.61	3.11	1.86	0.00	0.00	98.82
048 area 2	35.36	0.00	21.95	36.59	0.59	3.16	1.95	0.00	0.00	99.60
048 area 2	35.46	0.00	21.83	36.66	0.61	3.09	1.82	0.00	0.00	99.48
048 area 2	35.54	0.00	21.89	36.83	0.61	3.10	1.81	0.00	0.00	99.80
048 area 2	35.65	0.00	22.25	36.70	0.60	3.11	1.81	0.00	0.00	100.14
048 area 2	35.73	0.00	22.03	37.17	0.56	3.11	1.78	0.00	0.00	100.39
048 area 2	35.61	0.00	22.06	36.71	0.49	2.63	2.14	0.00	0.01	99.65
048 area 2	36.43	0.00	21.87	36.72	0.59	2.80	2.00	0.00	0.01	100.41
048 area 2	36.43	0.00	21.99	36.81	0.58	2.79	1.94	0.00	0.00	100.55
048 area 2	36.47	0.00	21.99	36.93	0.57	2.73	1.97	0.00	0.01	100.67
048 area 2	36.34	0.00	21.92	36.63	0.62	2.78	1.99	0.00	0.00	100.27
048 area 2	36.38	0.00	22.17	36.36	0.54	2.80	2.04	0.00	0.01	100.30
048 area 2	36.32	0.00	22.17	36.86	0.58	2.82	1.82	0.00	0.00	100.57
048 area 2	35.94	0.00	21.64	35.70	0.53	2.77	1.81	0.01	0.04	98.45
048 area 2	36.22	0.00	22.07	36.89	0.54	2.76	1.93	0.00	0.00	100.42
048 area 2	36.38	0.00	21.89	36.99	0.50	2.58	1.93	0.00	0.01	100.28
048 area 2	36.02	0.00	21.94	36.88	0.59	2.93	1.96	0.00	0.00	100.32
048 area 2	34.50	0.00	21.81	37.00	0.58	2.93	1.90	0.00	0.00	98.71
048 area 2	34.54	0.00	21.85	36.84	0.57	3.06	1.85	0.00	0.00	98.73
048 area 2	34.81	0.00	21.78	37.06	0.59	3.00	1.85	0.00	0.00	99.09
048 area 2	34.98	0.00	21.78	37.27	0.55	2.96	1.89	0.00	0.00	99.43
048 area 2	34.79	0.00	21.78	36.88	0.54	2.80	1.93	0.00	0.00	98.72
048 area 2	34.01	0.00	21.64	36.86	0.55	2.89	1.94	0.00	0.01	97.90
048 area 2	34.03	0.00	21.76	36.85	0.55	2.82	1.89	0.00	0.01	97.91
048 area 2	34.40	0.00	21.83	37.21	0.53	2.80	2.00	0.00	0.01	98.77
048 area 3	34.61	0.00	21.95	36.89	0.62	2.99	1.94	0.00	0.00	99.01
048 area 3	34.58	0.00	21.74	36.93	0.61	3.13	1.88	0.00	0.00	98.88
048 area 3	33.63	0.00	21.62	37.15	0.62	3.00	1.95	0.00	0.00	97.98
048 area 3	33.85	0.00	21.64	37.35	0.60	2.96	2.00	0.00	0.01	98.41
048 area 3	33.49	0.00	21.73	37.04	0.60	3.00	1.95	0.00	0.00	97.80
048 area 3	33.15	0.00	21.70	36.94	0.63	3.14	1.99	0.00	0.01	97.57
048 area 3	32.79	0.00	21.47	36.94	0.60	3.17	2.00	0.00	0.00	96.98
048 area 3	32.70	0.00	21.48	37.38	0.65	3.20	1.90	0.00	0.00	97.30
048 area 3	32.11	0.00	21.28	37.16	0.61	3.16	1.89	0.00	0.00	96.21
048 area 3	31.96	0.00	21.28	37.23	0.61	3.17	1.98	0.00	0.00	96.23
048 area 3	31.60	0.00	21.30	37.38	0.58	2.94	1.87	0.00	0.00	95.68
048 area 3	32.67	0.01	21.55	37.33	0.64	2.71	1.95	0.00	0.01	96.87
048 area 3	33.20	0.01	21.53	37.38	0.65	2.83	1.99	0.00	0.02	97.61
048 area 3	33.61	0.01	21.74	37.36	0.63	2.91	1.98	0.00	0.01	98.25
048 area 3	33.59	0.00	21.77	37.61	0.64	2.82	1.92	0.00	0.00	98.37
048 area 3	33.82	0.01	21.56	37.23	0.61	2.71	1.96	0.00	0.00	97.89
048 area 3	33.83	0.01	21.47	37.12	0.60	2.81	1.96	0.00	0.01	97.82
048 area 3	33.69	0.00	21.47	36.89	0.61	3.02	1.93	0.00	0.01	97.61

Location	SiO2	TiO2	Al2O3	FeO	MnO	MgO	CaO	Na2O	K2O	Total
048 area 3	33.20	0.00	21.54	37.17	0.60	2.94	1.95	0.00	0.00	97.41
048 area 3	34.21	0.00	21.83	37.05	0.54	2.97	1.89	0.00	0.01	98.51
048 area 3	34.43	0.00	21.72	37.44	0.55	2.88	1.90	0.00	0.01	98.93
048 area 3	33.90	0.00	21.87	37.26	0.55	2.92	2.00	0.01	0.00	98.52
048 area 3	33.37	0.00	21.76	37.11	0.56	2.98	1.97	0.00	0.00	97.74
048 area 3	34.62	0.00	21.51	36.60	0.54	2.87	2.02	0.00	0.00	98.17
048 area 3	34.24	0.00	21.55	36.82	0.52	2.69	1.95	0.00	0.01	97.79
048 area 3	34.20	0.00	21.51	36.55	0.55	2.96	1.86	0.00	0.01	97.65
048 area 3	34.38	0.00	21.50	36.62	0.60	3.08	1.77	0.00	0.00	97.95
048 area 3	34.02	0.00	21.44	36.29	0.64	3.11	2.09	0.00	0.00	97.58
048 area 3	34.21	0.00	21.33	36.33	0.62	3.10	1.91	0.00	0.00	97.51
048 area 3	34.08	0.00	21.49	36.50	0.61	3.18	1.90	0.00	0.00	97.75
048 area 3	33.72	0.00	21.43	36.70	0.61	2.98	1.89	0.00	0.01	97.33
048 area 3	33.73	0.00	21.41	36.63	0.60	2.85	1.95	0.00	0.01	97.17
048 area 3	33.19	0.00	21.37	36.49	0.60	2.79	1.92	0.00	0.01	96.37
048 area 3	33.11	0.00	21.33	36.51	0.62	2.87	1.98	0.00	0.00	96.42
048 area 3	33.04	0.00	21.07	36.32	0.67	3.00	1.96	0.00	0.00	96.06
048 area 3	32.81	0.00	21.21	36.45	0.64	3.02	1.91	0.00	0.00	96.05
048 area 3	32.59	0.00	21.04	36.25	0.64	3.10	1.86	0.00	0.00	95.48
048 area 3	32.08	0.00	21.13	36.22	0.60	3.12	1.85	0.00	0.00	95.00
048 area 3	32.09	0.00	21.04	36.13	0.62	3.19	1.86	0.00	0.00	94.93
048 area 3	31.85	0.00	20.84	36.21	0.60	3.18	1.92	0.00	0.00	94.60
048 area 3	31.83	0.00	20.95	36.36	0.60	3.19	1.75	0.00	0.00	94.69
048 area 3	31.51	0.00	20.86	36.56	0.56	2.97	1.78	0.00	0.00	94.25
048 area 3	31.34	0.00	20.67	36.52	0.57	2.97	1.90	0.00	0.00	93.98
048 area 3	31.41	0.00	20.88	36.59	0.51	2.86	1.81	0.00	0.00	94.07
048 area 3	31.65	0.00	20.99	36.59	0.54	2.91	1.85	0.00	0.00	94.54
048 area 3	31.59	0.00	20.80	36.61	0.56	2.89	1.90	0.00	0.00	94.35
048 area 3	31.70	0.00	20.94	36.83	0.58	2.87	1.89	0.00	0.00	94.80
048 area 3	34.49	0.00	21.45	36.56	0.61	2.92	1.96	0.00	0.00	98.00
048 area 3	34.46	0.00	21.40	36.64	0.64	3.08	1.94	0.00	0.00	98.18
048 area 3	34.70	0.00	21.32	36.69	0.62	2.89	1.91	0.00	0.01	98.15
048 area 3	34.49	0.01	21.33	36.64	0.63	2.99	1.88	0.00	0.01	97.98
048 area 3	34.46	0.00	21.45	36.54	0.63	2.86	1.93	0.00	0.01	97.88
048 area 3	34.75	0.00	21.56	36.57	0.61	2.87	1.96	0.00	0.01	98.33
048 area 3	34.58	0.00	21.75	36.92	0.53	2.64	1.89	0.01	0.01	98.33
048 area 3	35.02	0.00	21.83	36.48	0.56	2.79	1.92	0.00	0.00	98.60
048 area 3	35.33	0.00	21.74	36.38	0.55	2.84	2.00	0.00	0.01	98.83
048 area 3	33.71	0.00	21.47	36.89	0.55	2.81	1.79	0.00	0.00	97.21
048 area 3	34.46	0.00	21.51	36.78	0.53	2.72	1.94	0.00	0.00	97.95
048 area 3	34.26	0.00	21.54	36.55	0.55	2.83	1.97	0.00	0.00	97.71
048 area 6	35.22	0.00	22.02	37.09	0.54	2.64	2.11	0.00	0.02	99.65
048 area 6	35.37	0.00	21.85	36.99	0.58	3.00	1.87	0.00	0.01	99.68
048 area 6	35.02	0.00	21.79	37.46	0.58	2.99	1.91	0.00	0.01	99.76
048 area 6	34.61	0.00	21.86	37.24	0.52	3.02	2.00	0.00	0.00	99.26
048 area 6	34.53	0.00	21.76	37.40	0.57	2.99	1.94	0.00	0.00	99.19
048 area 6	34.30	0.00	21.69	37.70	0.58	2.72	1.96	0.00	0.02	98.97
048 area 6	34.51	0.01	21.67	37.88	0.55	2.70	1.88	0.00	0.02	99.22
048 area 6	34.39	0.01	21.71	37.89	0.56	2.57	1.91	0.00	0.02	99.05
048 area 6	34.30	0.00	21.57	37.69	0.58	2.54	1.95	0.00	0.03	98.66
048 area 6	36.46	0.00	22.90	36.93	0.54	3.07	1.87	0.03	0.03	101.82
048 area 6	34.18	0.00	21.61	37.45	0.53	2.78	1.87	0.00	0.01	98.43

Location	SiO2	TiO2	Al2O3	FeO	MnO	MgO	CaO	Na2O	K2O	Total
048 area 6	35.49	0.01	21.90	37.11	0.54	2.88	1.97	0.00	0.01	99.91
048 area 6	35.08	0.00	21.87	37.10	0.53	2.95	1.84	0.00	0.01	99.38
048 area 6	35.09	0.01	21.96	37.40	0.57	3.05	1.80	0.00	0.01	99.90
048 area 6	34.86	0.00	21.96	37.56	0.56	2.84	1.87	0.00	0.02	99.65
048 area 9	33.02	0.00	21.56	37.09	0.56	3.05	2.03	0.00	0.00	97.32
048 area 9	33.27	0.00	21.62	36.78	0.60	3.14	1.88	0.00	0.00	97.30
048 area 9	33.34	0.00	21.63	36.82	0.63	3.19	1.91	0.00	0.00	97.53
048 area 9	33.78	0.00	21.50	36.98	0.64	3.08	1.94	0.00	0.00	97.92
048 area 9	34.26	0.00	21.59	37.46	0.60	3.03	1.96	0.00	0.01	98.90
048 area 9	34.40	0.00	21.72	37.07	0.60	3.05	1.92	0.00	0.00	98.76
048 area 9	34.93	0.00	21.74	36.82	0.60	3.01	1.99	0.00	0.00	99.09
048 area 9	34.86	0.00	21.83	37.34	0.61	3.06	1.93	0.00	0.01	99.64
048 area 9	34.84	0.00	21.90	37.23	0.56	2.85	1.92	0.00	0.01	99.31
048 area 9	35.00	0.00	21.87	37.09	0.53	2.69	2.08	0.00	0.01	99.26
048 area 9	35.03	0.00	21.81	37.09	0.52	2.71	2.08	0.00	0.00	99.23
048 area 9	34.88	0.00	21.93	37.13	0.53	2.68	2.11	0.00	0.00	99.26
048 area 9	34.84	0.00	21.99	37.35	0.52	2.72	1.86	0.00	0.01	99.28
048 area 9	35.44	0.00	21.95	37.34	0.53	2.79	1.99	0.00	0.00	100.05
048 area 9	35.12	0.00	21.97	37.38	0.48	2.83	1.87	0.00	0.02	99.67
051 area 1	36.57	0.00	21.14	32.98	5.61	2.41	1.64	0.01	0.01	100.38
051 area 1	36.77	0.00	21.18	33.12	5.56	2.47	1.63	0.01	0.00	100.73
051 area 1	37.00	0.00	21.12	33.17	5.64	2.51	1.56	0.00	0.00	100.99
051 area 1	35.81	0.00	21.54	33.26	5.59	2.55	1.62	0.01	0.00	100.38
051 area 1	35.89	0.00	21.39	33.10	5.57	2.48	1.63	0.01	0.00	100.07
051 area 1	36.15	0.01	21.42	33.16	5.75	2.34	1.64	0.00	0.01	100.49
051 area 1	36.41	0.01	21.41	33.43	5.42	2.58	1.59	0.01	0.00	100.86
051 area 1	35.88	0.00	21.40	33.20	5.29	2.57	1.58	0.01	0.00	99.93
051 area 1	36.48	0.00	21.31	33.14	5.68	2.46	1.60	0.00	0.00	100.67
051 area 1	36.07	0.01	21.34	33.51	5.37	2.52	1.61	0.01	0.00	100.45
051 area 1	36.30	0.00	21.24	33.57	5.35	2.61	1.62	0.01	0.00	100.72
051 area 1	36.52	0.00	21.17	33.38	5.34	2.51	1.61	0.00	0.00	100.54
051 area 1	36.21	0.00	21.33	33.14	5.49	2.53	1.53	0.01	0.01	100.24
051 area 1	36.46	0.01	21.14	32.91	6.01	2.26	1.59	0.00	0.01	100.39
051 area 1	36.44	0.00	21.31	33.14	5.68	2.37	1.56	0.00	0.01	100.49
051 area 2	36.78	0.01	21.18	33.73	4.43	2.74	1.80	0.00	0.00	100.66
051 area 2	36.63	0.00	21.33	34.05	4.27	2.95	1.87	0.00	0.00	101.09
051 area 2	36.09	0.00	21.34	33.47	4.16	3.03	2.09	0.01	0.00	100.19
051 area 2	36.38	0.02	21.37	33.61	4.05	3.08	2.19	0.01	0.00	100.71
051 area 2	36.53	0.01	21.35	33.88	3.88	3.11	2.15	0.00	0.00	100.90
051 area 2	36.29	0.02	21.32	33.57	3.89	3.17	2.07	0.01	0.00	100.34
051 area 2	36.34	0.01	21.43	33.54	3.92	3.18	2.04	0.01	0.00	100.48
051 area 2	36.10	0.00	21.36	33.77	4.10	3.11	1.78	0.00	0.00	100.23
051 area 2	36.31	0.00	21.51	34.02	4.14	3.10	1.70	0.00	0.00	100.78
051 area 2	36.33	0.00	21.45	33.85	4.02	3.28	1.68	0.00	0.00	100.62
051 area 2	36.17	0.01	21.41	33.73	4.11	3.26	1.72	0.02	0.00	100.43
051 area 2	35.93	0.00	21.46	34.12	3.99	3.31	1.71	0.01	0.00	100.53
051 area 2	35.98	0.00	21.59	33.66	4.04	3.32	1.61	0.01	0.00	100.21
051 area 2	35.93	0.00	21.63	33.49	4.11	3.30	1.61	0.01	0.00	100.09
051 area 2	36.72	0.00	21.43	33.82	4.11	3.26	1.82	0.01	0.00	101.17
051 area 2	36.69	0.01	21.33	33.85	3.98	3.22	2.00	0.00	0.00	101.08
051 area 2	36.44	0.00	21.49	33.71	4.06	3.26	1.91	0.01	0.00	100.88
051 area 2	36.56	0.00	21.35	33.91	3.83	3.46	1.70	0.00	0.00	100.80

Location	SiO2	TiO2	Al2O3	FeO	MnO	MgO	CaO	Na2O	K2O	Total
051 area 2	37.01	0.00	21.35	33.82	4.04	3.25	1.66	0.00	0.00	101.11
051 area 2	36.93	0.00	21.30	33.70	3.97	3.26	1.86	0.00	0.00	101.03
051 area 2	36.18	0.00	21.41	34.11	4.16	3.09	1.63	0.01	0.00	100.60
051 area 2	36.38	0.01	21.36	33.77	4.10	3.32	1.78	0.00	0.00	100.72
051 area 2	36.54	0.00	21.12	33.45	4.40	2.98	1.66	0.01	0.00	100.16
052 area 2	34.81	0.00	21.37	35.46	3.68	1.90	1.29	0.01	0.00	98.52
052 area 2	34.97	0.00	21.43	35.88	3.61	2.06	1.15	0.01	0.00	99.12
052 area 2	35.02	0.00	21.33	35.73	3.17	2.35	1.29	0.00	0.01	98.90
052 area 2	35.18	0.00	21.52	36.52	3.01	2.43	1.29	0.00	0.00	99.96
052 area 2	35.32	0.00	21.39	36.00	2.70	2.51	1.34	0.00	0.00	99.27
052 area 2	35.57	0.00	21.39	35.89	2.69	2.52	1.28	0.00	0.00	99.34
052 area 2	35.48	0.00	21.37	35.87	2.85	2.34	1.28	0.00	0.01	99.21
052 area 2	35.29	0.01	21.47	36.30	2.82	2.27	1.28	0.00	0.02	99.46
052 area 2	35.55	0.00	21.50	36.10	2.87	2.38	1.29	0.00	0.01	99.70
052 area 2	35.64	0.00	21.59	36.12	2.79	2.55	1.37	0.00	0.00	100.07
052 area 2	35.69	0.00	21.52	36.13	2.64	2.56	1.29	0.00	0.00	99.84
052 area 2	35.93	0.00	21.56	36.03	2.73	2.49	1.30	0.00	0.00	100.05
052 area 2	36.15	0.00	21.53	35.61	2.84	2.55	1.31	0.00	0.01	100.01
052 area 2	36.22	0.00	21.64	35.99	3.17	2.46	1.34	0.00	0.01	100.84
052 area 2	35.97	0.00	21.72	35.37	3.29	2.48	1.33	0.00	0.01	100.17
052 area 2	36.23	0.00	21.69	35.33	3.46	2.40	1.31	0.00	0.02	100.45
052 area 2	36.06	0.00	21.78	35.24	3.40	2.35	1.30	0.00	0.02	100.15
052 area 2	35.99	0.00	21.63	34.93	3.43	2.36	1.28	0.00	0.02	99.63
052 area 2	35.94	0.00	21.47	35.93	3.43	2.07	1.30	0.00	0.00	100.15
052 area 2	35.86	0.00	21.49	36.18	3.46	2.16	1.30	0.00	0.01	100.46
052 area 2	34.86	0.00	21.41	35.35	3.49	2.37	1.30	0.00	0.00	98.78
052 area 2	34.79	0.00	21.31	35.32	3.53	2.24	1.35	0.01	0.00	98.56
052 area 2	34.92	0.00	21.40	35.80	3.63	2.15	1.22	0.01	0.00	99.13
052 area 2	34.79	0.00	21.29	35.90	4.01	1.73	1.24	0.00	0.00	98.97
052 area 4	35.52	0.00	21.49	35.89	3.57	2.31	1.15	0.00	0.01	99.94
052 area 4	35.39	0.00	21.28	35.60	3.37	2.24	1.26	0.00	0.00	99.14
052 area 4	35.33	0.00	21.48	36.09	3.16	2.31	1.24	0.00	0.01	99.61
052 area 4	35.26	0.00	21.63	36.24	2.99	2.37	1.24	0.00	0.00	99.74
052 area 4	34.64	0.00	21.48	36.08	2.92	2.42	1.24	0.00	0.00	98.79
052 area 4	34.73	0.00	21.25	36.24	2.93	2.25	1.26	0.00	0.00	98.65
052 area 4	34.60	0.00	21.41	36.11	2.88	2.34	1.20	0.00	0.00	98.54
052 area 4	34.30	0.00	21.29	35.86	2.85	2.46	1.28	0.00	0.00	98.04
052 area 4	34.45	0.00	21.49	36.76	2.83	2.53	1.29	0.00	0.00	99.37
052 area 4	34.41	0.08	21.58	36.45	2.92	2.53	1.27	0.00	0.00	99.24
052 area 4	34.24	0.00	21.51	36.45	3.00	2.48	1.29	0.00	0.00	98.96
052 area 4	34.09	0.00	21.50	35.79	3.27	2.36	1.16	0.00	0.01	98.19
052 area 4	33.94	0.00	21.54	35.76	3.27	2.48	1.32	0.00	0.02	98.32
052 area 4	33.88	0.00	21.47	36.06	3.28	2.40	1.30	0.00	0.01	98.40
052 area 4	33.67	0.00	21.34	35.45	3.25	2.57	1.26	0.01	0.00	97.54
052 area 4	33.78	0.00	21.44	35.97	3.30	2.55	1.31	0.00	0.00	98.36
052 area 4	34.69	0.00	21.28	35.27	3.38	2.39	1.28	0.00	0.00	98.30
052 area 4	35.02	0.00	21.52	35.61	3.58	2.47	1.36	0.00	0.00	99.56
052 area 4	34.94	0.00	21.35	35.48	3.52	2.30	1.31	0.00	0.00	98.88
052 area 4	35.38	0.05	21.47	36.39	3.35	2.14	1.24	0.00	0.02	100.04
052 area 4	35.02	0.00	21.36	35.87	3.10	2.42	1.27	0.00	0.01	99.05
052 area 4	34.72	0.00	21.50	35.90	2.92	2.46	1.25	0.00	0.00	98.73
052 area 7	35.59	0.00	21.37	34.92	4.80	1.71	1.17	0.00	0.04	99.60

Location	SiO2	TiO2	Al2O3	FeO	MnO	MgO	CaO	Na2O	K2O	Total
052 area 7	35.60	0.00	21.66	35.20	4.46	1.95	1.22	0.00	0.00	100.09
052 area 7	35.72	0.00	21.71	35.27	4.38	1.91	1.17	0.00	0.01	100.17
052 area 7	35.54	0.00	21.48	35.33	4.52	1.96	1.13	0.00	0.00	99.97
052 area 7	57.08	0.00	14.33	25.39	3.30	1.41	0.83	0.00	0.00	102.35
052 area 7	35.44	0.00	21.56	35.38	4.45	1.97	1.19	0.00	0.00	99.99
052 area 7	48.58	0.21	1.02	21.64	2.61	2.19	0.91	0.00	1.13	78.29
052 area 7	35.69	0.00	21.61	35.66	4.56	1.99	1.20	0.00	0.01	100.71
052 area 7	35.48	0.00	21.42	35.03	4.62	1.85	1.22	0.00	0.01	99.62
052 area 7	35.50	0.00	21.45	34.82	4.77	1.79	1.23	0.00	0.01	99.55
052 area 7	35.32	0.00	21.51	35.05	4.79	1.69	1.17	0.00	0.01	99.54
052 area 7	35.09	0.00	21.48	35.01	4.70	1.83	1.22	0.00	0.00	99.32
052 area 7	35.24	0.00	21.57	35.15	4.53	1.93	1.23	0.00	0.00	99.65
052 area 7	35.57	0.00	21.49	35.22	4.59	1.92	1.20	0.00	0.00	100.00
052 area 7	35.15	0.00	21.60	34.92	4.84	1.77	1.16	0.00	0.01	99.44
052 area 7	35.69	0.00	21.69	34.77	4.72	1.85	1.14	0.00	0.01	99.86
052 area 7	35.44	0.00	21.50	34.56	4.53	1.94	1.06	0.00	0.00	99.05
052 area 7	35.67	0.00	21.47	35.10	4.69	1.73	1.18	0.00	0.02	99.86
052 area 7	35.42	0.00	21.58	35.09	4.90	1.56	1.16	0.00	0.05	99.76
052 area 7	35.68	0.00	21.62	34.52	4.62	1.81	1.16	0.00	0.03	99.43
052 area 7	35.71	0.00	21.63	34.73	4.57	1.79	1.18	0.00	0.01	99.62
052 area 7	35.93	0.00	21.54	35.03	4.70	1.76	1.21	0.00	0.02	100.19
052 area 7	35.64	0.00	21.43	34.50	4.53	1.89	1.21	0.00	0.01	99.22
052 area 7	35.14	0.00	21.45	35.26	4.67	1.76	1.18	0.00	0.00	99.46
052 area 7	35.06	0.00	21.47	35.21	4.70	1.75	1.21	0.00	0.00	99.41
052 area 7	35.07	0.01	21.46	35.01	5.10	1.49	1.18	0.00	0.01	99.32
052 area 7	46.08	0.01	25.26	18.24	2.39	1.74	0.48	0.02	6.03	100.25
052 area 7	35.30	0.00	21.39	35.24	5.03	1.69	1.18	0.00	0.00	99.83
052 area 7	37.44	2.95	19.85	21.25	0.42	5.60	0.12	0.14	8.62	96.40
055 area 2	36.16	0.00	20.82	34.92	4.54	2.35	1.20	0.01	0.00	99.99
055 area 2	36.22	0.00	20.86	35.01	4.52	2.31	1.23	0.00	0.00	100.16
055 area 2	36.30	0.00	20.76	34.67	4.82	2.22	1.18	0.00	0.00	99.96
055 area 2	35.80	0.02	20.79	35.09	5.21	1.83	1.23	0.00	0.02	99.99
055 area 2	35.90	0.01	20.91	34.73	5.20	1.96	1.16	0.00	0.01	99.87
055 area 2	35.77	0.00	20.74	35.10	4.46	2.19	1.21	0.00	0.00	99.49
055 area 2	35.61	0.00	20.81	35.47	4.34	2.23	1.17	0.00	0.01	99.64
055 area 2	35.68	0.00	20.78	35.48	4.50	2.25	1.17	0.01	0.01	99.87
055 area 2	35.90	0.00	20.81	35.02	4.54	2.18	1.20	0.00	0.01	99.67
055 area 2	36.49	0.00	20.69	35.39	4.08	2.57	1.17	0.00	0.00	100.40
055 area 2	36.41	0.00	20.65	35.22	3.95	2.60	1.18	0.00	0.00	100.02
055 area 2	36.11	0.00	20.59	34.53	5.08	2.01	1.41	0.00	0.00	99.73
055 area 2	36.19	0.00	21.00	35.29	4.16	2.35	1.49	0.01	0.00	100.49
055 area 2	14.35	0.00	12.91	18.79	3.50	1.50	0.62	0.00	0.01	51.67
055 area 2	7.75	0.00	10.96	18.12	2.48	1.15	0.58	0.07	0.08	41.19
055 area 2	13.85	0.00	12.96	18.41	3.08	1.63	0.79	0.00	0.01	50.72
055 area 2	13.75	0.00	12.82	18.38	2.91	1.65	0.66	0.00	0.00	50.18
055 area 2	13.77	0.00	12.91	18.44	3.07	1.65	0.63	0.00	0.01	50.47
055 area 2	14.43	0.00	13.22	19.00	3.27	1.60	0.63	0.00	0.01	52.15
055 area 2	14.56	0.00	13.32	19.28	2.82	1.87	0.72	0.00	0.01	52.57
055 area 3	35.93	0.00	20.84	34.96	4.77	2.26	1.19	0.00	0.01	99.96
055 area 3	35.92	0.00	20.69	35.06	4.61	2.36	1.17	0.00	0.00	99.82
055 area 3	35.88	0.00	20.90	35.22	4.31	2.50	1.18	0.00	0.00	99.98
055 area 3	36.16	0.00	20.77	34.67	4.78	2.26	1.16	0.00	0.00	99.80

Location	SiO2	TiO2	Al2O3	FeO	MnO	MgO	CaO	Na2O	K2O	Total
055 area 3	35.80	0.00	20.86	34.90	4.90	2.13	1.22	0.00	0.00	99.81
055 area 3	35.85	0.00	20.87	34.99	4.60	2.31	1.20	0.00	0.00	99.82
055 area 3	36.18	0.00	20.59	35.09	4.79	2.18	1.24	0.00	0.00	100.09
055 area 3	36.37	0.00	20.59	35.08	5.10	2.00	1.23	0.00	0.00	100.38
055 area 3	36.64	0.00	20.51	35.01	5.24	1.92	1.15	0.00	0.00	100.48
055 area 4	36.55	0.00	20.59	34.64	5.41	1.98	1.14	0.00	0.00	100.32
055 area 4	36.24	0.00	20.66	34.71	5.20	2.14	1.15	0.00	0.00	100.11
055 area 4	36.54	0.00	20.48	34.80	5.42	2.04	1.16	0.00	0.01	100.47
055 area 4	36.28	0.00	20.69	35.13	5.22	2.13	1.15	0.00	0.00	100.60
055 area 4	36.08	0.00	20.76	34.64	4.96	2.14	1.15	0.00	0.00	99.74
055 area 4	35.96	0.00	20.69	34.55	5.34	2.07	1.10	0.00	0.00	99.71
055 area 4	35.96	0.00	20.64	34.30	5.53	1.99	1.14	0.00	0.00	99.56
055 area 4	35.74	0.00	20.72	34.55	5.49	1.98	1.14	0.00	0.00	99.62
055 area 4	36.56	0.00	20.57	34.43	5.40	2.03	1.12	0.00	0.01	100.11
055 area 4	36.59	0.00	20.60	34.60	5.42	2.06	1.16	0.00	0.01	100.45
055 area 3	33.99	0.00	20.74	34.37	5.19	1.95	1.15	0.00	0.01	97.41
055 area 3	33.75	0.00	20.93	34.31	5.29	2.06	1.15	0.00	0.01	97.51
055 area 3	33.55	0.00	20.70	34.09	5.16	1.98	1.19	0.01	0.00	96.67
055 area 3	32.66	0.00	20.73	33.96	4.51	2.43	1.16	0.00	0.00	95.46
055 area 3	32.70	0.00	20.74	34.27	4.46	2.46	1.19	0.00	0.00	95.83
055 area 3	33.04	0.00	20.78	34.03	4.56	2.43	1.22	0.00	0.00	96.06
059 area 1	34.19	0.01	21.37	38.08	1.93	1.96	1.08	0.00	0.00	98.63
059 area 1	33.84	0.00	21.55	38.12	1.60	2.24	0.99	0.00	0.00	98.33
059 area 1	34.12	0.00	21.58	38.05	1.51	2.25	1.04	0.00	0.01	98.56
059 area 1	33.97	0.00	21.38	37.99	1.43	2.46	1.09	0.00	0.00	98.31
059 area 1	34.77	0.01	21.39	38.14	1.40	2.40	1.15	0.00	0.00	99.27
059 area 1	34.35	0.00	21.40	37.88	1.39	2.51	1.11	0.00	0.00	98.63
059 area 1	34.30	0.00	21.44	38.04	1.42	2.51	1.03	0.00	0.00	98.74
059 area 1	34.17	0.00	21.51	37.59	1.56	2.26	1.05	0.00	0.01	98.15
059 area 1	34.42	0.00	21.56	37.58	1.66	2.21	1.00	0.00	0.00	98.44
059 area 1	35.39	0.00	21.55	37.82	1.80	1.99	1.05	0.00	0.01	99.60
059 area 1	35.34	0.00	21.53	38.04	2.10	1.68	1.03	0.00	0.01	99.73
059 area 1	35.17	0.00	21.62	37.87	2.47	1.44	1.04	0.00	0.03	99.64
059 area 1	35.11	0.00	21.52	37.94	2.19	1.66	1.04	0.00	0.01	99.46
059 area 1	34.96	0.00	21.34	38.33	2.22	1.58	1.01	0.00	0.02	99.46
059 area 1	35.08	0.00	21.46	38.07	2.17	1.61	1.05	0.00	0.02	99.46
059 area 1	34.91	0.00	21.46	38.00	2.04	1.81	1.05	0.00	0.01	99.30
059 area 1	35.12	0.00	21.57	38.01	1.86	1.85	1.05	0.00	0.02	99.49
059 area 1	32.38	0.00	21.18	37.97	1.79	2.10	0.98	0.00	0.02	96.40
059 area 1	32.27	0.00	21.03	37.83	1.86	2.18	1.01	0.00	0.03	96.21
059 area 1	32.73	0.00	21.15	37.99	1.79	2.21	0.99	0.00	0.03	96.89
059 area 1	32.51	0.00	21.23	37.40	1.74	2.23	0.97	0.00	0.03	96.11
059 area 1	32.86	0.00	21.25	37.75	1.62	2.34	1.00	0.00	0.00	96.82
059 area 1	32.85	0.00	21.34	37.89	1.63	2.41	0.99	0.00	0.00	97.11
059 area 3	33.58	0.00	21.58	37.74	1.78	2.18	1.02	0.00	0.00	97.88
059 area 3	33.86	0.00	21.53	38.34	1.68	2.29	1.04	0.00	0.00	98.74
059 area 3	33.91	0.00	21.46	38.07	1.45	2.49	1.25	0.00	0.00	98.64
059 area 3	33.81	0.01	21.50	37.98	1.32	2.57	1.22	0.00	0.00	98.42
059 area 3	34.16	0.01	21.49	37.65	1.15	2.77	1.51	0.00	0.00	98.74
059 area 3	34.41	0.02	21.77	37.61	1.13	2.81	1.58	0.00	0.00	99.32
059 area 3	32.63	0.02	20.58	36.81	1.07	2.62	1.51	0.01	0.05	95.30
059 area 3	34.44	0.01	21.61	37.58	1.09	2.88	1.50	0.00	0.01	99.11

Location	SiO2	TiO2	Al2O3	FeO	MnO	MgO	CaO	Na2O	K2O	Total
059 area 3	34.24	0.00	21.59	37.90	1.30	2.49	1.35	0.00	0.01	98.88
059 area 3	34.21	0.00	21.60	38.16	1.48	2.49	1.09	0.00	0.00	99.03
059 area 3	34.27	0.00	21.50	38.20	1.72	2.11	1.05	0.00	0.00	98.86
059 area 3	34.27	0.00	21.60	38.00	1.45	2.40	1.03	0.00	0.01	98.76
059 area 3	34.75	0.00	21.65	38.10	1.29	2.60	1.22	0.00	0.01	99.61
059 area 3	34.55	0.00	21.62	37.96	1.50	2.39	1.13	0.00	0.00	99.16
059 area 3	34.54	0.00	21.60	38.31	2.13	1.81	1.04	0.00	0.01	99.45
059 area 3	34.25	0.02	21.61	38.23	2.35	1.54	0.99	0.00	0.03	99.02
059 area 3	34.33	0.02	21.69	38.22	2.44	1.60	0.94	0.00	0.02	99.27
059 area 3	34.66	0.04	21.71	38.30	2.47	1.60	0.98	0.00	0.04	99.79
059 area 3	34.28	0.04	20.49	38.48	2.52	1.47	0.98	0.00	0.06	98.32
059 area 3	33.23	0.00	21.19	38.37	2.28	1.50	1.02	0.00	0.01	97.60
059 area 3	33.02	0.00	21.25	38.65	2.42	1.47	1.02	0.00	0.02	97.84
059 area 3	32.98	0.00	21.25	38.89	2.15	1.69	1.00	0.00	0.01	97.97
059 area 3	33.00	0.00	21.22	38.39	2.77	1.28	0.98	0.00	0.01	97.65
059 area 3	34.81	0.00	21.84	38.08	1.93	1.89	1.00	0.00	0.01	99.56
059 area 3	34.40	0.00	21.50	38.43	1.89	1.95	1.03	0.00	0.01	99.21
059 area 3	34.34	0.00	21.64	38.36	2.22	1.58	1.07	0.00	0.00	99.21
059 area 3	33.47	0.00	21.53	38.51	1.59	2.05	1.00	0.00	0.02	98.19
059 area 3	33.17	0.00	21.39	38.52	1.67	2.08	1.07	0.00	0.02	97.93
059 area 3	33.47	0.00	21.37	38.39	1.48	2.27	1.10	0.00	0.00	98.08
059 area 3	33.02	0.00	21.27	38.30	1.97	1.98	1.10	0.00	0.01	97.64
059 area 4	33.57	0.00	21.60	37.91	1.93	1.91	1.11	0.00	0.01	98.05
059 area 4	34.59	0.00	24.41	37.39	1.79	2.13	0.95	0.04	0.00	101.29
059 area 4	33.68	0.00	21.49	38.34	1.70	2.31	1.00	0.00	0.00	98.52
059 area 4	25.11	0.00	20.00	36.32	1.44	1.55	1.09	0.04	0.03	85.57
059 area 4	33.56	0.01	21.47	38.10	1.48	2.52	1.03	0.00	0.00	98.18
059 area 4	33.82	0.00	21.43	38.00	1.52	2.50	1.05	0.00	0.01	98.34
059 area 4	33.89	0.00	21.73	37.95	1.52	2.55	1.01	0.00	0.00	98.66
059 area 4	34.27	0.00	21.63	37.88	1.48	2.51	0.95	0.00	0.00	98.72
059 area 4	34.07	0.00	21.60	37.91	1.49	2.51	1.02	0.00	0.00	98.62
059 area 4	34.34	0.00	21.66	38.28	1.55	2.37	1.05	0.00	0.01	99.26
059 area 4	34.37	0.00	21.61	38.30	1.60	2.40	1.05	0.00	0.00	99.33
059 area 4	34.18	0.01	21.67	38.36	1.70	2.14	1.08	0.00	0.01	99.15
059 area 4	34.19	0.01	21.76	38.52	1.81	1.81	1.05	0.00	0.04	99.16
059 area 4	33.95	0.00	21.68	38.45	1.81	2.03	1.02	0.00	0.01	98.94
059 area 4	33.58	0.01	21.42	38.43	1.87	1.83	1.03	0.00	0.02	98.20
059 area 4	33.58	0.00	21.47	38.04	1.62	2.37	0.98	0.00	0.01	98.07
059 area 4	33.49	0.00	21.54	38.04	1.60	2.35	0.96	0.00	0.03	98.02
059 area 4	32.98	0.00	21.30	38.39	1.86	1.95	1.03	0.00	0.02	97.54
059 area 4	33.24	0.00	21.51	38.29	1.58	2.37	1.03	0.00	0.00	98.02
059 area 4	34.15	0.00	21.51	38.28	1.86	2.01	1.01	0.00	0.01	98.83
059 area 6	34.91	0.00	21.67	37.92	1.83	2.14	1.01	0.00	0.00	99.48
059 area 6	34.98	0.00	21.71	38.14	1.55	2.45	1.03	0.00	0.00	99.86
059 area 6	34.77	0.00	21.56	37.80	1.42	2.60	1.05	0.00	0.00	99.21
059 area 6	35.18	0.00	21.59	38.33	1.28	2.57	1.01	0.00	0.01	99.96
059 area 6	35.02	0.00	21.66	37.97	1.18	2.70	1.07	0.00	0.00	99.60
059 area 6	35.04	0.00	21.71	38.16	1.33	2.59	1.02	0.00	0.00	99.84
059 area 6	34.93	0.00	21.76	37.91	1.44	2.54	1.02	0.00	0.00	99.59
059 area 6	35.27	0.00	21.83	38.07	1.44	2.49	1.04	0.00	0.00	100.14
059 area 6	35.36	0.00	21.74	38.02	1.84	2.27	1.07	0.00	0.01	100.30
059 area 6	34.54	0.00	21.77	37.88	1.78	2.07	1.03	0.00	0.00	99.06

Location	SiO2	TiO2	Al2O3	FeO	MnO	MgO	CaO	Na2O	K2O	Total
059 area 6	34.88	0.00	21.38	38.04	1.96	1.98	1.05	0.00	0.01	99.29
059 area 6	33.05	0.00	21.21	38.27	2.51	1.50	1.03	0.00	0.05	97.61
059 area 6	33.37	0.00	21.37	38.29	2.06	1.83	1.01	0.00	0.02	97.95
059 area 6	32.20	0.00	21.31	38.58	2.19	1.83	1.01	0.00	0.02	97.13
059 area 6	31.76	0.00	21.24	38.25	1.70	2.23	0.98	0.00	0.00	96.15
059 area 6	31.16	0.02	21.30	39.07	1.51	1.80	0.97	0.00	0.07	95.90
059 area 6	31.70	0.00	20.98	38.21	1.45	2.39	1.01	0.00	0.01	95.76
059 area 6	31.94	0.00	20.91	38.38	2.05	2.06	1.00	0.00	0.01	96.34
059 area 6	32.07	0.00	21.05	38.62	1.93	1.99	1.00	0.00	0.00	96.68
059 area 6	33.53	0.00	21.39	38.55	1.99	2.02	0.99	0.00	0.00	98.46
059 area 6	33.38	0.00	21.31	38.24	2.05	1.92	1.05	0.00	0.01	97.96
059 area 6	36.05	0.00	21.54	37.89	1.25	2.55	1.08	0.00	0.00	100.37
059 area 6	35.79	0.00	21.46	37.90	1.30	2.49	1.09	0.00	0.01	100.04
059 area 6	35.87	0.00	21.71	37.99	1.27	2.60	1.11	0.00	0.01	100.56
059 area 6	35.82	0.00	21.57	37.52	1.50	2.47	1.02	0.00	0.01	99.92
059 area 6	35.94	0.00	21.59	38.27	1.37	2.44	1.04	0.00	0.01	100.66
059 area 6	35.97	0.00	21.63	37.71	1.43	2.34	1.04	0.00	0.01	100.13
059 area 6	36.15	0.00	21.70	37.46	1.41	2.47	1.06	0.00	0.01	100.26
059 area 6	35.85	0.00	21.60	37.68	1.54	2.22	1.11	0.00	0.00	100.00
059 area 6	35.97	0.00	21.42	37.81	1.57	2.18	1.05	0.00	0.01	100.00
059 area 6	36.07	0.00	21.69	37.48	1.58	2.41	1.01	0.00	0.00	100.25

APPENDIX B: Complete Microprobe analyses for muscovite

Location	SiO2	TiO2	Al2O3	FeO	MnO	MgO	CaO	Na2O	K2O	Total
013 area 1	45.49	0.22	36.70	1.09	0.00	0.61	0.04	1.02	8.13	93.30
013 area 1	45.09	0.26	36.58	1.90	0.01	1.27	0.04	0.80	8.65	94.59
013 area 1	39.64	0.43	30.30	4.31	0.00	3.58	0.50	0.94	3.67	83.36
013 area 1	44.12	0.23	35.73	1.35	0.01	0.80	0.06	0.87	8.99	92.15
013 area 1	40.98	0.31	34.59	1.34	0.01	0.84	0.08	0.78	8.66	87.59
013 area 1	43.73	0.28	35.55	1.12	0.00	0.63	0.02	0.66	9.00	91.00
013 area 1	46.33	0.27	38.13	1.08	0.01	0.68	0.06	0.78	7.90	95.24
013 area 2	45.37	0.26	36.34	1.61	0.02	0.64	0.04	0.85	9.17	94.30
013 area 2	44.84	0.25	36.29	1.45	0.00	0.67	0.01	0.91	8.99	93.40
013 area 2	45.00	0.25	36.44	1.75	0.00	0.74	0.01	0.96	8.82	93.98
013 area 2	44.46	0.26	35.51	1.64	0.01	0.84	0.02	0.95	9.40	93.09
013 area 2	43.48	0.26	36.97	3.21	0.00	1.39	0.04	0.74	8.22	94.31
013 area 2	44.37	0.30	35.51	3.45	0.00	1.19	0.09	0.72	8.54	94.17
013 area 2	38.23	0.23	32.79	11.64	0.01	3.32	0.19	0.53	6.08	93.03
013 area 2	44.90	0.26	35.36	1.06	0.00	0.65	0.00	0.78	8.88	91.89
013 area 3	44.54	0.27	36.73	2.53	0.01	0.67	0.06	0.91	8.49	94.21
013 area 3	43.07	0.31	35.86	1.70	0.01	0.89	0.04	0.78	9.35	91.99
013 area 3	44.57	0.22	33.60	3.81	0.01	1.88	0.12	0.60	7.79	92.60
013 area 3	44.64	0.27	36.63	1.28	0.00	0.68	0.07	0.79	8.63	92.99
013 area 3	44.74	0.36	35.76	2.19	0.00	1.37	0.00	0.82	9.02	94.26
013 area 3	45.24	0.28	37.24	1.09	0.00	0.69	0.00	0.74	8.98	94.27
013 area 3	44.27	0.42	34.17	3.55	0.00	1.74	0.02	0.65	8.89	93.71
013 area 3	44.85	0.28	36.07	1.83	0.00	0.77	0.01	0.76	9.47	94.03
013 area 3	35.44	0.22	27.69	16.66	0.00	4.44	0.14	0.36	4.65	89.60
013 area 3	46.67	0.29	36.41	1.10	0.00	0.92	0.00	0.85	8.75	94.99
013 area 3	45.40	0.26	36.65	1.02	0.00	0.81	0.02	0.83	8.74	93.75
013 area 3	45.67	0.28	35.88	1.26	0.00	0.79	0.02	0.81	9.26	93.97
013 area 3	45.70	0.26	35.95	1.48	0.00	0.77	0.02	0.72	8.76	93.67

Location	SiO2	TiO2	Al2O3	FeO	MnO	MgO	CaO	Na2O	K2O	Total
013 area 3	45.15	0.32	34.18	2.09	0.00	1.25	0.03	0.74	8.27	92.04
013 area 3	46.40	0.26	35.65	1.13	0.00	0.92	0.00	0.92	8.56	93.84
013 area 5	45.27	0.26	37.42	1.23	0.00	0.68	0.00	0.96	8.84	94.66
013 area 5	43.45	0.25	35.13	1.34	0.00	0.70	0.02	0.80	9.37	91.05
013 area 5	45.41	0.26	37.58	0.97	0.00	0.65	0.00	0.86	9.27	95.00
013 area 5	26.55	0.06	27.84	22.10	0.00	9.70	0.03	0.16	1.74	88.19
013 area 5	43.14	0.28	35.05	1.01	0.00	0.76	0.01	0.84	9.42	90.49
013 area 5	43.74	0.27	35.81	1.44	0.01	1.07	0.04	0.68	8.60	91.65
013 area 5	43.88	0.28	36.15	1.17	0.01	0.76	0.04	0.95	9.24	92.48
013 area 5	46.03	0.17	37.33	1.43	0.01	0.79	0.01	1.31	8.33	95.40
013 area 5	41.32	0.26	34.52	1.09	0.00	0.64	0.05	0.91	8.93	87.72
013 area 5	45.05	0.28	36.44	1.14	0.00	0.80	0.01	0.80	9.54	94.07
013 area 5	44.68	0.29	35.69	1.15	0.00	0.82	0.03	0.78	9.38	92.82
013 area 6	35.00	1.28	19.31	17.44	0.00	9.76	0.25	0.17	7.44	90.65
013 area 6	34.63	1.38	19.13	17.83	0.02	9.89	0.10	0.17	8.48	91.62
013 area 6	35.60	1.35	18.98	18.03	0.01	9.96	0.20	0.13	7.93	92.20
013 area 6	35.17	1.30	19.08	17.66	0.01	9.96	0.12	0.16	8.46	91.90
013 area 6	19.51	1.32	3.09	15.55	0.00	4.82	0.97	0.00	7.42	52.67
013 area 6	34.32	1.32	18.94	17.58	0.00	9.46	0.27	0.20	8.25	90.35
013 area 6	34.29	1.23	18.75	17.19	0.00	9.65	0.32	0.17	7.34	88.95
013 area 6	35.22	1.21	19.19	17.97	0.01	9.47	0.41	0.16	7.15	90.78
013 area 6	34.54	1.21	18.53	18.29	0.02	9.81	0.31	0.17	7.14	90.04
013 area 7	42.27	0.27	34.79	1.92	0.00	0.74	0.03	0.85	8.94	89.81
013 area 7	45.47	0.29	36.83	1.16	0.00	0.75	0.02	0.75	9.53	94.80
013 area 7	44.30	0.48	34.52	4.28	0.00	2.34	0.09	0.95	8.51	95.47
013 area 7	45.39	0.27	37.19	1.06	0.00	0.78	0.00	0.82	9.27	94.79
013 area 7	44.67	0.27	36.19	1.42	0.01	0.79	0.03	0.75	9.24	93.36
013 area 7	46.77	0.30	36.90	1.23	0.00	1.03	0.00	0.88	8.56	95.67
013 area 7	45.82	0.28	36.85	1.20	0.01	0.84	0.01	1.09	8.69	94.80
013 area 8	46.69	0.31	37.95	1.12	0.00	0.57	0.00	1.13	8.68	96.45
013 area 8	42.62	0.23	33.72	1.35	0.00	0.61	0.03	0.77	8.88	88.21
013 area 8	46.28	0.27	36.68	1.14	0.00	0.88	0.02	0.85	8.22	94.34
013 area 8	40.74	0.24	26.23	1.04	0.01	0.67	0.45	0.52	7.61	77.51
013 area 8	44.89	0.32	35.35	1.06	0.00	0.78	0.06	0.85	8.26	91.58
013 area 8	46.01	0.27	35.73	1.21	0.00	0.79	0.09	0.82	8.64	93.56
013 area 8	40.59	0.23	32.68	1.38	0.00	0.66	0.22	0.67	8.04	84.46
032 area 1	48.43	0.92	36.40	1.53	0.00	1.37	0.00	0.79	8.91	98.34
032 area 1	48.55	0.95	34.67	1.44	0.00	1.44	0.00	0.81	8.91	96.79
032 area 1	47.92	1.02	34.65	1.46	0.00	1.60	0.00	0.76	9.07	96.48
032 area 2	48.20	0.72	35.18	1.44	0.00	1.07	0.01	0.97	9.10	96.71
032 area 2	47.89	0.91	35.88	1.41	0.00	1.12	0.02	1.00	8.95	97.19
032 area 2	48.62	0.98	35.06	1.52	0.00	1.24	0.00	0.96	9.33	97.71
032 area 2	46.87	0.93	35.64	1.49	0.01	1.06	0.05	1.03	8.66	95.74
032 area 2	49.06	0.90	35.12	1.41	0.03	1.44	0.02	0.95	8.85	97.78
032 area 2	48.65	0.89	35.72	1.47	0.01	1.42	0.04	0.97	8.71	97.89
032 area 3	47.09	0.61	36.55	1.23	0.00	0.92	0.00	1.13	9.24	96.78
032 area 3	46.74	0.63	36.54	1.23	0.00	0.93	0.00	1.15	9.16	96.38
032 area 3	47.65	1.02	35.66	1.35	0.00	1.25	0.00	0.97	9.14	97.05
032 area 3	47.28	0.73	36.06	1.35	0.00	1.14	0.01	0.99	9.05	96.61
032 area 3	47.23	0.81	35.93	1.33	0.00	1.08	0.01	0.96	9.15	96.49
032 area 3	47.52	0.88	36.15	1.41	0.00	1.12	0.00	1.04	9.21	97.34
032 area 3	47.79	0.73	35.63	1.37	0.01	1.20	0.03	0.97	9.02	96.74

Location	SiO2	TiO2	Al2O3	FeO	MnO	MgO	CaO	Na2O	K2O	Total
032 area 3	47.19	0.74	35.65	1.40	0.00	1.15	0.00	0.93	8.96	96.01
032 area 3	47.00	0.61	35.76	1.30	0.00	1.12	0.00	1.04	9.27	96.11
032 area 3	47.01	0.55	36.24	1.27	0.01	1.12	0.00	1.10	9.40	96.72
032 area 3	46.48	1.25	35.06	1.34	0.00	1.03	0.00	1.00	9.30	95.46
032 area 3	46.87	0.82	35.37	1.37	0.00	1.26	0.00	1.03	9.38	96.11
032 area 3	47.00	0.73	35.33	1.32	0.00	1.22	0.00	0.98		95.94
032 area 4	46.91	0.70	37.32	1.24	0.00	1.02	0.04	1.12	9.02	97.37
032 area 4	47.07	0.48	36.35	1.44	0.01	0.94	0.05	1.16	9.19	96.68
032 area 4	47.83	0.74	36.34	1.45	0.00	1.07	0.06	1.14	9.09	97.73
032 area 4	47.62	0.13	38.25	1.29	0.01	0.61	0.08	1.38	8.75	98.13
032 area 4	46.99	0.12	37.67	1.42	0.01	0.91	0.06	1.23	8.97	97.37
032 area 4	46.98	0.69	36.16	1.32	0.00	1.21	0.00	1.13	9.35	96.85
032 area 4	46.82	0.66	36.52	1.28	0.00	0.87	0.02	1.01	8.90	96.08
032 area 4	46.48	0.70	35.93	1.30	0.00	1.12	0.00	1.08	9.19	95.78
032 area 4	47.20	0.68	36.17	1.39	0.00	1.02	0.00	1.09	9.37	96.94
032 area 4	46.75	0.71	36.34	1.23	0.00	1.08	0.00	1.05	9.22	96.39
032 area 6	45.91	0.85	34.84	1.45	0.00	1.30	0.00	1.01	9.30	94.67
032 area 6	47.74	0.86	35.41	1.49	0.01	1.30	0.00	1.01	9.40	97.23
032 area 6	46.87	0.83	35.28	1.48	0.00	1.21	0.00	1.06	9.27	96.01
032 area 6	47.18	0.47	37.48	1.07	0.01	0.63	0.04	1.53	8.57	96.97
032 area 6	46.65	0.27	37.43	1.14	0.00	0.60	0.01	1.42	8.77	96.28
032 area 6	47.48	0.84	35.39	1.55	0.01	1.19	0.01	0.99	9.22	96.70
032 area 6	47.59	0.85	35.44	1.77	0.01	1.31	0.01	0.93	9.05	96.97
035 area 1	47.54	0.62	34.27	3.01	0.01	0.89	0.01	0.71	8.23	95.28
035 area 1	47.48	0.44	34.94	2.90	0.00	0.78	0.01	0.79	8.26	95.60
035 area 1	48.17	0.63	33.91	3.08	0.01	0.91	0.00	0.69	8.41	95.81
035 area 1	47.24	0.66	33.78	3.04	0.00	0.90	0.03	0.71	8.30	94.66
035 area 1	47.95	0.70	35.08	3.12	0.01	1.08	0.01	0.76	8.09	96.80
035 area 1	48.97	0.73	33.98	2.96	0.00	1.02	0.00	0.67	8.28	96.62
035 area 1	48.41	0.78	33.07	3.29	0.00	1.17	0.00	0.66	8.04	95.41
035 area 1	48.60	0.62	34.51	3.17	0.03	0.91	0.00	0.73	8.36	96.94
035 area 1	47.76	0.57	34.48	2.91	0.01	0.85	0.01	0.71	7.99	95.28
035 area 1	47.53	0.72	33.10	3.18	0.01	1.11	0.01	0.64	8.16	94.45
035 area 1	48.36	0.67	34.16	2.78	0.00	0.96	0.00	0.68	8.45	96.05
035 area 1	49.10	0.45	34.85	3.42	0.05	0.93	0.02	0.73	8.43	97.99
035 area 1	48.43	0.54	34.15	3.59	0.04	1.29	0.00	0.73	8.51	97.28
035 area 1	48.37	0.48	34.80	3.34	0.03	0.80	0.00	0.73	8.51	97.07
035 area 3	49.33	0.76	34.07	3.08	0.00	1.14	0.00	0.65	8.28	97.32
035 area 3	48.23	0.73	33.33	3.24	0.01	1.09	0.04	0.59	8.05	95.31
035 area 3	48.59	0.59	35.11	2.74	0.00	0.79	0.00	0.77	8.52	97.10
035 area 3	49.01	0.97	33.44	3.42	0.01	1.25	0.00	0.83	8.09	97.01
035 area 3	49.53	0.74	33.86	3.14	0.01	1.14	0.00	0.70	8.39	97.52
035 area 3	48.29	0.76	34.00	3.07	0.01	1.08	0.01	0.70	8.39	96.30
035 area 3	49.08	0.72	34.24	2.99	0.00	1.01	0.00	0.70	8.67	97.41
035 area 3	49.03	0.66	34.14	3.00	0.01	0.93	0.00	0.66	8.43	96.87
035 area 3	48.60	1.03	33.26	3.25	0.03	1.20	0.00	0.78	8.30	96.43
035 area 3	48.65	1.01	33.19	3.42	0.01	1.22	0.00	0.81	8.29	96.61
035 area 3	47.56	0.54	34.06	2.98	0.01	0.86	0.00	0.62	8.33	94.97
035 area 3	49.10	1.00	33.01	3.33	0.01	1.25	0.03	0.73	8.04	96.50
035 area 3	46.81	0.70	33.50	3.09	0.00	1.03	0.00	0.73	8.65	94.51
035 area 3	47.98	0.70	34.22	3.18	0.00	1.00	0.00	0.82	8.68	96.58
035 area 4	21.89	0.59	19.48	16.91	0.15	4.47	0.29	0.36	7.61	71.74

Location	SiO2	TiO2	Al2O3	FeO	MnO	MgO	CaO	Na2O	K2O	Total
035 area 4	31.72	0.09	6.66	23.31	2.91	1.28	2.13	0.04	2.20	70.33
035 area 4	32.45	0.01	17.94	27.83	5.91	1.55	4.40	0.01	0.10	90.20
035 area 4	47.54	0.66	33.29	3.12	0.01	0.98	0.04	0.60	8.25	94.48
035 area 4	50.23	0.63	34.68	2.99	0.02	0.98	0.04	0.72	8.19	98.48
035 area 4	42.46	0.54	32.32	2.94	0.01	0.86	0.09	0.68	8.15	88.05
035 area 4	48.08	0.51	35.34	2.93	0.01	0.71	0.06	0.76	8.11	96.51
035 area 4	49.38	0.47	34.59	3.11	0.02	0.82	0.10	0.72	8.20	97.40
035 area 4	45.18	0.39	35.21	2.88	0.02	0.60	0.13	1.01	8.81	94.23
035 area 4	50.08	0.58	33.70	3.14	0.01	1.06	0.10	0.70	8.35	97.71
035 area 4	48.95	0.58	34.63	3.09	0.01	0.97	0.04	0.70	8.22	97.20
035 area 5	48.65	0.92	33.70	3.42	0.03	1.01	0.03	0.76	8.13	96.64
035 area 5	49.15	1.04	33.58	3.40	0.03	1.14	0.02	0.77	8.25	97.38
035 area 5	49.20	0.99	33.90	3.35	0.01	1.09	0.00	0.77	8.12	97.44
035 area 5	48.19	1.00	33.59	3.38	0.03	1.02	0.01	0.71	8.02	95.96
035 area 5	48.92	1.01	33.73	3.29	0.02	1.03	0.02	0.65	8.18	96.84
035 area 5	49.41	0.61	34.21	3.44	0.02	0.92	0.09	0.58	7.93	97.19
035 area 5	48.93	1.03	31.47	3.17	0.03	1.04	0.08	0.68	9.02	95.44
035 area 5	47.80	0.54	34.28	3.29	0.02	0.91	0.08	0.77	8.62	96.30
035 area 5	47.54	0.47	35.23	3.01	0.02	0.76	0.02	0.77	8.08	95.90
035 area 5	35.50	5.46	22.24	14.16	0.05	3.58	0.22	0.39	6.75	88.35
035 area 5	48.14	0.70	34.16	3.44	0.01	1.03	0.01	0.73	8.32	96.53
035 area 5	47.96	0.71	33.76	3.39	0.02	1.06	0.00	0.69	8.46	96.05
035 area 5	48.07	0.65	33.71	3.35	0.01	0.91	0.06	0.58	8.15	95.48
035 area 6	35.56	1.83	17.90	19.50	0.17	9.48	0.12	0.25	8.81	93.62
035 area 6	34.07	1.80	18.34	19.14	0.19	9.03	0.12	0.28	8.92	91.90
035 area 6	34.21	1.86	16.17	18.50	0.18	8.99	0.27	0.26	8.74	89.19
035 area 6	36.96	1.65	20.19	18.41	0.16	8.79	0.31	0.34	7.73	94.51
035 area 6	38.98	1.81	17.63	18.80	0.18	11.34	0.14	0.28	9.16	98.33
035 area 6	47.65	0.63	32.74	3.21	0.01	1.03	0.25	0.72	8.45	94.69
035 area 6	47.64	0.59	34.31	3.23	0.05	1.00	0.19	0.91	8.76	96.68
035 area 6	36.53	1.79	16.86	18.84	0.24	9.37	0.20	0.30	9.02	93.15
039 area 1	47.00	0.69	35.45	2.43	0.02	0.91	0.00	0.27	9.85	96.63
039 area 1	46.67	0.34	35.96	2.46	0.02	0.84	0.00	0.27	9.89	96.46
039 area 1	47.16	0.39	35.48	2.54	0.04	0.93	0.00	0.25	9.81	96.60
039 area 1	47.25	0.48	35.73	2.53	0.02	0.94	0.01	0.23	9.63	96.81
039 area 1	47.89	1.06	34.57	2.70	0.03	1.05	0.00	0.19	9.60	97.10
039 area 1	47.18	1.07	35.17	2.21	0.03	0.85	0.01	0.22	9.74	96.48
039 area 1	47.66	0.59	35.18	2.71	0.04	1.01	0.01	0.25	9.89	97.33
039 area 1	48.34	0.85	34.38	2.67	0.03	1.12	0.00	0.26	9.64	97.30
039 area 1	47.71	1.06	34.19	2.81	0.03	1.08	0.00	0.26	9.47	96.60
039 area 2	48.69	0.85	34.62	2.81	0.03	1.07	0.00	0.20	9.53	97.80
039 area 2	48.65	0.91	33.81	2.81	0.04	1.28	0.00	0.25	9.57	97.31
039 area 2	48.59	0.79	33.82	2.80	0.03	1.26	0.00	0.26	9.82	97.36
039 area 2	48.90	0.97	32.87	3.12	0.02	1.46	0.00	0.25	9.66	97.26
039 area 2	49.71	0.94	32.90	3.02	0.02	1.49	0.00	0.24	9.45	97.78
039 area 2	48.76	0.86	34.04	2.94	0.02	1.20	0.00	0.29	9.66	97.75
039 area 2	48.26	0.86	34.18	2.91	0.03	1.15	0.00	0.28	9.67	97.33
039 area 3	47.91	0.65	35.33	2.47	0.03	0.95	0.00	0.26	9.81	97.41
039 area 3	46.37	0.52	34.27	2.92	0.07	0.84	0.03	0.20	9.38	94.59
039 area 3	46.72	0.66	34.91	2.47	0.06	0.92	0.02	0.22	9.27	95.26
039 area 3	47.04	0.53	35.48	2.38	0.03	0.85	0.00	0.26	9.88	96.46
039 area 3	48.10	0.60	33.68	2.63	0.02	1.14	0.03	0.21	9.17	95.58

Location	SiO2	TiO2	Al2O3	FeO	MnO	MgO	CaO	Na2O	K2O	Total
039 area 3	47.50	0.60	34.43	2.52	0.03	0.94	0.01	0.22	9.14	95.39
039 area 3	46.98	0.54	34.45	2.55	0.03	0.93	0.01	0.24	9.17	94.90
039 area 3	46.79	0.52	34.96	2.45	0.03	0.97	0.01	0.26	9.15	95.14
039 area 4	46.71	0.96	34.49	2.79	0.05	1.08	0.00	0.26	9.55	95.88
039 area 4	46.48	0.99	34.17	2.82	0.04	1.09	0.00	0.27	9.62	95.49
039 area 4	46.98	0.94	34.87	2.81	0.05	1.02	0.00	0.28	9.69	96.64
039 area 4	47.31	1.03	34.18	2.83	0.02	1.16	0.00	0.26	9.66	96.46
039 area 4	47.17	0.99	34.41	2.71	0.03	1.10	0.00	0.27	9.42	96.11
039 area 4	47.39	0.97	34.46	2.70	0.03	1.11	0.00	0.28	9.59	96.54
039 area 4	47.30	1.03	34.32	2.72	0.04	1.10	0.01	0.23	9.66	96.41
039 area 4	47.32	0.97	34.40	2.78	0.04	1.11	0.00	0.26	9.40	96.28
039 area 4	47.54	1.00	34.52	2.68	0.01	1.10	0.00	0.27	9.59	96.70
039 area 6	47.00	1.17	34.90	2.44	0.02	1.04	0.00	0.28	9.66	96.52
039 area 6	46.68	1.53	33.97	2.67	0.02	1.07	0.00	0.25	9.49	95.68
039 area 6	48.24	1.10	32.35	2.92	0.03	1.50	0.00	0.25	9.99	96.38
039 area 6	34.85	3.19	18.17	23.06	0.21	6.46	0.00	0.06	9.35	95.35
039 area 6	46.75	1.35	33.31	2.72	0.01	1.20	0.00	0.24	9.17	94.75
039 area 6	47.96	1.35	33.72	2.66	0.01	1.22	0.00	0.27	9.46	96.65
039 area 6	47.32	1.26	33.68	2.78	0.02	1.23	0.00	0.28	9.59	96.16
046 area 1	47.33	0.99	35.34	1.55	0.01	0.70	0.03	0.90	9.38	96.23
046 area 1	45.91	1.02	35.76	1.54	0.00	0.74	0.02	0.82	9.00	94.82
046 area 1	46.69	1.03	36.79	1.49	0.01	0.72	0.01	0.83	9.06	96.63
046 area 1	46.31	1.08	36.89	1.56	0.00	0.70	0.01	0.84	9.09	96.49
046 area 1	45.62	1.13	35.04	1.56	0.01	0.76	0.02	0.75	8.96	93.85
046 area 1	46.71	1.04	35.96	1.58	0.01	0.73	0.01	0.81	8.93	95.78
046 area 1	46.32	1.07	36.55	1.44	0.00	0.69	0.03	0.83	8.85	95.79
046 area 2	45.60	0.56	35.47	1.29	0.00	0.70	0.05	1.09	9.02	93.78
046 area 2	48.02	0.62	35.66	1.39	0.00	0.77	0.05	1.06	9.12	96.69
046 area 2	44.90	0.53	35.77	1.27	0.00	0.68	0.06	1.21	8.85	93.28
046 area 2	43.16	0.55	35.10	1.29	0.00	0.61	0.05	1.23	8.93	90.93
046 area 2	18.57	4.25	14.52	12.34	0.22	1.73	0.06	0.56	4.47	56.72
046 area 2	34.63	2.14	19.28	20.57	0.03	8.76	0.06	0.22	8.65	94.33
046 area 2	34.26	1.88	19.42	18.92	0.00	9.04	0.09	0.29	8.26	92.17
046 area 2	33.60	0.36	30.97	6.10	0.00	0.67	0.12	1.39	6.57	79.79
046 area 2	45.76	0.56	36.76	1.44	0.01	0.69	0.06	1.33	8.78	95.40
046 area 2	44.54	0.69	34.75	2.22	0.01	0.80	0.13	1.14	8.54	92.82
046 area 2	37.02	0.43	27.21	3.36	0.01	0.75	0.17	0.97	7.23	77.16
046 area 2	46.62	1.02	36.94	1.37	0.00	0.64	0.00	0.88	9.49	96.96
046 area 2	46.90	1.07	36.36	1.48	0.00	0.73	0.00	0.81	9.56	96.92
046 area 2	47.11	1.13	35.66	1.55	0.00	0.81	0.01	0.77	9.44	96.49
046 area 2	46.25	0.99	36.55	1.28	0.00	0.60	0.00	0.85	9.52	96.05
046 area 2	44.97	0.87	36.28	2.82	0.00	0.65	0.02	0.82	9.17	95.60
046 area 2	46.03	0.44	37.04	1.55	0.00	0.66	0.02	0.83	9.38	95.95
046 area 2	46.27	0.62	37.30	1.57	0.00	0.64	0.00	0.86	9.47	96.73
046 area 4	46.29	1.04	36.87	1.31	0.00	0.57	0.00	0.84	9.52	96.44
046 area 4	46.11	1.12	36.38	1.36	0.01	0.63	0.00	0.85	9.54	96.00
046 area 4	46.37	1.09	36.45	1.40	0.00	0.66	0.00	0.77	9.35	96.09
046 area 4	46.75	1.24	35.69	1.64	0.01	0.85	0.00	0.80	9.62	96.60
046 area 4	46.72	1.26	34.57	1.80	0.00	1.05	0.00	0.72	9.57	95.68
046 area 4	47.07	1.16	34.89	1.82	0.00	1.10	0.00	0.71	9.61	96.36
046 area 4	46.75	1.16	36.58	1.46	0.00	0.68	0.00	0.81	9.79	97.23
046 area 4	47.15	1.17	35.18	1.67	0.00	0.99	0.00	0.76	9.84	96.77

Location	SiO2	TiO2	Al2O3	FeO	MnO	MgO	CaO	Na2O	K2O	Total
046 area 4	47.55	1.20	34.54	1.77	0.00	1.04	0.01	0.72	9.67	96.50
046 area 4	47.21	1.23	34.72	1.69	0.00	0.96	0.02	0.73	9.58	96.13
046 area 5	44.71	0.58	36.98	1.81	0.01	0.60	0.06	0.79	8.25	93.80
046 area 5	45.64	0.63	37.33	1.43	0.00	0.49	0.07	0.83	9.15	95.56
046 area 5	44.61	0.85	36.72	1.84	0.00	0.71	0.04	0.86	9.23	94.85
046 area 5	45.08	0.64	38.06	1.27	0.02	0.46	0.01	0.87	9.25	95.65
046 area 5	44.36	0.61	36.13	1.14	0.00	0.49	0.03	0.91	9.15	92.83
046 area 5	44.86	0.79	35.74	2.00	0.00	0.76	0.01	0.74	8.80	93.70
046 area 5	45.40	0.89	37.53	1.82	0.01	0.73	0.05	0.92	9.31	96.66
046 area 3	45.82	1.15	36.34	1.55	0.00	0.66	0.00	0.85	9.73	96.10
046 area 3	45.73	1.15	36.29	1.58	0.00	0.74	0.00	0.88	9.74	96.10
046 area 3	46.90	1.10	34.74	1.82	0.01	0.99	0.00	0.76	9.83	96.15
046 area 3	47.02	1.16	34.92	1.72	0.00	1.12	0.00	0.75	9.74	96.42
046 area 3	47.33	1.22	34.07	1.83	0.01	1.17	0.00	0.65	9.44	95.73
046 area 3	45.69	1.23	35.58	1.53	0.01	0.80	0.00	0.81	9.75	95.42
046 area 3	45.33	1.12	36.30	1.36	0.00	0.65	0.00	0.87	9.64	95.27
046 area 3	44.93	1.05	36.45	1.47	0.00	0.68	0.00	0.88	9.64	95.10
046 area 3	44.59	1.02	36.34	1.42	0.00	0.62	0.00	0.87	9.50	94.37
048 area 1	46.49	1.26	35.76	1.18	0.00	0.69	0.02	0.66	8.16	94.22
048 area 1	46.60	1.24	35.61	1.27	0.00	0.72	0.01	0.66	8.35	94.45
048 area 1	46.33	1.21	35.50	1.26	0.00	0.70	0.00	0.63	8.25	93.88
048 area 1	34.21	2.53	18.45	20.19	0.01	8.29	0.00	0.19	9.17	93.04
048 area 1	34.46	2.53	18.63	20.20	0.01	8.34	0.00	0.21	9.24	93.62
048 area 1	34.21	2.51	18.82	20.58	0.02	8.15	0.01	0.21	9.22	93.73
048 area 1	34.37	2.55	18.59	20.29	0.01	8.20	0.00	0.19	9.31	93.50
048 area 1	34.01	2.36	18.57	21.88	0.01	7.48	0.01	0.11	9.41	93.84
048 area 1	33.40	0.90	32.31	6.21	0.00	6.65	0.66	1.98	0.04	82.15
048 area 1	33.62	0.86	32.25	6.77	0.00	6.09	0.60	1.92	0.03	82.16
048 area 1	33.20	0.95	31.25	6.29	0.00	6.96	0.66	2.23	0.02	81.56
048 area 1	33.00	1.00	32.05	6.64	0.00	6.25	0.22	2.05	0.03	81.23
048 area 1	33.25	0.42	32.31	8.55	0.00	5.01	0.38	1.69	0.03	81.64
048 area 1	32.92	0.96	32.29	6.09	0.00	6.55	0.72	2.09	0.04	81.65
048 area 1	33.04	0.89	32.37	6.06	0.00	6.52	0.68	2.09	0.05	81.70
048 area 2	46.81	1.20	34.30	1.34	0.00	0.90	0.02	0.62	8.23	93.43
048 area 2	46.33	1.21	35.99	1.44	0.00	0.84	0.02	0.76	8.34	94.94
048 area 2	45.92	1.22	34.75	1.28	0.01	0.91	0.01	0.62	8.16	92.88
048 area 2	47.60	1.16	36.04	1.26	0.00	0.71	0.04	0.73	8.28	95.81
048 area 2	45.23	1.12	35.54	1.19	0.00	0.68	0.03	0.68	8.28	92.74
048 area 2	46.71	1.12	35.45	1.24	0.00	0.76	0.02	0.65	8.12	94.07
048 area 2	46.87	1.18	35.46	1.28	0.00	0.81	0.00	0.66	8.49	94.75
048 area 2	46.16	1.14	35.73	1.26	0.00	0.75	0.01	0.71	8.58	94.34
048 area 2	47.55	1.08	35.61	1.24	0.00	0.80	0.00	0.69	8.56	95.53
048 area 2	47.23	1.10	35.21	1.22	0.00	0.83	0.00	0.61	8.47	94.68
048 area 2	45.96	1.10	35.94	1.39	0.00	0.69	0.00	0.69	8.66	94.44
048 area 2	45.80	1.08	36.18	1.34	0.00	0.71	0.03	0.70	8.14	93.98
048 area 2	46.70	1.19	35.36	1.38	0.00	0.79	0.01	0.63	8.24	94.28
048 area 2	45.80	1.13	35.55	1.30	0.01	0.78	0.00	0.67	8.48	93.71
048 area 2	45.86	1.19	35.34	1.40	0.00	0.72	0.00	0.67	8.52	93.71
048 area 3	46.28	1.13	36.15	1.47	0.01	0.75	0.04	0.77	8.37	94.97
048 area 3	45.84	1.14	35.55	1.46	0.01	0.78	0.02	0.74	8.42	93.97
048 area 3	45.15	1.19	34.94	1.44	0.01	0.78	0.04	0.67	8.45	92.68
048 area 3	45.81	1.18	35.46	1.13	0.01	0.67	0.05	0.70	8.31	93.33

Location	SiO2	TiO2	Al2O3	FeO	MnO	MgO	CaO	Na2O	K2O	Total
048 area 3	44.15	1.17	34.93	1.20	0.01	0.74	0.05	0.69	8.06	90.99
048 area 3	44.97	1.18	35.11	1.24	0.00	0.75	0.02	0.66	8.44	92.37
048 area 4	47.19	1.14	33.56	1.40	0.00	0.82	0.09	0.57	8.30	93.07
048 area 4	45.91	1.16	35.83	1.14	0.00	0.57	0.08	0.71	8.58	93.97
048 area 4	45.76	1.14	34.69	1.26	0.00	0.73	0.05	0.63	8.34	92.60
048 area 4	45.79	1.12	34.42	1.30	0.00	0.70	0.07	0.63	8.36	92.39
048 area 4	43.39	0.63	36.32	1.55	0.00	0.46	0.06	0.68	8.44	91.52
048 area 4	46.79	1.19	34.73	1.38	0.00	0.70	0.09	0.69	8.84	94.41
048 area 4	43.55	1.25	34.42	1.45	0.00	0.68	0.05	0.60	8.40	90.39
048 area 4	46.68	1.08	33.95	1.48	0.00	0.84	0.07	0.61	8.50	93.22
048 area 4	44.88	1.09	35.02	1.34	0.01	0.78	0.07	0.59	8.24	92.01
048 area 4	46.24	1.14	33.86	1.40	0.00	0.86	0.04	0.55	8.29	92.38
048 area 4	46.70	1.06	33.98	1.57	0.00	1.04	0.04	0.56	8.35	93.31
048 area 4	46.83	1.06	34.71	1.47	0.00	0.99	0.05	0.60	8.23	93.95
048 area 6	46.05	0.92	36.35	1.05	0.01	0.66	0.02	0.70	8.50	94.26
048 area 6	46.95	0.92	36.06	1.15	0.00	0.71	0.01	0.65	8.61	95.06
048 area 6	45.16	1.04	34.86	1.17	0.00	0.62	0.04	0.64	8.28	91.81
048 area 6	47.06	1.07	35.63	0.91	0.00	0.60	0.04	0.65	8.38	94.34
048 area 6	46.20	1.10	35.78	1.21	0.02	0.72	0.04	0.68	8.34	94.08
048 area 6	46.05	1.14	34.43	1.21	0.00	0.73	0.05	0.58	8.04	92.22
048 area 6	47.13	1.10	35.81	1.12	0.00	0.71	0.02	0.69	8.47	95.06
048 area 6	47.79	1.14	35.20	1.12	0.00	0.71	0.04	0.65	8.36	95.00
048 area 6	48.59	1.16	35.60	1.31	0.00	0.77	0.03	0.64	8.54	96.62
048 area 6	47.18	1.11	36.55	1.31	0.00	0.72	0.03	0.73	8.33	95.95
048 area 6	47.22	1.24	37.02	1.28	0.00	0.65	0.05	0.76	8.10	96.32
048 area 6	46.42	1.02	35.43	1.52	0.01	0.66	0.05	0.71	8.38	94.20
048 area 6	45.92	1.12	36.54	1.21	0.00	0.70	0.08	0.81	8.29	94.66
048 area 8	44.16	0.51	36.33	1.14	0.00	0.58	0.02	0.80	8.72	92.26
048 area 8	43.31	1.12	34.81	1.26	0.00	0.72	0.03	0.64	8.27	90.16
048 area 8	43.83	1.09	34.81	1.42	0.00	0.80	0.01	0.64	8.48	91.08
048 area 8	44.54	1.15	34.38	1.45	0.00	0.89	0.00	0.61	8.54	91.57
048 area 8	44.14	1.14	34.22	1.43	0.01	0.86	0.01	0.61	8.51	90.92
048 area 8	44.04	1.16	34.32	1.37	0.00	0.83	0.01	0.64	8.57	90.94
048 area 8	43.26	1.04	34.84	1.23	0.00	0.69	0.04	0.66	8.33	90.09
048 area 8	45.46	1.12	35.41	1.59	0.01	1.02	0.01	0.68	8.41	93.70
048 area 8	45.97	1.09	34.62	1.59	0.01	0.96	0.01	0.59	8.37	93.20
051 area 1	62.46	0.02	19.27	0.32	0.05	0.00	0.03	1.28	14.79	98.21
051 area 1	61.58	0.01	19.22	0.25	0.03	0.00	0.03	1.34	14.57	97.03
051 area 1	61.50	0.01	19.21	0.46	0.07	0.00	0.02	1.17	14.89	97.35
051 area 1	62.37	0.02	19.26	0.40	0.04	0.00	0.02	1.38	14.55	98.05
051 area 1	61.46	0.01	19.33	0.42	0.05	0.00	0.03	1.39	14.55	97.25
051 area 1	61.65	0.02	19.21	0.38	0.04	0.00	0.04	1.30	14.69	97.31
051 area 2	45.28	0.82	36.77	1.35	0.01	0.77	0.02	0.32	9.57	94.91
051 area 2	44.03	0.90	36.88	1.35	0.00	0.65	0.02	0.35	9.60	93.79
051 area 2	44.48	0.89	36.96	1.41	0.00	0.67	0.02	0.36	9.48	94.28
051 area 2	44.44	0.85	37.21	1.54	0.01	0.66	0.03	0.33	8.89	93.96
051 area 3	46.20	1.19	36.39	1.33	0.02	0.55	0.02	0.27	9.32	95.27
051 area 3	46.22	1.04	37.15	1.35	0.01	0.62	0.04	0.34	9.53	96.30
051 area 3	46.99	1.08	36.57	1.41	0.01	0.70	0.04	0.30	9.43	96.52
051 area 3	45.57	1.07	37.00	1.31	0.01	0.56	0.05	0.31	9.39	95.29
051 area 3	44.54	1.09	37.66	1.40	0.00	0.60	0.05	0.34	9.30	94.98
051 area 3	46.44	0.66	37.19	1.17	0.00	0.62	0.04	0.27	9.45	95.85

Location	SiO2	TiO2	Al2O3	FeO	MnO	MgO	CaO	Na2O	K2O	Total
051 area 3	45.52	0.53	37.32	1.21	0.00	0.65	0.04	0.28	9.66	95.23
051 area 4	44.94	1.19	36.52	1.34	0.02	0.72	0.04	0.35	9.28	94.40
051 area 4	44.59	0.85	36.89	1.49	0.00	0.68	0.02	0.37	9.61	94.51
051 area 4	44.64	1.09	37.25	1.52	0.01	0.67	0.02	0.39	9.27	94.87
051 area 4	44.37	1.22	37.47	1.59	0.02	0.69	0.01	0.37	9.27	95.01
051 area 4	44.13	1.13	37.20	1.57	0.01	0.71	0.02	0.38	9.46	94.59
051 area 4	43.73	0.97	37.12	1.54	0.02	0.68	0.03	0.39	9.54	94.02
051 area 4	44.36	1.02	36.55	1.50	0.01	0.71	0.03	0.34	9.26	93.77
051 area 4	44.23	1.00	36.69	1.45	0.01	0.64	0.04	0.36	9.24	93.64
051 area 4	45.13	1.09	36.66	1.49	0.00	0.72	0.02	0.33	9.37	94.81
051 area 4	45.31	1.10	37.06	1.38	0.01	0.73	0.04	0.37	9.35	95.35
051 area 4	62.11	0.02	19.39	0.00	0.02	0.01	0.05	2.29	13.19	97.08
051 area 4	61.45	0.01	19.29	0.01	0.00	0.00	0.07	1.61	14.39	96.83
051 area 4	63.96	0.01	19.26	0.01	0.00	0.02	0.08	1.62	14.25	99.21
051 area 4	61.86	0.01	19.41	0.00	0.01	0.00	0.08	1.68	14.19	97.23
051 area 4	61.25	0.01	19.25	0.01	0.00	0.01	0.07	1.46	14.45	96.51
051 area 4	62.04	0.02	19.45	0.00	0.00	0.01	0.09	1.87	13.86	97.34
051 area 4	62.23	0.01	20.02	0.01	0.02	0.01	0.09	1.73	13.75	97.87
051 area 4	61.24	0.01	19.18	0.00	0.00	0.01	0.05	1.41	14.70	96.60
051 area 4	61.38	0.01	19.31	0.03	0.02	0.00	0.06	1.36	14.76	96.92
051 area 4	60.83	0.01	19.39	0.04	0.02	0.01	0.06	1.35	14.73	96.44
052 area 3	44.29	1.25	34.87	1.43	0.01	0.55	0.03	0.39	8.72	91.54
052 area 3	46.84	1.16	33.29	1.29	0.00	0.56	0.02	0.34	8.78	92.27
052 area 3	44.19	0.48	32.64	1.41	0.01	0.53	0.03	0.35	8.79	88.43
052 area 3	47.96	0.93	33.21	1.41	0.00	0.58	0.03	0.34	8.67	93.12
052 area 3	47.89	0.89	35.26	1.49	0.00	0.65	0.07	0.42	8.54	95.21
052 area 3	45.19	0.93	34.10	1.38	0.00	0.59	0.01	0.39	8.63	91.22
052 area 3	44.48	1.09	33.29	1.33	0.01	0.57	0.05	0.45	10.05	91.31
052 area 3	45.15	1.06	33.27	1.37	0.00	0.55	0.01	0.34	8.96	90.70
052 area 3	44.97	1.10	32.82	1.41	0.01	0.57	0.02	0.37	9.16	90.42
052 area 3	44.36	0.76	35.31	1.51	0.01	0.57	0.01	0.40	9.02	91.95
052 area 3	43.24	0.73	33.66	1.39	0.00	0.53	0.04	0.43	9.10	89.12
052 area 3	46.86	0.79	35.80	1.34	0.00	0.53	0.01	0.38	9.07	94.77
052 area 3	46.76	0.80	35.71	1.44	0.01	0.61	0.00	0.37	9.36	95.06
052 area 3	46.45	0.95	35.60	1.38	0.01	0.59	0.00	0.38	9.55	94.91
052 area 3	47.74	0.92	35.40	1.40	0.01	0.62	0.01	0.38	9.05	95.52
052 area 3	47.05	0.78	35.70	1.37	0.00	0.59	0.00	0.39	9.23	95.11
052 area 3	46.78	1.20	35.39	1.45	0.00	0.59	0.00	0.38	9.07	94.86
052 area 3	46.68	1.25	35.11	1.46	0.00	0.65	0.00	0.38	9.34	94.87
052 area 3	47.14	1.16	35.77	1.28	0.00	0.56	0.00	0.34	9.24	95.50
052 area 3	46.22	1.27	35.09	1.37	0.00	0.58	0.00	0.39	9.60	94.52
052 area 3	47.09	1.25	35.50	1.43	0.00	0.62	0.00	0.39	9.21	95.48
052 area 3	47.30	1.20	35.50	1.33	0.01	0.56	0.00	0.37	9.21	95.48
052 area 4	63.59	0.01	18.37	0.18	0.01	0.00	0.02	1.32	15.12	98.61
052 area 4	63.36	0.00	18.51	0.18	0.03	0.00	0.02	1.32	15.05	98.48
052 area 4	63.28	0.00	18.62	0.18	0.02	0.00	0.02	1.08	15.78	98.97
052 area 4	64.12	0.00	18.56	0.17	0.01	0.00	0.02	0.92	15.75	99.55
052 area 4	62.75	0.00	18.27	0.21	0.01	0.00	0.00	1.20	15.24	97.69
052 area 4	63.36	0.00	18.50	0.04	0.01	0.00	0.02	1.22	15.45	98.60
052 area 4	62.98	0.01	18.29	0.15	0.02	0.00	0.03	0.92	15.74	98.14
052 area 4	63.04	0.01	18.41	0.11	0.01	0.00	0.04	1.42	15.08	98.11
052 area 4	63.25	0.00	18.46	0.05	0.01	0.01	0.03	1.17	15.30	98.29

Location	SiO2	TiO2	Al2O3	FeO	MnO	MgO	CaO	Na2O	K2O	Total
052 area 4	63.08	0.01	18.35	0.03	0.02	0.00	0.03	1.32	15.07	97.91
052 area 4	63.49	0.00	18.46	0.20	0.02	0.00	0.02	1.33	14.91	98.43
052 area 4	64.28	0.00	18.96	0.15	0.01	0.00	0.03	1.62	14.13	99.18
052 area 4	62.95	0.00	18.29	0.28	0.02	0.00	0.03	1.24	14.45	97.25
052 area 4	63.87	0.00	18.45	0.27	0.03	0.00	0.01	1.31	15.12	99.06
052 area 4	63.99	0.01	18.58	0.32	0.02	0.00	0.02	1.45	15.09	99.49
052 area 4	62.83	0.01	17.80	0.24	0.01	0.00	0.00	1.02	15.25	97.16
052 area 5	63.22	0.03	18.62	0.23	0.01	0.00	0.01	1.77	14.45	98.32
052 area 5	62.61	0.01	18.32	0.08	0.00	0.00	0.02	1.48	14.99	97.50
052 area 5	63.22	0.01	18.40	0.05	0.01	0.00	0.02	1.79	14.62	98.12
052 area 5	63.09	0.01	18.43	0.04	0.01	0.00	0.01	1.46	15.30	98.35
052 area 5	63.04	0.01	18.57	0.03	0.01	0.00	0.03	1.94	14.69	98.32
052 area 5	63.53	0.01	18.40	0.03	0.00	0.00	0.06	1.68	14.84	98.54
052 area 5	63.03	0.01	18.31	0.04	0.01	0.00	0.04	1.27	15.12	97.82
052 area 5	63.88	0.02	18.51	0.08	0.00	0.00	0.01	1.71	14.53	98.73
052 area 5	64.17	0.01	18.57	0.06	0.00	0.01	0.03	1.68	14.77	99.29
052 area 5	64.26	0.02	18.62	0.18	0.01	0.00	0.02	2.13	13.62	98.85
052 area 5	46.46	0.55	33.77	1.97	0.00	0.86	0.04	0.27	9.11	93.02
052 area 5	45.74	1.24	34.11	1.37	0.00	0.52	0.03	0.38	8.70	92.11
052 area 5	46.41	1.21	36.04	1.35	0.01	0.56	0.03	0.44	9.28	95.34
052 area 5	44.39	0.81	35.50	1.37	0.00	0.55	0.05	0.51	9.38	92.56
052 area 5	45.78	0.65	30.11	1.26	0.00	0.58	0.05	0.35	9.85	88.63
052 area 5	45.49	0.66	33.70	1.37	0.01	0.52	0.02	0.36	8.85	90.98
052 area 5	46.54	0.76	37.07	1.29	0.00	0.54	0.04	0.59	9.74	96.57
052 area 5	46.36	0.56	35.53	1.34	0.00	0.53	0.04	0.45	9.39	94.21
052 area 5	44.85	0.81	35.15	1.32	0.00	0.63	0.00	0.42	9.37	92.55
052 area 5	45.14	1.13	35.24	1.33	0.01	0.52	0.00	0.39	9.34	93.10
052 area 5	45.20	1.14	34.85	1.48	0.00	0.60	0.00	0.38	9.16	92.79
052 area 5	45.41	1.01	35.28	1.41	0.00	0.51	0.00	0.40	9.09	93.12
052 area 7	47.87	0.60	37.09	1.48	0.03	0.57	0.03	0.42	9.15	97.23
052 area 7	56.95	0.84	31.37	1.27	0.03	0.55	0.03	0.43	8.65	100.13
052 area 7	47.58	0.87	36.54	1.49	0.01	0.59	0.01	0.43	8.96	96.47
052 area 7	48.08	0.82	35.29	1.26	0.04	0.52	0.03	0.40	8.82	95.25
052 area 7	47.93	0.79	36.29	1.38	0.01	0.56	0.01	0.42	9.10	96.49
052 area 7	47.47	0.92	36.18	1.21	0.02	0.55	0.00	0.39	9.04	95.77
052 area 7	48.11	0.92	35.89	1.35	0.01	0.60	0.02	0.40	8.96	96.28
052 area 7	47.91	0.63	37.02	1.55	0.06	0.58	0.02	0.42	9.11	97.31
052 area 7	46.31	1.11	35.45	1.19	0.01	0.56	0.02	0.34	8.98	93.96
052 area 7	46.35	0.84	35.32	2.14	0.01	0.65	0.03	0.36	8.95	94.64
052 area 7	47.93	0.98	36.10	1.27	0.01	0.53	0.04	0.37	8.82	96.03
052 area 7	47.41	0.95	36.07	1.33	0.01	0.61	0.01	0.36	9.07	95.83
052 area 7	46.80	0.88	35.85	1.35	0.00	0.55	0.00	0.39	9.06	94.88
052 area 7	46.87	0.89	35.79	1.32	0.01	0.58	0.00	0.38	9.19	95.03
052 area 7	47.37	1.05	36.23	1.24	0.00	0.53	0.00	0.38	9.50	96.30
052 area 7	47.59	1.02	36.03	1.34	0.00	0.63	0.00	0.36	9.14	96.10
052 area 8	63.08	0.00	24.00	0.08	0.01	0.00	5.26	8.52	0.16	101.11
052 area 8	48.84	1.24	36.09	1.20	0.01	0.58	0.02	0.40	9.07	97.44
052 area 8	48.67	1.43	36.58	1.19	0.00	0.45	0.00	0.38	9.34	98.04
052 area 8	48.25	1.17	36.71	1.24	0.01	0.50	0.00	0.42	9.39	97.69
052 area 8	47.99	1.44	36.26	1.36	0.00	0.56	0.00	0.40	9.10	97.10
052 area 8	48.54	1.41	36.36	1.37	0.00	0.59	0.00	0.42	9.02	97.71
052 area 8	48.69	1.40	36.35	1.42	0.02	0.56	0.00	0.43	8.98	97.84

Location	SiO2	TiO2	Al2O3	FeO	MnO	MgO	CaO	Na2O	K2O	Total
052 area 8	48.75	1.22	35.83	1.14	0.00	0.51	0.00	0.36	8.76	96.56
052 area 8	48.28	1.23	35.48	1.17	0.01	0.53	0.00	0.32	8.71	95.73
052 area 8	47.04	1.18	35.55	1.05	0.00	0.46	0.01	0.31	8.37	93.96
052 area 8	49.77	1.28	33.38	1.12	0.01	0.52	0.02	0.30	8.60	94.99
052 area 8	48.02	1.34	34.91	1.13	0.00	0.51	0.00	0.31	8.56	94.80
052 area 8	48.92	1.28	35.37	1.12	0.01	0.52	0.00	0.34	8.47	96.02
055 area 1	45.60	1.13	36.77	1.29	0.01	0.50	0.00	0.46	10.12	95.88
055 area 1	45.68	1.22	37.11	1.36	0.01	0.50	0.01	0.46	10.07	96.43
055 area 1	45.66	1.07	36.96	1.26	0.00	0.48	0.00	0.48	10.01	95.92
055 area 1	45.78	1.11	36.98	1.27	0.02	0.56	0.00	0.46	10.05	96.22
055 area 1	45.51	1.01	37.27	1.39	0.00	0.50	0.02	0.50	9.88	96.09
055 area 1	45.59	1.12	37.01	1.25	0.00	0.56	0.01	0.45	9.96	95.95
055 area 1	45.41	1.17	36.91	1.27	0.00	0.56	0.01	0.46	10.02	95.82
055 area 2	41.80	1.35	37.50	1.44	0.03	0.45	0.08	0.57	9.88	93.10
055 area 2	44.93	1.01	35.13	1.54	0.03	0.61	0.09	0.48	9.61	93.43
055 area 2	46.36	0.85	36.98	1.58	0.03	0.52	0.01	0.44	9.93	96.69
055 area 2	44.50	0.88	37.11	1.29	0.01	0.48	0.03	0.49	9.58	94.38
055 area 2	45.24	3.92	34.73	1.47	0.01	0.56	0.03	0.42	9.69	96.06
055 area 3	46.02	0.96	36.19	1.37	0.01	0.62	0.01	0.46	10.16	95.79
055 area 3	46.07	0.86	36.71	1.44	0.01	0.54	0.01	0.50	10.31	96.45
055 area 3	46.20	0.83	36.89	1.22	0.01	0.52	0.00	0.52	10.41	96.62
055 area 3	46.03	0.84	36.85	1.25	0.04	0.52	0.00	0.51	10.26	96.29
055 area 3	46.24	0.86	37.48	1.35	0.01	0.56	0.00	0.47	10.09	97.07
055 area 4	46.00	0.76	37.37	1.18	0.04	0.46	0.06	0.58	9.98	96.42
055 area 4	47.51	0.97	37.35	1.63	0.06	0.54	0.05	0.61	9.72	98.44
055 area 4	46.63	0.67	36.87	1.32	0.02	0.50	0.01	0.50	10.08	96.60
055 area 4	46.41	0.96	36.99	1.22	0.00	0.50	0.02	0.50	9.94	96.55
055 area 4	46.77	0.64	36.72	1.26	0.00	0.49	0.00	0.45	10.23	96.56
055 area 4	46.34	0.84	36.55	1.46	0.02	0.58	0.03	0.45	10.03	96.29
055 area 4	46.49	0.97	36.59	1.48	0.02	0.54	0.00	0.44	10.03	96.57
055 area 4	47.13	0.97	36.43	1.35	0.01	0.65	0.01	0.49	10.00	97.03
055 area 4	46.27	1.52	36.23	1.30	0.02	0.47	0.03	0.37	9.61	95.82
055 area 4	46.46	1.07	36.40	1.16	0.00	0.44	0.01	0.42	9.42	95.39
055 area 4	46.48	0.86	37.59	1.35	0.00	0.51	0.01	0.50	9.85	97.14
055 area 4	46.81	1.04	37.06	1.52	0.01	0.51	0.00	0.37	9.09	96.42
055 area 4	45.97	1.09	36.35	1.29	0.02	0.58	0.00	0.42	9.72	95.44
055 area 4	46.63	1.21	36.47	1.30	0.00	0.64	0.00	0.43	9.86	96.54
055 area 4	46.55	1.63	35.58	1.37	0.00	0.66	0.01	0.40	9.86	96.06
059 area 3	62.79	0.00	22.75	0.27	0.00	0.00	4.10	9.06	0.11	99.09
059 area 3	61.59	0.00	24.29	0.36	0.00	0.00	4.17	10.19	0.09	100.69
059 area 3	62.34	0.00	22.90	0.33	0.02	0.00	4.18	8.61	0.13	98.50
059 area 3	61.97	0.00	22.86	0.42	0.00	0.00	4.18	9.31	0.14	98.88
059 area 3	61.88	0.00	23.84	0.26	0.01	0.00	4.43	9.73	0.12	100.27
059 area 3	61.42	0.00	22.99	0.27	0.01	0.01	4.50	9.05	0.16	98.39
059 area 3	61.28	0.00	22.97	0.28	0.00	0.01	4.51	9.08	0.17	98.30
059 area 3	61.55	0.00	22.83	0.31	0.01	0.00	4.39	9.04	0.16	98.30
059 area 3	62.24	0.00	23.54	0.22	0.01	0.00	4.41	9.28	0.10	99.79
059 area 6	45.92	0.52	36.21	1.59	0.00	0.54	0.00	0.38	9.37	94.53
059 area 6	45.36	0.60	36.00	1.47	0.00	0.54	0.00	0.42	9.29	93.68
059 area 6	45.88	0.59	36.60	1.47	0.00	0.49	0.00	0.42	9.28	94.73
059 area 6	45.44	0.56	36.30	1.38	0.00	0.44	0.00	0.43	9.24	93.78
059 area 6	43.78	0.61	34.39	1.49	0.00	0.57	0.04	0.44	10.05	91.36

Location	SiO2	TiO2	Al2O3	FeO	MnO	MgO	CaO	Na2O	K2O	Total
059 area 6	46.06	0.66	36.00	1.53	0.00	0.56	0.00	0.41	9.14	94.36
059 area 6	46.62	0.61	36.43	1.36	0.00	0.48	0.04	0.43	8.96	94.93
059 area 6	45.84	0.59	36.34	1.43	0.00	0.48	0.00	0.38	9.05	94.10
059 area 6	46.55	0.48	36.14	1.43	0.00	0.61	0.02	0.34	9.27	94.83
059 area 6	46.05	0.41	36.76	1.25	0.00	0.46	0.00	0.40	9.25	94.59
059 area 6	45.48	0.70	36.49	1.13	0.00	0.44	0.00	0.37	9.25	93.85
059 area 6	64.70	0.01	18.78	0.46	0.01	0.00	0.03	1.12	15.34	100.44
059 area 6	57.23	0.09	18.28	3.60	0.04	1.07	0.03	0.61	14.74	95.69
059 area 6	64.67	0.01	18.83	0.28	0.01	0.00	0.04	1.48	15.21	100.53
059 area 6	65.09	0.01	18.80	0.24	0.01	0.00	0.04	1.35	15.15	100.68
059 area 6	64.86	0.01	18.71	0.21	0.00	0.00	0.03	1.22	15.47	100.51
059 area 6	65.92	0.00	18.69	0.53	0.03	0.00	0.02	1.13	15.62	101.94
059 area 6	65.02	0.01	18.60	0.26	0.01	0.00	0.01	0.82	16.10	100.84
059 area 6	64.61	0.01	18.67	0.12	0.01	0.00	0.03	1.09	15.80	100.34
059 area 6	63.87	0.00	22.66	0.45	0.02	0.00	3.82	9.14	0.15	100.11

APPENDIX B: Complete Microprobe analyses for plagioclase

Location	SiO2	TiO2	Al2O3	FeO	MnO	MgO	CaO	Na2O	K2O	Total
032 area 1	61.32	0.00	25.34	0.01	0.00	0.00	6.43	8.27	0.08	101.45
032 area 1	60.83	0.00	22.16	0.00	0.00	0.00	5.97	8.28	0.09	97.34
032 area 1	61.89	0.00	24.99	0.00	0.01	0.00	5.75	8.43	0.07	101.14
032 area 1	61.44	0.00	25.11	0.00	0.00	0.00	6.25	8.26	0.06	101.13
032 area 2	62.99	0.00	24.30	0.06	0.00	0.00	4.81	8.90	0.08	101.15
032 area 2	61.74	0.00	24.75	0.03	0.00	0.00	5.54	8.88	0.10	101.03
032 area 2	60.78	0.00	25.18	0.04	0.01	0.00	6.12	8.41	0.07	100.61
032 area 2	61.42	0.00	24.92	0.12	0.00	0.01	5.76	8.67	0.07	100.97
032 area 2	61.30	0.00	24.23	0.09	0.01	0.00	5.00	9.26	0.08	99.98
032 area 2	61.21	0.00	24.35	0.01	0.01	0.00	4.98	9.13	0.10	99.79
032 area 2	61.68	0.00	23.99	0.00	0.00	0.00	4.61	9.29	0.10	99.67
032 area 4	61.15	0.01	24.64	0.08	0.00	0.00	5.70	8.74	0.07	100.39
032 area 4	61.12	0.02	25.53	0.09	0.01	0.00	5.45	9.39	0.11	101.72
032 area 4	61.38	0.00	25.03	0.05	0.01	0.00	5.79	8.73	0.06	101.07
032 area 4	61.05	0.00	25.00	0.06	0.00	0.00	5.76	8.71	0.07	100.65
032 area 5	61.46	0.00	25.03	0.00	0.00	0.00	5.77	8.55	0.08	100.89
032 area 5	61.83	0.00	24.80	0.00	0.01	0.00	5.56	8.73	0.09	101.02
032 area 5	61.38	0.01	24.75	0.00	0.00	0.00	5.57	8.70	0.11	100.53
032 area 5	61.43	0.00	24.87	0.00	0.00	0.00	5.72	8.59	0.08	100.69
032 area 5	61.59	0.00	24.88	0.00	0.00	0.00	5.68	8.58	0.10	100.82
032 area 5	61.58	0.00	24.99	0.00	0.00	0.00	5.75	8.77	0.11	101.21
032 area 5	61.49	0.00	24.90	0.01	0.01	0.00	5.67	8.58	0.07	100.73
032 area 6	60.01	0.00	24.82	0.04	0.00	0.00	5.92	8.57	0.08	99.44
032 area 6	60.38	0.00	24.72	0.02	0.00	0.00	5.49	8.82	0.09	99.53
032 area 6	60.36	0.00	24.51	0.02	0.01	0.00	5.52	8.75	0.09	99.25
032 area 6	60.52	0.00	24.35	0.00	0.00	0.00	5.47	8.69	0.11	99.14
032 area 6	60.33	0.00	26.13	0.03	0.00	0.00	5.77	9.30	0.09	101.63
032 area 6	61.06	0.00	24.36	0.02	0.00	0.00	5.53	8.77	0.08	99.82
035 area 1	63.52	0.00	24.17	0.00	0.00	0.00	4.82	8.57	0.11	101.19
035 area 1	63.30	0.00	24.09	0.05	0.00	0.00	4.85	8.64	0.11	101.04
035 area 1	63.07	0.00	24.09	0.04	0.01	0.00	4.84	8.68	0.15	100.88
035 area 1	63.45	0.00	24.03	0.04	0.00	0.00	4.82	8.71	0.15	101.21
035 area 1	63.30	0.00	24.26	0.04	0.00	0.00	4.80	8.56	0.14	101.11
035 area 1	63.34	0.01	24.26	0.03	0.00	0.00	4.90	8.46	0.16	101.16

Location	SiO2	TiO2	Al2O3	FeO	MnO	MgO	CaO	Na2O	K2O	Total
035 area 1	63.36	0.00	24.13	0.05	0.00	0.00	4.87	8.53	0.15	101.09
035 area 1	63.98	0.01	24.15	0.21	0.01	0.06	4.74	8.20	0.22	101.60
035 area 1	63.04	0.00	24.14	0.04	0.02	0.00	4.90	8.50	0.17	100.81
035 area 1	63.39	0.00	24.20	0.07	0.01	0.01	4.90	8.54	0.16	101.29
035 area 1	63.08	0.01	24.24	0.07	0.01	0.01	4.97	8.43	0.18	100.98
035 area 1	62.95	0.01	24.17	0.03	0.01	0.00	4.96	8.44	0.16	100.73
035 area 1	63.32	0.00	24.34	0.04	0.00	0.00	4.95	7.91	0.15	100.71
035 area 1	63.43	0.00	24.10	0.05	0.00	0.00	4.89	8.62	0.15	101.25
035 area 1	61.32	0.00	23.57	0.05	0.00	0.01	4.98	7.95	0.14	98.02
035 area 1	63.15	0.00	24.26	0.06	0.00	0.00	4.90	8.71	0.11	101.19
035 area 1	62.82	0.00	24.32	0.08	0.01	0.01	5.19	8.49	0.09	101.01
035 area 1	63.02	0.00	24.09	0.03	0.00	0.00	4.89	8.74	0.09	100.86
035 area 1	63.21	0.00	24.15	0.03	0.02	0.00	4.84	8.78	0.08	101.11
035 area 2	62.51	0.00	23.94	0.02	0.01	0.00	4.78	8.91	0.09	100.26
035 area 2	62.10	0.00	24.23	0.02	0.01	0.00	5.12	8.44	0.09	100.02
035 area 2	59.47	0.00	21.68	0.03	0.00	0.00	4.78	7.03	0.08	93.07
035 area 2	62.62	0.00	23.79	0.03	0.00	0.00	4.53	9.04	0.12	100.12
035 area 2	63.65	0.01	23.80	0.05	0.00	0.00	4.51	8.72	0.14	100.87
035 area 2	63.27	0.00	23.71	0.04	0.01	0.00	4.51	8.91	0.14	100.58
035 area 2	63.13	0.00	23.71	0.03	0.00	0.00	4.54	8.27	0.13	99.81
035 area 2	63.23	0.00	23.82	0.02	0.00	0.00	4.49	8.84	0.15	100.54
035 area 2	63.02	0.00	23.70	0.03	0.02	0.00	4.47	8.96	0.13	100.33
035 area 2	62.50	0.00	23.88	0.03	0.00	0.00	4.66	8.85	0.11	100.03
039 area 1	60.02	0.01	25.15	0.49	0.06	0.00	5.54	8.58	0.15	100.00
039 area 1	60.60	0.01	25.08	0.43	0.06	0.00	5.36	8.55	0.20	100.29
039 area 1	60.21	0.01	25.11	0.25	0.04	0.01	5.50	8.39	0.19	99.70
039 area 1	59.83	0.01	24.84	0.10	0.01	0.01	5.27	8.59	0.23	98.89
039 area 1	60.47	0.00	24.72	0.16	0.02	0.00	5.21	8.58	0.24	99.39
039 area 2	54.85	0.00	21.87	0.05	0.00	0.01	4.47	7.61	0.22	89.08
039 area 2	60.51	0.00	24.45	0.01	0.00	0.01	5.00	8.79	0.20	98.97
039 area 2	60.70	0.00	24.51	0.02	0.01	0.00	5.03	8.72	0.16	99.15
039 area 2	61.07	0.00	24.57	0.04	0.01	0.01	5.03	8.84	0.18	99.76
039 area 2	60.87	0.00	24.51	0.04	0.01	0.01	5.01	8.71	0.20	99.37
039 area 2	61.08	0.00	24.57	0.03	0.01	0.00	5.00	8.72	0.20	99.61
039 area 2	60.59	0.00	24.46	0.06	0.01	0.00	5.14	8.74	0.20	99.19
039 area 2	95.12	0.00	0.00	0.07	0.00	0.00	0.00	0.00	0.01	95.20
039 area 2	61.09	0.00	24.67	0.05	0.00	0.00	4.89	8.11	0.21	99.01
039 area 2	60.01	0.01	24.34	0.07	0.00	0.00	4.87	8.81	0.23	98.35
039 area 2	59.32	0.01	24.32	0.07	0.01	0.01	5.04	8.78	0.13	97.67
039 area 3	62.18	0.00	24.38	0.06	0.00	0.01	4.86	8.61	0.28	100.38
039 area 3	61.43	0.00	24.35	0.02	0.02	0.00	4.90	8.67	0.30	99.69
039 area 3	62.25	0.00	24.22	0.02	0.01	0.00	4.63	8.76	0.28	100.18
039 area 3	62.13	0.00	24.15	0.02	0.01	0.00	4.58	8.74	0.36	99.99
039 area 3	62.63	0.00	24.02	0.01	0.00	0.00	4.48	8.76	0.36	100.26
039 area 3	61.09	0.00	24.07	0.02	0.00	0.00	4.54	8.78	0.36	98.87
039 area 3	61.07	0.00	24.29	0.00	0.00	0.00	4.70	8.73	0.34	99.14
039 area 3	61.76	0.00	24.27	0.01	0.01	0.00	4.75	8.84	0.28	99.92
039 area 3	60.94	0.00	24.16	0.04	0.01	0.01	4.85	8.38	0.23	98.60
039 area 7	60.01	0.00	25.13	0.12	0.01	0.01	5.88	8.23	0.24	99.63
039 area 7	57.45	0.00	24.91	0.06	0.00	0.02	6.37	7.72	0.27	96.80
039 area 7	59.27	0.00	25.29	0.01	0.00	0.01	6.09	8.13	0.30	99.10
039 area 7	59.68	0.00	25.06	0.01	0.01	0.00	5.70	8.16	0.34	98.96

Location	SiO2	TiO2	Al2O3	FeO	MnO	MgO	CaO	Na2O	K2O	Total
039 area 7	58.93	0.00	25.26	0.02	0.00	0.00	6.04	8.07	0.31	98.62
039 area 7	58.50	0.00	25.33	0.00	0.00	0.01	6.14	8.09	0.30	98.37
039 area 7	58.57	0.01	25.67	0.02	0.01	0.00	6.49	7.65	0.27	98.70
039 area 7	58.80	0.00	25.56	0.02	0.00	0.02	6.29	7.84	0.25	98.79
039 area 7	59.06	0.01	25.37	0.06	0.00	0.02	6.05	8.13	0.17	98.88
039 area 8	60.33	0.00	25.31	0.06	0.01	0.00	5.93	8.23	0.21	100.09
039 area 8	60.24	0.00	25.33	0.09	0.02	0.00	5.96	8.10	0.21	99.95
039 area 8	59.56	0.01	25.25	0.07	0.01	0.01	5.88	8.42	0.11	99.32
039 area 8	59.35	0.00	25.53	0.09	0.00	0.01	6.05	8.07	0.14	99.25
039 area 8	58.90	0.00	25.52	0.05	0.00	0.00	6.24	8.06	0.21	98.99
039 area 8	59.22	0.00	25.32	0.00	0.01	0.00	6.02	8.08	0.11	98.77
039 area 8	59.57	0.00	25.34	0.00	0.01	0.00	6.00	8.12	0.22	99.25
039 area 8	59.34	0.00	25.34	0.00	0.02	0.00	6.00	8.00	0.20	98.90
039 area 8	59.33	0.00	25.30	0.00	0.01	0.00	6.01	8.07	0.20	98.93
039 area 8	59.36	0.00	25.27	0.01	0.01	0.01	5.92	8.11	0.12	98.82
044 area 1	58.36	0.00	25.74	0.00	0.01	0.00	6.72	7.78	0.31	98.92
044 area 1	58.28	0.00	25.79	0.01	0.00	0.00	6.80	7.67	0.32	98.88
044 area 1	58.30	0.00	25.90	0.00	0.00	0.00	6.83	7.68	0.31	99.02
044 area 1	58.41	0.00	26.08	0.01	0.00	0.00	6.86	7.73	0.28	99.37
044 area 1	59.44	0.00	25.86	0.01	0.01	0.01	6.80	7.77	0.17	100.07
044 area 1	60.82	0.01	24.45	0.01	0.01	0.00	5.21	8.66	0.13	99.30
044 area 1	59.55	0.01	25.45	0.02	0.00	0.00	6.32	7.92	0.22	99.49
044 area 1	59.35	0.00	25.64	0.01	0.00	0.01	6.55	7.60	0.28	99.44
044 area 1	59.38	0.00	25.55	0.01	0.01	0.01	6.47	7.75	0.33	99.52
044 area 1	59.37	0.00	25.57	0.00	0.00	0.01	6.49	7.82	0.29	99.56
044 area 1	60.21	0.01	25.25	0.00	0.01	0.01	6.04	8.10	0.27	99.89
044 area 1	60.06	0.00	25.15	0.01	0.00	0.00	6.01	8.15	0.18	99.56
044 area 1	59.17	0.00	25.67	0.10	0.00	0.01	6.59	7.78	0.17	99.49
044 area 3	74.66	0.01	6.76	1.30	0.08	0.05	1.56	2.13	0.69	87.23
044 area 3	48.13	0.00	28.12	0.25	0.03	0.00	6.58	8.83	0.18	92.12
044 area 3	55.51	0.00	25.53	0.56	0.04	0.04	1.69	7.74	2.59	93.72
044 area 3	54.95	0.00	28.10	0.51	0.07	0.01	6.33	8.49	0.19	98.65
044 area 3	60.91	0.01	24.70	0.28	0.03	0.00	5.75	8.06	0.23	99.98
044 area 3	56.98	0.00	27.13	0.26	0.02	0.01	6.51	8.82	0.14	99.88
044 area 3	58.30	0.00	25.87	0.14	0.02	0.00	6.50	8.09	0.10	99.03
044 area 3	59.94	0.00	26.42	0.14	0.01	0.01	6.24	7.18	0.13	100.08
044 area 3	58.18	0.00	25.71	0.09	0.00	0.00	6.47	7.99	0.11	98.56
044 area 4	57.89	0.00	25.52	0.02	0.00	0.00	6.52	7.89	0.20	98.05
044 area 4	58.18	0.00	25.56	0.02	0.02	0.01	6.57	7.92	0.24	98.51
044 area 4	58.69	0.00	25.05	0.03	0.00	0.00	6.07	8.22	0.27	98.33
044 area 4	59.25	0.00	24.92	0.00	0.00	0.00	5.87	8.30	0.22	98.56
044 area 4	59.20	0.01	25.05	0.00	0.02	0.00	5.92	8.32	0.19	98.72
044 area 4	59.58	0.00	25.00	0.00	0.01	0.01	5.95	8.20	0.23	98.98
044 area 4	59.86	0.00	24.99	0.01	0.00	0.01	5.78	8.32	0.19	99.17
044 area 5	58.35	0.00	25.94	0.21	0.02	0.00	7.02	7.56	0.17	99.28
044 area 5	56.89	0.00	26.10	0.18	0.02	0.00	7.05	7.72	0.18	98.14
044 area 5	57.46	0.00	25.84	0.08	0.01	0.00	6.97	7.70	0.13	98.20
044 area 5	57.26	0.00	25.89	0.03	0.02	0.02	6.98	7.77	0.14	98.10
044 area 8	58.35	0.01	23.95	0.45	0.03	0.02	6.45	7.11	0.18	96.54
044 area 8	56.93	0.00	26.90	0.26	0.02	0.02	7.69	7.32	0.17	99.32
044 area 8	58.23	0.02	25.49	0.21	0.01	0.00	6.48	8.03	0.20	98.67
044 area 8	59.16	0.00	25.50	0.41	0.05	0.01	6.52	7.55	0.13	99.35

Location	SiO2	TiO2	Al2O3	FeO	MnO	MgO	CaO	Na2O	K2O	Total
044 area 8	57.47	0.01	26.86	0.43	0.04	0.02	6.48	8.62	0.16	100.10
044 area 8	58.02	0.00	25.43	0.24	0.02	0.02	6.57	7.72	0.13	98.15
046 area 1	65.80	0.00	23.09	0.00	0.01	0.00	3.02	9.97	0.06	101.94
046 area 1	65.60	0.00	23.03	0.00	0.00	0.00	3.02	9.94	0.07	101.67
046 area 1	65.75	0.00	22.95	0.00	0.00	0.00	3.02	9.72	0.08	101.53
046 area 1	64.90	0.00	22.88	0.00	0.00	0.00	3.30	9.65	0.09	100.83
046 area 1	65.35	0.00	22.77	0.00	0.00	0.00	2.98	9.97	0.09	101.15
046 area 1	65.67	0.00	22.65	0.00	0.00	0.00	3.00	9.87	0.10	101.29
046 area 2	64.99	0.00	23.33	0.12	0.01	0.00	3.39	9.29	0.08	101.21
046 area 2	64.45	0.00	23.26	0.04	0.00	0.00	3.23	9.30	0.09	100.36
046 area 2	64.43	0.00	23.46	0.02	0.00	0.00	3.38	9.92	0.09	101.30
046 area 3	63.97	0.00	22.87	0.01	0.00	0.00	3.02	10.09	0.09	100.06
046 area 3	63.15	0.00	23.13	0.03	0.01	0.00	3.30	10.00	0.06	99.69
046 area 3	63.61	0.00	23.05	0.00	0.00	0.00	3.11	10.17	0.09	100.03
046 area 4	64.81	0.00	23.18	0.01	0.00	0.00	3.00	10.08	0.09	101.17
046 area 4	65.35	0.00	22.40	0.00	0.01	0.00	2.45	10.41	0.14	100.76
046 area 4	65.19	0.00	22.31	0.00	0.00	0.00	2.46	10.44	0.16	100.56
046 area 4	65.60	0.00	22.51	0.00	0.00	0.00	2.40	10.46	0.17	101.13
046 area 4	65.75	0.00	22.22	0.00	0.00	0.00	2.42	10.44	0.13	100.96
046 area 4	65.58	0.00	22.49	0.00	0.00	0.00	2.40	10.41	0.11	101.00
046 area 4	65.65	0.01	22.38	0.00	0.01	0.00	2.47	10.32	0.10	100.92
046 area 4	65.90	0.00	22.31	0.00	0.00	0.00	2.51	10.29	0.10	101.11
046 area 4	65.71	0.00	22.45	0.00	0.01	0.00	2.61	10.25	0.09	101.12
046 area 4	65.90	0.00	22.23	0.05	0.00	0.00	2.70	10.21	0.08	101.16
046 area 5	64.14	0.00	23.26	0.11	0.00	0.00	3.69	9.63	0.08	100.91
046 area 5	57.16	0.00	20.10	0.08	0.00	0.00	3.17	8.40	0.10	89.01
046 area 5	63.56	0.01	21.60	2.07	0.00	0.49	1.72	9.95	0.11	99.51
046 area 5	44.52	0.05	21.78	17.98	0.05	4.42	1.58	5.35	0.21	95.94
046 area 5	64.34	0.01	23.13	0.28	0.00	0.00	3.32	9.95	0.07	101.10
048 area 6	58.01	0.00	24.66	0.04	0.00	0.00	5.98	8.02	0.10	96.81
048 area 6	57.65	0.00	24.25	0.02	0.00	0.01	5.76	8.27	0.11	96.06
048 area 6	57.90	0.00	24.25	0.02	0.00	0.01	5.55	8.48	0.08	96.30
048 area 6	57.90	0.01	23.71	0.02	0.00	0.00	5.19	8.42	0.15	95.40
048 area 6	56.71	0.00	24.16	0.00	0.01	0.01	5.90	8.09	0.15	95.03
048 area 6	58.82	0.00	23.83	0.01	0.00	0.00	5.20	8.17	0.12	96.14
048 area 6	58.36	0.00	23.55	0.02	0.00	0.00	4.92	8.69	0.17	95.71
048 area 6	58.48	0.00	23.54	0.00	0.00	0.01	4.90	8.68	0.16	95.77
048 area 6	57.74	0.00	23.65	0.00	0.01	0.00	5.14	8.21	0.16	94.91
048 area 6	57.67	0.00	23.52	0.01	0.00	0.02	5.09	8.54	0.18	95.03
048 area 6	59.89	0.00	23.74	0.01	0.00	0.00	5.03	8.58	0.19	97.44
048 area 6	59.68	0.00	24.15	0.03	0.01	0.00	5.49	8.25	0.18	97.78
048 area 6	59.18	0.00	23.36	0.01	0.00	0.00	4.88	8.06	0.15	95.64
048 area 6	60.26	0.00	23.89	0.02	0.00	0.00	4.96	8.56	0.17	97.86
048 area 6	63.52	0.00	24.94	0.03	0.00	0.00	4.81	8.26	0.16	101.72
048 area 6	61.06	0.00	23.92	0.01	0.01	0.00	4.93	8.59	0.21	98.72
048 area 6	62.75	0.00	23.36	0.02	0.00	0.00	4.13	8.47	0.22	98.95
048 area 6	58.17	0.00	24.69	0.02	0.00	0.00	5.92	8.34	0.12	97.27
048 area 8	59.07	0.00	24.33	0.01	0.00	0.00	5.64	8.35	0.14	97.54
048 area 8	58.79	0.00	24.39	0.03	0.00	0.00	5.64	8.40	0.11	97.36
048 area 8	58.76	0.00	23.56	0.03	0.00	0.00	5.20	7.14	0.19	94.88
048 area 8	59.47	0.00	23.85	0.04	0.00	0.00	5.00	8.71	0.20	97.27
048 area 8	59.02	0.00	23.69	0.02	0.00	0.00	4.91	8.69	0.20	96.52

Location	SiO2	TiO2	Al2O3	FeO	MnO	MgO	CaO	Na2O	K2O	Total
048 area 8	59.09	0.00	23.64	0.02	0.01	0.00	4.89	8.69	0.21	96.56
048 area 8	58.09	0.00	23.48	0.00	0.00	0.00	4.91	8.62	0.23	95.32
048 area 8	58.42	0.00	23.63	0.01	0.00	0.00	5.03	8.57	0.21	95.88
048 area 8	57.97	0.00	23.59	0.02	0.00	0.00	5.05	8.43	0.21	95.28
048 area 8	58.25	0.00	23.50	0.02	0.00	0.01	5.06	8.40	0.19	95.43
048 area 8	58.08	0.00	23.60	0.03	0.01	0.01	5.02	8.43	0.20	95.39
048 area 8	59.21	0.00	23.71	0.02	0.00	0.00	4.97	8.75	0.21	96.87
048 area 8	58.95	0.00	24.32	0.04	0.00	0.02	5.67	8.16	0.13	97.29
048 area 8	58.87	0.00	24.44	0.04	0.00	0.00	5.66	8.13	0.13	97.26
048 area 8	58.78	0.00	24.46	0.02	0.00	0.00	5.56	8.30	0.14	97.27
048 area 8	59.88	0.01	24.11	0.01	0.00	0.00	4.94	7.93	0.20	97.08
048 area 8	58.19	0.00	23.83	0.05	0.01	0.00	5.13	8.44	0.22	95.88
048 area 8	57.98	0.00	23.62	0.02	0.00	0.01	5.04	8.64	0.21	95.52
048 area 8	58.09	0.00	23.75	0.04	0.00	0.00	5.06	8.39	0.17	95.51
048 area 8	57.76	0.00	23.42	0.03	0.00	0.01	4.99	8.45	0.19	94.85
048 area 8	57.54	0.00	23.56	0.03	0.00	0.00	5.01	8.58	0.18	94.90
048 area 8	58.32	0.00	23.08	0.02	0.00	0.00	4.36	8.86	0.14	94.78
048 area 8	57.79	0.00	22.81	0.04	0.00	0.00	4.24	9.09	0.10	94.07
048 area 8	58.04	0.00	23.12	0.05	0.00	0.00	4.39	8.92	0.09	94.61
051 area 1	59.72	0.00	24.63	0.06	0.01	0.01	5.47	8.46	0.16	98.52
051 area 1	62.25	0.01	19.07	0.13	0.03	0.00	0.03	0.73	15.54	97.78
051 area 1	59.81	0.00	24.63	0.08	0.02	0.00	5.61	8.36	0.19	98.70
051 area 1	59.16	0.01	24.68	0.10	0.01	0.00	5.67	8.40	0.20	98.22
051 area 1	59.04	0.00	24.74	0.06	0.03	0.01	5.61	8.37	0.23	98.09
051 area 1	59.12	0.00	24.50	0.04	0.01	0.00	5.37	8.55	0.18	97.77
051 area 1	59.30	0.01	24.76	0.14	0.02	0.00	5.60	8.42	0.20	98.45
051 area 1	60.09	0.00	24.87	0.20	0.03	0.02	5.58	8.40	0.18	99.36
051 area 1	58.92	0.00	24.92	0.13	0.03	0.00	5.66	8.47	0.17	98.30
051 area 1	59.36	0.01	24.92	0.19	0.04	0.00	5.65	8.49	0.15	98.80
051 area 2	60.23	0.00	24.90	0.18	0.02	0.01	5.67	8.32	0.22	99.55
051 area 2	60.21	0.00	24.89	0.16	0.01	0.01	5.60	8.28	0.15	99.29
051 area 2	60.17	0.00	24.67	0.09	0.01	0.01	5.63	8.24	0.19	99.01
051 area 2	60.09	0.00	24.79	0.03	0.01	0.00	5.61	8.30	0.22	99.05
051 area 2	60.22	0.01	25.01	0.06	0.00	0.02	5.60	8.45	0.19	99.54
051 area 2	60.29	0.01	24.95	0.12	0.03	0.00	5.56	8.38	0.20	99.55
051 area 2	60.24	0.00	25.00	0.11	0.01	0.00	5.71	8.23	0.21	99.51
051 area 2	60.27	0.00	24.97	0.20	0.02	0.01	5.64	8.36	0.17	99.64
051 area 3	59.13	0.00	24.79	0.00	0.02	0.01	5.61	8.25	0.32	98.13
051 area 3	59.16	0.00	24.66	0.01	0.00	0.01	5.36	8.41	0.37	97.99
051 area 3	59.39	0.00	24.63	0.00	0.01	0.00	5.32	8.33	0.41	98.10
051 area 3	59.82	0.00	24.71	0.00	0.02	0.00	5.34	8.35	0.40	98.64
051 area 3	59.74	0.01	24.57	0.00	0.01	0.00	5.34	8.38	0.39	98.44
051 area 3	59.84	0.00	24.68	0.00	0.00	0.01	5.32	8.29	0.37	98.51
051 area 3	59.83	0.00	24.79	0.02	0.01	0.00	5.37	8.39	0.37	98.78
051 area 3	59.45	0.00	24.98	0.02	0.01	0.00	5.65	8.24	0.38	98.74
051 area 3	59.81	0.00	24.97	0.00	0.01	0.00	5.65	8.26	0.36	99.07
051 area 3	59.82	0.00	25.00	0.00	0.00	0.01	5.70	8.35	0.25	99.13
051 area 3	60.35	0.01	25.09	0.09	0.01	0.00	5.69	8.43	0.27	99.93
051 area 4	60.56	0.00	24.57	0.08	0.00	0.01	5.38	8.83	0.27	99.69
051 area 4	60.58	0.00	24.19	0.00	0.01	0.01	5.01	8.86	0.43	99.08
051 area 4	60.27	0.00	24.30	0.00	0.01	0.00	5.03	8.83	0.45	98.91
051 area 4	59.79	0.00	24.29	0.01	0.00	0.00	5.06	8.80	0.47	98.42

Location	SiO2	TiO2	Al2O3	FeO	MnO	MgO	CaO	Na2O	K2O	Total
051 area 4	59.87	0.00	24.26	0.02	0.00	0.00	5.05	8.80	0.46	98.46
051 area 4	59.57	0.00	24.40	0.01	0.01	0.01	5.31	8.71	0.36	98.39
052 area 1	62.80	0.00	18.78	0.03	0.01	0.00	0.04	1.33	15.04	98.03
052 area 1	63.64	0.01	19.18	0.02	0.00	0.00	0.05	2.36	13.15	98.41
052 area 1	63.02	0.00	18.97	0.03	0.01	0.00	0.04	1.44	14.91	98.43
052 area 1	62.91	0.01	18.95	0.03	0.00	0.00	0.04	1.45	15.10	98.48
052 area 1	64.11	0.00	19.18	0.02	0.01	0.00	0.05	1.99	13.67	99.03
052 area 1	63.09	0.00	18.86	0.02	0.00	0.00	0.02	1.54	15.06	98.60
052 area 1	62.57	0.00	18.89	0.02	0.00	0.00	0.06	1.38	15.07	97.98
052 area 1	62.56	0.01	18.90	0.03	0.00	0.01	0.05	1.46	14.81	97.82
052 area 1	62.91	0.00	18.92	0.04	0.00	0.00	0.04	1.39	15.02	98.32
052 area 1	62.74	0.00	18.84	0.02	0.00	0.00	0.01	1.31	14.95	97.87
052 area 1	63.08	0.01	18.95	0.04	0.01	0.00	0.03	1.37	15.28	98.75
052 area 1	63.10	0.01	18.95	0.04	0.01	0.00	0.01	1.22	15.23	98.56
052 area 2	61.65	0.00	23.72	0.36	0.03	0.00	4.83	8.52	0.17	99.27
052 area 2	62.86	0.00	24.09	0.53	0.05	0.00	4.76	8.51	0.19	100.99
052 area 2	61.50	0.00	23.45	0.41	0.04	0.04	4.55	7.18	0.24	97.41
052 area 2	22.59	0.01	16.16	20.07	1.78	0.52	0.94	1.72	0.31	64.09
052 area 2	62.91	0.00	23.91	0.48	0.04	0.01	4.71	8.04	0.26	100.35
052 area 2	44.80	0.01	21.07	7.08	0.47	0.16	1.41	7.56	0.62	83.16
052 area 2	60.82	0.00	24.36	0.21	0.01	0.00	5.49	8.18	0.24	99.31
052 area 2	62.14	0.00	23.61	0.20	0.02	0.01	4.49	8.41	0.23	99.10
052 area 2	50.75	0.00	34.68	1.15	0.05	0.08	0.35	2.48	6.98	96.53
052 area 2	60.15	0.00	24.22	0.06	0.01	0.00	5.42	8.29	0.28	98.43
052 area 2	60.50	0.00	24.26	0.08	0.00	0.00	5.45	8.16	0.27	98.73
052 area 2	53.56	0.03	24.28	0.66	0.04	0.09	4.08	8.32	0.44	91.50
052 area 2	44.44	0.65	34.18	1.62	0.02	0.58	0.04	0.39	9.67	91.58
052 area 2	45.41	0.61	36.15	1.60	0.02	0.60	0.03	0.40	9.17	93.99
052 area 2	34.48	2.79	16.61	19.77	0.08	8.06	0.09	0.21	9.38	91.47
052 area 2	43.84	0.92	35.39	1.48	0.00	0.51	0.04	0.36	9.06	91.61
052 area 2	44.63	0.85	35.89	1.49	0.02	0.61	0.02	0.38	9.12	93.03
052 area 2	47.16	1.02	34.51	1.47	0.01	0.64	0.04	0.36	9.28	94.49
052 area 3	63.53	0.03	18.59	0.25	0.00	0.00	0.00	0.64	15.93	98.97
052 area 3	62.74	0.01	18.78	0.07	0.01	0.00	0.02	1.46	14.84	97.93
052 area 3	63.30	0.00	18.75	0.03	0.00	0.00	0.01	1.48	14.87	98.44
052 area 3	62.35	0.01	18.69	0.06	0.01	0.00	0.03	1.55	14.70	97.40
052 area 3	62.21	0.01	18.65	0.03	0.00	0.00	0.02	1.54	14.84	97.30
052 area 3	62.29	0.01	18.72	0.02	0.01	0.00	0.02	1.60	14.90	97.58
052 area 3	62.30	0.01	18.81	0.03	0.00	0.00	0.03	1.46	14.45	97.09
052 area 3	61.53	0.01	18.75	0.03	0.01	0.00	0.04	1.56	14.98	96.90
052 area 3	61.85	0.00	18.86	0.03	0.01	0.00	0.05	1.56	14.70	97.05
052 area 4	60.80	0.00	24.08	0.21	0.00	0.00	4.98	8.48	0.16	98.72
052 area 4	62.73	0.00	25.04	0.32	0.02	0.01	4.47	9.96	0.15	102.69
052 area 4	63.69	0.00	23.80	0.18	0.00	0.00	5.01	8.21	0.13	101.04
052 area 4	62.59	0.00	23.82	0.37	0.03	0.00	4.32	7.81	0.21	99.15
052 area 4	63.09	0.00	24.22	0.17	0.02	0.01	5.05	8.52	0.27	101.36
052 area 4	62.48	0.01	24.61	0.29	0.03	0.00	4.92	8.34	0.20	100.86
052 area 4	62.68	0.00	24.03	0.23	0.01	0.00	4.96	7.69	0.23	99.82
052 area 4	42.29	0.00	13.69	0.61	0.00	0.07	2.26	4.64	0.35	63.90
052 area 4	62.52	0.00	23.71	0.17	0.03	0.01	4.67	8.20	0.16	99.48
052 area 4	61.54	0.00	23.98	0.24	0.03	0.00	4.86	8.13	0.18	98.95
052 area 4	61.55	0.00	24.50	0.33	0.03	0.00	4.33	9.41	0.30	100.45

Location	SiO2	TiO2	Al2O3	FeO	MnO	MgO	CaO	Na2O	K2O	Total
052 area 4	62.59	0.00	24.11	0.35	0.01	0.00	4.70	8.22	0.18	100.17
052 area 4	61.30	0.01	22.91	0.89	0.01	0.16	1.52	7.36	1.58	95.75
052 area 4	63.95	0.01	23.61	0.40	0.01	0.05	3.09	8.51	0.73	100.35
052 area 4	56.16	0.00	27.53	1.06	0.01	0.30	0.49	4.64	5.24	95.42
055 area 1	61.01	0.00	24.85	0.00	0.02	0.00	5.48	8.71	0.29	100.37
055 area 1	61.83	0.00	24.07	0.00	0.00	0.00	4.62	9.04	0.22	99.78
055 area 1	60.44	0.00	24.63	0.00	0.00	0.00	5.51	8.42	0.32	99.33
055 area 1	60.63	0.00	24.66	0.00	0.02	0.00	5.52	8.55	0.34	99.72
055 area 1	60.70	0.00	24.57	0.00	0.01	0.00	5.42	8.66	0.29	99.65
055 area 1	61.76	0.00	24.80	0.01	0.01	0.00	5.16	8.86	0.22	100.81
055 area 2	64.62	0.00	23.70	0.65	0.03	0.17	0.61	8.07	2.21	100.05
055 area 2	62.02	0.00	24.52	0.23	0.05	0.00	4.95	9.14	0.22	101.13
055 area 2	61.38	0.00	24.57	0.12	0.00	0.00	5.28	8.86	0.22	100.45
055 area 2	61.35	0.00	24.29	0.19	0.03	0.00	4.90	9.02	0.21	99.99
055 area 2	61.89	0.00	24.42	0.26	0.03	0.00	4.36	9.01	0.63	100.60
055 area 2	61.87	0.00	24.95	0.05	0.00	0.00	5.64	8.27	0.26	101.04
055 area 2	33.70	3.79	19.45	22.62	0.12	6.72	0.00	0.13	9.61	96.13
055 area 2	35.50	3.55	21.05	21.31	0.13	6.27	0.01	0.13	8.95	96.89
055 area 2	34.57	3.62	19.44	22.95	0.17	6.83	0.00	0.13	9.54	97.25
055 area 2	34.98	3.64	19.83	22.75	0.14	6.69	0.00	0.14	9.57	97.73
055 area 2	34.72	3.27	19.74	23.10	0.13	6.78	0.00	0.12	9.63	97.50
055 area 2	34.35	3.46	19.32	24.31	0.15	6.52	0.00	0.15	9.21	97.46
055 area 2	62.53	0.00	24.42	0.09	0.00	0.00	4.92	8.94	0.19	101.10
055 area 3	61.41	0.00	24.57	0.13	0.02	0.00	5.60	8.67	0.21	100.62
055 area 3	57.51	0.00	24.50	0.13	0.01	0.00	5.66	8.80	0.22	96.84
055 area 3	58.09	0.00	23.82	0.11	0.01	0.00	5.02	9.11	0.21	96.37
055 area 3	56.92	0.00	24.00	0.06	0.01	0.00	5.50	8.82	0.26	95.57
055 area 3	57.42	0.00	23.89	0.05	0.00	0.00	5.40	8.86	0.21	95.83
055 area 3	57.68	0.00	23.95	0.17	0.01	0.00	5.29	8.92	0.22	96.23
055 area 3	57.41	0.00	23.85	0.11	0.00	0.00	5.37	8.90	0.24	95.88
055 area 4	61.55	0.00	24.40	0.07	0.01	0.00	5.12	8.88	0.22	100.24
055 area 4	61.95	0.00	23.94	0.12	0.02	0.00	4.71	9.25	0.16	100.15
055 area 4	61.82	0.00	24.01	0.12	0.01	0.00	4.71	8.87	0.11	99.64
055 area 4	61.49	0.00	24.19	0.17	0.02	0.00	4.89	9.09	0.11	99.95
055 area 4	60.58	0.00	24.28	0.00	0.01	0.00	5.45	8.49	0.28	99.09
055 area 4	60.50	0.00	24.47	0.00	0.00	0.00	5.40	8.64	0.18	99.20
059 area 1	60.98	0.00	18.90	0.19	0.00	0.00	0.01	1.15	15.74	96.97
059 area 1	61.03	0.00	18.77	0.18	0.01	0.00	0.01	1.13	15.82	96.95
059 area 1	60.25	0.01	18.75	0.11	0.01	0.00	0.01	0.84	16.10	96.07
059 area 1	60.98	0.00	18.65	0.10	0.01	0.00	0.00	0.99	15.72	96.47
059 area 1	60.92	0.00	18.74	0.16	0.00	0.00	0.02	1.07	15.76	96.68
059 area 1	60.99	0.00	18.73	0.25	0.02	0.00	0.01	0.96	16.06	97.02
059 area 1	61.13	0.00	18.75	0.20	0.03	0.00	0.01	1.13	15.92	97.18
059 area 1	62.58	0.01	18.96	0.24	0.02	0.00	0.03	1.30	15.32	98.45
059 area 1	65.38	0.01	20.01	0.22	0.01	0.00	0.11	8.01	2.15	95.88
059 area 1	62.27	0.01	18.91	0.13	0.00	0.00	0.02	1.21	15.77	98.32
059 area 1	62.49	0.00	18.88	0.08	0.01	0.00	0.02	1.36	15.45	98.29
059 area 1	62.79	0.01	19.10	0.03	0.00	0.00	0.04	1.56	14.68	98.20
059 area 1	64.32	0.00	19.57	0.07	0.00	0.00	0.04	2.26	12.27	98.53
059 area 1	63.19	0.01	19.18	0.07	0.00	0.00	0.04	1.24	15.31	99.04
059 area 1	63.35	0.01	19.28	0.04	0.01	0.00	0.05	1.70	14.61	99.05
059 area 2	62.14	0.00	18.91	0.03	0.00	0.00	0.04	1.37	15.24	97.74

Location	SiO2	TiO2	Al2O3	FeO	MnO	MgO	CaO	Na2O	K2O	Total
059 area 2	61.37	0.00	18.77	0.03	0.00	0.00	0.06	1.32	14.81	96.37
059 area 2	62.11	0.01	19.07	0.02	0.00	0.00	0.04	1.59	14.83	97.66
059 area 2	61.92	0.00	19.07	0.02	0.00	0.00	0.04	1.20	14.93	97.17
059 area 2	61.43	0.00	18.75	0.03	0.01	0.00	0.04	1.34	15.49	97.10
059 area 2	61.89	0.00	18.87	0.05	0.01	0.00	0.05	1.37	14.95	97.20
059 area 2	60.49	0.01	18.77	0.03	0.01	0.00	0.05	1.35	15.23	95.92
059 area 2	61.74	0.00	18.88	0.01	0.00	0.00	0.04	1.07	15.63	97.37
059 area 2	61.16	0.00	18.64	0.04	0.01	0.00	0.06	1.56	14.90	96.36
059 area 2	60.48	0.01	18.65	0.03	0.01	0.00	0.05	1.40	15.37	96.00
059 area 2	60.70	0.00	18.80	0.04	0.01	0.00	0.04	1.16	15.23	95.98
059 area 2	60.50	0.00	18.58	0.02	0.02	0.00	0.04	1.28	15.54	95.98
059 area 2	59.73	0.00	18.54	0.02	0.00	0.00	0.04	1.21	15.58	95.12
059 area 2	59.38	0.01	18.54	0.07	0.01	0.00	0.04	1.28	14.95	94.27
059 area 2	60.59	0.00	18.69	0.03	0.01	0.00	0.06	1.50	14.98	95.88
059 area 2	61.01	0.00	18.80	0.02	0.01	0.00	0.06	1.54	14.86	96.31
059 area 2	60.70	0.00	18.70	0.01	0.01	0.00	0.04	1.39	15.28	96.14
059 area 3	61.84	0.01	19.18	1.16	0.05	0.17	3.63	5.45	0.39	91.88
059 area 3	58.34	0.00	23.80	0.60	0.02	0.00	4.45	9.11	0.09	96.41
059 area 3	58.50	0.00	23.54	0.52	0.01	0.00	4.60	9.04	0.11	96.31
059 area 3	58.88	0.00	24.03	0.42	0.01	0.00	4.71	9.02	0.08	97.14
059 area 3	60.15	0.01	23.62	0.35	0.01	0.00	4.86	8.62	0.12	97.73
059 area 3	60.26	0.00	23.90	0.36	0.01	0.00	3.99	7.45	0.16	96.13
059 area 3	59.81	0.00	19.65	0.29	0.01	0.01	0.04	1.19	14.86	95.86
059 area 3	64.10	0.00	19.46	0.11	0.02	0.00	0.03	1.13	14.93	99.77
059 area 3	65.44	0.00	19.15	0.03	0.01	0.01	0.05	1.42	14.49	100.59
059 area 3	63.75	0.01	19.07	0.06	0.01	0.00	0.05	1.32	15.27	99.53
059 area 3	63.90	0.01	19.15	0.06	0.00	0.00	0.04	1.26	15.17	99.60
059 area 3	62.65	0.01	19.00	0.08	0.00	0.00	0.02	0.88	16.03	98.68
059 area 3	63.21	0.00	19.09	0.35	0.02	0.00	0.01	1.09	14.95	98.73
059 area 3	63.92	0.00	19.17	0.11	0.00	0.00	0.03	1.11	15.33	99.68
059 area 3	64.13	0.01	19.04	0.14	0.00	0.00	0.05	1.49	15.08	99.94
059 area 3	63.72	0.00	19.24	0.08	0.00	0.00	0.05	1.46	14.88	99.43
059 area 3	63.43	0.01	19.24	0.07	0.01	0.00	0.04	1.39	15.13	99.31
059 area 3	64.35	0.01	19.39	0.03	0.01	0.00	0.04	1.62	14.29	99.75
059 area 3	64.85	0.01	19.52	0.05	0.00	0.00	0.05	1.74	14.38	100.61
059 area 3	62.22	0.00	19.53	0.04	0.00	0.00	0.06	1.36	14.93	98.13
059 area 3	61.82	0.01	19.28	0.08	0.00	0.00	0.04	1.39	15.35	97.97
059 area 3	62.15	0.01	18.97	0.03	0.00	0.00	0.05	1.44	15.19	97.86
059 area 3	61.76	0.00	18.93	0.04	0.01	0.00	0.06	1.81	14.72	97.32
059 area 3	61.14	0.01	19.01	0.05	0.01	0.00	0.04	1.46	15.13	96.84
059 area 3	61.86	0.01	19.05	0.03	0.00	0.00	0.04	1.32	15.30	97.62
059 area 3	60.61	0.01	18.79	0.03	0.01	0.00	0.04	1.35	15.38	96.22
059 area 3	61.56	0.01	19.00	0.03	0.00	0.00	0.05	1.65	14.79	97.08
059 area 3	34.06	0.00	21.45	37.60	1.90	1.87	1.09	0.00	0.00	97.98
059 area 3	34.29	0.00	21.46	38.09	1.88	2.08	1.03	0.00	0.01	98.83
059 area 4	59.24	0.01	23.73	0.24	0.01	0.00	5.06	8.56	0.19	97.05
059 area 4	60.17	0.01	23.14	0.30	0.00	0.01	5.07	8.03	0.22	96.95
059 area 4	64.20	0.00	21.26	0.36	0.01	0.00	2.34	6.87	0.28	95.32
059 area 4	53.70	0.00	22.83	0.38	0.00	0.00	3.51	7.56	0.17	88.15
059 area 4	64.05	0.00	23.91	0.14	0.00	0.01	3.85	9.58	0.11	101.66
059 area 4	58.69	0.00	24.72	0.12	0.00	0.01	4.36	9.80	0.20	97.90
059 area 4	40.00	0.01	27.77	1.16	0.01	0.10	1.55	3.42	0.32	74.34

Location	SiO2	TiO2	Al2O3	FeO	MnO	MgO	CaO	Na2O	K2O	Total
059 area 4	60.16	0.00	23.34	0.09	0.00	0.00	4.72	8.61	0.14	97.05
059 area 4	59.77	0.00	23.42	0.12	0.00	0.00	4.89	8.81	0.18	97.20
059 area 4	62.52	0.00	23.14	0.22	0.01	0.02	4.35	8.91	0.14	99.30
059 area 4	60.14	0.00	23.26	0.14	0.00	0.00	4.69	8.75	0.22	97.21
059 area 4	59.66	0.00	23.49	0.03	0.00	0.00	5.01	8.54	0.26	97.01
059 area 4	60.62	0.01	23.60	0.05	0.01	0.00	5.08	8.26	0.24	97.88
059 area 4	60.18	0.00	23.87	0.07	0.02	0.00	5.15	8.62	0.19	98.09
059 area 4	59.95	0.01	23.62	0.02	0.00	0.00	5.12	8.47	0.31	97.49
059 area 4	61.31	0.00	23.69	0.05	0.00	0.01	4.84	8.66	0.30	98.86
059 area 4	62.75	0.00	18.56	0.47	0.01	0.00	0.03	1.18	15.29	98.29
059 area 4	62.54	0.00	18.62	0.29	0.00	0.00	0.04	1.02	15.83	98.34
059 area 4	62.62	0.01	18.70	0.31	0.02	0.00	0.03	1.19	15.72	98.60
059 area 4	62.47	0.01	18.75	0.26	0.01	0.00	0.04	1.25	15.24	98.03
059 area 4	62.81	0.01	18.73	0.19	0.01	0.00	0.04	1.17	15.57	98.52
059 area 4	62.93	0.00	18.84	0.13	0.00	0.00	0.05	1.20	15.34	98.50
059 area 4	64.19	0.00	18.47	0.15	0.01	0.00	0.03	1.17	15.41	99.42
059 area 4	63.44	0.00	18.64	0.22	0.00	0.01	0.02	0.79	15.86	98.97
059 area 4	63.85	0.00	17.90	0.34	0.02	0.00	0.05	1.21	15.27	98.64
059 area 4	62.55	0.00	18.60	0.17	0.00	0.00	0.02	1.38	15.16	97.88
059 area 4	62.04	0.00	18.54	0.22	0.02	0.00	0.02	1.15	15.74	97.73
059 area 4	63.11	0.01	18.42	0.21	0.02	0.00	0.01	0.85	15.54	98.18
059 area 4	61.51	0.00	18.76	0.28	0.01	0.00	0.02	1.19	15.71	97.49
059 area 6	64.62	0.03	22.11	0.67	0.01	0.09	2.12	8.81	0.46	98.93
059 area 6	62.25	0.00	24.19	0.17	0.01	0.00	4.69	8.58	0.18	100.06
059 area 6	58.32	0.01	21.06	0.59	0.01	0.00	2.59	7.95	0.23	90.77
059 area 6	63.55	0.00	24.62	0.39	0.02	0.00	1.40	11.41	0.23	101.62
059 area 6	63.99	0.00	22.87	0.50	0.02	0.00	3.52	8.84	0.17	99.91
059 area 6	60.90	0.00	24.02	0.23	0.01	0.00	4.93	8.63	0.24	98.96
059 area 6	60.63	0.00	24.23	0.29	0.00	0.01	5.17	8.37	0.23	98.94
059 area 6	60.81	0.00	23.99	0.18	0.01	0.00	4.93	8.65	0.26	98.82
059 area 6	60.99	0.00	24.04	0.19	0.00	0.00	4.97	8.58	0.24	99.03
059 area 6	61.18	0.01	24.01	0.25	0.01	0.00	4.88	8.67	0.14	99.14
059 area 6	61.02	0.01	24.15	0.20	0.00	0.00	5.01	8.50	0.21	99.08
059 area 6	62.17	0.01	23.58	0.15	0.01	0.00	4.36	8.62	0.26	99.16

APPENDIX C: Trace element data from monazite with associated 2se errors

Spot location	La_ppm	2se	Ce_ppm	2se	Pr_ppm	2se	Nd_ppm	2se
046_Gt1_1	6.21E+04	6.40E+03	1.43E+05	1.50E+04	1.56E+04	1.80E+03	6.20E+04	1.50E+04
046_Gt1_2	5.82E+04	9.00E+03	1.35E+05	1.40E+04	1.50E+04	2.10E+03	5.00E+04	1.60E+04
046_Gt5_1	6.30E+04	1.10E+04	1.33E+05	1.10E+04	1.48E+04	1.40E+03	5.50E+04	1.50E+04
046_Gt5_2	6.61E+04	8.10E+03	1.20E+05	1.30E+04	1.73E+04	1.60E+03	3.76E+04	9.30E+03
046_Gt5_3	5.75E+04	8.40E+03	1.34E+05	1.40E+04	1.61E+04	1.30E+03	5.30E+04	1.30E+04
046_Gt5_4	5.52E+04	9.20E+03	1.30E+05	8.60E+03	1.66E+04	1.50E+03	6.40E+04	1.90E+04
046_Gt5_5	6.40E+04	1.00E+04	1.27E+05	1.00E+04	1.54E+04	1.70E+03	6.30E+04	1.90E+04
046_Gt6_2	5.31E+04	7.90E+03	1.30E+05	1.00E+04	1.59E+04	1.30E+03	7.30E+04	2.30E+04
046_Gt6_3	5.70E+04	1.00E+04	1.42E+05	1.10E+04	1.47E+04	1.50E+03	4.80E+04	1.40E+04
046_Gt8_1	5.93E+04	8.90E+03	1.40E+05	9.80E+03	1.59E+04	1.50E+03	7.10E+04	1.90E+04
046_Gt9_1	5.80E+04	1.10E+04	1.38E+05	1.10E+04	1.79E+04	1.80E+03	5.60E+04	1.50E+04
046_Gt14_1	6.45E+04	5.60E+03	1.46E+05	1.30E+04	1.83E+04	1.60E+03	5.90E+04	1.10E+04
046_Gt14_3	6.40E+04	1.00E+04	1.41E+05	1.60E+04	1.68E+04	2.20E+03	5.40E+04	1.90E+04
046_Gt14_4	5.52E+04	7.20E+03	1.37E+05	1.30E+04	1.72E+04	1.70E+03	5.60E+04	1.50E+04
046_Gt16_1	6.87E+04	8.90E+03	1.36E+05	1.10E+04	1.89E+04	2.00E+03	5.60E+04	1.70E+04
046_Gt16_2	5.65E+04	6.90E+03	1.39E+05	7.50E+03	1.70E+04	1.30E+03	5.70E+04	1.70E+04
046_Gt16_3	5.85E+04	8.10E+03	1.42E+05	1.40E+04	1.92E+04	1.50E+03	6.10E+04	1.40E+04
046_Gt16_4	5.52E+04	6.50E+03	1.45E+05	1.20E+04	1.65E+04	1.50E+03	5.60E+04	1.70E+04
046_Gt16_5	6.06E+04	7.60E+03	1.38E+05	1.50E+04	1.66E+04	1.80E+03	6.00E+04	1.00E+04
052_Gt1_1	4.02E+04	7.80E+03	8.00E+04	8.20E+03	8.70E+03	1.10E+03	2.95E+04	9.60E+03
052_Gt1_2	3.00E+04	8.10E+03	7.11E+04	8.60E+03	8.80E+03	1.00E+03	1.91E+04	9.70E+03
052_Gt1_3	3.78E+04	7.80E+03	7.85E+04	9.70E+03	9.60E+03	1.10E+03	4.20E+04	1.20E+04
052_Gt3_2	5.03E+04	7.50E+03	1.16E+05	1.60E+04	1.45E+04	1.30E+03	5.40E+04	1.40E+04
052_Gt3_3	5.48E+04	9.30E+03	1.07E+05	8.90E+03	1.45E+04	1.50E+03	5.40E+04	1.90E+04
052_Gt3_4	5.13E+04	9.20E+03	1.24E+05	9.60E+03	1.51E+04	1.40E+03	4.50E+04	1.20E+04
052_Gt3_5	4.35E+04	7.20E+03	1.10E+05	1.10E+04	1.37E+04	1.60E+03	4.20E+04	1.10E+04
052_Gt3_7	4.63E+04	9.10E+03	1.13E+05	1.10E+04	1.35E+04	1.80E+03	3.70E+04	1.20E+04
052_Gt3_8	2.36E+04	5.30E+03	6.60E+04	1.10E+04	7.40E+03	1.30E+03	2.47E+04	8.30E+03
052_Gt3_10	6.13E+04	6.20E+03	1.11E+05	1.10E+04	1.59E+04	1.50E+03	3.90E+04	1.20E+04
052_Gt5_1	5.34E+04	9.00E+03	1.22E+05	1.30E+04	1.60E+04	2.50E+03	6.80E+04	2.00E+04
052_Gt5_2	4.80E+04	6.20E+03	1.16E+05	1.10E+04	1.66E+04	1.60E+03	5.60E+04	1.30E+04
052_Gt5_3	4.52E+04	7.00E+03	1.30E+05	1.10E+04	1.46E+04	1.60E+03	6.90E+04	1.30E+04
052_Gt5_4	4.92E+04	6.10E+03	1.23E+05	1.10E+04	1.50E+04	1.80E+03	6.80E+04	1.50E+04
052_Gt6_1	5.44E+04	8.10E+03	1.25E+05	1.10E+04	1.42E+04	1.30E+03	5.80E+04	1.60E+04
052_Gt6_2	6.03E+04	5.50E+03	1.28E+05	1.00E+04	1.45E+04	1.30E+03	5.50E+04	1.60E+04
052_Gt6_3	5.32E+04	8.30E+03	1.16E+05	8.70E+03	1.47E+04	1.30E+03	6.40E+04	1.40E+04
052_Gt8_1	5.57E+04	5.30E+03	1.29E+05	1.60E+04	1.44E+04	1.70E+03	6.40E+04	1.50E+04
052_Gt8_2	5.08E+04	8.50E+03	1.22E+05	1.10E+04	1.41E+04	1.40E+03	5.70E+04	1.40E+04
052_Gt12_2	5.38E+04	5.30E+03	1.08E+05	1.20E+04	1.31E+04	1.20E+03	4.65E+04	9.10E+03
052_Gt12_3	4.37E+04	8.00E+03	1.01E+05	9.30E+03	13790	990	5.00E+04	1.50E+04
052_Gt14_1	5.59E+04	9.30E+03	1.16E+05	9.10E+03	14220	930	4.70E+04	1.10E+04
052_Gt17_1	5.76E+04	7.20E+03	1.25E+05	1.50E+04	1.55E+04	1.20E+03	8.10E+04	1.60E+04
052_Gt17_2	5.08E+04	6.90E+03	1.25E+05	1.20E+04	1.47E+04	1.90E+03	5.60E+04	1.50E+04
052_Gt17_3	6.80E+04	1.00E+04	1.41E+05	1.40E+04	1.83E+04	2.00E+03	6.90E+04	2.10E+04
052_Gt18_1	6.40E+04	1.00E+04	1.42E+05	1.10E+04	15930	970	7.40E+04	1.70E+04
052_Gt18_2	5.93E+04	8.60E+03	1.36E+05	7.80E+03	1.78E+04	1.90E+03	7.30E+04	1.90E+04
052_Gt18_3	5.67E+04	7.20E+03	1.28E+05	1.40E+04	1.68E+04	1.80E+03	6.50E+04	1.10E+04
052_Gt18_4	5.30E+04	7.10E+03	1.13E+05	1.30E+04	1.65E+04	2.00E+03	6.70E+04	1.90E+04
048_Gt1_1	4.23E+04	7.50E+03	1.01E+05	5.80E+03	1.05E+04	1.60E+03	4.43E+04	5.50E+03
048_Gt1_2	5.50E+04	5.50E+04	1.20E+05	1.20E+05	1.30E+04	1.30E+04	5.60E+04	5.60E+04
048_Gt1_3	4.71E+04	9.80E+03	1.08E+05	2.30E+04	1.20E+04	3.10E+03	4.64E+04	5.90E+03

Spot location	La_ppm	2se	Ce_ppm	2se	Pr_ppm	2se	Nd_ppm	2se
048_Gt1_4	5.06E+04	4.50E+03	1.24E+05	1.80E+04	7740	650	4.90E+04	1.10E+04
048_Gt1_5	4.90E+04	2.90E+03	1.25E+05	6.50E+03	1.38E+04	2.10E+03	5.12E+04	6.30E+03
048_Gt1_6	4.80E+04	4.80E+04	1.20E+05	1.20E+05	1.30E+04	1.30E+04	5.30E+04	5.30E+04
048_Gt1_7	5.26E+04	5.00E+03	1.15E+05	6.90E+03	8650	730	4.68E+04	8.90E+03
048_Gt1_8	4.90E+04	1.20E+04	1.18E+05	4.10E+03	1.12E+04	4.60E+03	4.59E+04	2.20E+03
048_Gt1_9	5.10E+04	5.10E+04	1.10E+05	1.10E+05	8.80E+03	8.80E+03	4.60E+04	4.60E+04
048_Gt1_10	6.57E+04	6.80E+03	1.49E+05	1.30E+04	1.92E+04	1.30E+03	6.07E+04	2.70E+03
048_Gt1_11	6.28E+04	4.00E+03	1.43E+05	1.70E+04	18690	660	5.94E+04	8.80E+03
048_Gt1_12	6.34E+04	3.00E+03	1.39E+05	7.70E+03	1.84E+04	2.90E+03	6.54E+04	2.00E+03
048_Gt6_1	6.33E+04	1.80E+03	1.50E+05	3.40E+03	2.18E+04	6.00E+03	6.49E+04	6.60E+03
048_Gt6_2	6.40E+04	1.00E+04	1.48E+05	1.80E+04	1.45E+04	6.50E+03	6.00E+04	1.20E+04
048_Gt6_3	6.41E+04	8.50E+03	1.51E+05	1.30E+04	1.78E+04	1.20E+03	5.78E+04	8.50E+03
048_Gt6_4	6.08E+04	7.40E+03	1.52E+05	1.30E+04	1.53E+04	7.40E+03	6.28E+04	8.10E+03
048_Gt6_5	6.06E+04	5.00E+03	1.37E+05	1.10E+04	10630	610	5.77E+04	9.60E+03
048_Gt6_6	5.50E+04	5.50E+04	1.30E+05	1.30E+05	9.40E+03	9.40E+03	5.50E+04	5.50E+04
048_Gt7_1	6.70E+04	6.70E+04	1.50E+05	1.50E+05	1.80E+04	1.80E+04	6.40E+04	6.40E+04
048_Gt7_2	5.80E+04	5.80E+04	1.40E+05	1.40E+05	1.00E+04	1.00E+04	5.60E+04	5.60E+04
048_Gt7_3	6.38E+04	1.50E+03	1.60E+05	2.50E+04	11090	930	6.02E+04	2.80E+03
048_Gt7_4	6.44E+04	2.30E+03	1.49E+05	1.20E+04	10527	75	5.82E+04	5.10E+03
048_Gt7_5	6.50E+04	6.50E+04	1.50E+05	1.50E+05	1.80E+04	1.80E+04	5.80E+04	5.80E+04
048_Gt7_6	57840	340	1.36E+05	7.30E+03	1.77E+04	2.20E+03	6.20E+04	1.00E+04
048_Gt9_1	6.32E+04	4.10E+03	1.40E+05	3.40E+03	10760	950	5.38E+04	3.60E+03
048_Gt9_2	5.94E+04	6.20E+03	1.40E+05	1.40E+04	1.80E+04	1.30E+04	5.90E+04	8.20E+03
048_Gt9_3	6.79E+04	6.40E+03	1.51E+05	8.50E+03	1.90E+04	1.60E+03	5.83E+04	4.10E+03
048_Gt9_4	6.61E+04	1.40E+03	1.39E+05	2.40E+04	1.82E+04	3.60E+03	5.01E+04	7.90E+03
048_Gt9_5	61540	960	1.54E+05	1.30E+04	11980	360	5.48E+04	7.80E+03
048_Gt9_6	6.04E+04	2.30E+03	1.42E+05	1.10E+04	19330	440	5.58E+04	5.80E+03
048_Gt9_7	6.38E+04	1.80E+03	1.51E+05	1.50E+04	1.92E+04	2.00E+03	5.40E+04	1.20E+04
048_Gt9_8	6.57E+04	9.50E+03	1.48E+05	2.40E+04	2.03E+04	1.30E+03	5.85E+04	5.50E+03
048_Gt9_9	60510	240	1.52E+05	6.20E+03	21980	370	5.26E+04	9.80E+03
048_Gt9_10	5.96E+04	6.40E+03	1.73E+05	4.00E+04	2.32E+04	1.20E+03	5.27E+04	3.10E+03
048_Gt9_11	6.34E+04	2.20E+03	1.49E+05	2.90E+04	2.55E+04	2.00E+03	5.26E+04	2.80E+03
048_Gt9_12	5.94E+04	2.40E+03	1.47E+05	2.80E+03	2.56E+04	1.60E+03	5.51E+04	6.60E+03
048_Gt9_13	6.43E+04	6.60E+03	1.51E+05	1.70E+04	2.49E+04	4.70E+03	5.73E+04	7.10E+03
048_Gt9_14	6.16E+04	4.70E+03	1.41E+05	2.40E+03	2.89E+04	3.80E+03	5.26E+04	5.10E+03
048_Gt9_15	5.99E+04	3.50E+03	1.46E+05	1.60E+04	1.80E+04	1.30E+03	5.05E+04	4.70E+03
048_Gt9_16	6.09E+04	8.40E+03	1.35E+05	2.50E+04	2.74E+04	1.30E+03	5.43E+04	6.40E+03
048_Gt9_17	6.20E+04	4.30E+03	1.45E+05	2.00E+04	1.76E+04	2.00E+03	5.80E+04	6.20E+03
048_Gt9_18	6.32E+04	2.70E+03	1.49E+05	1.60E+04	1.48E+04	1.50E+03	5.85E+04	8.60E+03
048_Gt9_19	6.07E+04	8.20E+03	1.38E+05	9.10E+03	2.32E+04	3.20E+03	5.36E+04	2.60E+03
048_Gt9_20	6.20E+04	6.20E+04	1.40E+05	1.40E+05	2.10E+04	2.10E+04	6.20E+04	6.20E+04
048_Gt9_21	6.20E+04	6.20E+04	1.60E+05	1.60E+05	2.00E+04	2.00E+04	5.70E+04	5.70E+04
048_Gt9_22	6.13E+04	9.10E+03	1.58E+05	2.60E+04	1.83E+04	1.60E+03	5.97E+04	9.10E+03
048_Gt9_23	6.42E+04	6.00E+03	1.49E+05	3.30E+03	1.88E+04	1.50E+03	5.94E+04	9.50E+03
048_Gt9_24	6.20E+04	1.20E+04	1.42E+05	7.50E+03	11160	840	5.85E+04	9.90E+03
048_Gt9_25	6.82E+04	8.20E+03	1.49E+05	1.40E+04	1.59E+04	4.70E+03	5.75E+04	5.40E+03
048_Gt9_26	6.19E+04	5.30E+03	1.50E+05	7.00E+03	1.86E+04	2.40E+03	5.70E+04	7.50E+03
048_Gt9_27	7.01E+04	6.70E+03	1.59E+05	7.80E+03	1.99E+04	2.70E+03	5.83E+04	4.10E+03
048_Gt9_28	6.60E+04	6.60E+04	1.50E+05	1.50E+05	2.20E+04	2.20E+04	5.70E+04	5.70E+04
048_Gt9_29	6.27E+04	8.10E+03	1.64E+05	1.10E+04	2.27E+04	2.50E+03	5.70E+04	1.30E+04
048_Gt9_30	6.40E+04	6.00E+03	1.92E+05	5.00E+04	13940	550	5.37E+04	1.90E+03
048_Gt9_31	6.02E+04	9.00E+03	1.50E+05	1.80E+04	2.30E+04	3.50E+03	5.31E+04	6.80E+03

Spot location	La_ppm	2se	Ce_ppm	2se	Pr_ppm	2se	Nd_ppm	2se
048_Gt9_32	5.99E+04	1.70E+03	1.32E+05	1.70E+03	2.57E+04	3.60E+03	5.93E+04	6.90E+03
048_Gt9_33	6.80E+04	6.80E+04	1.50E+05	1.50E+05	2.80E+04	2.80E+04	6.50E+04	6.50E+04
048_Gt9_34	6.18E+04	3.80E+03	1.41E+05	2.60E+04	3.18E+04	1.70E+03	5.88E+04	9.40E+03
048_Gt9_35	6.90E+04	1.50E+04	1.49E+05	3.10E+04	33890	280	6.46E+04	4.60E+03
048_Gt9_36	6.41E+04	9.10E+03	1.53E+05	9.80E+03	3.52E+04	3.00E+03	6.82E+04	5.50E+03
048_Gt9_37	6.30E+04	1.10E+04	1.48E+05	1.60E+04	3.06E+04	2.80E+03	5.92E+04	3.80E+03
048_Gt9_38	59560	690	1.45E+05	1.40E+04	3.04E+04	3.30E+03	6.04E+04	6.40E+03
048_Gt9_39	6.09E+04	3.60E+03	1.56E+05	1.10E+04	1.52E+04	1.10E+03	5.99E+04	3.80E+03
048_Gt9_40	5.95E+04	9.20E+03	1.58E+05	2.40E+04	2.39E+04	2.90E+03	7.02E+04	3.60E+03
048_Gt9_41	5.52E+04	9.20E+03	1.38E+05	1.80E+04	1.81E+04	3.00E+03	6.31E+04	8.60E+03
048_Gt9_42	5.70E+04	5.70E+04	2.10E+05	2.10E+05	1.20E+04	1.20E+04	6.40E+04	6.40E+04
048_Gt9_43	5.45E+04	4.20E+03	1.35E+05	1.00E+04	10850	190	5.79E+04	8.00E+03
051_Gt1_1	7.00E+04	1.10E+04	1.46E+05	1.10E+04	1.94E+04	1.80E+03	5.70E+04	1.20E+04
051_Gt1_2	7.10E+04	1.40E+04	1.59E+05	1.50E+04	1.87E+04	2.10E+03	5.80E+04	1.40E+04
051_Gt1_3	6.30E+04	9.60E+03	1.35E+05	9.50E+03	1.81E+04	1.80E+03	7.00E+04	1.30E+04
051_Gt5_1	7.50E+04	1.00E+04	1.31E+05	1.10E+04	1.79E+04	1.40E+03	5.16E+04	9.80E+03
051_Gt5_2	6.90E+04	1.10E+04	1.43E+05	1.10E+04	1.73E+04	1.70E+03	5.40E+04	1.30E+04
051_Gt5_3	6.76E+04	5.80E+03	1.37E+05	1.20E+04	1.71E+04	1.70E+03	6.00E+04	1.50E+04
051_Gt6_1	6.08E+04	9.70E+03	1.15E+05	1.20E+04	1.57E+04	1.80E+03	5.80E+04	1.80E+04
051_Gt6_2	7.12E+04	8.60E+03	1.49E+05	9.70E+03	1.92E+04	1.30E+03	5.70E+04	1.30E+04
051_Gt6_3	6.50E+04	1.10E+04	1.39E+05	1.60E+04	1.65E+04	1.30E+03	6.60E+04	1.70E+04
051_Gt6_5	6.39E+04	6.70E+03	1.51E+05	1.20E+04	1.64E+04	1.70E+03	6.30E+04	1.60E+04
051_Gt10_1	6.00E+04	1.10E+04	1.29E+05	1.20E+04	1.68E+04	2.00E+03	5.60E+04	1.60E+04
051_Gt10_2	6.45E+04	9.00E+03	1.51E+05	1.30E+04	1.88E+04	1.60E+03	7.20E+04	1.80E+04
051_Gt10_3	6.44E+04	9.00E+03	1.43E+05	1.20E+04	1.78E+04	1.50E+03	6.60E+04	1.50E+04
051_Gt10_4	6.14E+04	8.50E+03	1.49E+05	1.40E+04	1.75E+04	1.70E+03	6.30E+04	1.50E+04
051_Gt11_1	6.80E+04	1.30E+04	1.39E+05	1.40E+04	1.80E+04	1.60E+03	5.60E+04	1.20E+04
051_Gt11_2	7.46E+04	9.30E+03	1.52E+05	1.60E+04	2.06E+04	1.70E+03	5.70E+04	1.30E+04
051_Gt11_3	7.20E+04	1.20E+04	1.62E+05	1.40E+04	2.16E+04	2.70E+03	8.10E+04	1.70E+04
051_Gt11_4	6.77E+04	9.70E+03	1.43E+05	1.60E+04	1.64E+04	2.30E+03	3.90E+04	1.10E+04
051_Gt11_5	7.80E+04	1.40E+04	1.69E+05	1.90E+04	2.19E+04	1.80E+03	7.80E+04	2.10E+04
051_Gt11_6	7.20E+04	1.00E+04	1.56E+05	1.60E+04	1.76E+04	1.90E+03	6.50E+04	1.30E+04
051_Gt11_7	7.20E+04	1.00E+04	1.47E+05	1.20E+04	1.79E+04	1.90E+03	7.30E+04	1.40E+04
051_Gt11_8	8.60E+04	2.00E+04	2.02E+05	4.10E+04	2.19E+04	4.40E+03	7.40E+04	3.50E+04
051_Gt11_9	7.30E+04	1.20E+04	1.45E+05	1.80E+04	1.85E+04	2.10E+03	7.00E+04	1.60E+04
051_Gt11_10	7.80E+04	1.00E+04	1.60E+05	2.00E+04	1.83E+04	1.40E+03	6.30E+04	1.90E+04
051_Gt11_11	7.09E+04	9.30E+03	1.69E+05	1.40E+04	1.99E+04	2.20E+03	5.30E+04	1.30E+04
051_Gt11_12	7.30E+04	1.10E+04	1.62E+05	1.20E+04	1.88E+04	1.30E+03	6.20E+04	1.70E+04
051_Gt11_13	6.25E+04	9.60E+03	1.44E+05	1.50E+04	1.78E+04	1.80E+03	7.80E+04	1.80E+04
051_Gt11_14	6.80E+04	1.10E+04	1.70E+05	1.40E+04	1.79E+04	2.30E+03	7.70E+04	2.00E+04
051_Gt11_15	7.80E+04	1.10E+04	1.44E+05	1.40E+04	1.89E+04	2.00E+03	7.00E+04	1.10E+04
051_Gt11_16	6.08E+04	8.00E+03	1.43E+05	1.40E+04	1.95E+04	2.10E+03	7.10E+04	1.50E+04
051_Gt11_17	7.30E+04	1.10E+04	1.47E+05	1.40E+04	1.85E+04	2.00E+03	6.60E+04	1.10E+04
055_Gt1_1	7.00E+04	1.10E+04	1.53E+05	1.20E+04	1.90E+04	2.00E+03	5.40E+04	1.50E+04
055_Gt1_2	6.58E+04	9.10E+03	1.60E+05	1.20E+04	1.89E+04	2.20E+03	8.30E+04	1.50E+04
055_Gt1_4	6.90E+04	1.10E+04	1.53E+05	1.60E+04	1.93E+04	2.00E+03	6.90E+04	1.10E+04
055_Gt1_5	7.00E+04	1.00E+04	1.45E+05	1.40E+04	1.88E+04	2.10E+03	6.50E+04	1.40E+04
055_Gt1_6	8.90E+04	2.00E+04	1.76E+05	2.00E+04	2.40E+04	3.30E+03	8.50E+04	4.90E+04
055_Gt1_7	8.10E+04	1.10E+04	1.58E+05	1.30E+04	2.02E+04	1.90E+03	9.40E+04	1.70E+04
055_Gt1_8	7.60E+04	1.10E+04	1.57E+05	1.00E+04	1.95E+04	1.50E+03	7.40E+04	2.00E+04
055_Gt1_9	7.45E+04	9.00E+03	1.68E+05	1.60E+04	1.93E+04	2.20E+03	6.30E+04	1.90E+04
055_Gt1_10	8.59E+04	8.70E+03	1.70E+05	2.10E+04	2.13E+04	2.00E+03	8.40E+04	2.20E+04

Spot location	La_ppm	2se	Ce_ppm	2se	Pr_ppm	2se	Nd_ppm	2se
055_Gt1_11	7.50E+04	1.40E+04	1.59E+05	1.50E+04	1.99E+04	2.20E+03	6.40E+04	1.30E+04
055_Gt1_12	7.60E+04	1.00E+04	1.51E+05	1.40E+04	2.08E+04	2.30E+03	8.10E+04	2.60E+04
055_Gt1_13	7.60E+04	1.00E+04	1.62E+05	1.20E+04	2.29E+04	1.90E+03	6.90E+04	1.30E+04
055_Gt1_14	5.00E+04	1.10E+04	1.31E+05	1.70E+04	1.59E+04	1.70E+03	6.80E+04	2.30E+04
055_Gt18_1	8.10E+04	1.20E+04	1.70E+05	1.40E+04	2.01E+04	2.90E+03	6.30E+04	2.10E+04
055_Gt18_2	7.20E+04	1.20E+04	1.42E+05	1.50E+04	1.98E+04	1.90E+03	4.80E+04	1.70E+04
055_Gt18_3	6.05E+04	6.10E+03	1.31E+05	1.30E+04	1.83E+04	2.70E+03	7.30E+04	1.70E+04
055_Gt18_4	7.10E+04	1.20E+04	1.60E+05	1.50E+04	1.95E+04	2.40E+03	6.80E+04	1.50E+04
055_Gt8_1	7.60E+04	1.30E+04	1.57E+05	1.40E+04	1.93E+04	2.20E+03	6.20E+04	1.50E+04
055_Gt8_2	1.64E+04	9.40E+03	3.82E+04	9.80E+03	4.10E+03	1.60E+03	6.90E+03	8.80E+03
055_Gt8_3	8.00E+04	9.80E+03	1.68E+05	1.50E+04	2.10E+04	1.60E+03	5.90E+04	1.20E+04
055_Gt8_4	8.40E+04	1.10E+04	2.04E+05	1.70E+04	2.28E+04	2.70E+03	7.50E+04	2.80E+04
055_Gt9_1	6.60E+04	2.30E+04	1.12E+05	3.40E+04	1.30E+04	2.50E+03	7.40E+04	1.50E+04
055_Gt9_2	7.30E+04	1.40E+04	1.47E+05	9.00E+03	1.88E+04	1.10E+03	6.00E+04	1.50E+04
055_Gt9_3	7.70E+04	1.10E+04	1.63E+05	1.90E+04	2.13E+04	2.60E+03	6.40E+04	2.10E+04
055_Gt9_4	7.40E+04	1.30E+04	1.43E+05	1.40E+04	1.76E+04	2.80E+03	4.50E+04	1.90E+04
055_Gt9_5	7.52E+04	8.10E+03	1.67E+05	1.70E+04	2.03E+04	1.60E+03	5.20E+04	1.50E+04
055_Gt9_6	8.07E+04	9.00E+03	1.59E+05	1.60E+04	1.80E+04	1.70E+03	5.60E+04	1.90E+04
055_Gt9_7	6.95E+04	9.20E+03	1.58E+05	1.70E+04	1.94E+04	1.80E+03	6.20E+04	1.20E+04
055_Gt9_8	6.69E+04	9.20E+03	1.53E+05	1.60E+04	2.11E+04	2.50E+03	7.80E+04	1.80E+04
055_Gt9_9	8.80E+04	1.50E+04	1.75E+05	2.00E+04	2.20E+04	2.70E+03	7.90E+04	3.10E+04
055_Gt9_10	7.46E+04	9.00E+03	1.66E+05	1.60E+04	2.03E+04	1.40E+03	7.20E+04	1.20E+04
059_Gt6_1	6.81E+04	7.90E+03	1.54E+05	1.50E+04	1.62E+04	1.60E+03	4.90E+04	1.80E+04
059_Gt9-1	5.36E+04	9.10E+03	1.30E+05	1.20E+04	1.60E+04	1.20E+03	5.00E+04	1.20E+04
059_Gt9-2	4.42E+04	5.00E+03	8.66E+04	9.50E+03	10080	980	3.82E+04	9.90E+03
059_Gt19_1	5.21E+04	6.00E+03	1.00E+05	9.40E+03	1.17E+04	1.30E+03	4.08E+04	8.70E+03
059_Gt19_2	5.13E+04	5.70E+03	1.11E+05	9.80E+03	1.25E+04	1.30E+03	5.20E+04	1.00E+04

APPENDIX C: Trace element data with associated 2se errors

Spot location	Sm_ppm	2se	Eu_ppm	2se	Gd_ppm	2se	Tb_ppm	2se	Dy_ppm
046_Gt1_1	1.10E+04	3.90E+03	578	54	8620	620	1049	71	5190
046_Gt1_2	1.18E+04	3.80E+03	580	88	9490	750	1041	63	5340
046_Gt5_1	1.10E+04	3.40E+03	747	66	6860	430	358	36	671
046_Gt5_2	9.98E+03	3.20E+03	671	67	5970	400	332	29	770
046_Gt5_3	1.10E+04	3.70E+03	679	95	6120	310	419	53	1200
046_Gt5_4	9.10E+03	3.40E+03	604	75	7550	780	780	110	3380
046_Gt5_5	9.50E+03	3.60E+03	515	71	5740	440	495	66	2000
046_Gt6_2	9.60E+03	4.30E+03	696	76	6560	530	516	62	1500
046_Gt6_3	9.40E+03	3.80E+03	636	64	6470	620	333	33	520
046_Gt8_1	7.10E+03	3.30E+03	556	82	7810	490	719	53	3240
046_Gt9_1	8.20E+03	3.60E+03	554	75	6390	520	522	44	1550
046_Gt14_1	1.11E+04	4.00E+03	713	82	5820	410	317	33	592
046_Gt14_3	1.50E+04	4.60E+03	630	120	5670	470	305	24	601
046_Gt14_4	1.01E+04	3.80E+03	440	45	5980	470	610	40	3040
046_Gt16_1	1.10E+04	4.00E+03	710	130	5960	420	388	32	808
046_Gt16_2	8.80E+03	3.90E+03	499	68	6920	440	811	55	4210
046_Gt16_3	1.09E+04	4.00E+03	610	120	5100	250	270	21	450
046_Gt16_4	1.11E+04	3.70E+03	680	100	6580	550	452	33	989
046_Gt16_5	4.80E+03	2.30E+03	726	64	6930	470	395	49	707
052_Gt1_1	4.50E+03	2.70E+03	148	39	4960	350	648	62	3120
052_Gt1_2	4.80E+03	2.20E+03	113	37	5240	360	645	32	3560
052_Gt1_3	4.70E+03	2.60E+03	129	35	4870	350	593	49	3230
052_Gt3_2	5.90E+03	3.50E+03	116	41	8150	600	908	78	4270
052_Gt3_3	7.70E+03	2.90E+03	185	37	8830	860	919	81	5300
052_Gt3_4	8.30E+03	3.20E+03	272	60	6020	550	740	83	4110
052_Gt3_5	9.90E+03	4.50E+03	189	34	7370	660	876	89	5020
052_Gt3_7	1.12E+04	3.70E+03	314	41	5970	440	693	42	3840
052_Gt3_8	7.00E+03	3.30E+03	52	15	3220	430	421	64	2340
052_Gt3_10	1.17E+04	4.50E+03	88	37	6370	520	727	54	3310
052_Gt5_1	1.86E+04	5.50E+03	671	79	4430	450	232	38	660
052_Gt5_2	1.06E+04	4.20E+03	338	51	5850	420	662	57	3730
052_Gt5_3	1.76E+04	4.00E+03	332	47	5960	460	562	45	3500
052_Gt5_4	1.41E+04	4.80E+03	369	55	6420	570	628	52	3510
052_Gt6_1	1.07E+04	3.60E+03	229	62	6720	490	672	48	3880
052_Gt6_2	1.83E+04	4.90E+03	131	30	6620	520	862	59	4880
052_Gt6_3	9.60E+03	4.10E+03	280	58	6730	340	723	56	3810
052_Gt8_1	1.13E+04	3.80E+03	440	79	5980	630	515	39	2222
052_Gt8_2	1.16E+04	4.40E+03	623	75	6040	540	628	47	2810
052_Gt12_2	8.90E+03	3.80E+03	460	59	6030	480	738	48	3680
052_Gt12_3	9.00E+03	3.00E+03	165	50	6230	550	762	68	4330
052_Gt14_1	1.29E+04	3.20E+03	655	97	6000	530	471	35	2030
052_Gt17_1	8.40E+03	3.20E+03	762	96	5090	270	265	26	820
052_Gt17_2	1.57E+04	5.30E+03	229	45	6360	470	698	74	3840
052_Gt17_3	1.51E+04	6.30E+03	472	67	7780	680	671	89	2440
052_Gt18_1	1.36E+04	5.00E+03	1005	88	6750	560	485	57	1270
052_Gt18_2	1.79E+04	4.70E+03	588	96	6640	710	410	31	1490
052_Gt18_3	1.32E+04	4.70E+03	98	36	7060	540	773	47	4250
052_Gt18_4	1.02E+04	3.40E+03	128	28	7550	520	803	63	4620
048_Gt1_1	7.10E+03	1.10E+03	502	73	6760	940	649	82	2740
048_Gt1_2	8.40E+03	8.40E+03	530	530	4.90E+03	4.90E+03	460	460	580
048_Gt1_3	7.80E+03	1.20E+03	507	56	5840	170	580	92	1300

Spot location	Sm_ppm	2se	Eu_ppm	2se	Gd_ppm	2se	Tb_ppm	2se	Dy_ppm
048_Gt1_4	7800	440	488.6	9.1	4000	720	420.9	6.4	530
048_Gt1_5	7350	270	494	63	3930	300	420	46	525
048_Gt1_6	8.40E+03	8.40E+03	550	550	5.40E+03	5.40E+03	630	630	1.50E+03
048_Gt1_7	7.70E+03	1.70E+03	490.9	8.6	4850	110	523	25	880
048_Gt1_8	7.60E+03	1.20E+03	539	68	6.60E+03	1.90E+03	666	6	1820
048_Gt1_9	8.50E+03	8.50E+03	530	530	4.60E+03	4.60E+03	450	450	570
048_Gt1_10	11160	220	647	33	6340	700	662	16	1010
048_Gt1_11	1.05E+04	1.10E+03	693	24	6.10E+03	1.00E+03	600	90	809
048_Gt1_12	10400	550	715	15	6260	600	726	66	863
048_Gt6_1	10640	610	707	10	5770	290	654	11	708
048_Gt6_2	10710	970	750	150	6.80E+03	1.20E+03	698	17	1060
048_Gt6_3	10110	520	654	72	6310	290	653	85	920
048_Gt6_4	10420	650	704	52	8.10E+03	1.40E+03	918	94	1630
048_Gt6_5	10290	830	686	74	8770	840	1019	81	2140
048_Gt6_6	9.80E+03	9.80E+03	610	610	8.70E+03	8.70E+03	970	970	4.90E+03
048_Gt7_1	1.10E+04	1.10E+04	670	670	5.60E+03	5.60E+03	690	690	640
048_Gt7_2	1.00E+04	1.00E+04	650	650	8.90E+03	8.90E+03	980	980	4.30E+03
048_Gt7_3	10760	470	701	78	6130	90	700	65	700
048_Gt7_4	1.02E+04	1.40E+03	661	67	6150	560	716	25	845
048_Gt7_5	1.10E+04	1.10E+04	740	740	9.00E+03	9.00E+03	1.20E+03	1.20E+03	2.20E+03
048_Gt7_6	1.08E+04	1.30E+03	678	80	6070	570	690	150	692.8
048_Gt9_1	10690	710	729.5	6.5	7920	310	838	37	1335
048_Gt9_2	10840	180	723	14	7110	770	755	35	841
048_Gt9_3	10585	87	668	43	5790	780	700	100	613
048_Gt9_4	9.70E+03	1.30E+03	559	78	5330	910	642.6	9.7	610
048_Gt9_5	10120	530	660	130	5375	43	640	100	629
048_Gt9_6	1.05E+04	2.50E+03	691	38	6550	980	684	65	758
048_Gt9_7	1.08E+04	1.50E+03	660	32	6160	880	711	67	744
048_Gt9_8	1.07E+04	1.30E+03	656	29	6040	170	678	77	688
048_Gt9_9	1.04E+04	1.50E+03	634	66	6410	810	704	53	790
048_Gt9_10	9.90E+03	1.10E+03	665	87	7.20E+03	1.30E+03	874.2	8.3	1229
048_Gt9_11	10940	580	660	130	5640	190	714	34	680
048_Gt9_12	1.06E+04	1.40E+03	661	60	6210	590	740	150	670
048_Gt9_13	1.16E+04	2.00E+03	700	110	6200	370	800	130	662
048_Gt9_14	10500	850	725	17	1.02E+04	1.10E+03	1286	63	2730
048_Gt9_15	10260	840	714	92	1.17E+04	2.00E+03	1333	13	3100
048_Gt9_16	10530	220	720	240	1.23E+04	1.10E+03	1396	50	4180
048_Gt9_17	1.09E+04	1.40E+03	770	110	1.28E+04	2.10E+03	1408	58	3580
048_Gt9_18	10680	370	745	54	1.28E+04	1.20E+03	1478	40	4060
048_Gt9_19	10930	760	729	82	12260	900	1400	190	4480
048_Gt9_20	1.10E+04	1.10E+04	690	690	6.30E+03	6.30E+03	770	770	780
048_Gt9_21	1.20E+04	1.20E+04	720	720	1.10E+04	1.10E+04	1.10E+03	1.10E+03	3.20E+03
048_Gt9_22	11490	520	759	86	1.00E+04	1.40E+03	1150	140	2190
048_Gt9_23	1.25E+04	1.20E+03	766	43	6890	740	890	110	1059.6
048_Gt9_24	12530	320	726	7.2	6960	290	763.5	5.2	738.3
048_Gt9_25	1.20E+04	1.70E+03	714	64	7.20E+03	1.10E+03	830	150	900
048_Gt9_26	1.22E+04	1.20E+03	625	15	6460	340	729	50	756
048_Gt9_27	11200	610	614	20	6.00E+03	1.10E+03	700	150	686
048_Gt9_28	1.30E+04	1.30E+04	630	630	5.90E+03	5.90E+03	680	680	700
048_Gt9_29	12470	260	613	93	5882	91	662	60	667
048_Gt9_30	1.22E+04	1.90E+03	581	48	5690	900	630	130	648
048_Gt9_31	11150	950	567	84	5380	860	590	87	619

Spot location	Sm_ppm	2se	Eu_ppm	2se	Gd_ppm	2se	Tb_ppm	2se	Dy_ppm
048_Gt9_32	11380	920	630	110	6470	790	730	140	872
048_Gt9_33	1.30E+04	1.30E+04	630	630	6.30E+03	6.30E+03	700	700	690
048_Gt9_34	12850	650	640	100	5980	160	692	63	717
048_Gt9_35	12990	770	708	87	6430	850	690	110	687
048_Gt9_36	1.38E+04	2.60E+03	690	110	6450	420	700	130	760
048_Gt9_37	1.20E+04	2.10E+03	670	52	6269	94	674	44	700
048_Gt9_38	1.18E+04	1.80E+03	588	30	5800	750	680	160	710
048_Gt9_39	1.13E+04	3.70E+03	590	100	5730	680	640	110	667
048_Gt9_40	11810	640	663	25	6.60E+03	1.20E+03	728	85	784.5
048_Gt9_41	1.08E+04	1.10E+03	691	48	11980	950	1230	59	6490
048_Gt9_42	1.10E+04	1.10E+04	630	630	8.00E+03	8.00E+03	960	960	2.20E+03
048_Gt9_43	1.03E+04	2.30E+03	632	77	9.70E+03	2.10E+03	1010	280	3.80E+03
051_Gt1_1	1.05E+04	3.40E+03	518	94	8290	580	881	53	4870
051_Gt1_2	9.10E+03	4.30E+03	296	32	9160	320	1004	66	5470
051_Gt1_3	1.69E+04	4.20E+03	259	26	8240	470	957	65	5290
051_Gt5_1	9.90E+03	3.60E+03	250	20	8600	540	950	80	5410
051_Gt5_2	1.74E+04	5.10E+03	328	37	9120	570	1014	71	5510
051_Gt5_3	1.29E+04	3.80E+03	851	63	8490	660	955	72	5940
051_Gt6_1	7.90E+03	2.80E+03	401	37	7500	630	883	46	5230
051_Gt6_2	1.22E+04	4.00E+03	832	49	9410	670	1168	82	7200
051_Gt6_3	1.57E+04	5.60E+03	790	45	8880	710	1159	77	6650
051_Gt6_5	1.02E+04	3.10E+03	1000	88	10460	830	1180	120	7420
051_Gt10_1	4.80E+03	3.20E+03	690	70	8830	530	1092	72	6650
051_Gt10_2	1.22E+04	3.70E+03	671	60	9570	770	1060	69	6590
051_Gt10_3	1.74E+04	5.10E+03	283	31	9820	560	1161	75	6370
051_Gt10_4	1.87E+04	5.30E+03	313	34	9890	510	1217	73	6970
051_Gt11_1	1.40E+04	5.00E+03	676	74	9000	820	911	63	3920
051_Gt11_2	1.05E+04	3.40E+03	706	61	8740	720	964	83	4500
051_Gt11_3	1.66E+04	4.80E+03	667	65	8840	840	925	60	3900
051_Gt11_4	9.30E+03	4.80E+03	597	41	7640	610	790	52	3260
051_Gt11_5	1.60E+04	6.90E+03	821	80	1.08E+04	1.10E+03	1202	82	5070
051_Gt11_6	9.80E+03	3.80E+03	623	50	10220	910	1094	98	4940
051_Gt11_7	8.20E+03	3.00E+03	454	42	9220	560	1000	68	4650
051_Gt11_8	1.35E+04	9.10E+03	780	110	9810	900	1088	97	3930
051_Gt11_9	1.08E+04	4.00E+03	642	68	8670	650	858	56	3390
051_Gt11_10	1.31E+04	3.50E+03	596	65	8550	560	852	69	3260
051_Gt11_11	1.17E+04	3.20E+03	694	54	9240	580	977	79	3680
051_Gt11_12	1.34E+04	4.20E+03	729	69	9620	680	978	71	3970
051_Gt11_13	1.09E+04	3.70E+03	802	64	10700	730	1103	98	5340
051_Gt11_14	1.02E+04	4.30E+03	611	49	8230	580	815	59	3220
051_Gt11_15	1.60E+04	5.40E+03	682	59	9400	640	1079	85	5950
051_Gt11_16	1.85E+04	5.90E+03	289	29	9950	760	1247	94	6470
051_Gt11_17	1.44E+04	5.80E+03	418	52	8760	950	990	130	4940
055_Gt1_1	1.34E+04	4.10E+03	195	32	1.32E+04	1.00E+03	1370	100	6150
055_Gt1_2	1.71E+04	5.60E+03	166	21	10490	550	1067	63	5820
055_Gt1_4	1.45E+04	4.50E+03	313	44	9310	540	1101	36	6450
055_Gt1_5	1.18E+04	3.40E+03	274	34	9800	660	1065	71	6270
055_Gt1_6	2.64E+04	4.70E+03	321	47	1.38E+04	1.30E+03	1380	120	8030
055_Gt1_7	1.73E+04	5.70E+03	177	20	10280	560	1133	80	5870
055_Gt1_8	1.56E+04	3.70E+03	277	34	10390	920	1092	70	6960
055_Gt1_9	1.12E+04	4.40E+03	349	31	11760	790	1189	70	6530
055_Gt1_10	1.20E+04	4.30E+03	360	31	1.29E+04	1.20E+03	1410	140	8040

Spot location	Sm_ppm	2se	Eu_ppm	2se	Gd_ppm	2se	Tb_ppm	2se	Dy_ppm
055_Gt1_11	1.09E+04	4.50E+03	316	29	9880	780	1060	60	6370
055_Gt1_12	2.10E+04	3.90E+03	155	17	9920	610	1089	60	6840
055_Gt1_13	1.49E+04	4.90E+03	510	32	9630	890	739	61	2920
055_Gt1_14	1.11E+04	8.40E+03	205	62	8520	520	1019	73	5810
055_Gt18_1	1.17E+04	6.30E+03	157	20	9370	790	892	69	5350
055_Gt18_2	1.78E+04	6.40E+03	155	19	9850	460	1032	84	6380
055_Gt18_3	9.20E+03	5.10E+03	151	33	10350	740	1019	89	5930
055_Gt18_4	1.08E+04	4.10E+03	181	18	9750	630	1067	72	6180
055_Gt8_1	1.19E+04	5.30E+03	308	28	12030	750	1483	95	8450
055_Gt8_2	3.80E+03	4.80E+03	52	35	2850	660	304	79	1720
055_Gt8_3	1.91E+04	4.80E+03	320	36	12430	880	1430	110	8340
055_Gt8_4	2.53E+04	5.70E+03	308	37	13540	990	1582	70	8870
055_Gt9_1	1.32E+04	9.30E+03	209	29	6210	740	672	82	4420
055_Gt9_2	1.16E+04	3.40E+03	230	30	10510	890	1123	69	5540
055_Gt9_3	1.84E+04	8.80E+03	361	45	11790	900	1246	77	7060
055_Gt9_4	6.30E+03	4.30E+03	170	35	8460	510	1067	75	5350
055_Gt9_5	1.39E+04	4.80E+03	342	41	8630	550	739	42	3080
055_Gt9_6	1.10E+04	5.00E+03	119	23	7710	620	999	65	5100
055_Gt9_7	2.00E+04	6.70E+03	221	30	9950	690	1167	93	6360
055_Gt9_8	1.57E+04	6.30E+03	152	21	9190	740	1050	95	5410
055_Gt9_9	1.51E+04	6.70E+03	180	31	9520	790	1010	61	6490
055_Gt9_10	2.31E+04	8.10E+03	361	31	9640	570	1076	58	5410
059_Gt6_1	8.60E+03	3.10E+03	620	110	3980	580	270	49	924
059_Gt9-1	1.26E+04	4.10E+03	350	120	3610	350	261	27	639
059_Gt9-2	8.20E+03	2.30E+03	210	67	5990	520	510	54	1690
059_Gt19_1	9.10E+03	2.90E+03	209	54	5920	510	519	47	1830
059_Gt19_2	1.18E+04	3.30E+03	292	65	5330	560	418	49	1670

APPENDIX C: Trace element data from monazite with associated 2se errors

Spot location	2se	Ho_ppm	2se	Er_ppm	2se	Tm_ppm	2se	Yb_ppm	2se	Lu_ppm
046_Gt1_1	330	530	32	724	44	56.2	5.3	87.3	6.5	2.79
046_Gt1_2	330	509	38	728	44	47.8	4.4	87.2	7.6	2.38
046_Gt5_1	91	33.4	8.9	21.1	7.4	1.9	1	2.8	1.6	0.13
046_Gt5_2	160	50	20	64	32	6.4	2.7	6.7	3.7	0.27
046_Gt5_3	140	87	17	111	21	9.5	2.6	15.8	4	0.341
046_Gt5_4	500	349	52	451	84	36.9	6.9	67	13	2.14
046_Gt5_5	200	193	20	271	27	19.3	2.7	36.2	4.5	1.2
046_Gt6_2	280	116	24	155	38	9.2	2.2	19.3	7.1	0.69
046_Gt6_3	32	19	2.8	11.3	3.9	0.39	0.61	0.13	0.26	0.05
046_Gt8_1	190	316	22	360	27	28.2	4.3	46.2	3.9	1.32
046_Gt9_1	190	132	16	144	20	11.2	2.1	18.6	3.8	0.55
046_Gt14_1	49	23.4	3.1	13.3	3.4	0.96	0.51	0.91	0.7	0.018
046_Gt14_3	78	29.5	8.6	34	15	1.42	0.88	4	2.6	0.19
046_Gt14_4	210	319	17	420	24	39	2.6	71.2	6.2	2.39
046_Gt16_1	58	30.5	2.7	13	2.8	1.07	0.61	0.65	0.47	-0.0001946
046_Gt16_2	310	449	30	618	41	52.2	5	100.7	7	3.09
046_Gt16_3	39	20.6	2.1	13.5	2.4	1.4	0.57	0.65	0.57	0.042
046_Gt16_4	82	45.7	5.3	26.7	5.2	1.99	0.66	2.1	0.76	0.009
046_Gt16_5	48	34.7	4	19.6	5.2	0.86	0.6	1.4	1	0.039
052_Gt1_1	220	347	19	488	36	37.3	4	63.5	5.4	1.62
052_Gt1_2	270	383	28	551	50	46	5.4	92.2	6.7	2.64
052_Gt1_3	230	360	25	547	58	40	3.3	77.8	9.7	2.33
052_Gt3_2	260	378	20	413	25	25.9	3.5	33.8	3.8	1.12
052_Gt3_3	340	510	38	612	35	37.4	3.4	64.7	5.1	1.89
052_Gt3_4	270	509	44	747	44	73.3	5.9	152	14	4.19
052_Gt3_5	300	515	39	645	48	47.7	5.3	80.9	8.6	2.32
052_Gt3_7	220	458	31	722	62	71.7	6.8	150	13	4.87
052_Gt3_8	300	276	36	400	57	32.7	5.9	64	11	2.21
052_Gt3_10	170	303	24	342	36	24	3.8	33.5	3.9	0.95
052_Gt5_1	63	37.7	4.1	33.4	7.4	4.9	1.7	4.8	1.4	0.14
052_Gt5_2	220	488	28	770	44	67.5	6.7	149	12	5.17
052_Gt5_3	250	442	30	737	46	69.5	4	148	12	5.01
052_Gt5_4	460	404	46	690	100	57	10	128	17	4.33
052_Gt6_1	230	420	24	594	51	47.8	7.8	91	13	3.13
052_Gt6_2	380	568	44	784	63	65.8	5.7	113	13	3.09
052_Gt6_3	210	454	39	728	41	61	7.1	142	13	4.46
052_Gt8_1	75	229	17	366	22	34.1	5	71.6	6.5	2.3
052_Gt8_2	200	295	30	356	39	23.2	4.1	46.6	5.9	1.3
052_Gt12_2	240	465	27	692	42	69.4	8.6	140.8	9.1	4.57
052_Gt12_3	280	512	40	706	40	61.6	5.4	107	11	3.44
052_Gt14_1	130	173	11	196	14	12.6	1.8	22.5	3.5	0.83
052_Gt17_1	160	65	17	74	19	4.2	1.3	6.5	2	0.199
052_Gt17_2	380	471	42	765	57	74.1	6.3	156	16	4.54
052_Gt17_3	370	265	42	336	55	30.6	6.7	45.4	6.6	1.49
052_Gt18_1	140	71.6	6.8	60.3	7.6	3	1.1	3.4	1.1	0.136
052_Gt18_2	110	103.8	7.8	93	11	4.4	1.3	7	1.6	0.24
052_Gt18_3	260	532	36	753	42	51.8	3.9	109	12	3.04
052_Gt18_4	370	537	46	767	59	57	4.7	114.3	8.4	3.06
048_Gt1_1	600	299	53	288	42	14.4	3.5	10.9	3.8	0.36
048_Gt1_2	580	61	61	57	57	1.8	1.8	0.57	0.57	0.067
048_Gt1_3	120	130.1	7.7	119	33	4.8	1	2.8	1.7	0.098

Spot location	2se	Ho_ppm	2se	Er_ppm	2se	Tm_ppm	2se	Yb_ppm	2se	Lu_ppm
048_Gt1_4	110	55.3	5.9	48.9	2	2.23	0.23	2.8	1.7	0.05332
048_Gt1_5	53	64	10	48	8.1	2.7	1.3	2.21	0.43	0.0634
048_Gt1_6	1.50E+03	140	140	130	130	6.5	6.5	5.3	5.3	0.2
048_Gt1_7	130	96	16	75	17	3.61	0.32	2.61	0.86	0.116
048_Gt1_8	430	198	32	182	23	9.07	0.5	6.0363	0.0012	0.193414
048_Gt1_9	570	54	54	56	56	2.6	2.6	2.6	2.6	0.077
048_Gt1_10	130	120.8	5.1	92.5	7	3.58	0.96	4.4	1.7	0.0632
048_Gt1_11	95	81.6	7.5	65	15	3.27	0.32	0.8	1.3	0.043
048_Gt1_12	63	93.4	5.3	81.1	3.2	3.6	1.1	4.03	0.87	0.057
048_Gt6_1	26	81	13	65.8	1.8	2.63	0.046	1.64	0.43	0.0417
048_Gt6_2	130	115	16	94	23	4.8	1.1	2.5	1.3	0.064
048_Gt6_3	120	102	20	86.9	4.9	4.2	1.1	3.4	2.4	0.062
048_Gt6_4	140	184	14	151	32	7.78	0.92	5.3	1.7	0.1414
048_Gt6_5	240	244	33	196	26	8.51	0.99	6.64	0.51	0.185
048_Gt6_6	4.90E+03	590	590	610	610	38	38	40	40	0.86
048_Gt7_1	640	73	73	51	51	1.8	1.8	2.8	2.8	0.032
048_Gt7_2	4.30E+03	510	510	550	550	33	33	39	39	1.1
048_Gt7_3	120	77.2	5.6	60	19	2.89	0.69	2.35	0.43	0.062
048_Gt7_4	72	88	12	64	19	3.04	0.79	3.41	0.87	0.076
048_Gt7_5	2.20E+03	250	250	190	190	9.7	9.7	7.7	7.7	0.16
048_Gt7_6	4.8	75.1	5.4	60.2	3.5	2.5	1.3	1.8	1.3	0.062
048_Gt9_1	83	142.2	5.7	122.2	7.7	5.11	0.93	4.8	1.3	0.124
048_Gt9_2	19	79.3	1.7	75	16	2.98	0.19	4.1	1.7	0.0766
048_Gt9_3	56	67.6	7.6	54.4	2.6	2.19	0.74	1.44	0.29	0.037
048_Gt9_4	110	65	13	53.81	0.34	2.82	0.33	2.29	0.43	0.0764
048_Gt9_5	47	72	15	57.2	9.7	3	1.6	1.47	0.44	0.052
048_Gt9_6	16	86.14	0.22	72.8	0.34	3.13	0.37	2.14458	0.00085	0.069
048_Gt9_7	9.2	79.9	5.4	63.7	5.5	3.35	0.42	2.6	2.6	0.0606
048_Gt9_8	35	80	15	64.5	7.7	2.62	0.37	2.8	1.3	0.064
048_Gt9_9	140	82	17	69.8	7.9	2.98	0.71	1.7	1.3	0.075
048_Gt9_10	92	146	23	119.1	4.9	5.3	1.1	5.1	3	0.136
048_Gt9_11	120	72.7	8.5	58.4	3.2	2.26	0.19	1.2	0.43	0.063
048_Gt9_12	100	73.7	9.4	57.4	3.7	2.06	0.42	3.01	0.49	0.048
048_Gt9_13	12	74	10	52.8	4.9	2.19	0.71	1.71	0.84	0.062
048_Gt9_14	150	319.2	1.9	263.1	5	12.56	0.38	8.54	0.42	0.242
048_Gt9_15	340	329	37	285	51	13.64	0.14	11.7	1.7	0.33
048_Gt9_16	180	448	51	426	39	21.3	2.8	22.2	7.5	0.575
048_Gt9_17	510	414	21	387	40	20.1	1.8	11.5	3.8	0.43
048_Gt9_18	250	436	65	433	73	22.7	1.6	19.7	1.2	0.6
048_Gt9_19	300	459	16	494	81	28.1	2.3	25.6	2.1	0.757
048_Gt9_20	780	89	89	80	80	3.4	3.4	4.1	4.1	0.1
048_Gt9_21	3.20E+03	340	340	310	310	16	16	13	13	0.42
048_Gt9_22	200	254	12	201	55	9.4	1.2	5.7	3.8	0.176
048_Gt9_23	9.4	125	27	93.3	9	5.27	0.72	2.66	0.83	0.122
048_Gt9_24	3.3	84.8	2.2	62.8	2.9	2.72	0.53	1.07	0.85	0.063
048_Gt9_25	110	96	14	77	14	3.39	0.17	1.7	1.6	0.068
048_Gt9_26	74	85.5	9.7	69.1	5.3	3	2	2.3	1.3	0.032
048_Gt9_27	96	69.8	8.2	50.8	4.1	2.1	0.44	1.68	0.84	0.049
048_Gt9_28	700	70	70	53	53	3.8	3.8	0.82	0.82	0.064
048_Gt9_29	73	72.1	2.8	60	10	2.8	1.3	2.7	1.3	0.088
048_Gt9_30	45	78	11	64.3	5.9	2.6	0.24	2.7	2.1	0.043
048_Gt9_31	83	70	13	55.9	7.3	2.7	0.76	2.23	0.73	0.057

Spot location	2se	Ho_ppm	2se	Er_ppm	2se	Tm_ppm	2se	Yb_ppm	2se	Lu_ppm
048_Gt9_32	79	93.7	6.7	78	20	3.16	0.29	2.24	0.42	0.0834
048_Gt9_33	690	89	89	61	61	2.6	2.6	3.3	3.3	0.069
048_Gt9_34	53	76	8.4	58.5	4.3	2.73	0.68	2	2.5	0.043
048_Gt9_35	48	77	15	58	10	2.44	0.59	3.28	0.84	0.068
048_Gt9_36	190	78.8	9.2	60.7	9.4	2.57	0.83	2.03	0.84	0.07996
048_Gt9_37	110	85.9	9.8	61.8	2.2	2.72	0.34	2.3	2.1	0.059
048_Gt9_38	110	74	14	55	14	3.014	0.049	1.4	1.2	0.07
048_Gt9_39	88	71.5	3.6	57	4.4	2.4	1.1	2.7	1.3	0.084
048_Gt9_40	5.7	85.8	1.6	64.2	2.4	3.12	0.84	1.7	2.1	0.09
048_Gt9_41	630	719	55	730	110	45.7	1.6	41.4	5.4	1.439
048_Gt9_42	2.20E+03	270	270	290	290	14	14	14	14	0.49
048_Gt9_43	1.10E+03	410	130	450	130	30.9	9.9	28	15	0.96
051_Gt1_1	260	599	29	1105	49	121	8.4	354	21	13.54
051_Gt1_2	270	652	36	1038	55	101	14	233	24	9.4
051_Gt1_3	270	606	29	1042	74	120	12	289	29	11.1
051_Gt5_1	380	624	38	964	66	106.1	7.7	256	19	10.7
051_Gt5_2	350	647	35	947	48	78.1	7.5	198	17	6.08
051_Gt5_3	350	727	50	1240	110	135.2	8	319	21	12.3
051_Gt6_1	310	609	43	955	88	75.5	7	176	15	5.86
051_Gt6_2	430	832	63	1307	66	120.8	9.5	262	22	8.83
051_Gt6_3	440	773	51	1325	71	125.3	8.3	281	16	9.77
051_Gt6_5	740	765	80	1240	120	110.2	7.8	217	26	7.58
051_Gt10_1	380	767	37	1247	76	121	14	247	24	8.76
051_Gt10_2	390	760	41	1105	52	100.4	6.9	203	14	7.74
051_Gt10_3	390	757	43	966	83	72.1	5.4	129	13	3.95
051_Gt10_4	470	754	58	967	56	67.6	8.1	95.8	5.8	3.21
051_Gt11_1	390	344	32	393	48	30.6	4.6	44.2	9.7	1.32
051_Gt11_2	360	415	37	553	49	42	5.1	89	10	2.79
051_Gt11_3	320	323	22	319	28	20.9	3.8	32.8	3.8	0.99
051_Gt11_4	240	277	21	285	23	19.2	3.1	25.5	2.1	0.77
051_Gt11_5	410	477	39	531	61	42.2	5.9	65	15	1.89
051_Gt11_6	440	501	61	650	110	44.5	9.3	76	17	2.57
051_Gt11_7	270	509	31	606	42	50.8	3.9	71.2	5.9	2.03
051_Gt11_8	390	388	25	380	23	23.4	7.4	34.3	8.1	0.77
051_Gt11_9	240	319	22	309	16	21	2.7	31.9	3.7	0.79
051_Gt11_10	230	308	24	325	27	19.8	2.2	32.2	2.9	0.96
051_Gt11_11	290	333	21	315	29	18.4	2.2	26.7	3.5	0.9
051_Gt11_12	230	344	29	383	35	26.6	4	34.9	4.1	1.01
051_Gt11_13	390	591	44	816	88	59.4	6.7	113	12	3.73
051_Gt11_14	260	303	22	306	28	19.3	2.3	28	5	0.9
051_Gt11_15	280	776	45	1250	70	113	8.5	239	19	8.08
051_Gt11_16	460	835	72	1130	110	86.6	8.3	156	13	4.56
051_Gt11_17	790	510	110	680	170	46	13	79	24	2.36
055_Gt1_1	440	495	27	405	35	19.1	2.3	26.5	3.2	0.4
055_Gt1_2	450	626	33	825	35	51.6	4.9	93	8	2.87
055_Gt1_4	400	745	42	1104	57	89.2	7.4	170	9.5	5.46
055_Gt1_5	500	723	55	1035	85	87.4	7.5	162	15	5.45
055_Gt1_6	570	960	97	1384	49	89.7	3.5	162	26	5.28
055_Gt1_7	300	623	37	725	56	44.3	5.3	78.3	8.1	2.13
055_Gt1_8	370	763	40	1108	50	81.8	7.4	159	12	4.96
055_Gt1_9	400	609	40	790	54	51.3	4.9	90.2	7.9	2.85
055_Gt1_10	480	945	74	1304	77	109.8	9.9	194	12	6.48

Spot location	2se	Ho_ppm	2se	Er_ppm	2se	Tm_ppm	2se	Yb_ppm	2se	Lu_ppm
055_Gt1_11	340	754	46	1025	49	80.7	8.5	145	16	4.95
055_Gt1_12	250	726	42	949	76	75.3	6.8	120	10	4
055_Gt1_13	250	210	15	222	23	13	1.7	23.8	4.3	0.65
055_Gt1_14	500	697	45	1027	79	81	10	155	19	4.72
055_Gt18_1	320	652	46	869	59	64.8	7.2	116.8	9.3	3.74
055_Gt18_2	460	753	33	1096	75	82	6.9	147	15	4.74
055_Gt18_3	380	659	28	788	62	51.4	8.8	83.8	7.9	3.37
055_Gt18_4	490	737	50	940	65	77	7.1	139	13	3.89
055_Gt8_1	600	857	51	1143	73	94	10	166	12	5.01
055_Gt8_2	400	181	44	218	78	17.7	9.8	32	13	1.08
055_Gt8_3	510	928	67	1205	58	85.2	6.2	156	13	5.6
055_Gt8_4	590	922	45	1297	67	93.1	9.2	180	24	4.85
055_Gt9_1	350	508	30	702	41	56	12	108	11	4.21
055_Gt9_2	220	554	26	570	38	37.5	3.9	54.7	5.1	1.52
055_Gt9_3	480	803	50	1023	64	89	14	140	15	4.52
055_Gt9_4	250	657	31	926	36	79.4	8.1	130	11	4.17
055_Gt9_5	150	264	17	298	17	17.6	2.6	24	2.7	0.57
055_Gt9_6	430	643	48	912	53	78.9	9.5	112.9	9.8	3.55
055_Gt9_7	320	689	51	869	63	54.1	5.2	80	8	2.67
055_Gt9_8	300	624	50	741	69	54.3	4.6	71	7.3	2.36
055_Gt9_9	390	759	28	1063	83	87	13	148	16	5.68
055_Gt9_10	300	600	33	887	56	68.8	5.2	96.7	8.2	3.23
059_Gt6_1	83	70.9	6.5	75	10	7.8	2	10.9	2.8	0.22
059_Gt9-1	48	37.8	4	38.4	4.3	2.31	0.79	4.3	1.6	0.111
059_Gt9-2	140	122	12	119	11	8.6	1.7	14	2.5	0.39
059_Gt19_1	150	114.7	9.3	104	11	5.4	1.4	10	1.9	0.293
059_Gt19_2	160	107	12	98	14	5.6	1.1	9.2	1.9	0.298

APPENDIX C: Trace element data from monazite with associated 2se errors

Spot location	2se	^{206}Pb_ppm	2se	^{207}Pb_ppm	2se	^{208}Pb_ppm	2se	Total HREE	Gd/Yb
046_Gt1_1	0.39	103	14	105	13	99	9.4	16259.29	98.74
046_Gt1_2	0.35	123	17	96	17	96	12	17245.38	108.83
046_Gt5_1	0.064	103	17	91	12	104	10	7948.33	2450.00
046_Gt5_2	0.14	121	13	123	15	119	12	7199.37	891.04
046_Gt5_3	0.099	140	23	145	15	111	15	7962.64	387.34
046_Gt5_4	0.41	94	14	83	8.4	93	12	12616.04	112.69
046_Gt5_5	0.27	116	20	109	14	119.6	8.9	8755.70	158.56
046_Gt6_2	0.23	103	10	92	12	100	14	8876.19	339.90
046_Gt6_3	0.04	104	13	90	12	129.2	7.9	7353.87	49769.23
046_Gt8_1	0.2	101	17	86	12	98	12	12520.72	169.05
046_Gt9_1	0.14	147	18	111	17	120.6	8.3	8768.35	343.55
046_Gt14_1	0.025	115	20	93	13	118	12	6767.59	6395.60
046_Gt14_3	0.1	102	25	89	17	106	18	6645.11	1417.50
046_Gt14_4	0.36	82	17	64	7.2	83	9.3	10481.59	83.99
046_Gt16_1	2.9E-07	111	18	120	10	129	14	7201.22	9169.23
046_Gt16_2	0.34	97	13	81	11	84	11	13163.99	68.72
046_Gt16_3	0.034	167	23	158	18	118	10	5856.19	7846.15
046_Gt16_4	0.018	110	20	103.8	7.9	112	11	8097.50	3133.33
046_Gt16_5	0.042	86	17	85	11	116	13	8088.60	4950.00
052_Gt1_1	0.21	58	14	45.9	6.9	32.3	6	9665.42	78.11
052_Gt1_2	0.41	52	17	37.8	7.8	51.9	5.7	10519.84	56.83
052_Gt1_3	0.36	51	11	36.5	9	48.8	9.9	9720.13	62.60
052_Gt3_2	0.17	62	11	45.7	9.7	68	9	14179.82	241.12
052_Gt3_3	0.38	50	12	45.3	7.1	63.2	9.5	16274.99	136.48
052_Gt3_4	0.43	70	12	75.6	7.8	76.8	8.9	12355.49	39.61
052_Gt3_5	0.29	78	16	76.4	7.9	57.5	7.8	14556.92	91.10
052_Gt3_7	0.54	84	15	79	12	76	10	11909.57	39.80
052_Gt3_8	0.46	25	5.7	24.3	4.7	42.2	9.9	6755.91	50.31
052_Gt3_10	0.25	57	18	38.7	8.2	61	13	11110.45	190.15
052_Gt5_1	0.076	146	23	145	15	153	15	5402.94	922.92
052_Gt5_2	0.49	65.3	9.1	59.1	9.9	104.5	9.3	11721.67	39.26
052_Gt5_3	0.42	76	13	64.7	9.7	93.4	9.5	11423.51	40.27
052_Gt5_4	0.61	56	11	79.2	9.9	104	13	11841.33	50.16
052_Gt6_1	0.48	59	12	58	10	101	13	12427.93	73.85
052_Gt6_2	0.34	52	12	30.5	8.5	83.3	9.8	13895.89	58.58
052_Gt6_3	0.45	71	14	51.7	8.3	93	14	12652.46	47.39
052_Gt8_1	0.25	85	14	60.6	6.5	103	13	9420.00	83.52
052_Gt8_2	0.27	120	20	107	10	108	11	10200.10	129.61
052_Gt12_2	0.39	82	17	75	12	78.1	8.3	11819.77	42.83
052_Gt12_3	0.43	53	13	53.2	6	62.8	9.4	12712.04	58.22
052_Gt14_1	0.15	141	19	120	11	113	12	8905.93	266.67
052_Gt17_1	0.076	165	33	181	17	143	16	6324.90	783.08
052_Gt17_2	0.54	57	12	53.5	9.3	111	10	12368.64	40.77
052_Gt17_3	0.31	104	18	97	16	132	14	11569.49	171.37
052_Gt18_1	0.066	160	25	176	17	145	14	8643.44	1985.29
052_Gt18_2	0.13	181	32	148	13	132	21	8748.44	948.57
052_Gt18_3	0.35	57	12	36.8	6	97	10	13531.84	64.77
052_Gt18_4	0.42	59	11	29.7	7.3	92	11	14451.36	66.05
048_Gt1_1	0.13	710	210	50	22	112	30	10761.66	620.18
048_Gt1_2	0.067	1.20E+03	1.20E+03	53	53	110	110	6060.44	8596.49
048_Gt1_3	0.01	890	720	69.9	2.3	117	82	7976.80	2085.71

Spot location	2se	^{206}Pb_ppm	2se	^{207}Pb_ppm	2se	^{208}Pb_ppm	2se	Total HREE	Gd/Yb
048_Gt1_4	0.00021	710	720	65	26	116	21	5060.18	1428.57
048_Gt1_5	0.0049	980	900	58	17	120	10	4991.97	1778.28
048_Gt1_6	0.2	1.20E+03	1.20E+03	48	48	160	160	7812.00	1018.87
048_Gt1_7	0.084	1180	350	58	45	108	30	6430.34	1858.24
048_Gt1_8	0.000084	850	900	55	21	109	49	9481.30	1093.39
048_Gt1_9	0.077	110	110	72	72	79	79	5735.28	1769.23
048_Gt1_10	0.005	1520	890	92	28	128	29	8233.34	1440.91
048_Gt1_11	0.016	600	360	61	19	133	39	7659.71	7625.00
048_Gt1_12	0.022	920	170	82	19	161	39	8031.19	1553.35
048_Gt6_1	0.0051	1.40E+03	1.10E+03	69.4	7	144.7	9.4	7283.11	3518.29
048_Gt6_2	0.011	1330	530	71	9.4	185	77	8774.36	2720.00
048_Gt6_3	0.022	710	210	55	15	170	55	8079.56	1855.88
048_Gt6_4	0.0049	1.30E+03	2.00E+03	85	26	164	47	10996.22	1528.30
048_Gt6_5	0.048	1470	310	74	5.6	144	33	12384.34	1320.78
048_Gt6_6	0.86	1.60E+03	1.60E+03	40	40	95	95	15848.86	217.50
048_Gt7_1	0.032	1.60E+03	1.60E+03	68	68	68	68	7058.63	2000.00
048_Gt7_2	1.1	1.60E+03	1.60E+03	53	53	120	120	15313.10	228.21
048_Gt7_3	0.027	880	710	85	16	209	56	7672.50	2608.51
048_Gt7_4	0.017	880	710	62	21	161	74	7869.53	1803.52
048_Gt7_5	0.16	1.10E+03	1.10E+03	77	77	150	150	12857.56	1168.83
048_Gt7_6	0.038	1500	180	71	2.4	149	18	7592.46	3372.22
048_Gt9_1	0.033	1060	710	75	26	149	91	10367.43	1650.00
048_Gt9_2	0.0055	1230	710	115	19	166.9026	0.008	8867.46	1734.15
048_Gt9_3	0.018	1400	700	82	18	178	38	7228.67	4020.83
048_Gt9_4	0.0055	1490	530	63	25	146.5	9	6706.60	2327.51
048_Gt9_5	0.044	1753.847	0.029	80.5397	0.0036	169	36	6777.72	3656.46
048_Gt9_6	0.044	1.40E+03	1.10E+03	92	37	204	36	8156.28	3054.21
048_Gt9_7	0.0055	1.40E+03	1.10E+03	82	58	199	45	7764.61	2369.23
048_Gt9_8	0.022	1310	180	94	11	180	63	7555.98	2157.14
048_Gt9_9	0.061	2.10E+03	1.80E+03	57	35	157.3	8.7	8060.56	3770.59
048_Gt9_10	0.017	1120	880	72.9	4.5	147.1	8.7	9578.84	1411.76
048_Gt9_11	0.039	1640	530	74.6	2.3	150	18	7168.62	4700.00
048_Gt9_12	0.036	1550	880	70	18	115	36	7756.22	2063.12
048_Gt9_13	0.062	2080	350	99.3	2.4	160	26	7792.76	3625.73
048_Gt9_14	0.04	1570	350	61.9	4.6	170	17	14819.64	1194.38
048_Gt9_15	0.13	960	520	65	48	138.3	8.8	16772.67	1000.00
048_Gt9_16	0.091	1.80E+03	1.20E+03	79	6.9	116	35	18794.08	554.05
048_Gt9_17	0.2	1120	520	77	11	128	26	18621.03	1113.04
048_Gt9_18	0.023	920.9	1.6	64	25	128	17	19250.00	649.75
048_Gt9_19	0.074	820	170	58.9	2.3	128	35	19147.46	478.91
048_Gt9_20	0.1	1.70E+03	1.70E+03	80	80	140	140	8026.60	1536.59
048_Gt9_21	0.42	1.20E+03	1.20E+03	71	71	110	110	15979.42	846.15
048_Gt9_22	0.064	1300	170	80	55	129	35	13810.28	1754.39
048_Gt9_23	0.053	870	350	83	11	111.867	0.048	9065.95	2590.23
048_Gt9_24	0.029	1130	870	77	50	142.3	8.6	8613.25	6504.67
048_Gt9_25	0.034	1270	500	80	16	132	37	9108.16	4235.29
048_Gt9_26	0.012	430	520	85	14	150	26	8104.93	2808.70
048_Gt9_27	0.03	1381.143	0.037	78	20	152	51	7510.43	3571.43
048_Gt9_28	0.064	2.10E+03	2.10E+03	64	64	84	84	7407.68	7195.12
048_Gt9_29	0.024	1380	340	88	13	189	25	7348.69	2178.52
048_Gt9_30	0.03	1290	170	81	2.4	188.8	8.4	7115.64	2107.41
048_Gt9_31	0.023	1720	700	82	11	122	16	6719.89	2412.56

Spot location	2se	^{206}Pb_ppm	2se	^{207}Pb_ppm	2se	^{208}Pb_ppm	2se	Total HREE	Gd/Yb
048_Gt9_32	0.0059	670	690	89.9	6.7	197.5	8.3	8249.18	2888.39
048_Gt9_33	0.069	1.80E+03	1.80E+03	48	48	110	110	7845.97	1909.09
048_Gt9_34	0.018	1440	340	63	12	154	49	7528.27	2990.00
048_Gt9_35	0.042	2.10E+03	1.70E+03	54	18	134	24	7947.79	1960.37
048_Gt9_36	0.00027	1050	510	65.2	4.7	137	97	8054.18	3177.34
048_Gt9_37	0.024	1070	520	78.9	6.9	141	56	7795.78	2725.65
048_Gt9_38	0.018	1010	690	63	31	92	40	7323.48	4142.86
048_Gt9_39	0.012	900	1700	81	11	161	55	7170.68	2122.22
048_Gt9_40	0.019	1460	510	51	43	132	47	8267.41	3882.35
048_Gt9_41	0.086	1110	510	71	20	91	47	21237.54	289.37
048_Gt9_42	0.49	1.20E+03	1.20E+03	63	63	140	140	11748.49	571.43
048_Gt9_43	0.28	770	510	44	16	123.5	7.8	15429.86	346.43
051_Gt1_1	0.93	61	10	53.4	5.5	83.2	6.5	16233.54	23.42
051_Gt1_2	0.95	47.6	8.1	63	12	83.6	8.4	17667.40	39.31
051_Gt1_3	1.3	63	11	56.9	9	83.2	9.2	16555.10	28.51
051_Gt5_1	1.1	62	12	54	10	73	11	16920.80	33.59
051_Gt5_2	0.61	62	16	51.3	7.7	86	13	17520.18	46.06
051_Gt5_3	1.3	74	15	56.1	9.4	82	11	17818.50	26.61
051_Gt6_1	0.82	56	12	61	10	79	15	15434.36	42.61
051_Gt6_2	0.77	103	18	78	10	93	14	20308.63	35.92
051_Gt6_3	0.92	84	11	59.6	9	90	13	19203.07	31.60
051_Gt6_5	0.99	109	18	73	11	90	12	21399.78	48.20
051_Gt10_1	0.79	119	19	85	10	100	13	18962.76	35.75
051_Gt10_2	0.63	94	20	86.3	9.4	87.3	7.7	19396.14	47.14
051_Gt10_3	0.37	64	13	46.5	7.6	84.1	9.8	19279.05	76.12
051_Gt10_4	0.31	66	15	45.7	7.5	86.1	7.7	19964.61	103.24
051_Gt11_1	0.36	103	17	90	15	125.2	9.4	14644.12	203.62
051_Gt11_2	0.46	126	22	92	13	129	17	15305.79	98.20
051_Gt11_3	0.12	105	12	104	15	139	17	14361.69	269.51
051_Gt11_4	0.17	99	22	93	13	110	16	12297.47	299.61
051_Gt11_5	0.3	133	23	88	13	113	12	18189.09	166.15
051_Gt11_6	0.71	87	18	96	11	112	11	17528.07	134.47
051_Gt11_7	0.22	92	16	71	13	100	11	16109.03	129.49
051_Gt11_8	0.25	132	24	123	28	160	20	15654.47	286.01
051_Gt11_9	0.17	117	17	94	10	127	16	13599.69	271.79
051_Gt11_10	0.24	121	18	97	18	123	13	13347.96	265.53
051_Gt11_11	0.16	90	13	97	10	119	11	14591.00	346.07
051_Gt11_12	0.17	100	18	99	12	117	14	15357.51	275.64
051_Gt11_13	0.56	92	17	84.5	8.7	125	10	18726.13	94.69
051_Gt11_14	0.23	110	13	87	13	118	15	12922.20	293.93
051_Gt11_15	0.73	86	16	76.7	9.8	96	12	18815.08	39.33
051_Gt11_16	0.43	73	13	46.2	6.6	98	13	19879.16	63.78
051_Gt11_17	0.74	81	17	68	12	114	11	16007.36	110.89
055_Gt1_1	0.12	108	16	114	16	127	16	21666.00	498.11
055_Gt1_2	0.27	82	15	60.7	6.3	119	11	18975.47	112.80
055_Gt1_4	0.45	89	12	58	8.8	138	14	18974.66	54.76
055_Gt1_5	0.39	62	12	60	11	143	17	19147.85	60.49
055_Gt1_6	0.72	98	31	65	21	122	17	25810.98	85.19
055_Gt1_7	0.36	85	16	61	11	143	16	18755.73	131.29
055_Gt1_8	0.48	84	14	59	12	122	14	20558.76	65.35
055_Gt1_9	0.37	100	16	87	12	141	14	21022.35	130.38
055_Gt1_10	0.82	93	28	58	13	163	16	24909.28	66.49

Spot location	2se	^{206}Pb_ppm	2se	^{207}Pb_ppm	2se	^{208}Pb_ppm	2se	Total HREE	Gd/Yb
055_Gt1_11	0.56	92	16	60	10	139	12	19319.65	68.14
055_Gt1_12	0.54	79	19	45	11	117	20	19723.30	82.67
055_Gt1_13	0.17	87	15	107	11	143	16	13758.45	404.62
055_Gt1_14	0.58	44	18	34.3	4.4	146	27	17313.72	54.97
055_Gt18_1	0.52	81	14	45	10	127	14	17318.34	80.22
055_Gt18_2	0.55	64	16	54.7	9	139	15	19344.74	67.01
055_Gt18_3	0.84	56	14	48	13	121	12	18884.57	123.51
055_Gt18_4	0.39	66	11	54.9	6.2	137	18	18893.89	70.14
055_Gt8_1	0.33	94	19	75	11	101	11	24228.01	72.47
055_Gt8_2	0.37	191	33	194	39	78	30	5323.78	89.06
055_Gt8_3	0.54	94	13	70	12	116	12	24579.80	79.68
055_Gt8_4	0.31	114	38	72	16	102	17	26488.95	75.22
055_Gt9_1	0.59	96	25	48	20	69	19	12680.21	57.50
055_Gt9_2	0.22	93	20	67	9.2	137	17	18390.72	192.14
055_Gt9_3	0.43	94	23	79	16	132	19	22155.52	84.21
055_Gt9_4	0.52	70	19	53.9	8	131	16	16673.57	65.08
055_Gt9_5	0.11	119	18	79	11	155	18	13053.17	359.58
055_Gt9_6	0.49	41	13	51.2	6.5	121	18	15559.35	68.29
055_Gt9_7	0.35	85	16	59.5	9.5	132	16	19171.77	124.38
055_Gt9_8	0.41	72	12	47.8	6.8	117	15	17142.66	129.44
055_Gt9_9	0.67	58	16	47	12	131	25	19082.68	64.32
055_Gt9_10	0.34	93	13	77	12	135	18	17781.73	99.69
059_Gt6_1	0.15	60	13	52.2	9.6	81	12	5338.82	365.14
059_Gt9-1	0.082	45.3	8.6	48.1	5.9	66	8.7	4592.92	839.53
059_Gt9-2	0.13	44.2	7.8	35.8	4.1	40.2	6.1	8453.99	427.86
059_Gt19_1	0.095	44.3	6.6	30.5	5.8	63.1	5.8	8503.39	592.00
059_Gt19_2	0.083	66.5	8.1	39.2	4.8	65.8	8.6	7638.10	579.35